Fault Detection and Isolation in a Networked Multi-Vehicle Unmanned System

Nader Meskin

A Thesis

in

The Department

of

Electrical and Computer Engineering

Presented in Partial Fulfillment of the Requirements

for the Degree of Doctor of Philosophy at

Concordia University

Montréal, Québec, Canada

October 2008

© Nader Meskin, 2008

Library and Archives Canada

Published Heritage Branch

395 Wellington Street
Ottawa ON K1A 0N4
Canada

Bibliothèque et Archives Canada

Direction du Patrimoine de l'édition

395, rue Wellington
Ottawa ON K1A 0N4
Canada

Your file Votre référence
ISBN: 978-0-494-63395-3
Our file Notre référence
ISBN: 978-0-494-63395-3

NOTICE:

The author has granted a non-exclusive license allowing Library and Archives Canada to reproduce, publish, archive, preserve, conserve, communicate to the public by telecommunication or on the Internet, loan, distribute and sell theses worldwide, for commercial or non-commercial purposes, in microform, paper, electronic and/or any other formats.

The author retains copyright ownership and moral rights in this thesis. Neither the thesis nor substantial extracts from it may be printed or otherwise reproduced without the author's permission.

AVIS:

L'auteur a accordé une licence non exclusive permettant à la Bibliothèque et Archives Canada de reproduire, publier, archiver, sauvegarder, conserver, transmettre au public par télécommunication ou par l'Internet, prêter, distribuer et vendre des thèses partout dans le monde, à des fins commerciales ou autres, sur support microforme, papier, électronique et/ou autres formats.

L'auteur conserve la propriété du droit d'auteur et des droits moraux qui protège cette thèse. Ni la thèse ni des extraits substantiels de celle-ci ne doivent être imprimés ou autrement reproduits sans son autorisation.

In compliance with the Canadian Privacy Act some supporting forms may have been removed from this thesis.

While these forms may be included in the document page count, their removal does not represent any loss of content from the thesis.

Conformément à la loi canadienne sur la protection de la vie privée, quelques formulaires secondaires ont été enlevés de cette thèse.

Bien que ces formulaires aient inclus dans la pagination, il n'y aura aucun contenu manquant.

Canada

ABSTRACT

Fault Detection and Isolation in a Networked Multi-Vehicle Unmanned System

Nader Meskin, Ph.D.

Concordia Unviersity, 2008

Recent years have witnessed a strong interest and intensive research activities in the area of networks of autonomous unmanned vehicles such as spacecraft formation flight, unmanned aerial vehicles, autonomous underwater vehicles, automated highway systems and multiple mobile robots. The envisaged networked architecture can provide surpassing performance capabilities and enhanced reliability; however, it requires extending the traditional theories of control, estimation and Fault Detection and Isolation (FDI). One of the many challenges for these systems is development of autonomous cooperative control which can maintain the group behavior and mission performance in the presence of undesirable events such as failures in the vehicles. In order to achieve this goal, the team should have the capability to detect and isolate vehicles faults and reconfigure the cooperative control algorithms to compensate for them.

This dissertation deals with the design and development of fault detection and isolation algorithms for a network of unmanned vehicles. Addressing this problem is the main step towards the design of autonomous fault tolerant cooperative control of network of unmanned systems. We first formulate the FDI problem by considering ideal communication channels among the vehicles and solve this problem corresponding to three different architectures, namely centralized, decentralized, and semi-decentralized. The necessary and sufficient solvability conditions for each architecture are also derived based on geometric FDI approach. The effects of large environmental disturbances are subsequently taken into account in the design of FDI

algorithms and robust hybrid FDI schemes for both linear and nonlinear systems are developed. Our proposed robust FDI algorithms are applied to a network of unmanned vehicles as well as Almost-Lighter-Than-Air-Vehicle (ALTAV).

The effects of communication channels on fault detection and isolation performance are then investigated. A packet erasure channel model is considered for incorporating stochastic packet dropout of communication channels. Combining vehicle dynamics and communication links yields a discrete-time Markovian Jump System (MJS) mathematical model representation. This motivates development of a geometric FDI framework for both discrete-time and continuous-time Markovian jump systems. Our proposed FDI algorithm is then applied to a formation flight of satellites and a Vertical Take-Off and Landing (VTOL) helicopter problem.

Finally, we investigate the problem of fault detection and isolation for time-delay systems as well as linear impulsive systems. The main motivation behind considering these two problems is that our developed geometric framework for Markovian jump systems can readily be applied to other class of systems. Broad classes of time-delay systems, namely, retarded, neutral, distributed and stochastic time-delay systems are investigated in this dissertation and a robust FDI algorithm is developed for each class of these systems. Moreover, it is shown that our proposed FDI algorithms for retarded and stochastic time-delay systems can potentially be applied in an integrated design of FDI/controller for a network of unmanned vehicles. Necessary and sufficient conditions for solvability of the fundamental problem of residual generation for linear impulsive systems are derived to conclude this dissertation.

In the name of God

To my wife

Mojdeh,

and my daughter

Melina

ACKNOWLEDGEMENTS

I would like to express deep gratitude to my dissertation advisor Prof. K. Khorasani for his consistent encouragement, motivation, guidance and support throughout my study at Concordia University. He has provided me with unquenchable enthusiasm, vision, and wisdom, which inspired me from the beginning to the end.

I would like to thank all my dissertation committee members, including Dr. T. Chen, Dr. Hashtrudi zad, Dr. L. Rodrigues, and Dr. W. P. Zhu. I sincerely appreciate the time, advice, and support they offered me during my doctoral study. I also wish to thank Dr. A. Aghdam for providing me the opportunity to study at Concordia University.

My good friends, Amin Mannani, Behzad Samadi, Hani Khoshdel Nikkho, Ehsan Sobhani, Rasul Mohammadi, Amitabh Barua, Farzaneh Abdollahi, Elham Semsar, Mohsen Zamani, Mohsen Azizi, and Mohammad El Bouyoucef, with whom I spent a lot of time both at work and in spare time, deserve big thanks. They made my four-year stay at Montreal enjoyable and memorable.

Finally, I would like to thank my wife, Mojdeh, for her love and support over the years. She has always been a pillar of strength, inspiration and support. I could never thank my parents for their unconditional love and prayers, without which I would never have come so far.

TABLE OF CONTENTS

List of Figures xii

List of Tables xvii

List of Symbols and Abbreviations xviii

1 Introduction **1**

1.1 Motivation 1

1.2 Literature Review 3

1.2.1 Fault Detection and Isolation 3

1.2.2 Network of Unmanned Vehicles 9

1.3 General Problem Statement 12

1.4 Contributions of the Thesis 13

1.5 Organization of the Thesis 16

1.6 Notation 18

2 Geometric Approach to Fault Detection and Isolation **20**

2.1 Structured Fault Detection and Isolation 20

2.2 Geometric Approach to FDI of Linear Systems 25

2.3 Geometric Approach to FDI of Nonlinear Systems 33

2.4 Actuator Fault Modes 37

3 Fault Detection and Isolation in a Network of Unmanned Vehicles: Ideal Communication Channels **39**

3.1 FDI Problem Formulation in a Network of Unmanned Vehicles 40

3.1.1 Centralized Architecture 42

3.1.2 Decentralized Architecture 43

3.1.3 Semi-decentralized Architecture 44

3.2 Proposed Structured Fault Detection and Isolation Scheme 45

3.3 Actuator Fault detection and Isolation in a Network of Unmanned Vehicles 55
3.3.1 Centralized Architecture 55
3.3.2 Semi-decentralized Architecture 57
3.3.3 Simulation Results For Formation Flight of Satellites 60
3.4 Fault Detection and Isolation of F-18 HARV 66
3.5 Fault Detection and Isolation of Redundant Reaction Wheels 68
3.6 Conclusions 78

4 A Robust Fault Detection and Isolation Scheme with a Disturbance Decoupling Property 79

4.1 Introduction 80
4.2 Hybrid FDI approach 84
4.2.1 Bank of Continuous-Time Residual Generators 86
4.2.2 Residual Evaluation Criteria 92
4.2.3 DES Fault Diagnoser 94
4.3 Actuator Fault Detection and Isolation in a Network of Unmanned Vehicles 101
4.3.1 Simulation Results 103
4.4 Hybrid FDI Design for the ALTAV System 109
4.4.1 ALTAV System 109
4.4.2 Design of a Hybrid FDI Scheme for the ALTAV System 111
4.4.3 Simulation Results 115
4.5 Conclusions 125

5 Compensating for Communication Channels Effects in Fault Detection and Isolation 126

5.1 Introduction 128

5.2 The Packet Erasure Channel Model 131
5.3 A Network of Unmanned Vehicles in the Presence of Imperfect Communication Channels 134
5.4 Discrete-time Markovian Jump Systems 139
5.4.1 Unobservable and Unobservability Subspaces 140
5.4.2 Fault Detection and Isolation Based on Geometric Approach . 152
5.4.3 H_∞-based Fault Detection and Isolation Design 158
5.4.4 FDI of a Formation Flight of Satellites 162
5.5 Continuous-time Markovian Jump Systems 164
5.5.1 Unobservable and Unobservability Subspaces 167
5.5.2 Fault Detection and Isolation Based on Geometric Approach . 171
5.5.3 H_∞-based Fault Detection and Isolation Design 176
5.5.4 A Case Study 182
5.6 Conclusions 186

6 Robust Fault Detection and Isolation of Time-Delay Systems 188
6.1 Introduction 189
6.2 Retarded and Neutral Time-Delay Systems 191
6.2.1 Finite Unobservability Subspaces for Time-delay Systems . . . 191
6.2.2 H_∞-based FDI for Retarded Time-Delay Systems 194
6.2.3 H_∞-based FDI for Neutral Time-Delay Systems 200
6.3 Distributed Delay Systems 205
6.3.1 Finite Unobservability Subspace for Distributed Delay Systems 206
6.3.2 H_∞-based FDI Strategy of Distributed Delay Systems 208
6.4 FDI of Markovian Jump Systems with Time-delays 212
6.4.1 Background and Preliminary Results 212
6.4.2 Unobservability Subspace for Markovian Jump Systems with Time-delay (MJSD) 216

6.4.3 H_∞-based Fault Detection and Isolation Strategy for Markovian Jump Systems with Mode-dependent Time delays 218
6.5 Fault Detection and Isolation Decision Criteria 221
6.6 Numerical Examples 222
6.6.1 Retarded Time-Delay System 223
6.6.2 Neutral Time-Delay System 225
6.6.3 Distributed Time-delay systems 228
6.6.4 Combustion System in a Rocket Motor Chamber 232
6.6.5 Markovian Jump Systems with Mode-dependent Delay 236
6.7 Conclusions 241

7 Fault Detection and Isolation of Linear Impulsive Systems 242
7.1 Introduction 243
7.2 Unobservability Subspaces for Linear Impulsive Systems 244
7.3 Fault Detection and Isolation of Linear Impulsive Systems 247
7.4 Two Case Studies 253
7.4.1 Mass-spring system with constraint buffers 253
7.4.2 System with impulsive control 255
7.5 Conclusions 256

8 Perspectives and Future Directions of Research 258
8.1 Research Directions Considered in this Dissertation 259
8.1.1 Fault Detection and Isolation in a Network of Unmanned Vehicles: Ideal Communication Channels 259
8.1.2 Fault Detection and Isolation in a Network of Unmanned Vehicles Subject to Large Environmental Disturbances 260
8.1.3 Fault Detection and Isolation in a Network of Unmanned Vehicles with Imperfect Communication Links 261

8.1.4 Fault Detection and Isolation for Time-delay Systems 262

8.1.5 Fault Detection and Isolation for Linear Impulsive Systems . . 263

A Finite Unobservability Subspaces for Time-delay Systems 264

B Integrated Fault Detection, Isolation and Control for a Network of Unmanned Vehicles 269

B.1 Integrated Fault Detection, Isolation and Control for Networked Control Systems 270

B.2 Integrated Fault Detection, Isolation and Control for a Network of Unmanned Vehicles 271

References 274

List of Figures

1.1 Comparison between hardware and analytical redundancy schemes. . 4

1.2 Scheme for the model-based FDI. 5

1.3 Structured residual set. 7

3.1 The residuals corresponding to multiple fault scenario $r_1, ...r_6$ (centralized architecture). 63

3.2 The residuals corresponding to multiple fault scenario $r_7, ..., r_{12}$ (centralized architecture). 64

3.3 The residuals corresponding to multiple fault scenario (semi-decentralized architecture). 64

3.4 The residuals corresponding to multiple fault scenario (semi-decentralized architecture). 65

3.5 Residual outputs corresponding to the hard-over fault in the leading edge flap deflection. 68

3.6 Residual outputs corresponding to 60% loss of effectiveness in the trailing edge flap deflection. 69

3.7 Residual outputs corresponding to concurrent hard over faults in the throttle and trailing edge flap deflection. 70

3.8 Gyrostat with four reaction wheels in a tetrahedron configuration [1]. 70

3.9 Residuals corresponding to the normal mode (Healthy operation). . . 75

3.10 Residuals corresponding to a 20% loss of effectiveness in the reaction wheel #3. 75

3.11 Residual L_2 norm corresponding to the normal mode. 76

3.12 Residual L_2 norm corresponding to a 20% loss of effectiveness in the reaction wheel # 3. 76

3.13 Residual corresponding to a 40% loss of effectiveness in the reaction wheel #3 and 50% loss of effectiveness in reaction wheel #1. 77
3.14 Residuals L_2 norm corresponding to 40% loss of effectiveness in the reaction wheel #3 and 50% loss of effectiveness in the reaction wheel #1. 77

4.1 General architecture of our proposed hybrid diagnoser. 85
4.2 The transition function corresponding to Example 1. 96
4.3 Residual evaluation functions corresponding to a fault in the first actuator of the vehicle 2. 107
4.4 Fault diagnoser state corresponding to fault in the first actuator of the vehicle 2. 107
4.5 Residual evaluation functions corresponding to a 50% loss of effectiveness fault in the second actuator of the vehicle 2. 108
4.6 Fault diagnoser state corresponding to a 50 % loss of effectiveness fault in the second actuator of the vehicle 2. 108
4.7 Schematic of an Almost-Lighter-Than-Air-Vehicle (ALTAV) [2]. . . . 110
4.8 The reference trajectory (dashed line) and the ALTAV trajectory (solid line) corresponding to a healthy operation. 117
4.9 Residual evaluation functions corresponding to a float fault in the F_1 actuator (the dashed dots correspond to the threshold values $J^1_{th_i} = 6e-4, i = 1, ..., 4$ and $J^1_{th_5} = 3e-5$, the dashed lines correspond to the threshold value $J^2_{th_i} = 4.5e-3$). 119
4.10 Fault diagnoser state corresponding to a float fault in the F_1 actuator. 119
4.11 Residuals corresponding to a float fault in the F_1 actuator. 120

4.12 Residual evaluation functions corresponding to a hard over fault in the F_2 actuator (the dashed dots correspond to the threshold values $J^1_{th_i} = 6e-4, i = 1, ..., 4$ and $J^1_{th_5} = 3e-5$, the dashed lines correspond to the threshold value $J^2_{th_i} = 4.5e-3$). 121
4.13 Fault diagnoser state corresponding to a hard over fault in the F_2 actuator. 121
4.14 Residual evaluation functions corresponding to a 50% loss of effectiveness in the F_3 actuator (the dashed dots correspond to the threshold values $J^1_{th_i} = 6e-4, i = 1, ..., 4$ and $J^1_{th_5} = 3e-5$, the dashed lines correspond to the threshold value $J^2_{th_i} = 4.5e-3$). 122
4.15 Fault diagnoser state corresponding to a 50% loss of effectiveness in the F_3 actuator. 122
4.16 Residual evaluation functions corresponding to multiple faults in the F_1 and F_4 actuators (the dashed dot corresponds to the threshold values $J^1_{th_i} = 6e-4, i = 1, ..., 4$ and $J^1_{th_5} = 3e-5$, the dashed lines correspond to the threshold value $J^2_{th_i} = 4.5e-3$). 124
4.17 Fault diagnoser state corresponding to multiple faults in the F_1 and F_4 actuators. 124

5.1 The Gilbert-Elliott model 133
5.2 FDI in sensor networks 139
5.3 Residual evaluation functions corresponding to a fault in the first actuator of satellite 1. 165
5.4 Residual evaluation functions corresponding a fault in the second actuator of satellite 2. 166
5.5 Residual signal: (a) $m_2(t) = 0.1, t > 10sec$; (b) $m_1(t) = 0.1, t > 15sec$ 175

5.6 Residual signals and their evaluation functions corresponding to a float fault in the first actuator $m_1 = -u_1$ (the dashed line in J_{r_i} denotes the threshold). 185
5.7 Residual signals and their evaluation functions corresponding to a lock-in-place (LIP) fault in the second actuator $m_2 = -u_2 + 0.1$ (the dashed line in J_{r_i} denotes the threshold). 185
5.8 Residual signals and their evaluation functions corresponding to multiple faults in actuators, namely a 50% loss of effectiveness fault in the first actuator and a lock in place fault in the second actuator (the dashed line in J_{r_i} denotes the threshold). 186

6.1 Evaluation functions corresponding to multiple faults that are injected in both actuators. 224
6.2 System states corresponding to multiple faults scenario. 225
6.3 Evaluation functions corresponding to multiple faults that are injected in both actuators. 227
6.4 Residual signals and their evaluation functions corresponding to a fault in the first actuator. 232
6.5 Residual signals and their evaluation functions corresponding to concurrent faults in both actuators. 233
6.6 Residual signal and its evaluation function corresponding to the normal mode (healthy operation). 235
6.7 Residual signal and its evaluation function corresponding to a fault in the actuator. 236
6.8 Residual signals and their evaluation functions corresponding to the normal mode (healthy operation). 240
6.9 Residual signals and their evaluation functions corresponding to concurrent faults in both actuators. 240

6.10 Residual signals and their evaluation functions corresponding to an intermittent fault in the first actuator. 241

7.1 The mass-spring system. 254

7.2 The positions response of the healthy system subject to an energy-based controller. 256

7.3 Residual evaluation functions corresponding to multiple fault scenario in the actuators F_1 and F_2 (based on our proposed approach). 256

7.4 Residual evaluation functions corresponding to multiple fault scenario in the actuators F_1 and F_2 (based on the standard continuous-time approach [3]). 256

7.5 Residual evaluation functions corresponding to single fault scenario in the second impulsive actuator (based on our proposed approach). . 257

B.1 The structure of a networked control system. 271

B.2 Integrated FDI/Controller structure of a network of unmanned vehicles. 273

List of Tables

3.1 Orbital Disturbances 74

3.2 Residual threshold values 78

4.1 Finite states of the plant 95

4.2 Output map of the plant 97

4.3 Transition function of state s_0 98

4.4 Transition function of state s_D 99

4.5 Transition function of state s_i, $i \in \mathbf{k}$ 99

4.6 Transition function of states s_F, $s_{F,D}$, $s_{i,D}$ and $s_{i,j}$ 100

4.7 Transition function of Example 4.1 101

4.8 ALTAV parameters 110

4.9 Transition function of the ALTAV DES fault diagnoser 116

4.10 Output measurement noise characteristics 118

4.11 Tolerable disturbance input $\mathfrak{D}_1$ characteristics 118

5.1 The specific values for the parameters of the VTOL helicopter 183

List of Symbols and Abbreviations

AHS	Automated Highway Systems
AHS	Almost-Lighter-Than- Air-Vehicle
AUV	Autonomous Underwater Vehicle
DES	Discrete Event System
EFPRG	Extended Fundamental Problem in Residual Generation
ESA	European Space Agency
FDI	Fault Detection and Isolation
FPRG	Fundamental Problem in Residual Generation
HARV	High Angle of Attack Research Vehicle
HEFPRG	H_∞-based EFPRG
HFD	Hybrid Fault Diagnoser
LMI	Linear Matrix Inequality
lNFPRG	Locally Nonlinear FPRG
LTI	Linear Time-Invariant
MEMS	Micro-Electro-Mechanical Systems
MJS	Markovian Jump System
MJSD	Markovian Jump System with time-Delay
NCS	Networked Control System
SFDIP	Structured Fault Detection and Isolation Problem
TPF	Terrestrial Planet Finder
VTOL	Vertical Take-Off and Landing
UAV	Unmanned Aerial Vehicle
UIO	Unknown Input Observer
u.o.s.	UnObservability Subspace

Chapter 1

Introduction

1.1 Motivation

Recent technological advances have spurred a broad interest in cooperative control of systems composed of autonomous unmanned vehicles such as spacecraft, unmanned aerial vehicles, autonomous underwater vehicles, automated highway systems and multiple mobile robots. The explosion in computation and communication capabilities, the advent of miniaturization technologies such as MEMS, and the development of powerful control techniques have created numerous research interests in vehicles that can interact autonomously with environment and other vehicles to perform tasks beyond the capabilities of individual vehicles. The overambitious goal of these systems is *autonomy*, meaning the ability to accomplish the mission goals in the face of significant uncertainty and unexpected events such as faults without human intervention.

Unmanned vehicles such as unmanned aerial vehicles (UAVs) are indeed among the most complicated systems that are being developed. Since they operate in an environment subjected to a high degree of uncertainties and disturbances, the problem of precise and accurate control of such vehicles is difficult and requires complicated

control systems theory. On the other hand, with an increasing requirement for control systems to be more secure and reliable, fault tolerance in such control systems is becoming more and more critical and important.

In the presence of undesirable effects such as failures in the actuators or sensors, the vehicle control systems must be responsive and adaptive to such failures. Under these circumstances there may be a necessity to adjust the control laws to recover the vehicle from the effects of anomalies and failures. Furthermore, the required adjustments of control laws must be done expeditiously in a relatively short period of time to guarantee the operation of the safety critical subsystems of the vehicle. Specifically, it is required to develop an autonomous fault diagnosis and reconfigurable control system.

In particular for a network of unmanned vehicles, if any of the vehicles undergoes a failure and the vehicle controller is not equipped with autonomous fault tolerant capabilities, the stability of the entire network may not be maintainable and could lead to instability. Therefore, fault tolerant control systems for a network of unmanned vehicles needs to be fully investigated.

Advanced computers have resulted in more capable and advanced vehicle control systems. Thus, activities such as navigation and maneuver planning, command planning and sequencing, and fault diagnosis and recovery can all potentially be autonomously handled onboard the vehicle. Aside from the obvious cost savings realized by smaller operations staff, there are traditional advantages to placing some of these functions on the vehicle. For example, onboard fault diagnosis and recovery algorithms can detect, identify, and remedy vehicle faults, both minor and major, *in real-time*, possibly saving the mission in the process. Moreover, the ability to plan the vehicle activities onboard allows one to respond to major instrument failures or other anomalies without impacting the remaining healthy subsystems. In the event of a major anomaly, the vehicle can respond quickly and generate a new sequence

of commands to carry out the remaining possible mission objectives.

Cooperative control of networked unmanned vehicles poses many interesting challenges such as optimal control of vehicles, collision and obstacle avoidance during reconfiguration, information flow among the vehicles and development of advanced hardware such as sensors and actuators. One of the main challenges in these systems is developing autonomous cooperative control which can maintain the group behavior and mission performance in the presence of undesirable events such as failures in vehicles sensors, actuators, or other components. In order to achieve this goal, the team should have the capability of detecting and isolating faults in its vehicles and reconfigure the cooperative control algorithms to compensate for the faults. This thesis explores the *Fault Detection and Isolation (FDI)* issue in these systems.

1.2 Literature Review

1.2.1 Fault Detection and Isolation

Modern control systems are becoming increasingly more complex and issues of availability, cost efficiency, reliability, operating safety, and environmental protection concerns are receiving more attention. This requires a fault diagnosis system that is capable of detecting plant, actuator and sensor faults when they occur and of identifying and isolating the faulty component. A fault diagnosis algorithm consists of fault detection, isolation and identification steps. A traditional approach to fault diagnosis is based on the *hardware redundancy* method which uses multiple sensors, actuators, computers and software to measure or control a particular value. Typically, a voting scheme is applied to the hardware redundant system to decide if and when a fault has occurred and its likely location among redundant components. The major problems encountered with hardware redundancy are the extra equipment, maintenance cost and the additional space required to accommodate the equipment.

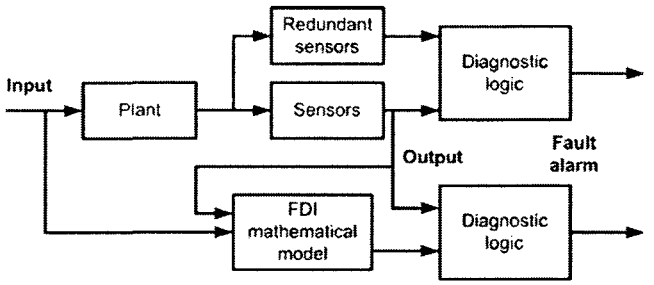

Figure 1.1: Comparison between hardware and analytical redundancy schemes.

An alternative approach for fault diagnosis is based on *analytical redundancy* which uses the redundant analytical relationships among system inputs and measured system outputs to generate residual signals where no extra hardware is required in this approach. In analytical redundancy schemes, the resulting difference generated from consistency checks of different variables is called a *residual* signal. Analytical redundancy makes uses of a mathematical model of the monitored system and is often referred to as the *model-based approach* to fault diagnosis. Figure 1.1 illustrates the concepts of hardware and analytical redundancy [4].

The principle of model-based fault detection and isolation is depicted in Figure 1.2. Model-based residual generation techniques have been categorized by Patton et al. [5–7], Basseville and Nikiforov [8], Gertler [9] as **a)** observer-based approach, **b)** parity equation, and **c)** identification and parameter estimation.

In observer or filter-based approaches, the outputs of the system are estimated from the measurements (or subset of measurements) by using either Luenberger observers in the deterministic setting [10–22] or Kalman filters in a stochastic setting [8, 23–28]. Then the weighted output estimation error (or innovations in the stochastic case) is used as a residual. The flexibility in selecting observer gains has been fully utilized in the literature yielding a rich variety of FDI schemes. The increasing popularity of state-space models as well as the wide usage of observers in modern control theory and applications have made the observer-based FDI approach as one of the most common approaches in this domain. In parity space

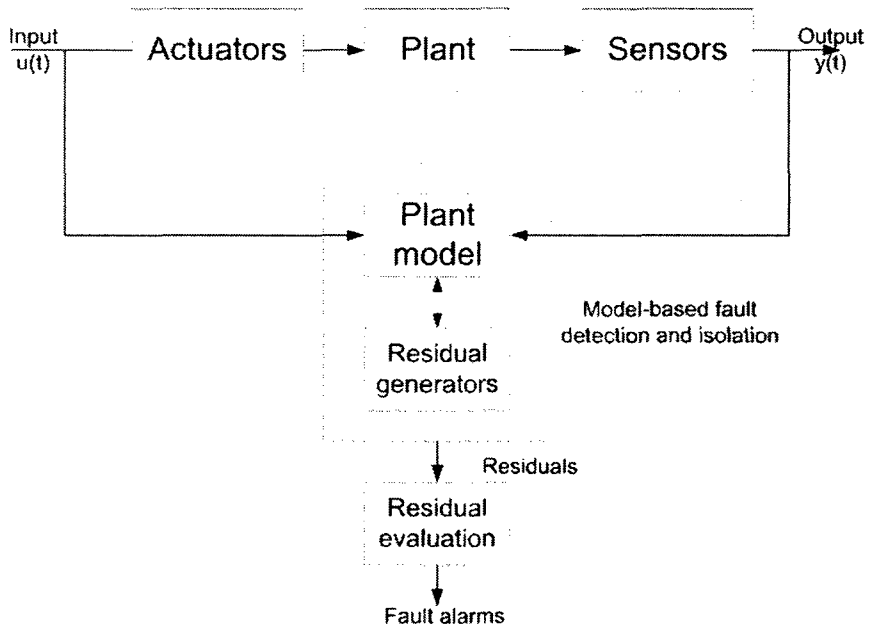

Figure 1.2: Scheme for the model-based FDI.

approach [9, 29–32] residual signals (or parity vector) are generated based upon consistency checks on system input and output data over a given time window. It has been shown that there exists some correspondence between observer-based and parity relation approaches [5, 33–35]. In other words, the parity relation approach is equivalent to the use of a dead-beat observer and a residual signal generated by a non dead-beat observer is equivalent to a post-filtered residual generated by a dead-beat observer. This implies that the parity space method provides less design flexibility when compared with methods which are based on observers without any restriction [6].

Parameter estimation method [36–38] is developed based on system identification techniques. In this approach, the faults are reflected in the physical system parameters such as friction, mass, viscosity, resistance, inductance, capacitance, etc. The basic idea of the detection method is that the parameters of the actual process are estimated on-line using well-known parameter estimation methods and the results are compared with the parameters of the reference model obtained initially

under the fault-free condition. It should be pointed out that a typical limitation on parameter estimation-based approaches is the fact that the input signal should be persistently exciting. This condition is satisfied if the input signal provides enough information to estimate the parameters. However, many industrial systems may not allow feeding such persistently exciting signals as inputs [39].

The successful fault detection of a fault is followed by the fault isolation procedure which will isolate a particular fault from others. While a single residual signal is sufficient to detect faults, a set of residuals is usually required for fault isolation. One way to fulfill the fault isolation task is to design a set of structured residuals. Each residual is designed to be sensitive to a subset of faults, whilst remaining insensitive to the other faults. The residual set which has the required sensitivity to specific faults and insensitivity to other faults is known as the *structured residual set* [40]. The design procedure consists of two steps [6]. The first step is to specify the sensitivity and insensitivity relationships between residuals and faults according to the assigned isolation task, and the second step is to design a set of residual generators according to the desired sensitivity and insensitivity relationships. In the second step different residual generation techniques such as observer-based or parity space approaches can be used for designing a residual set. The main advantage of the structured residual set is that the diagnostic analysis is simplified to determining which of the residuals have exceeded their thresholds. Several special residual schemes have been suggested in the literature [3, 5, 41]. In the dedicated residual set [3], all faults can be detected simultaneously, however it is difficult to design such residual sets for many practical systems, and generally there are no design degrees of freedom to achieve other desirable performance specifications and requirements such as robustness against uncertainty and modeling errors. More importantly, the necessary condition for designing such a residual set is *independence* of the fault signatures. In [5], a generalized residual set is introduced which can only detect a single

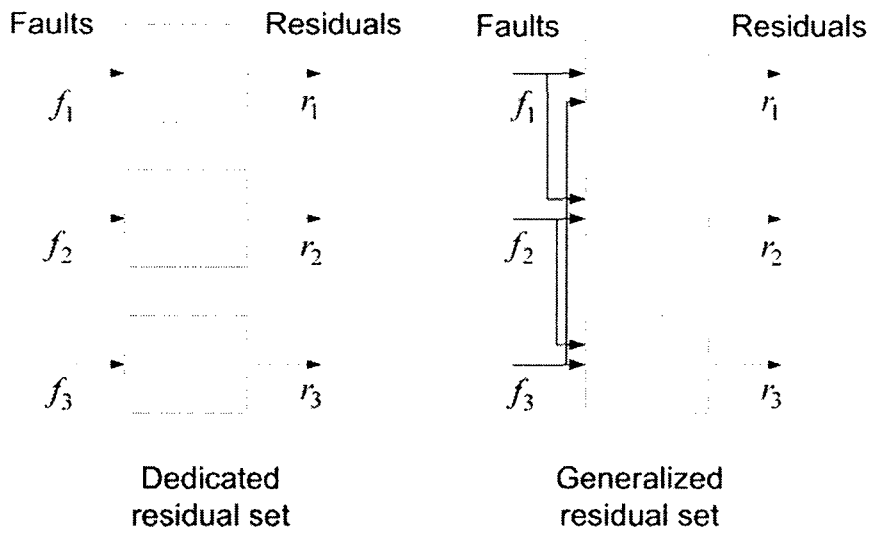

Figure 1.3: Structured residual set.

fault although it has design degree of freedom for achieving robustness against uncertainty and modeling errors. Figure 1.3 depicts the above two different structured residual sets for isolating three different faults $\{f_1, f_2, f_3\}$.

An alternative way of achieving the isolability of faults is to design a *directional* residual vector [10–13] which in response to a particular fault, a residual vector lies in a fixed and fault-specified direction in the residual space. With fixed directional residual vector, the fault isolation problem is to determine which of the known fault signature directions the generated residual vector lies the closest to. The solvability conditions for generating a structured residual set are generally more relaxed when compared to the directional residual vector since in the later approach, the design objective is to generate one residual vector with the above isolability condition while in the former approach a set of residuals is generated and one may have more design degree of freedom [12].

Recent years have witnessed a strong interest and considerable research activities on the design and analysis of FDI schemes for nonlinear systems [6, 39, 42, 43].

Most techniques in the literature constitute direct extension of the approaches described above for linear systems. In [44], an extension of the parity space approach to nonlinear polynomial dynamic systems is proposed. Parity relation for a more general class of nonlinear systems was proposed in [45]. In [46], the concept of the parity relation and parameter estimation fault detection techniques are combined for nonlinear systems. Many observer-based FDI approaches have also been developed in the literature for solving nonlinear system FDI problem [47, 48]. The unknown input observer approach was extended to include nonlinear terms in [49–51]. Adaptive nonlinear observer based FDI scheme was proposed in [52, 53], and sliding mode observers have been designed in [54–58] for nonlinear FDI problem. Persis and Isidori [59, 60] have extended Massoumnia's method [3, 12] to nonlinear systems. They showed that the problem of fault detection and isolation for nonlinear systems is solvable if and only if there is an unobservability distribution that leads to a quotient subsystem which is unaffected by all faults but one. In [61] the result of [60] is extended to a more realistic situation when measurement noise is present in the state affine system. Furthermore, the approach was extended to a special class of nonlinear systems. Hammouri et. al. [62] addressed the problem of fault detection and isolation for bilinear systems using the same geometric approach. In [63] the nonlinear geometric approach was successfully applied to a nonlinear longitudinal model of an aircraft subject to various types of actuator faults.

Model-based fault diagnosis approaches relay on the key assumption that a perfectly accurate and complete mathematical model of the system under supervision is available. However, such assumption may not always be valid in practice. This problem has contributed to the rapid development of soft computing-based FDI methods [64]. Generally, the most popular soft computing techniques that are used in the FDI framework can be divided into three groups [39]: **a)** neural

networks [64–73], **b)** Fuzzy logic-based techniques [64], and **c)** Evolutionary algorithms [66, 74, 75].

In this thesis, we adopt the model-based FDI approach based on structured residual set concept and the geometric FDI approach [3,60] is considered as the main methodology of this dissertation. In general, a primary advantage of geometric-type techniques is the formulation of the results in terms of very simple and intuitive concepts that gives the feeling of problems not being masked by heavy, complex mathematics and they are easily reduced to matrix arithmetic as soon as one needs to compute them. Moreover, as it will be shown in this thesis, FDI problem for linear and nonlinear systems can be tackled in one framework.

1.2.2 Network of Unmanned Vehicles

Research in the cooperative control of vehicles is currently progressing in multiple directions and domains. Some examples are discussed in the paragraphs below.

Spacecraft Formation Flight: In recent years, there has been increased research interest in the formation control of spacecraft [76–83]. The use of multiple spacecraft has the potential to expand functionality, performance and reduce operational cost. For instance, a formation of interferometric imaging spacecraft can achieve an optical imaging system with an aperture of kilometers giving the resolution required to image planets in the other solar systems. Many space missions planned for the upcoming decades such as NASA's terrestrial planet finder (TPF) [84], ESA Darwin project [85] involve spacecraft formations.

Unmanned Aerial Vehicles: Advances in avionics and flight control techniques have led unmanned aerial vehicle (UAV) technology to a point where it is routinely used in commercial and military applications. These advances have renewed a lot of research interest in UAV cooperative control. Applications of this technology include coordinated rendezvous of UAV [86–88], cooperative forest fire

surveillance [89], cooperative search [90–92], and drag reduction via close formation flight [93–97].

Autonomous Underwater Vehicles: Over the last decade, numerous research and development activities have occurred in the area of autonomous underwater vehicles (AUVs) where they have been used in commercial, scientific and military applications [98]. Recently, researchers have turned to AUV formations to accomplish more challenging tasks. Potential applications of AUV formations include oceanographic surveying at deep sea [99], operations under ice for exploration of Arctic areas and efficient monitoring sub-sea oil installations [100].

Automated Highway Systems: In the last two decades, there has been a lot of research in automated highway systems (AHS) and new advances in computation and machine vision are bringing this technology closer to completion [101, 102].

Multiple Mobile Robots: Coordinated control of land mobile robots has been investigated in last decade [103–106]. Cooperative robots can be used to perform tasks that are too difficult for a single robot to perform alone. For example, a group of robots can be used to move large awkward objects [107, 108] , or to move a large number of objects [109]. Moreover, groups of robots can be used for terrain model acquisition [109], planetary exploration [110], or measuring radiation levels over a large area [111]. In [112], a group of robots are used for path obstruction.

While each of the above areas has its own unique challenges, several common themes can be found [113,114]. In most cases, the vehicles are *dynamically decoupled* which implies that the motion of one does not directly affect the others. However, the vehicles are coupled through the goal they are trying to achieve. Each vehicle, through its sensors or communication links has limited information about the other vehicles which may be subjected to uncertainty and information transmission delays. The interactions between the vehicles motions make the network of vehicles an interconnected dynamic system whose behavior depends not only on the individual

vehicles dynamics, but also on the nature of their interactions.

In recent years, only a few results on fault tolerant cooperative control of unmanned vehicle systems have been developed. In [115], a software architecture was developed to facilitate the fault tolerant cooperative control of teams of heterogenous mobile robots. In this architecture, if a robot fails, it cannot necessarily communicate its failure to its teammate and behavior-based fault detection approach was used to detect the failure in the robots. In this approach, each robot knows the tasks of other robots and if the specific task has not been completed in certain interval, this will be interpreted as a failure in the corresponding robot.

A conversation protocol for failure detection is proposed in [116] where the robots can communicate with each other and send their faulty status to other robots. A fault tolerant algorithm is developed in [117] for the formation flight of UAVs in the presence of a failure of one or more of UAVs. In this approach, it is assumed that the communication channel faults can be detected by the UAVs and the algorithm was proposed to reconfigure the formation according to the type of the fault.

In [118] a decentralized fault detection filter is designed as a combination of a game theoretic fault detection filter [18] with the decentralized filtering introduced in [119]. The approach is applied to a platoon of cars in an advanced vehicle control system. In [120], a decentralized detection filter for a large homogeneous collection of LTI systems is developed, with inspiration from platoons of vehicles with typical "look-ahead" structure. Recently in [121] a distributed, model-based, qualitative fault diagnosis scheme in developed for multi robots formation.

1.3 General Problem Statement

The main objective of this thesis is to explore the fault detection and isolation issues in networked multi-vehicle systems. These systems can be modeled as interconnected dynamical systems whose behavior depends not only on the individual vehicle dynamics, but on the nature of their interaction. FDI is one of the main challenges in autonomous network of unmanned vehicles. In this dissertation, we first investigate the development of and comparison among three different FDI architectures for a network of unmanned vehicles, namely, centralized, decentralized and semi-decentralized.

Each FDI architecture has its own challenges. In the centralized scheme, all the information is sent to a central FDI unit through communication network channels. Conceptually, the FDI algorithms used are similar to those for a single system and hence relatively simple. However, the effects of communication channels such as data dropout and time delay have a negative impact on the performance of FDI algorithms that should be investigated. In a decentralized scheme, all the information is processed locally and there is no central processing unit. In this scheme, FDI problem should be solved locally at each vehicle on the basis of local observations, commands and information communicated from neighboring vehicles. The FDI solvability condition will be investigated in this thesis for the centralized, decentralized and semi-decentralized architectures and the comparison will be made among them.

One of the main challenges in the design of FDI algorithms is to distinguish the effect of disturbances from faults and develop a robust FDI scheme without comprising the detection of incipient faults in the vehicles. In unmanned vehicles such UAV's, this problem is more challenging due to the small size feature and more sensitivity of them with respect to disturbances such as wind gust. In this thesis, we investigate development and design of robust hybrid FDI approach for both linear and nonlinear systems to tackle this problem.

In this thesis, the FDI problem for time-delay systems as well as linear impulsive systems are also investigated. A great deal of attention has recently been devoted to time-delay systems. However, only few results on FDI of time-delay systems have been developed in the literature [122–129]. It should be emphasized that the presently available FDI algorithms in the literature cannot generate the structured residual signals for time-delay systems. In these algorithms [124–129], faults that one needs to be decoupled are considered as unknown inputs and the algorithms seek to attenuate the effects of faults on the residual. Therefore, these types of algorithms cannot decouple fault effects from the residuals. In this dissertation, we investigate design of FDI algorithms for retarded, neutral, distributed delay and stochastic time-delay systems based on the geometric approach.

Another research area that has witnessed a great deal of interest in the last decade is in modeling and control of hybrid systems. A subclass of hybrid systems are impulsive dynamical systems in which the states behave according to a continuous-time dynamics and which are also subjected to time-driven or event-driven impulsive effects where the states of the system are changed instantaneously. In the past few years research has been conducted on stability, controllability and observability of these systems. However, no FDI results have been reported for linear impulsive systems. In the last part of the thesis, we try to develop a fault detection and isolation scheme for linear impulsive systems based on the geometric approach.

1.4 Contributions of the Thesis

The main contributions of this thesis are as follows.

- **Fault detection and isolation (FDI) of systems with dependent fault signatures**

  Motivated by the FDI problem in a network of unmanned vehicles, we study

systems with dependent fault signatures. For many classes of dynamical systems such as overactuated systems, fault signatures are generally dependent. This fault signature dependency may arise due to redundant actuators or coupling effects among sensors, actuators and plant faults. The first contribution of this thesis is in the development, design, and analysis of fault detection and isolation schemes for systems with dependent fault signatures.

- **FDI for a network of unmanned vehicles with relative state measurements corresponding to three architectures, namely, centralized, decentralized and semi-decentralized**

  Our proposed structured residual set is applied to the problem of actuators fault detection and isolation in a multi-vehicle system. Three different architectures, namely centralized, decentralized and semi-decentralized, are investigated for solving this problem and the necessary and sufficient solvability conditions for centralized and semi-decentralized architectures are derived based on the dynamics of each vehicle. Moreover, it is shown that the FDI problem does not have a solution for the decentralized architecture.

- **Robust hybrid FDI scheme for systems subject to large disturbances**

  A robust hybrid FDI scheme is developed for systems that are subject to large disturbances. A hybrid architecture is composed of a bank of continuous-time residual generators and a discrete-event system (DES) fault diagnoser. The main advantage of the proposed FDI algorithm in comparison with previous works in the literature is that our algorithm is capable of distinguishing the effects of disturbances and incipient faults without imposing any limitation on the number of detectable faults in the system.

- **Fault detection and isolation of Markovian jump systems**

  A geometric FDI framework is developed for both discrete-time and continuous time Markovian Jump Systems (MJS). A new geometric unobservable subspace property is derived for MJS systems and the notion of unobservability subspaces is introduced for these systems. The necessary and sufficient conditions for solvability of the fundamental problem of residual generation (FPRG) are derived for both discrete-time and continuous-time MJS systems. We also present and develop sufficient conditions for designing H_∞-based FDI algorithms for MJS systems subject to input disturbances.

- **FDI for a network of unmanned vehicles in the presence of imperfect communication channels**

  By combining a packet erasure channel model of each communication channel and the vehicle dynamics yields a discrete-time Markovian jump system. Our proposed FDI algorithm for discrete-time Markovian jump systems is then applied for solving the FDI problem in a network of unmanned vehicles in the presence of imperfect communication links.

- **FDI of time-delay systems: a geometric approach**

  Fault detection and isolation algorithms are developed for broad classes of time-delay systems, namely, retarded, neutral, distributed and stochastic. A geometric framework is developed for solving the FDI problem in time-delay systems based on our developed results for Markovian jump systems. A robust H_∞-based FDI algorithm is proposed for each class of the time-delay systems.

- **FDI of linear impulsive systems**

  We consider the problem of fault detection and isolation for linear impulsive systems and it is shown that the notion of unobservability subspaces and its corresponding algorithms developed for MJS systems is also applicable

to linear impulsive systems. Based on this fact, the necessary and sufficient conditions for the FPRG in linear impulsive systems are developed and derived.

To summarize, the contributions of this dissertation provide the first step towards the design of fault tolerant control systems for a network of unmanned vehicles by developing new fault detection and isolation schemes. We tackle different issues in these systems such as different FDI architectures, robustness to external disturbances and compensating the effects of communication channels in the framework of Markovian jump systems. Moreover, it is shown that our proposed FDI algorithm for Markovian jump systems can be utilized for solving FDI problems for other classes of systems such as time-delay and linear impulsive systems.

1.5 Organization of the Thesis

We begin in Chapter 2 with the brief review of Structured Fault Detection and Isolation (SFDIP) for both linear and nonlinear systems. A geometric FDI framework for solving the SFDIP problem is presented for linear and nonlinear systems in Sections 2.2 and 2.3, respectively.

In Chapter 3, we focus on the problem of fault detection and isolation in a network of unmanned vehicles without considering the effect of communication channels. It is shown in Section 3.1 that the actuator fault signatures in a network of unmanned vehicles with relative state measurements are dependent and the entire network can be considered as an overactuated system. This motivate us to develop a novel coding scheme applicable to systems with dependent fault signatures. Moreover, it is shown in Section 3.1.2 that the FDI problem for a network of unmanned vehicles does not have a solution for the decentralized architecture and vehicles need to exchange information. We tackle the FDI problem in a network of unmanned vehicles corresponding to centralized and semi-decentralized architectures in Sections

3.3.1 and 3.3.2, respectively. The necessary and sufficient conditions for solvability of the FDI problem are derived for centralized and semi-decentralized architectures. Our proposed FDI scheme is applied to the actuator FDI problem in the formation flight of satellites in Section 3.3.3. To show the applicability of our proposed structured residual set, two other case studies, namely, F18-HARV and a satellite with redundant reaction wheels are also presented in Sections 3.4 and 3.5, respectively.

In Chapter 4, a network of unmanned vehicles subject to large environmental disturbances is considered and a hybrid FDI scheme is developed to achieve robustness with respect to external disturbances. A hybrid architecture for a robust FDI is introduced in Section 4.2 that is composed of a bank of continuous-time residual generators and a DES fault diagnoser. Moreover, our proposed hybrid FDI algorithms are developed for both linear and nonlinear systems. Our developed hybrid scheme is applied to a network of unmanned vehicles and an Almost-Lighter-Than-Air-Vehicle (ALTAV) in Sections 4.3 and 4.4, respectively.

In Chapter 5, we consider the effects of communication channels on fault detection and isolation. In Section 5.2, a communication channel is modeled using the packet erasure model. By combining the vehicle dynamics and the channel packet erasure model a discrete-time Markovian jump model is obtained for the "entire" network. This motivate us to investigate the FDI problem for both discrete-time and continuous-time Markovian Jump Systems (MJS) in Sections 5.4 and 5.5, respectively and a novel geometric framework is introduced for solving this problem. We then apply our proposed algorithm to two case studies, namely, formation flight of satellites in the presence of imperfect communication links in Section 5.4.4 and VTOL (vertical take-off and landing) helicopter in Section 5.5.4.

In Chapter 6, we focus on the fault detection and isolation for broad classes of time-delay systems, namely, retarded, neutral, distributed and stochastic systems in Sections 6.2.2, 6.2.3, 6.3 and 6.4, respectively. In this chapter, we show how

our proposed notion of unobservability subspaces for Markovian jump systems in Chapter 5 can be invoked for time-delay systems. In this chapter, the notion of finite unobservability subspaces are introduced for different types of time-delay systems and an H_∞-based FDI algorithm is developed for each of them.

In Chapter 7, we consider another important class of systems, namely linear impulsive systems and show in Section 7.2 that similar to the notion of unobservability for Markovian jump system, the same can be defined for linear impulsive systems. Consequently, the developed algorithm in Chapter 5 can be invoked for constructing unobservability subspaces for linear impulsive systems. Based on our developed geometric approach, the necessary and sufficient conditions for solvability of the fundamental problem of residual generation are derived in Section 7.3. Two case studies, namely mass-spring system with buffer constraint and systems with impulsive control are considered in Section 7.4 to show the effectiveness of our proposed FDI algorithm.

In the final Chapter 8, we outline future research directions in which more research is needed to be conducted.

1.6 Notation

The following notation is used throughout this dissertation. Script letters $\mathcal{X}, \mathcal{U}, \mathcal{Y}, ..$ denote real vector spaces. Matrices and linear maps are denoted by capital italic letters $A, B, C, ...$; the same symbol is used both for a matrix and its map; the zero space and zero vectors are denoted by 0. $\mathcal{B} = \text{Im } B$ denotes the image of B; Ker C denotes the kernel of C. The spectrum of A is denoted by $\sigma(A)$. A set Λ is said to be symmetric if $\lambda \in \Lambda$ implies $\lambda^* \in \Lambda$ where $*$ denotes the complex conjugate. For any positive integer k, $\mathbf{k}$ denotes the finite set $\{1, 2, \cdots, k\}$. If a map C is epic (onto), i.e. the matrix representation of C has full row rank), then C^{-r} denotes

the right inverse of C(i.e., $CC^{-r} = I$). A subspace $\mathcal{S} \subseteq \mathcal{X}$ is termed A-invariant if $A\mathcal{S} \subseteq \mathcal{S}$. For A-invariant subspace $\mathcal{S} \subseteq \mathcal{X}$, $A : \mathcal{S}$ denotes the restriction of A to $\mathcal{S}$, and $A : \mathcal{X}/\mathcal{S}$ denotes the map induced by A on the factor space $\mathcal{X}/\mathcal{S}$. For a linear system (C, A, B), $<$ Ker $C|A>$ denotes the unobservable subspace of (C, A). $\otimes$ denotes the Kronecker product of matrices and for a given matrix A, A^N denotes $I_N \otimes A$ where I_N is $N \times N$ identity matrix. For a given set $\mathbf{n}$, a *combination* is an unordered collection of the elements of $\mathbf{n}$ and is a subset of $\mathbf{n}$. The order of the elements in a combination is not important and the elements cannot be repeated. $C(n, k)$ denotes a number of k combinations (k-subset) of $\mathbf{n}$ which is equal to $\frac{n!}{k!(n-k)!}$. We denote by $||.||$ the standard norm in $\mathbb{R}^n$ and $\mathfrak{L}_2$ denotes the set of L_2 norm bounded signals. The symbol $*$ within a matrix represents the symmetric term of the matrix. For a given set N, $|N|$ denotes the cardinality of N.

A *directed graph* $\mathcal{G}$ consists of a set of vertices, or nodes, denoted $\mathcal{V}$ and a set of arcs $\mathcal{A} \subset \mathcal{V}^2$, where $a = (v, w) \in \mathcal{A}$ and $v, w \in \mathcal{V}$. A directed graph is called weakly connected if there exist a path between every pair of distinct vertices ignoring the direction of arcs.

Chapter 2

Geometric Approach to Fault Detection and Isolation

In this chapter, we briefly review a structured fault detection and isolation problem (SFDIP) for both linear and nonlinear systems based on geometric approaches that are developed in [3] and [60].

This chapter is organized as follows. In Section 2.1 the Structured Fault Detection and Isolation Problem (SFDIP) is presented. The geometric FDI framework for linear and nonlinear systems are then reviewed in Sections 2.2 and 2.3, respectively. In 2.4, common actuator fault modes that we consider in this thesis are presented.

2.1 Structured Fault Detection and Isolation

In this section, the structured fault detection and isolation problems for both linear and nonlinear systems are reviewed. As pointed out in Chapter 1, the structured residual set is one of the common way for fulfilling the fault isolation task and it has more design degrees of freedom with respect to other approaches such as directional residual vector. The design procedure consists of two steps [6], the first step is to specify the sensitivity and insensitivity relationships between residuals

and faults according to the assigned isolation task, and the second step is to design a set of residual generators according to the desired sensitivity and insensitivity relationships. In the second step different residual generation techniques such as observer-based or parity space approach can be used for designing a residual set. In this thesis, we adopt the geometric FDI approach for designing the residual generators which will be discussed in Sections 2.2 and 2.3.

Consider the following linear time-invariant system

$$\begin{aligned} \dot{x}(t) &= Ax(t) + Bu(t) + \sum_{i=1}^{k} L_i m_i(t) \\ y(t) &= Cx(t) \end{aligned} \tag{2.1}$$

and the nonlinear system

$$\begin{aligned} \dot{x}(t) &= f(x(t)) + g(x(t))u(t) + \sum_{i=1}^{k} l_i(x(t)) m_i(t) \\ y(t) &= h(x(t)) \end{aligned} \tag{2.2}$$

where $x \in \mathcal{X}$ is the state of the system with dimension n, $u \in \mathcal{U}, y \in \mathcal{Y}$ are input and output signals with dimensions m and q, respectively, $m_i \in \mathcal{M}_i$ are fault modes with dimension k_i and L_i's ($l_i(x)$) are fault signatures.

The fault modes together with the fault signatures may be used to model the effects of actuator faults, sensor faults (for linear systems only) and system faults on the dynamics of the system. For modeling a fault in the i-th actuator, L_i ($l_i(x)$) is chosen as the i-th column of matrix B ($g(x)$) and the fault mode m_i is chosen to model the type of a fault. For example a complete failure of an actuator can be represented and modeled by $m_i = -u_i$. A system fault can be represented by a potential variation in the parameters of the matrix A for linear system (2.1) as shown below:

$$\begin{aligned} \dot{x}(t) &= (A + \Delta A)x(t) + Bu(t) \\ y(t) &= Cx(t) \end{aligned} \tag{2.3}$$

As an example, a change in the i-th row and the j-th column element of the matrix A can be modeled according to [6]:

$$\Delta A x(t) = I_i \Delta a_{ij} x_j(t).$$

where x_j is the j-th element of the vector x and I_i is the n-dimensional vector with all zero elements except a 1 in the i-th element. Defining a signal $m_i(t) \triangleq \Delta a_{ij} x_j(t)$ as an external input and fault signature $L_i = I_i$, then equation (2.3) can be rewritten as:

$$\begin{aligned} \dot{x}(t) &= Ax(t) + Bu(t) + L_i m_i(t) \\ y(t) &= Cx(t) \end{aligned}$$

Similarly, a system fault for nonlinear system (2.2) can be represented by a potential variation in the parameters of the vector field $f(x)$.

It should be noted that sensor faults can initially be modeled as additive inputs in the measurement equation

$$y(t) = Cx(t) + \sum_{j=1}^{q} E_j n_j(t) \tag{2.4}$$

where E_j is an $q \times 1$ unit vector with a one at the j-th position and $n_j \in \mathbb{R}$ is a sensor fault mode, which correspond to a fault in the j-th sensor. For example a complete failure of the j-th sensor can be represented and modeled by $n_j(t) = -c_j x(t)$ where c_j is the j-th row of the matrix C. The sensor fault signature can also be modeled as an input to the system [3,18,130]. Following [18], let f_j be the solution to $E_j = Cf_j$. The new states can be defined according to $\bar{x} = x + \sum_{j=1}^{q} f_j n_j$, where the state space representation for the new states can be written as

$$\begin{aligned} \dot{\bar{x}}(t) &= A\bar{x}(t) + Bu(t) + \sum_{j=1}^{q} L_j m_j(t) \\ y(t) &= C\bar{x}(t) \end{aligned} \tag{2.5}$$

where $L_j = \begin{bmatrix} f_j & Af_j \end{bmatrix}$ and $m_j(t) = \begin{bmatrix} \dot{n}_j(t) & -n_j(t) \end{bmatrix}^{\top}$.

The Structured Fault Detection and Isolation Problem (SFDIP) as introduced in [3], [40] is defined formally as design of a dynamic residual generator that takes the observables $u(t)$ and $y(t)$ as inputs and generates a set of residual signals $r_i(t), i \in \mathbf{p}$ with the following properties.

1. When no failure is present, all the residuals $r_i(t)$ decay asymptotically to zero.

2. The residuals $r_i(t)$ for $i \in \Omega_j$ are affected by a fault of the j-th component, and the other residuals $r_\alpha(t)$ for $\alpha \in \mathbf{p} - \Omega_j$ are decoupled from this fault.

The prespecified family of *coding sets* $\Omega_j \subseteq \mathbf{p}, j \in \mathbf{k}$ should be chosen such that, by knowing which of the $r_i(t)$ are zero and which are not, we can uniquely identify the fault. The resulting residual set which has the corresponding required sensitivity to specific faults and insensitivity to other faults is known as the *structured residual set* [40]. For detecting all possible faults in the system, no coding set should be empty. The minimum requirement for fault isolation is that all coding sets be distinct. Coding sets satisfying these two requirements are defined as *weakly isolating* .

Definition 2.1 ([40]). *The weakly isolating coding sets $\Omega_i, i \in \boldsymbol{k}$ are defined as being* strongly isolating *if for each $i, j \in \boldsymbol{k}$, $i \neq j$*

$$\Omega_i \nsubseteq \Omega_j \tag{2.6}$$

A strongly isolating coding set prevents incorrect fault detection when some of the residuals in Ω_i do not exceed the respective thresholds while the others do.

In the Extended Fundamental Problem of Residual Generation (EFPRG) introduced in [3] for linear systems and in the nonlinear fundamental problem in residual generation (lNFPRG) introduced in [60] for nonlinear system, the coding set of $\Omega_i = \{i\}$ was chosen. This coding set is also called a *dedicated residual set* [6] which is inspired by the dedicated observer scheme that was proposed by Clark [131]

(Figure 1.3). In this coding scheme, one looks to design a set of filters which generates k residuals $r_i(t), i \in \mathbf{k}$ such that a fault in the i-th component $m_i(t) \neq 0$ can only affect the residual $r_i(t)$ and no other residuals $r_j(t)(i \neq j)$. With this coding scheme one can detect and isolate all faults simultaneously. Another commonly used scheme in designing the residual set is to make each residual sensitive to all but one fault which is known as a *generalized residual set* [5]. By utilizing this residual set one cannot simultaneously detect and isolate faults in two or more channels.

Once the residual signals are generated according to given coding sets $\Omega_i, i \in \mathbf{k}$, the final step for performing fault detection and isolation is to determine the threshold values J_{th_i} and the evaluation functions $J_{r_i}(t)$. Various evaluation functions have been introduced in [132] as follows:

- Instantaneous value of the residual signal, i.e. $J_{r_i} = r_i$.
- The average value of the residual signal over a time interval $[t-T, t]$, i.e.

$$J_{r_i} = ||r||_a = \frac{1}{T}\int_{t-T}^{t} r(\tau)d\tau \tag{2.7}$$

- Root-mean-square (RMS) which measures the average energy over a time interval $(0, T)$, i.e.,

$$J_{r_i} = \Big(\frac{1}{T}\int_{0}^{T} ||r(\tau)||^2 d\tau\Big)^{1/2} \tag{2.8}$$

- Truncated RMS which measures the average energy over a time interval $[t-T, t]$, i.e

$$J_{r_i} = \frac{1}{T}\int_{t-T}^{t} ||r(\tau)||^2 d\tau \tag{2.9}$$

The threshold value for each of the above residual evaluation functions can be selected as

$$J_{th_i} = \sup_{m_i=0, d\in\mathfrak{D}} J_{r_i} \tag{2.10}$$

where d represents the input disturbance or measurement noise and $\mathfrak{D}$ denotes the set of allowable disturbances, for instance, $\mathfrak{D} = \mathfrak{L}_2$ or $\mathfrak{D}$ can be selected as a set of Gaussian white noise. Based on the thresholds and the evaluation functions, the occurrence of a fault can then be detected and isolated by using the following decision logic

$$J_{r_j}(t) > J_{th_j}, \quad \forall j \in \Omega_i \Longrightarrow m_i \neq 0, \quad i \in \mathbf{k} \tag{2.11}$$

2.2 Geometric Approach to FDI of Linear Systems

In this section the geometric approach that was introduced in [3] for the SFDIP of linear systems is reviewed. In general, a primary advantage of geometric-type techniques is the formulation of the results in terms of very simple and intuitive concepts that gives the feeling of problems not being masked by heavy, complex mathematics and they are easily reduced to matrix arithmetic as soon as one needs to compute them. In the geometric approach to fault detection and isolation certain subspaces play a central role.

Definition 2.2 ([133]). *A subspace $\mathcal{W}$ is a (C, A)-invariant subspaces (conditioned invariant) if $A(\mathcal{W} \cap Ker\ C) \subseteq \mathcal{W}$.*

It is simple to show that $\mathcal{W}$ is (C, A)-invariant if and only if there exists a map $D : \mathcal{Y} \rightarrow \mathcal{X}$ such that $(A + DC)\mathcal{W} \subseteq \mathcal{W}$. The set of all (C, A)-invariant subspaces containing a given subspace $\mathcal{L} \subseteq \mathcal{X}$ is denoted by $\mathfrak{W}(A, C, \mathcal{L})$. It can be shown that $\mathfrak{W}(A, C, \mathcal{L})$ is closed under intersection and nonempty ($\mathcal{X} \in \mathfrak{W}(A, C, \mathcal{L})$); therefore, it admits an infimum, the *minimal (C, A)-invariant containing $\mathcal{L}$*, which will be denoted by $\mathcal{W}^* = \inf\ \mathfrak{W}(A, C, \mathcal{L})$. The following algorithm [133] can be used for finding $\mathcal{W}^*$.

Algorithm 2.1 ([133]). *Subspace $\mathcal{W}^*$ coincides with the last term of the sequence*

$$\mathcal{Z}_0 = \mathcal{L}$$
$$\mathcal{Z}_i = \mathcal{L} + A(\mathcal{Z}_{i-1} \cap \ Ker\ C), \quad (i \in \boldsymbol{k})$$

where the value of $k \leq n$ is determined by condition $\mathcal{Z}_{k+1} = \mathcal{Z}_k$.

The dual of the (C, A)-invariant subspace is the (A, B)-invariant (controlled invariant), which is defined as follows:

Definition 2.3 ([133, 134]). *A subspace $\mathcal{V} \subseteq \mathcal{X}$ is said to be (A, B)-invariant (controlled invariant) if*

$$A\mathcal{V} \subseteq \mathcal{V} + Im\ B \tag{2.12}$$

Similarly, the set of all (A, B)-invariants contained in a given subspace $\mathcal{E}$ (denoted by $\mathfrak{V}(A, B, \mathcal{E})$)is closed under the subspace addition operator and nonempty, hence, it admits a supermum, which is denoted by $\mathcal{V}^* = \max \mathfrak{V}(A, B, \mathcal{E})$. The following algorithm [133] can be used for finding $\mathcal{V}^*$.

Algorithm 2.2 ([133]). *Subspace $\mathcal{V}^*$ coincides with the last term of the sequence*

$$\mathcal{Z}_0 = \mathcal{E}$$
$$\mathcal{Z}_i = \mathcal{E} \cap A^{-1}(\mathcal{Z}_{i-1} + ImB), \quad (i \in \boldsymbol{k})$$

where the value of $k \leq n$ is determined by condition $\mathcal{Z}_{k+1} = \mathcal{Z}_k$.

Next, some specific subclass of (C, A)-invariants is introduced.

Definition 2.4 ([133]). *Let $\mathcal{S}$ be a (C, A)-invariant subspace containing a subspace $\mathcal{L} \subseteq \mathcal{X}$, $\mathcal{S}$ is said to be self-hidden with respect to $\mathcal{L}$ if*

$$\mathcal{S} \subseteq \mathcal{W}^* + \ Ker\ C \tag{2.13}$$

where $\mathcal{W}^* = \inf\ \mathfrak{W}(A, C, \mathcal{L})$.

It can be shown that the class $\Psi_{(C,\mathcal{L})}$ of (C, A)-invariants self-hidden with respect to $\mathcal{L}$, i.e.

$$\Psi_{(C,\mathcal{L})} = \{\mathcal{S} \ : \ A(\mathcal{S} \cap \text{Ker } C) \subseteq \mathcal{S}, \mathcal{L} \subseteq \mathcal{S}, \mathcal{S} \subseteq \mathcal{W}^* + \text{Ker } C\} \tag{2.14}$$

is closed under the subspace addition and hence it has the supremum element which can be found by the following lemma.

Lemma 2.1 ([133]). *The supremum of* $\Psi_{(C,\mathcal{L})}$ *is*

$$\mathcal{W}^* + \mathcal{V}_2^* \tag{2.15}$$

where $\mathcal{V}_2^* = \max \mathfrak{V}(A, \mathcal{L}, Ker\ C)$.

In the *geometrical approach* to fault detection and isolation certain unobservability subspaces play a central role [3, 12] as defined below.

Definition 2.5. *A subspace* $\mathcal{S}$ *is a* (C, A) unobservability subspace *(u.o.s.) [12] if* $\mathcal{S} =< Ker\ HC|A + DC >$ *for some output injection map* $D : \mathcal{Y} \to \mathcal{X}$ *and measurement mixing map* $H : \mathcal{Y} \to \mathcal{Y}$.

It can be shown [12] that for an unobservability subspace $\mathcal{S}$,

$$\mathcal{S} =< \mathcal{S} + \text{Ker } C|A + DC > \tag{2.16}$$

The next theorem provides an alternative characterization of the u.o.s. for the system Σ which is independent of the maps D and H (this is the dual to Theorem 5.3 in [134] for controllability subspaces).

Theorem 2.1. *Let* $\mathcal{S} \subseteq \mathcal{X}$ *and define the family* $\mathcal{G}_{(A,C)}$ *as follows*

$$\mathcal{G}_{(A,C)} = \{\mathscr{S} : \mathscr{S} = \mathcal{S} + A^{-1}\mathscr{S} \cap \ Ker\ C\} \tag{2.17}$$

$\mathcal{S}$ *is an* (C, A) *u.o.s. if and only if*

$$A(\mathcal{S} \cap \ Ker\ C) \subseteq \mathcal{S} \quad (\mathcal{S} \textit{ is conditioned invariant}) \tag{2.18}$$

and

$$\mathcal{S} = \mathscr{S}^* \tag{2.19}$$

where $\mathscr{S}^*$ is the maximal element of $\mathcal{G}_{(A,C)}$.

The maximal element $\mathscr{S}^*$ can be computed by invoking the following algorithm

$$\mathscr{S}^0 = \mathcal{X}; \quad \mathscr{S}^\mu = \mathcal{S} + A^{-1}\mathscr{S}^{\mu-1} \cap \text{ Ker } C, \quad \mu \in \mathbf{n} \tag{2.20}$$

Given an u.o.s. $\mathcal{S}$, a measurement mixing map H can be computed from $\mathcal{S}$ by solving the equation KerHC = Ker$C + \mathcal{S}$. Let $\underline{D}(\mathcal{S})$ denote the class of all maps $D : \mathcal{Y} \to \mathcal{X}$ such that $(A + DC)\mathcal{S} \subseteq \mathcal{S}$. The notation $\mathfrak{S}(A, C, \mathcal{L})$ refers to the class of u.o.s. containing $\mathcal{L} \subseteq \mathcal{X}$. The class of u.o.s. is closed under intersection; therefore, it contains an infimal element $\mathcal{S}^* = \inf \mathfrak{S}(A, C, \mathcal{L})$. Moreover,

$$\mathcal{S}^* =< \text{Ker } C + \mathcal{W}^* | A + DC > \tag{2.21}$$

The following lemma shows the equivalency between the infimal unobservability subspace $\mathcal{S}^*$ containing a given subspace $\mathcal{L}$ and the supremum element of class $\Psi_{(C,\mathcal{L})}$.

Lemma 2.2 ([133]). *The infimal (C, A)-unobservability subspace $\mathcal{S}^*$ containing $\mathcal{L}$ is the supremum (C, A)-invariant self-hidden with respect to $\mathcal{L}$, i.e. $\mathcal{S}^* = \mathcal{W}^* + \mathcal{V}_2^*$.*

The above lemma provides an easy way for finding $\mathcal{S}^*$ using Algorithms 2.1 and 2.2. In [12] an alternative algorithm for computing $\mathcal{S}^*$ is proposed as follows.

Algorithm 2.3 ([12]). *The subspace $\mathcal{S}^*$ coincides with the last term of the sequence*

$$\mathcal{Z}_0 = \mathcal{X}$$

$$\mathcal{Z}_i = \mathcal{W}^* + (A^{-1}\mathcal{Z}_{k-1}) \cap Ker\, C \quad (i \in \boldsymbol{k})$$

where the value of $k \leq n$ is determined by condition $\mathcal{Z}_{k+1} = \mathcal{Z}_k$.

The next theorem provides the necessary and sufficient conditions for solvability of EFPRG problem ($\Omega_i = \{i\}$) based on the concept of unobservability subspaces.

Theorem 2.2 ([3]). *EFPRG problem has a solution if and only if there exist* (C, A) *unobservability subspaces*

$$\mathcal{S}_i^* = \inf \mathfrak{S}(A, C, \sum_{j=1, j\neq i}^{k} \mathcal{L}_j), \quad i \in \boldsymbol{k} \tag{2.22}$$

such that $\mathcal{S}_i^* \cap \mathcal{L}_i = 0$, $i \in \boldsymbol{k}$.

The major step in generating the residual r_i is to incorporate the image of the fault signatures that requires to decouple $(L_j(j \neq i))$ in the unobservability subspace of r_i and then factor out the unobservable subspace in a manner that in the remaining factor space those faults do not appear. The associated necessary condition for this purpose states that the image of L_i should not intersect with the unobservable subspace of r_i, so that a fault in the i-th component is manifested in the residual r_i.

According to [3], let $\mathcal{S}_i^*$ be an u.o.s. that satisfies Theorem 2.2, then there exists a map $D_0 \in \underline{D}(\mathcal{S}_i^*)$ and H_i such that $\mathcal{S}_i^* =< \text{Ker } H_iC|A + D_0C >$, where H_i is a solution to Ker $H_iC = \mathcal{S}_i^* + \text{Ker } C$. Let M_i be a unique solution of $M_iP_i = H_iC$ and $A_0 = (A + D_0C : \mathcal{X}/\mathcal{S}_i^*)$, P_i is the canonical projection of $\mathcal{X}$ on $\mathcal{X}/\mathcal{S}_i^*$ and $(A + D_0C : \mathcal{X}/\mathcal{S}_i^*)$ denotes an induced map of $A + D_0C$ on the factor space $\mathcal{X}/\mathcal{S}_i^*$ which satisfies the following equation

$$P_i(A + D_0C) = (A + D_0C : \mathcal{X}/\mathcal{S}_i^*)P_i \tag{2.23}$$

By construction, the pair (M_i, A_0) is observable, hence there exists a D_1 such that $\sigma(F_i) = \Lambda$, where $F_i = A_0 + D_1M_i$ and Λ is an arbitrary symmetric set. Let $D = D_0 + P_i^{-r}D_1H_i$, $E_i = P_iD$ and $G_i = P_iB$. The following detection filter generates the desired residual which is only affected by L_i and is decoupled from

other faults,

$$\begin{aligned} \dot{w}_i(t) &= F_i w_i(t) - E_i y(t) + G_i u(t) \\ r_i(t) &= M_i w_i(t) - H_i y(t) \end{aligned} \tag{2.24}$$

Definition 2.6 ([134]). *Let $p = (p_1, ..., p_N) \in \mathbb{R}^N$ and consider polynomials $\phi_i(\alpha_1, ..., \alpha_N), i \in \boldsymbol{k}$ with coefficient in $\mathbb{R}$. A* variety *$V \subseteq \mathbb{R}^N$ is defined to be the locus of common zeros of a finite number of polynomials $\phi_1, ..., \phi_k$. V is* proper *if $V \neq \mathbb{R}^N$. Let $A, B, ...$ be matrices with elements in $\mathbb{R}$ and suppose $\prod(A, B, ...)$ is some property which may be asserted about them. Let V be a proper variety. We say that $\prod$ is* generic relative *to V provided the property $\prod$ does not hold only for points $p \in V$, and $\prod$ is* generic *provided such a V exists. In other words, the set of points on which the generic property does not hold has a Lebesgue measure of zero.*

The generic solvability conditions for EFPRG problem are stated as follows [3].

Proposition 2.1 ([3]). *Let A, C and L_i be arbitrary matrices of dimensions $n \times n$, $q \times n$ and $n \times k_i$, respectively, let $v = \sum_{i=1}^{k} k_i$. EFPRG problem generically has a solution if and only if*

$$v \leq n \tag{2.25}$$

and

$$v - \min\{k_i, i = 1, ..., k\} < q \tag{2.26}$$

In the next theorem, the solvability condition for the SFDIP problem is presented. For given coding sets $\Omega_j, j \in \mathbf{k}$, the finite sets $\Gamma_i, i \in \mathbf{p}$ are defined as the collection of all $j \in \mathbf{k}$ for which the j-th failure mode affects the i-th residual, i.e. $\Gamma_i = \{j \in \mathbf{k} | i \in \Omega_j\}$. It follows that the sets Γ_i contain all the information corresponding to the coding sets $\Omega_j, j \in \mathbf{k}$.

Theorem 2.3. *For a given family of coding sets, the SFDIP problem has a solution if and only if*

$$\mathcal{S}^*_{\Gamma_i} \cap \mathcal{L}_j = 0, \quad j \in \Gamma_i, \quad i \in \boldsymbol{p} \tag{2.27}$$

where

$$\mathcal{S}^*_{\Gamma_i} = \inf \mathfrak{S}(A, C, \sum_{j \notin \Gamma_i} \mathcal{L}_j), \qquad i \in \boldsymbol{p} \tag{2.28}$$

Proof: According to Theorem 2.2, the SFDIP problem can be solved as p separate EFPRG problem. Each residual $r_i(t), i \in \mathbf{p}$ can be generated by applying EFPRG results to the following model

$$\begin{aligned} \dot{x}(t) &= Ax(t) + Bu(t) + \bar{L}_1 \bar{m}_1(t) + \bar{L}_2 \bar{m}_2(t) \\ y(t) &= Cx(t) \end{aligned}$$

where $\bar{L}_1 = \{L_j | j \in \Gamma_i\}$, $\bar{L}_2 = \{L_j | j \in \mathbf{k} - \Gamma_i\}$, $\bar{m}_1 = \{m_j | i \in \Gamma_i\}$ and $\bar{m}_2 = \{m_j | i \in \mathbf{k} - \Gamma_i\}$. Hence, based on Theorem 2.2 in order to be able to decouple the residual $r_i(t)$ from $\bar{m}_2(t)$, there should exists an unobservability subspace that contains all fault signature in $\bar{L}_2$, i.e. $\mathcal{S}^*_{\Gamma_i} = \inf \mathfrak{S}(A, C, \sum_{j \notin \Gamma_i} \mathcal{L}_j)$. Moreover, the necessary condition for manifesting the effect of faults in components $m_j, j \in \Gamma_i$ in the residual r_i is that $\mathcal{S}^*_{\Gamma_i}$ does not have intersection with $L_j, j \in \Gamma_i$, i.e. condition (2.27). ■

A family of fault signatures satisfying the conditions of Theorem 2.2 is designated as a *strongly detectable* family. It follows from Theorem 2.2 that a necessary condition for existence of a solution to EFPRG problem is that

$$\text{Rank}\{[L_1, L_2, ..., L_k]\} = \sum_{i=1}^{k} k_i \tag{2.29}$$

which implies that there should be no dependency among the fault signatures. The following example demonstrates situations in which the family of fault signatures is not *strongly detectable.*

Example 2.1. *Consider the following overactuated system*

$$\begin{aligned} \dot{x}(t) &= Ax(t) + Bu(t) + \sum_{i}^{4} B_i m_i(t) \\ y(t) &= Cx(t) \end{aligned} \tag{2.30}$$

where

$$A = \begin{bmatrix} 1 & 1 & 1 \\ 0 & -1 & 2 \\ 2 & 0 & -4 \end{bmatrix}, B = \begin{bmatrix} 1 & 0 & 1 & 1 \\ 0 & 1 & 1 & 0 \\ 0 & 1 & 0 & 1 \end{bmatrix}, C = \begin{bmatrix} 0 & 1 & 0 \\ 0 & 0 & 1 \\ 1 & 0 & 2 \end{bmatrix}$$

This system has 4 inputs such that rank $B = 3$. Therefore, the family of actuator fault signatures for this system is clearly not strongly detectable.

Example 2.2. *Consider the following system*

$$\dot{x}(t) = Ax(t) + Bu(t) \tag{2.31}$$

$$y(t) = Cx(t) + \sum_{j=1}^{3} E_j \mu_j \tag{2.32}$$

where

$$A = \begin{bmatrix} 1 & 2 & 1 & 0 & 0 \\ 0 & 1 & 3 & -1 & 2 \\ 3 & -1 & 2 & 0 & 1 \\ 0 & 1 & 1 & 1 & 1 \\ 0 & 0 & 2 & 1 & 1 \end{bmatrix}, B = \begin{bmatrix} 1 & 0 \\ 1 & 0 \\ 0 & 1 \\ 0 & 1 \\ 0 & 0 \end{bmatrix}, C = \begin{bmatrix} 1 & 1 & 0 & 0 & 1 \\ 0 & 1 & 1 & 0 & 0 \\ 0 & 0 & 1 & 1 & 0 \end{bmatrix}$$

As mentioned earlier, sensor faults can be modeled as input faults to the system. Using the state space coordinate transformation $\bar{x} = x + \sum_{j=1}^{3} f_j \mu_j$, the state space representation for the new state is written according to equation (2.5) *where*

$$L_1 = \begin{bmatrix} 1 & 1 \\ 0 & 0 \\ 0 & 3 \\ 0 & 0 \\ 0 & 0 \end{bmatrix}, L_2 = \begin{bmatrix} -2 & 1 \\ 2 & -1 \\ -1 & -10 \\ 0 & 1 \\ 0 & -2 \end{bmatrix}, L_3 = \begin{bmatrix} 0 & 0 \\ 0 & -1 \\ 0 & 0 \\ 1 & 1 \\ 0 & 1 \end{bmatrix} \tag{2.33}$$

If one considers the actuator faults L_4 and L_5 as the first and second column of B, it can be easily checked that the family of fault signatures $L_1, ..., L_5$ is not strongly detectable. Therefore, one cannot detect all fault simultaneously in this system.

2.3 Geometric Approach to FDI of Nonlinear Systems

In this section, the geometric FDI approach introduced in [60] for nonlinear systems is briefly reviewed. This scheme provides us with the necessary and sufficient conditions for solving the problem of generating a structured residual set for general nonlinear systems. It is assumed that the nonlinear system is described by the following model:

$$\begin{aligned} \dot{x}(t) &= f(x(t)) + g(x(t))u + \sum_{i=1}^{k} l_i(x(t))m_i(t) \\ y(t) &= h(x(t)) \end{aligned} \tag{2.34}$$

with the state x is defined in a neighborhood $\mathcal{X}$ of the origin in $\mathbb{R}^n$; the input is denoted by $u \in \mathbb{R}^m$; the output is denoted by $y \in \mathbb{R}^q$; the fault modes are denoted by $m_i \in \mathbb{R}^{k_i}$, $l_i(x)$'s are the fault signatures, $f(x)$, $g(x)$ and $l_i(x)$'s are smooth vector fields, $h(x)$ is a nonlinear smooth mapping, and $f(0) = 0, h(0) = 0$. It is assumed that $span\{l_i^1(x), ..., l_i^{k_i}(x)\}, i \in \mathbf{k}$ is nonsingular where l_i^j denotes the j-th column of l_i.

Definition 2.7 ([135]). *The distribution Δ is said to be* conditioned invariant *(or (h, f) invariant) for (2.34) if it satisfies*

$$[g_i, \Delta \cap Ker\{dh\}] \subseteq \Delta, \quad for\ all\ i = 0, ..., m \tag{2.35}$$

where $g_0(x) = f(x)$, $Ker\{dh\}$ is the distribution annihilating the differentials of the rows of the mapping $h(x)$ and $[f, g]$ denotes the Lie derivative of f and g.

For a given distribution $\mathcal{L}$, the following algorithm is proposed in [59] to determine the smallest condition invariant distribution which contains $\mathcal{L}$ (denoted by $\Sigma_*^{\mathcal{L}}$):

Algorithm 2.4 ([59]). *Consider the following sequence of distributions*

$$\mathcal{S}_0 = \bar{\mathcal{L}}$$

$$\mathcal{S}_{k+1} = \bar{\mathcal{S}}_k + \sum_{i=0}^{m} \left[g_i, \bar{\mathcal{S}}_k \cap Ker\,\{dh\}\right]$$

where $\bar{\mathcal{S}}$ denotes the involutive closure of $\mathcal{S}$. Suppose there is an integer k^* such that $\mathcal{S}_{k^*+1} = \bar{\mathcal{S}}_{k^*}$, then $\Sigma_*^{\mathcal{L}} = \bar{\mathcal{S}}_{k^*}$ and $\Sigma_*^{\mathcal{L}}$ is involutive and is the smallest conditioned invariant contains $\mathcal{L}$.

According to [59], it is more convenient to work with a dual object, i.e. with a codistribution as defined next.

Definition 2.8 ([60]). *A codistribution Π is said to be conditioned invariant if*

$$L_{g_i}\Pi \subseteq \Pi + span\{dh\}, \quad for\ all\ i = 0, ..., m \tag{2.36}$$

where $span\{dh\}$ is the codistribution spanned by the differentials of the rows of the mapping $h(x)$.

It is shown in [135] that if $\Delta \cap \mathrm{Ker}\{dh\}$ is a smooth distribution and $\Pi = \Delta^{\perp}$ is a smooth codistribution, then Π satisfies (2.36). In [59], the following algorithm was proposed for defining an observability codistribution associated with system (2.34).

Algorithm 2.5 ([59]). *Consider system (2.34) and let Θ be a fixed codistribution. The observability codistribution algorithm (o.c.a.) that characterizes this codistribution is given according to the following procedure:*

$$Q_0 = \Theta \cap span\{dh\}$$

$$Q_{k+1} = \Theta \cap \Big(\sum_{i=0}^{m} L_{g_i} Q_k + span\{dh\}\Big)$$

Suppose all codistributions of the sequences are nonsingular, so that there is an integer $k^* \leq n-1$ such that $Q_k = Q_{k^*}$ for all $k > k^*$ and set $\Pi^* = Q_{k^*}$. The following notation is then used to stress the dependency of Π^* on Θ:

$$\Pi^* = o.c.a.(\Theta) \tag{2.37}$$

Definition 2.9. *The codistribution* Π *is an* observability codistribution *for (2.34) if it satisfies (2.36) and*

$$o.c.a.(\Pi) = \Pi \tag{2.38}$$

If Θ is a conditioned invariant codistribution, then o.c.a.(Θ) is the maximal observability codistribution contained in Θ. The next theorem which is proposed in [59] states one of the important properties of the observability codistribution.

Theorem 2.4 ([59]). *Consider system (2.34) with* $m_i = 0$. *Let* Π *be an observability codistribution such that* $\Pi = span\{\Phi_1\}$ *where* $\Phi_1 : U^\circ \to \mathbb{R}^{n_1}$ *and* U° *is a neighborhood of fixed point* x°. *One can then find a local state diffeomorphism at* x° *and a local output diffeomorphism at* $y^\circ = h(x^\circ)$ *such that in the new local coordinates system (2.34) is described by the following equations*

$$\begin{aligned}
\dot{z}_1 &= f_1(z_1, z_2) + g_1(z_1, z_2)u \\
\dot{z}_2 &= f_2(z_1, z_2, z_3) + g_2(z_1, z_2, z_3)u \\
\dot{z}_3 &= f_3(z_1, z_2, z_3) + g_3(z_1, z_2, z_3)u \\
y_1 &= h(z_1) \\
y_2 &= z_2
\end{aligned} \tag{2.39}$$

where $z_1 = \Phi_1(x)$, *and in the new coordinates any vector field* $l(x)$ *in* $\Pi^\perp$ *will be expressed in the form*

$$\begin{pmatrix} 0 & l_2^\top(z_1, z_2, z_3) & l_3^\top(z_1, z_2, z_3) \end{pmatrix}^\top \tag{2.40}$$

The observability codistribution is a special type of condition invariant codistribution where the z_1-subsystem, in which z_2 can be replaced by y_2 and viewed as an independent "input", namely system

$$\begin{aligned}
\dot{z}_1 &= f_1(z_1, y_2) + g_1(z_1, y_2)u \\
y_1 &= h_1(z_1)
\end{aligned} \tag{2.41}$$

satisfies the observability rank condition and where by imposing certain mild assumptions [59], one can design an asymptotic observer for the state z_1.

In the nonlinear fundamental problem in residual generation (lNFPRG) that is introduced in [60], the family of coding sets $\Omega_i = \{i\}$ was chosen. The solvability of the lNFPRG problem is stated as follows.

Theorem 2.5 ([60]). *The lNFPRG has a solution if and only if there exist observability codistributions*

$$\Pi_i^* = o.c.a.((\Sigma_*^{\mathcal{L}_i})^{\perp}) \tag{2.42}$$

such that

$$(span\{l_i\})^{\perp} + \Pi_i^* = T^*X \tag{2.43}$$

where $\mathcal{L}_i = span\{l_1(x), ..., l_{i-1}(x), l_{i+1}(x), ..., l_m(x)\}$.

If such observability codistribution exist, then by using Theorem 2.4, the z_1-subsystem corresponding to each Π_i^* is described in the new coordinates by

$$\begin{aligned} \dot{z}_1 &= f_1(z_1, y_2) + g_{i1}(z_1, y_2)u_i + l_{i1}(z_1, y_2)m_i \\ y_1 &= h_1(z_1) \end{aligned} \tag{2.44}$$

Consequently, it is now possible to design an observer for the above subsystem which generates the state estimate $\hat{z}_1$. In [60], one way to design an observer for the z_1-subsystem (2.44) is presented based on a result from Gauthier-Kupca [136]. Once the observer is designed, the residual signal r_i can be generated according to

$$r_i = y_1 - h_1(\hat{z}_1) \tag{2.45}$$

The next theorem provides the necessary and sufficient conditions for the solvability of the SFDIP problem for given coding sets Ω_i's for the nonlinear system (2.34).

Theorem 2.6. *The SFDIP problem for nonlinear system* (2.34) *has a solution for given coding sets Ω_i's if and only if there exist observability codistributions*

$$\Pi^*_{\Gamma_i} = o.c.a.((\Sigma_*^{\mathcal{L}_{\Gamma_i}})^{\perp}), \qquad i \in \boldsymbol{p} \tag{2.46}$$

such that

$$(span\{l_j\})^{\perp} + \Pi^*_i = T^*X, \quad \forall j \in \Gamma_i, \quad i \in \boldsymbol{p} \tag{2.47}$$

where $\mathcal{L}_{\Gamma_i} = span\{l_j(x)|j \notin \Gamma_i\}$, $i \in \boldsymbol{p}$.

Proof: According to Theorem 2.5, the SFDIP problem can be solved as p separate lNFPRG problem. Each residual $r_i(t), i \in \mathbf{p}$ can be generated by applying EFPRG results to the following model

$$\dot{x} = f(x) + g(x)u + \bar{L}_1(x)\bar{m}_1(t) + \bar{L}_2(x)\bar{m}_2(t)$$
$$y = h(x)$$

where $\bar{L}_1 = \{l_i(x)|i \in \Gamma_i\}$, $\bar{L}_2 = \{l_i(x)|i \in \mathbf{k} - \Gamma_i\}$, $\bar{m}_1 = \{m_i|i \in \Gamma_i\}$ and $\bar{m}_2 = \{m_i|i \in \mathbf{k} - \Gamma_i\}$. The residual $r_i(t)$ should be decoupled from all faults in the components $\bar{(m)}_2$ and should be affected by faults in the components $m_j, j \in \Gamma_i$. Hence, based on Theorem 2.5, there should exist an observability codistribution that contains all fault signatures in $\bar{L}_2$, i.e. $\Pi^*_{\Gamma_i} = \text{o.c.a.}((\Sigma_*^{\mathcal{L}_{\Gamma_i}})^{\perp})$. Moreover, the necessary condition for manifesting the effect of faults in components $m_j, j \in \Gamma_i$ is (2.47). ■

2.4 Actuator Fault Modes

Actuator faults that are considered in this dissertation for simulation include [137]: (i) freezing or lock in-place (LIP) fault, (ii) float fault, (iii) hard-over fault (HOF), and (iv) loss of effectiveness (LOE) fault. In case of the LIP fault, the actuator states freezes at a particular value and will not respond to subsequent commands. HOF is

characterized by the actuator moving to its upper or lower saturation limits regardless of the commanded signal. The actuator transient response time is bounded by its rate limits. Float fault occurs when the actuator floats with zero output and does not contribute to the control authority. Loss of effectiveness is characterized and represented by lowering the actuator gain with respect to its nominal value. The various types of actuator faults discussed above are mathematically parameterized as follows [137]:

$$u_{true} = \begin{cases} u_{cmd} & \text{No Fault} \\ k(t)u_{cmd} & 0 < \varepsilon \leq k(t) < 1, \forall t \geq t_F \text{ (LOE)} \\ 0 & \forall t \geq t_F \text{ (Float)} \\ u_{cmd}(t_F) & \forall t \geq t_F \text{ (LIP)} \\ u_m \quad \text{or} \quad u_M & \forall t \geq t_F \text{ (HOF)} \end{cases} \tag{2.48}$$

where t_F denotes the time of fault occurrence in the actuator, k denotes the loss of effectiveness coefficient where $k \in [\varepsilon, 1]$ and ε denotes the minimum loss of effectiveness, and u_m and u_M denote the minimum and maximum values of the input, respectively. The general model below integrates the above cases into a single representation, $u_{true} = \sigma k u_{cmd} + (1 - \sigma)\bar{u}$ where u_{true} is the actuator output, u_{cmd} is the output of the controller (which at the same time is an input to the actuator), $\sigma = 1$ and $k = 1$ correspond to the no fault operating regime, $\sigma = 1$ and $\varepsilon < k < 1$ correspond to the loss of effectiveness fault, and $\sigma = 0$ corresponds to other types of fault scenarios, namely Float, LIP and HOF. Finally, $u_m \leq \bar{u} \leq u_M$ denotes the state at which the actuator is locked for the float, lock-in-place, and hard-over faults cases.

It should be emphasized that all the algorithms that are developed throughout the thesis do not depend on the above fault modeling and the above actuator faults are only used in simulation results throughout the thesis.

Chapter 3

Fault Detection and Isolation in a Network of Unmanned Vehicles: Ideal Communication Channels

In this chapter, we address the problem of actuator fault detection and isolation in a network of unmanned vehicles in three different architectures, namely centralized, decentralized and semi-decentralized. It is shown that the fault signatures in a network of unmanned vehicles with relative state measurement are dependent and the overall system is overactuated. This motivates us to investigate the development, design, and analysis of a fault detection and isolation scheme for both linear and nonlinear systems with dependent fault signatures. The work presented in this chapter has partly appeared in [138–141].

This chapter is organized as follows. In Section 3.1, the actuator fault detection and isolation problem in a network of unmanned vehicles is formulized within different architectures, namely centralized, decentralized and semi-decentralized. In Section 3.2, new coding sets are introduced for fault detection and isolation of both linear and nonlinear systems with dependent fault signatures. In Section 3.3, our

proposed FDI algorithm is applied to the actuator fault detection and isolation in a network of unmanned vehicles. Simulation results for FDI in formation flight of satellites is presented in Section 3.3.3. Moreover, two other case studies, namely, actuator FDI problem of F18-HARV and FDI of a satellite with redundant reaction wheel configuration are considered in Sections 3.4 and 3.5, respectively.

Contributions

The main contributions of this chapter are now summarized below.

- A new structured residual set is introduced for systems with dependent fault signatures.
- The actuator fault detection and isolation problem in a network of unmanned vehicles with relative state measurement is investigated corresponding to three architectures, namely, centralized, decentralized and semi-decentralized. The necessary and sufficient conditions for solvability of the actuator FDI problem in centralized and decentralized architectures are provided. Moreover, it is shown that the actuator FDI problem does not have a solution in the decentralized architecture.
- Three cases studies, namely, formation flight of satellites, overactuated F18-HARV aircraft and a satellite with redundant reaction wheels are considered as potential applications of our developed algorithm.

3.1 FDI Problem Formulation in a Network of Unmanned Vehicles

In this section, the problem of actuator fault detection and isolation in a network of N homogenous (for sake of simplicity) vehicles is formulized. It is assumed that

each vehicle dynamics is governed by the following linear model:

$$\dot{x}_i(t) = Ax_i(t) + Bu_i(t) + \sum_{k=1}^{a} L_k m_{ik}(t) \tag{3.1}$$

where the fault signature L_k represents a fault in the k-th actuator of a vehicle, i.e, L_k is the k-th column of B. It is assumed that the matrix B is full rank (Rank(B)=a). Each vehicle has the following relative state measurements:

$$z_{ij}(t) = C(x_i(t) - x_j(t)) \qquad j \in \mathrm{N}_i \tag{3.2}$$

where the set $\mathrm{N}_i \subseteq \mathbf{N} \setminus i$ represents the set of vehicles that vehicle i can sense ($\mathbf{N} = \{1, ..., N\}$) and is designated as the neighboring set of vehicle i, and $z_{ij} \in \mathcal{Z}_i, j \in \mathrm{N}_i$ represent the state measurement relative to the other vehicles.

It is assumed that the pair (A, C) is observable. Let $\mathrm{N}_i = \{i_1, i_2, ..., i_{|\mathrm{N}_i|}\}$. We have $z_i(t) = [z_{ii_1}^{\top}(t), z_{ii_2}^{\top}(t), \cdots, z_{ii_{|\mathrm{N}_i|}}^{\top}(t)]^{\top}$, and equation (3.2) can be rewritten as $z_i(t) = C_i x(t)$, where $x(t) = [x_1^{\top}(t), x_2^{\top}(t), \cdots, x_N^{\top}(t)]^{\top}$ and C_i can be constructed from the neighboring set N_i and matrix C. The vehicles and their neighborhood sets together form a directed graph, where each node represents a vehicle and an arc leads from node i to node j if $j \in \mathrm{N}_i$. It is assumed that this graph is weakly connected, i.e. there exists a path between every pair of distinct vertices ignoring the direction of arcs.

In the following discussions we will formulate three different architectures for FDI of actuator faults in the above network of unmanned vehicles. Namely, we are interested in centralized, decentralized and semi-decentralized configurations as described and defined below. It will be shown that actuator fault signatures in the centralized and semi-decentralized architectures are dependent and therefore, new coding schemes need to be developed for systems with dependent fault signatures (Section 3.2). Moreover, we will show that the actuator FDI problem does not have a solution in the decentralized architecture.

In this chapter, it is assumed that the communication links among the vehicles

and the FDI units are ideal, i.e. there exist no networked-induced delay, packet dropout and quantization error due to communication links. This assumption will be relaxed in Chapter 5.

3.1.1 Centralized Architecture

In the centralized architecture, all information should be sent to a central FDI unit through the "entire" communication network channels. The overall system can be modeled as follows:

$$\begin{aligned} \dot{x}(t) &= A^N x(t) + B^N u(t) + \sum_{k=1}^{N}\sum_{j=1}^{a} \bar{L}_{kj} m_{kj}(t) \\ z(t) &= \bar{C} x(t) \end{aligned} \tag{3.3}$$

where $A_N = I_N \otimes A$, $B_N = I_N \otimes B$, $\otimes$ denotes the Kronecker product, N is a positive integer, I_N is an $N \times N$ identity matrix, $u = [u_1^\top, u_2^\top, \cdots, u_N^\top]^\top$, $\bar{L}_{kj}$ is the $(k-1)\times a + j$-th column of B^N, $z = [z_1^\top, z_2^\top, \cdots, z_N^\top]^\top$ and $\bar{C}^\top = [C_1^\top, C_2^\top, \cdots, C_N^\top]$. It is clear that the entire state x is not fully observable from the relative state measurements z and states of the centroid of the vehicles cannot be determined from z. Since the pair $(A^N, \bar{C})$ in not observable, one can first determine the observable subspace of system (3.3) as

$$\begin{aligned} \dot{x}^O(t) &= A^{N-1} x^O(t) + \bar{B}^O u(t) + \sum_{k=1}^{N}\sum_{j=1}^{a} \bar{L}^O_{kj} m_{kj}(t) \\ \bar{z}(t) &= C^{N-1} x^O(t) \end{aligned} \tag{3.4}$$

where $x^O(t) = [x_1^\top(t) - x_2^\top(t), x_1^\top(t) - x_3^\top(t), \cdots, x_1^\top(t) - x_N^\top(t)]^\top$, $C^{N-1} = I_{N-1} \otimes C$,

$$\bar{B}^O = \begin{bmatrix} B & -B & 0 & \cdots & 0 \\ B & 0 & -B & \cdots & 0 \\ \vdots & & \ddots & & \vdots \\ B & 0 & 0 & \cdots & -B \end{bmatrix}_{(N-1)\times N} \tag{3.5}$$

$\bar{L}^O_{kj}$ is the $(k-1)\times a + j$-th column of $\bar{B}^O$, and $\bar{z}(t) = Tz(t)$, where T is an output transformation that specifies the relative states with respect to the first vehicle. Such a transformation exists since it is assumed that the graph of the network is weakly connected. Without loss of generality, the relative states between vehicle one and other vehicles are taken as observable states of the entire network. It can be verified that the rank of $\bar{B}^O$ is $a \times (N-1)$ and system (3.4) is overactuated.

3.1.2 Decentralized Architecture

In this section, the decentralized architecture is considered where there exist no communication links between the vehicles and we wish to determine whether each vehicle can detect and isolate its own faults using only local signals, namely u_i and z_i. Since the output measurement z_i depends on the state of the neighboring vehicles, the following nodal model should be considered for the i-th vehicle for designing a decentralized FDI filter, namely

$$\begin{aligned} \dot{x}_{\mathrm{N}_i}(t) &= A^{|\mathrm{N}_i|+1}x_{\mathrm{N}_i}(t) + B^{|\mathrm{N}_i|+1}u_{\mathrm{N}_i}(t) + \sum_{j=1}^{a}\bar{L}_{1j}m_{1j}(t) + \sum_{k=2}^{|\mathrm{N}_i|+1}\sum_{j=1}^{a}\bar{L}_{kj}m_{kj}(t) \\ z_i(t) &= \bar{C}_{\mathrm{N}_i}x_{\mathrm{N}_i}(t) \end{aligned} \tag{3.6}$$

where $x^\top_{\mathrm{N}_i}(t) = [x^\top_i(t), x^\top_{i_1}(t), \cdots, x^\top_{i_{|\mathrm{N}_i|}}(t)]^\top$, $u_{\mathrm{N}_i}(t) = [u^\top_i(t), u^\top_{i_1}(t), \cdots, u^\top_{i_{|\mathrm{N}_i|}}(t)]^\top$, $z_i(t) = [z^\top_{ii_1}(t), z^\top_{ii_2}(t), \cdots, z^\top_{ii_{|\mathrm{N}_i|}}(t)]^\top$, and $\bar{L}_{kj}$ is the $(k-1)\times a + j$-th column of $B^{|\mathrm{N}_i|+1}$. It should be noted that $\bar{L}_{1j}$'s represent the fault signatures of the i-th vehicle in the nodal system (3.6). It is clear that the entire state x_{N_i} is not fully observable from the relative state measurements z_i, and the states of the centroid of vehicle i and its neighbors cannot be determined from z_i. Since the pair $(A^{|\mathrm{N}_i|+1}, \bar{C}_{\mathrm{N}_i})$ is not observable, one can first try to obtain the observable part of system (3.6) as

$$\begin{aligned} \dot{x}^O_{\mathrm{N}_i}(t) &= A^{|\mathrm{N}_i|}x^O_{\mathrm{N}_i}(t) + \bar{B}^O_{\mathrm{N}_i}u_{\mathrm{N}_i}(t) + \sum_{j=1}^{a}\bar{L}^O_{1j}m_{1j}(t) + \sum_{k=2}^{|\mathrm{N}_i|+1}\sum_{j=1}^{a}\bar{L}^O_{kj}m_{kj}(t) \\ z_i(t) &= C^{|\mathrm{N}_i|}x^O_{\mathrm{N}_i}(t) \end{aligned} \tag{3.7}$$

where $x^O_{\mathrm{N}_i}(t) = [x_i^\top(t) - x_{i_1}^\top(t), x_i^\top(t) - x_{i_2}^\top(t), \cdots, x_i^\top(t) - x_{i_{|\mathrm{N}_i|}}^\top(t)]^\top$ and $\bar{B}^O_{\mathrm{N}_i} = [\bar{B}^O_i, \bar{B}^O_{i_1} \cdots, \bar{B}^O_{i_{\mathrm{N}_i}}]$ has the same structure as the matrix $\bar{B}^O$ in (3.5) with dimension $|N_i - 1| \times |N_i|$ and $\bar{L}^O_{kj}$ is the $(k-1) \times a + j$-th column of $\bar{B}^O_{\mathrm{N}_i}$. We are now in the position to introduce our main theorem in this subsection.

Theorem 3.1. *The decentralized FDI problem is not solvable for a network of unmanned vehicles* (3.6) *using only the relative state measurements.*

Proof: In order to generate the residual signals $r_{ij}, j \in \mathbf{a}$ for the i-th vehicle by using only the signals u_i and z_i, the residual signals should be decoupled from both faults in the neighboring vehicles $\sum_{k=2}^{|\mathrm{N}_i|+1} \sum_{j=1}^{a} \bar{L}^O_{kj} m_{kj}(t)$ and input signals $u_j, j \neq i$. However, since the fault signatures $\bar{L}^O_{kj}$'s are the columns of $\bar{B}^O_{\mathrm{N}_i}$, the term $\sum_{k=1}^{|\mathrm{N}_i|} \mathcal{B}^O_{i_k}$ includes both fault signatures and input channel matrices of other vehicles. Therefore, by invoking the result of Theorem 2.3, the existence of the $(C^{|\mathrm{N}_i|}, A^{|\mathrm{N}_i|})$ unobservability subspaces $\mathcal{S}^*_j = \inf \underline{\mathcal{S}}(\sum_{k=1}^{|\mathrm{N}_i|} \bar{\mathcal{B}}^O_{i_k} + \sum_{k=1,k\neq j}^{a} \bar{\mathcal{L}}^O_{1k})$ such that $\mathcal{S}^*_j \cap \bar{\mathcal{L}}_{1j} = 0, j \in \mathbf{a}$, is the necessary and sufficient condition for generating the residual signal $r_{ij}(t)$. This residual signal is only affected by m_{1j} and is decoupled from all other fault signatures of the i-th vehicle and $\sum_{k=1}^{|\mathrm{N}_i|} \mathcal{B}^O_{i_k}$. However, it is clear from equation (3.5) that $\bar{\mathcal{L}}_{1j} \subset \sum_{k=1}^{|\mathrm{N}_i|} \bar{\mathcal{B}}^O_{i_k}, j \in \mathbf{a}$ and $\bar{\mathcal{L}}_{1j} \subseteq \mathcal{S}^*_j, j \in \mathbf{a}$. Therefore, it can be concluded that the above decentralized FDI problem does not have a solution for a network of unmanned vehicles using only relative state measurements, and each vehicle cannot even detect its own fault by using the local information u_i and z_i. ■

3.1.3 Semi-decentralized Architecture

In the semi-decentralized architecture, it is assumed that local communication links exist between each vehicle and its neighbors and the control signals u_i are communicated among them. The problem is to determine how each vehicle detects and isolates not only its own actuator faults but also actuator faults of its neighbors

using the signals u_{N_i} and z_i. The observable nodal model (3.7) is considered for the i-th vehicle.

It can be verified that the rank of $\bar{B}^O_{\mathrm{N}_i}$ is $a \times |\mathrm{N}_i|$ and the fault signatures $\bar{L}^O_{kj}$'s are not strongly detectable. This is due to the fact that one needs to control $|\mathrm{N}_i|$ vehicles in the nodal system (3.7) in order to control the relative states of $|\mathrm{N}_i| + 1$ vehicles. In other words, actuator redundancy is present and the system can be categorized as an overactuated system.

As shown above, in centralized and semi-decentralized architectures, the fault signatures are dependents and hence concurrent faults in all actuators cannot be detected and isolated. This provides us with the motivation to determine and investigate a suitable coding sets for a family of dependent fault signatures. In the next section, we propose the structured residual set for both linear and nonlinear systems with dependent fault signatures.

3.2 Proposed Structured Fault Detection and Isolation Scheme

For many class of dynamical systems such as overactuated systems, fault signatures are generally dependent. Generally speaking, fault signatures are called *dependent* if effect of one fault can be written as a linear combination of effects of other faults. This fault signature dependency may arise due to redundant actuators or coupling effects among sensor, actuator and plant faults. In this section, we investigate the development, design, and analysis of a fault detection and isolation scheme for both linear and nonlinear systems with dependent fault signatures. Due to dependency among fault signatures, the dedicated residual set cannot be utilized and consequently all faults cannot be detected simultaneously. To determine a suitable residual set, a isolability index μ is first introduced for a family of fault signatures as

the maximum number of concurrent faults that can be detected and isolated. Next, two structured residual sets are proposed and developed for achieving a specific isolability index. The geometric approach of [3] and [60] is used for generating these new residual sets for linear and nonlinear systems, respectively.

Definition 3.1. *For a family of fault signatures $L_1, \cdots, L_k$ for linear system* (2.1) *($l_1(x), \cdots, l_k(x)$ for nonlinear system* (2.34)*), the maximum value of $\mu \leq k$ where one can detect and isolate the occurrence of up to μ concurrent faults is denoted as the isolability index.*

According to the above definition, Theorem 2.2 shows that the isolability index of a family of k fault signatures is k if and only if the family is *strongly detectable.*

The next theorem provides the necessary and sufficient conditions for a given coding sets that can be used for detecting and isolating up to μ concurrent faults in a given family of fault signatures $\mathcal{FL} = \{L_1, L_2, ..., L_k\}$ for linear system (2.1). The same statement can be derived for nonlinear system by substituting $l_i(x)$'s with L_i's.

Theorem 3.2. *Consider the weakly isolating coding sets $\Omega_i, i \in \boldsymbol{k}$ and a given family of fault signatures $\mathcal{FL} = \{L_1, L_2, ..., L_k\}$ for linear system* (2.1)*. Let for each l combination $L_{i_1}, ..., L_{i_l}$ of L_i's, $\Omega_{i_1 i_2 ... i_l} = \bigcup_{j=i_1}^{i_l} \Omega_j$. The family of fault signatures $\mathcal{FL}$ has a isolability index of μ if and only if the SFDIP problem has a solution for the coding sets $\Omega_i, i \in \boldsymbol{k}$ with the following property that for each two different $1 \leq l, h \leq \mu$ combinations $L_{i_1}, ..., L_{i_l}$ and $L_{j_1}, ..., L_{j_h}$ of L_i's*

$$\Omega_{i_1 i_2 ... i_l} \neq \Omega_{j_1 j_2 ... j_h} \tag{3.8}$$

Proof: (only if) Let a family of fault signatures $L_1, ..., L_k$ has the isolability index of μ, then for any occurrence of $l \leq \mu$ concurrent faults, there should exists a unique set of residuals that is affected by these faults. According to the definition of the coding

sets, a set of residuals that is affected by l faults $L_{i_1}, ..., L_{i_l}$ is $\Omega_{i_1 i_2 ... i_l}$. Therefore, the uniqueness of $\Omega_{i_1 i_2 ... i_l}$ leads to the equation (3.8).

(if) It is trivial to observe that if the SFDIP problem has a solution for the coding sets $\Omega_i, i \in \mathbf{k}$ with the above property, then one can detect and isolate up to μ concurrent faults. ■

It should be emphasized that for $\mu = k$, there exists only one k-combination of L_i's, namely $L_1, ..., L_k$ and hence condition (3.8) implies that for having an isolability index of $\mu = k$, we should have

$$\Omega_{i_1 i_2 ... i_l} \neq \Omega_{1...k}$$

for any $l < k$ where $\Omega_{1...k} = \bigcup_{j=1}^{k} \Omega_j$.

Remark 3.1. *It can be shown that the coding sets of the EFPRG problem [3] ($\Omega_i = \{i\}$) and the coding sets of the generalized residual set [5] ($\Omega_i = \boldsymbol{k} - \{i\}$) satisfy the necessary and sufficient conditions of the above theorem for $\mu = k$ and $\mu = 1$, respectively.*

As mentioned in Section 2.1, in order to prevent incorrect fault detection and isolation, the coding sets Ω_i should be strongly isolating. The same criteria can be considered for the coding sets $\Omega_{i_1 i_2 ... i_l}$.

Definition 3.2. *The coding sets that satisfy the condition of Theorem 3.2 are said to be strongly isolating with index μ if for each two different $1 \leq l \leq \mu$ combination $L_{i_1}, ..., L_{i_l}$ and $L_{j_1}, ..., L_{j_l}$ of L_i's*

$$\Omega_{i_1 i_2 ... i_l} \nsubseteq \Omega_{j_1 j_2 ... j_l}, \quad \textbf{and} \quad \Omega_{i_1 i_2 ... i_l} \nsupseteq \Omega_{j_1 j_2 ... j_l} \tag{3.9}$$

Moreover, if the SFDIP problem for a given family of fault signatures has a solution for a strongly isolating coding set with index μ, then we call the isolability index of that family as a strongly isolability index μ.

Lemma 3.1. *The strong isolability index μ of a given family of fault signatures is either $\mu = k$ or $\mu < k - 1$.*

Proof: Let $\Omega_i, i \in \mathbf{k}$ be strongly isolating with index $\mu = k - 1$. Consider that concurrent faults have occurred in all fault signatures. Since Ω_i's are weakly isolating (none of them is empty), all residuals will be affected by these concurrent faults. Moreover, since the strong isolability of fault signatures is μ, it is clear that for each $k - 1$ combination $L_{i_1}, ..., L_{i_{k-1}}$ of L_i's, we have $\Omega_{i_1 i_2 ... i_{k-1}} \neq \Omega_{1,...,k} = \bigcup_{j=1}^{k} \Omega_j$. Therefore, one can also detect that there exist concurrent faults in all channels. Moreover by assumption, one can detect and isolate up to $k - 1$ concurrent faults. Hence $\mu = k$. ■

It should be emphasized not every coding sets that satisfy Theorem 3.2 is strongly isolating with index μ. For instance, consider the coding sets $\Omega_1 = 1, 2$, $\Omega_2 = 3, 4$ and $\Omega_3 = 2, 3$. It can easily be verified that these coding sets satisfy the condition of Theorem 3.2 with $\mu = 2$ but they are not strongly isolating with index 2. Indeed it is clear that $\Omega_{2,3} \subset \Omega_{1,2}$.

Since strong isolability index is more desirable and it prevents incorrect detection and isolation, we will focus on strong isolability index. The next theorem illustrates how one can construct coding sets that have the strong isolability index $\mu < k - 1$.

Theorem 3.3. *Let $\Gamma_i, i \in \boldsymbol{p}$ be defined as the $k - \mu$ combinations of the set $\boldsymbol{k}$. Then the corresponding sets $\Omega_i, i \in \boldsymbol{k}$ defined as*

$$\Omega_i = \{j \in \boldsymbol{p} | i \in \Gamma_j\} \tag{3.10}$$

are strongly isolating with index μ.

Proof: Consider two different $1 \leq l, h \leq \mu$ combinations $i_1, ..., i_l$ and $j_1, ..., j_h$ of the set $\mathbf{k}$. In order to show that equation (3.8) holds it is sufficient to show that the

complement sets $\mathbf{p} - \Omega_{i_1 i_2 \ldots i_l}$ and $\mathbf{p} - \Omega_{j_1 j_2 \ldots j_h}$ are not equal where

$$\mathbf{p} - \Omega_{i_1 i_2 \ldots i_l} = \{j \in \mathbf{p} | i_k \notin \Gamma_j, \ \forall i_k \in \{i_1, \ldots, i_l\}\} \tag{3.11}$$

Assume that $l \leq h$. Since two combinations $i_1, \ldots, i_l$ and $j_1, \ldots, j_h$ are different, there exists $j_t \in \{j_1, \ldots, j_h\}$ such that $j_t \in \mathbf{k} - \{i_1, i_2, \ldots, i_l\}$. Since the sets $\Gamma_i, i \in \mathbf{p}$ are defined as $k - \mu$ combinations of the set $\mathbf{k}$ and $l \leq \mu$, there exists a combination Γ_j such that $j_t \in \Gamma_j$ and $i_k \notin \Gamma_j$, $\forall i_k \in \{i_1, \ldots, i_l\}$, therefore $j \notin \mathbf{p} - \Omega_{j_1 j_2 \ldots j_h}$ and $j \in \mathbf{p} - \Omega_{i_1 i_2 \ldots i_l}$ which shows that equation (3.11) holds. The combination Γ_j can be found by first selecting j_t and then selecting $k - \mu - 1$ elements from the set $\mathbf{k} - \{i_1, i_2, \ldots, i_l, j_t\}$. It is clear that since $l \leq \mu$, then $|\mathbf{k} - \{i_1, i_2, \ldots, i_l\}| \geq k - \mu$ and one can find the combination Γ_j. Similarly it can be shown that the coding sets Ω_i's satisfies conditions (3.9) and hence are strongly isolating.

In order to show that μ is the maximum number of combinations that satisfy equation (3.8), it should be noted that $|\mathbf{p} - \Omega_{i_1 i_2 \ldots i_l}| = C(k - l, k - \mu)$, therefore for $l > \mu$, the set $\mathbf{p} - \Omega_{i_1 i_2 \ldots i_l}$ is empty and for any different l combinations $i_1, \ldots, i_l$ and $j_1, \ldots, j_l$, we have $\Omega_{i_1 i_2 \ldots i_l} = \Omega_{j_1 j_2 \ldots j_l}$. ■

It can be shown for $\mu = 1$, the above coding sets results in the generalized residual set [5]. For simplicity, we mean isolability index as strongly isolability index and drop the term "strongly".

Theorem 3.4. *1. A necessary condition for the SFDIP problem for linear system* (2.1) *to have a solution for the above coding sets and a given family of fault signatures is that for each $\mu+1$ combination $L_{i_1}, \ldots, L_{i_{\mu+1}}$ of L_i's, $[L_{i_1}, \ldots, L_{i_{\mu+1}}]$ is full rank.*

2. A necessary condition for the SFDIP problem for nonlinear system (2.34) *to have a solution for the above coding sets and a given family of fault signatures is that for each $\mu + 1$ combination $l_{i_1}(x), \ldots, l_{i_{\mu+1}}(x)$ of $l_i(x)$'s, the dimension of distribution $\Delta = span[l_{i_1}(x), \ldots, l_{i_{\mu+1}}(x)]$ is $v_i = \sum_{j=1}^{\mu+1} k_{i_j}$.*

Proof:

1. If there exists a $\mu+1$ combination $L_{i_1}, ..., L_{i_{\mu+1}}$ of L_i's such that $[L_{i_1}, ..., L_{i_{\mu+1}}]$ is not full rank, then $\mathcal{L}_{i_{\mu+1}} \subset \sum_{j=1}^{\mu} \mathcal{L}_{i_j}$. It is evident that one of the sets Γ_i is equal to $\mathbf{k} - \{i_1, i_2, ..., i_\mu\}$ and $\mathcal{L}_{i_{\mu+1}} \subset S^*_{\Gamma_i}$.

2. Similarly if there exists a $\mu + 1$ combination $l_{i_1}(x), ..., l_{i_{\mu+1}}(x)$ of $l_i(x)$'s such that the dimension of distribution $\Delta = \text{span}[l_{i_1}(x), ..., l_{i_{\mu+1}}(x)]$ is less than $v_i = \sum_{j=1}^{\mu+1} k_{i_j}$, then there exists $x \in \mathcal{X}$ such that $l_{i_{\mu+1}}(x) \subset \Delta_i = \text{span}\{l_{i_1}(x), ..., l_{i_\mu}(x)\}$. It is evident that one of the sets Γ_i is equal to $\mathbf{k} - \{i_1, i_2, ..., i_\mu\}$ and $\text{span}\{l_{i_{\mu+1}}\} \subset (\Pi^*)^\perp = o.c.a.((\Sigma_*^{\Delta_i})^\perp)$. ■

The above necessary condition provides a test to determine the possible values of the isolability index for a family of fault signatures. For sake of subsequent further referencing, this coding scheme is designated as the <u>*coding scheme 1*</u>.

Theorem 3.5. *Let A, C and L_i be arbitrary matrices of dimensions $n \times n$, $q \times n$ and $n \times k_i$, respectively, then the SFDIP problem for linear system* (2.1) *generically has a solution for the coding sets of Theorem 3.3 if and only if*

1. *For each $\mu + 1$ combination $L_{i_1}, ..., L_{i_{\mu+1}}$ of L_i's let $v_i = \sum_{j=1}^{\mu+1} k_{i_j}$ and $v = \max_i v_i$, then*

$$v \leq n \tag{3.12}$$

2. *For each μ combination $L_{i_1}, ..., L_{i_\mu}$ of L_i's,*

$$\sum_{j=1}^{\mu} k_{i_j} < q \tag{3.13}$$

Proof: (only if) It readily follows that L_i's should satisfy Theorem 3.4, hence (3.12) is immediate. Moreover, if for a given combination $L_{i_1}, ..., L_{i_\mu}$ of L_i's, $q < \sum_{j=1}^{\mu} k_{i_j}$, then generically $S^*_{\Gamma_i} = \mathcal{X}$ for $\Gamma_i = \mathbf{k} - \{i_1, ..., i_\mu\}$, and therefore condition (3.13) is necessary.

(if) Inequality (3.12) implies that $L_i, i \in \mathbf{k}$ generically satisfies the necessary condition of Theorem 3.4. Also, inequality (3.13) implies that for any μ combination $L_{i_1}, ..., L_{i_\mu}$ of L_i's, generically $S^*_{\Gamma_i} = \sum_{j=1}^{\mu} \mathcal{L}_{i_j}$. Therefore, from Theorem 3.4 it follows that the SFDIP problem is generically solvable for the coding sets of Theorem 3.3.

■

The above coding scheme needs to generate $C(k, k-\mu)$ residuals for detection and isolation of μ concurrent faults. However, under certain special circumstances one can solve the problem with fewer number of residuals.

Theorem 3.6. *Assume that a given family of fault signatures can be categorized into m subsets $FL_1, FL_2, ..., FL_m$ such that*

1. *For $FL_i = \{L_{i_1}, L_{i_2}, ...L_{i_{b_i}}\}$, then $[L_{i_1}, ..., L_{i_{b_i}}]$ is not full rank.*
2. *Any $\mu_i + 1$ combination of fault signatures in FL_i is linearly independent.*

For each subset FL_i, $\Gamma_{ij}, j = 1, .., C(b_i, b_i - \mu_i)$ are defined as $b_i - \mu_i$ combinations of FL_i, then the coding sets Ω_i's are strongly isolating with index $\mu = \min_i \mu_i$.

Proof: It should be shown that for any two different $1 \leq l, h \leq \mu$ combinations $L_{i_1}, ..., L_{i_l}$ and $L_{j_1}, ..., L_{j_h}$, equation (3.8) holds. If both combinations are from one subfamily FL_k, then according to Theorem 3.3, equation (3.8) holds. If combinations are from different subfamilies then using the fact that for each two fault signatures L_i and L_j from two different subfamilies,

$$\Omega_i \cap \Omega_j = 0 \tag{3.14}$$

it follows that equation (3.8) holds. Let $L_{i_1}, ..., L_{i_{l_1}}$ and $L_{j_1}, ..., L_{j_{h_1}}$ be from a same subfamily FL_i and $L_{i_{l_1+1}}, ..., L_{i_l}$ and $L_{j_{h_1+1}}, ..., L_{j_h}$ be from a different subfamily

FL_j. Then using Theorem 3.3, we have

$$\Omega_{i_1,\ldots i_{l_1}} \neq \Omega_{j_1,\ldots j_{h_1}} \tag{3.15}$$

$$\Omega_{i_{l_1+1},\ldots i_l} \neq \Omega_{j_{h_1+1},\ldots j_h}$$

Also, using equation (3.14), we have

$$\Omega_{i_1,\ldots i_{l_1}} \cap \Omega_{j_{h_1+1},\ldots j_h} = 0 \tag{3.16}$$

$$\Omega_{i_{l_1+1},\ldots i_l} \cap \Omega_{j_1,\ldots j_{h_1}} = 0 \tag{3.17}$$

Therefore, it follows that

$$\Omega_{i_1,\ldots i_l} \neq \Omega_{j_1,\ldots j_h}$$

The same procedure can be used if $L_{i_1}, \ldots, L_{i_l}$ and $L_{j_1}, \ldots, L_{j_h}$ can be categorized into more than two subfamilies. ■

The same result can be derived for a nonlinear system with the family of fault signatures $l_i(x)$'s. For the coding sets of Theorem 3.6, the number of residuals are $p = \sum_{i=1}^{m} C(b_i, b_i - \mu_i)$ which may be much smaller than $C(k, \mu)$ when $\mu = \min_i \mu_i$.

Remark 3.2. *It should be noted that by utilizing the coding sets of Theorem 3.6, one may detect more than μ concurrent faults in cases where the faults are not all from one of the subfamilies FL_i's. For example, consider the two different $\mu_i + \mu_j$ combinations $L_{i_1}, \ldots, L_{i_{\mu_i+\mu_j}}$ and $L_{j_1}, \ldots, L_{j_{\mu_i+\mu_j}}$ such that $L_{i_1}, \ldots, L_{i_{\mu_i}}$ and $L_{j_1}, \ldots, L_{j_{\mu_i}}$ are from the same subfamily FL_i and $L_{i_{\mu_i+1}}, \ldots, L_{i_{\mu_i+\mu_j}}$ and $L_{j_{\mu_i+1}}, \ldots, L_{j_{\mu_i+\mu_j}}$ are from a different subfamily FL_j, then it follows that*

$$\Omega_{i_1,\ldots i_{\mu_i+\mu_j}} \neq \Omega_{j_1,\ldots j_{\mu_i+\mu_j}}$$

so that one can indeed detect and isolate these two combination of concurrent faults. The maximum number of concurrent faults that one can detect and isolate is $\sum_{i=1}^{m} \mu_i$, where only μ_i fault signatures are selected from the subfamily FL_i.

Theorem 3.7. *1. The SFDIP problem for linear system* (2.1) *has a solution for the coding sets of Theorem 3.6 and a given family of fault signatures if* $\mathcal{FL}_i \cap L_{k_j} = 0, \forall i, k_j$ *where* $\mathcal{FL}_i = \sum_{j=1}^{b_i} \mathcal{L}_{i_j}$ *and* $L_{k_j} \in FL_k, k \neq i$.

2. The SFDIP problem for nonlinear system (2.34) *has a solution for the coding sets of Theorem 3.6 and a given family of fault signatures if* $span l_{k_j}(x) \nsubseteq FL_i \ \forall i, k_j$ *where* $FL_i == span\{l_{i_1}(x), ..., l_{i_{b_i}}(x)\}$ *and* $l_{k_j} \in FL_k, k \neq i$.

Proof:

1. If there exists $L_{k_j} \in FL_k, k \neq i$ such that $\mathcal{FL}_i \cap L_{k_j} \neq 0$ for some $i \in \mathbf{m}$, then there exists a Γ_{kl} such that $k_j \in \Gamma_{kl}$, but since $\mathcal{FL}_i \cap L_{k_j} \neq 0$, then $L_{k_j} \cap S^*_{\Gamma_{kl}} \neq 0$, and therefore the SFDIP problem does not have a solution for Γ_{kl}.

2. The proof is similar to part 1 and is omitted. ■

The next example illustrates some details regarding the above coding scheme. For subsequent referencing, the coding scheme in Theorem 3.6 is designated as the <u>*coding scheme 2.*</u>

Example 3.1. *Consider the following family of fault signatures:*

$$FL = \begin{bmatrix} 1 & -0.5 & -0.5 & 0 & 0 & 0 & 0 & 0 \\ 0 & 0 & 0 & 0 & 1 & -0.5 & -0.5 & 0 \\ 0 & 0.5 & -0.5 & 0 & 0 & 0 & 0 & 0 \\ 0 & 0 & 0 & 0 & 0 & 0.5 & -0.5 & 0 \\ 0 & 0 & -0.5 & 0.5 & 0 & 0 & 0 & 0 \\ 0 & 0 & 0 & 0 & 0 & 0 & 0.5 & -0.5 \end{bmatrix} \tag{3.18}$$

One can categorize the above family into two sets FL_1 and FL_2 such that

$$FL_1 = \begin{bmatrix} 1 & -0.5 & -0.5 & 0 \\ 0 & 0 & 0 & 0 \\ 0 & 0.5 & -0.5 & 0 \\ 0 & 0 & 0 & 0 \\ 0 & 0 & -0.5 & 0.5 \\ 0 & 0 & 0 & 0 \end{bmatrix} = \begin{bmatrix} L_1 & L_2 & L_3 & L_4 \end{bmatrix} \tag{3.19}$$

$$FL_2 = \begin{bmatrix} 0 & 0 & 0 & 0 \\ 1 & -0.5 & -0.5 & 0 \\ 0 & 0 & 0 & 0 \\ 0 & 0.5 & -0.5 & 0 \\ 0 & 0 & 0 & 0 \\ 0 & 0 & 0.5 & -0.5 \end{bmatrix} = \begin{bmatrix} L_5 & L_6 & L_7 & L_8 \end{bmatrix} \tag{3.20}$$

where $\mu_1 = \mu_2 = 2$ and $b_1 = b_2 = 4$ as defined in Theorem 3.6. The sets Γ_{ij} are selected as $\Gamma_{11} = \{1,2\}$, $\Gamma_{12} = \{1,3\}$, $\Gamma_{13} = \{1,4\}$, $\Gamma_{14} = \{2,3\}$, $\Gamma_{15} = \{2,4\}$, $\Gamma_{16} = \{3,4\}$, $\Gamma_{21} = \{5,6\}$, $\Gamma_{22} = \{5,7\}$, $\Gamma_{23} = \{5,8\}$, $\Gamma_{24} = \{6,7\}$, $\Gamma_{25} = \{6,8\}$, and $\Gamma_{26} = \{7,8\}$. Utilizing the coding scheme of Theorem 3.6, one needs to generate only 12 residuals, whereas by utilizing the coding scheme of Theorem 3.3, $C(8,2) = 28$ residuals need to be generated. Moreover, by assuming that there are concurrent faults in L_1, L_2, L_5, L_6, then all residuals except r_{16} and r_{26} will be affected by this fault, with r_{ij} denoting the residual generated by Γ_{ij}. Therefore, one can detect and isolate the occurrence of 4 concurrent faults in these fault signatures.

3.3 Actuator Fault detection and Isolation in a Network of Unmanned Vehicles

In the following discussions, our proposed structured residual set is utilized to solve the actuator fault detection and isolation problem in a network of unmanned vehicles. We will investigate the development of and comparison among two architectures for FDI of actuator faults in the network of unmanned vehicles. Namely, we are interested in centralized and semi-decentralized configurations as described and defined in Sections 3.1.1 and 3.1.3, respectively.

3.3.1 Centralized Architecture

As pointed out in Section 3.1.1, system (3.4) is overactuated and the rank of $\bar{B}^O$ in system (3.4) is $a \times (N-1)$. Hence, the first step is to determine the possible isolability index of actuator fault signatures in the centralized architecture. It can be verified that the family of $a \times N$ fault signatures $\bar{L}^O_{kj}, k \in \mathbf{N},\ j \in \mathbf{a}$ satisfies the necessary condition of Theorem 3.4 with $\mu = N-2$ isolability index. If the SFDIP problem has a solution for the *coding scheme 1*, then one needs to generate $C(a \times N, N-2)$ residuals for detecting and isolating $N-2$ multiple faults. However, since matrix B is full rank and in view of the structure of the matrix $\bar{B}^O$, one can categorize the family of fault signatures into the following a subfamilies $FL_i, i \in \mathbf{a}$ such that $FL_i = \{\bar{L}^O_{ki}, k \in \mathbf{N}\}$ satisfies the condition of Theorem 3.6 with $b_i = N$ and $\mu_i = N-2$. In other words, each subfamily FL_i contains the fault signatures of the i-th actuator of all the vehicles. If the SFDIP problem has a solution for the *coding scheme 2*, then one needs to generate $a \times C(N, N-2) = a \times N \times (N-1)/2$ residuals for detecting and isolating $N-2$ multiple faults, which is much smaller than $C(a \times N, N-2)$. Moreover, according to Remark 3.2, one is able to detect multiple faults in <u>all</u> actuators of each vehicle since fault signatures of each vehicle

are in different subfamilies.

Theorem 3.8 presented below provides the necessary and sufficient conditions for generating the residual signals for the centralized architecture using the *coding scheme 2*. The following lemma is needed and will be used in the proof of this theorem.

Lemma 3.2. *Consider the following diagonal dynamical system*

$$\begin{aligned} \dot{x}(t) &= A^M x(t) + B^M u(t) + L^M m(t) \\ y(t) &= C^M x(t) \end{aligned} \tag{3.21}$$

where $L = [L_1, \cdots, L_a]$ *and* $M > 1$ *(*$A^M = I_M \otimes A$, $B^M = I_M \otimes B$, $L^M = I_M \otimes L$*). Let* $L_{ij}, i \in \boldsymbol{M} = \{1, ..., M\}, j \in \boldsymbol{k}$ *denote the* $(i-1) \times a + j$*-th column of* L^M*, then the family of fault signatures* L_{ij}*'s in* (3.21) *is strongly detectable if and only if the family of fault signatures* L_i*'s is strongly detectable in the following system*

$$\begin{aligned} \dot{x}(t) &= Ax(t) + Bu(t) + \sum_{k=1}^{a} L_k m_k(t) \\ y(t) &= Cx(t) \end{aligned} \tag{3.22}$$

Proof: The fault signatures L_{ij}'s are strongly detectable if and only if there exists (C^M, A^M) unobservability subspace $\mathcal{S}_{ij}^{M^*} = \inf \underline{\mathcal{S}}^M(\bar{\mathcal{L}}_{ij}^M)$ such that $\mathcal{S}_{ij}^{M^*} \cap \mathcal{L}_{ij} = 0$, where $\bar{L}_{ij}^M, i \in \mathbf{M}, j \in \mathbf{k}$ are obtained by setting the column L_{ij} of L^M to zero. By using Algorithms 2.1 and 2.3, it can be easily shown that $\mathcal{S}_{ij}^{M^*} = \text{diag}\{\mathcal{S}^*(\mathcal{L}), \mathcal{S}^*(\mathcal{L}), \cdots, \mathcal{S}^*(\bar{\mathcal{L}}_j), \cdots, \mathcal{S}^*(\mathcal{L})\}$ where $\bar{L}_j, j \in \mathbf{k}$ are obtained by setting the j-th column of L to zero and $\mathcal{S}^*(\mathcal{L}) = \inf \underline{\mathcal{S}}(\mathcal{L})$ is (C, A) unobservability subspace. Hence, $\mathcal{S}_{ij}^{M^*} \cap \mathcal{L}_{ij} = 0$ if and only if $\mathcal{S}^*(\bar{\mathcal{L}}_j) \cap \mathcal{L}_j = 0$, implying that L_j's should be strongly detectable. ■

We are now in the position to introduce our main theorem in this subsection.

Theorem 3.8. *The centralized SFDIP problem has a solution for the* coding scheme 2 *if and only if the actuator fault signatures* L_k*'s are strongly detectable for the system* (3.22).

Proof: According to Theorem 3.6, for each subfamily FL_i, the sets Γ_{ij} are defined as the 2-combination of N fault signatures corresponding to the i-th actuator of each vehicle. Therefore, each residual r_{ij} should only be affected by the i-th actuator fault signatures of the two vehicles and should be decoupled from all other actuator fault signatures. Since the observable state x^O is considered as the relative state of the vehicles with respect to the state of vehicle 1, we consider generating the residual signals r_{ij}'s such that the residual signal r_{ij} is affected by the i-th actuator of vehicle 1 and vehicle j and is decoupled from all other actuator fault signatures in the entire system. In generating such residual signals, system (3.4) can be rewritten as follows:

$$\begin{aligned} \dot{x}^O(t) &= A^{N-1}x^O(t) + B^{N-1}u^O(t) + L^{N-1}m^O(t) \\ \bar{z}(t) &= C^{N-1}x^O(t) \end{aligned} \tag{3.23}$$

where $u^O = [u_1^\top(t) - u_2^\top(t), \cdots, u_1^\top(t) - u_N^\top(t)]^\top$, $m^O(t) = [m_1^\top(t) - m_2^\top(t), ..., m_1^\top(t) - m_N^\top(t)]^\top$, and $m_i^\top(t) = [m_{i1}^\top(t), ..., m_{ia}^\top(t)]^\top$. Using the result of the Lemma 3.2, it is clear that the residual signals r_{ij}'s can be generated if and only if L_j's are strongly detectable in system (3.22). The same approach can be considered for generating the residual signals that are only affected by the i-th actuator fault signatures of vehicles $k, j \neq 1$ by rewriting the observable subsystem in terms of the relative states with respect to vehicle k. ■

In the next section, it is shown that by considering only "local" communication links among neighboring vehicles, the vehicles with more than one neighbor can detect and isolate not only their own faults but also faults of their neighboring vehicles.

3.3.2 Semi-decentralized Architecture

As pointed out in Section 3.1.3, the family of actuator fault signatures in the nodal model (3.7) is dependent and system (3.7) is also overactuated. It can be verified that the family of $a \times (|\mathrm{N}_i|+1)$ fault signatures $\bar{L}_{kj}^O$, $k = 1, ..., |\mathrm{N}_i|+1$, $j \in \mathbf{a}$ in system

(3.7) satisfies the necessary condition of Theorem 3.4 with the isolability index of $\mu = |\mathrm{N}_i| - 1$. If the SFDIP problem has a solution for the *coding scheme 1*, then one needs to generate $C(a \times (|\mathrm{N}_i| + 1), |\mathrm{N}_i| - 1)$ residuals for detecting and isolating $|\mathrm{N}_i| - 1$ multiple faults. However, since matrix B is full rank, and by considering the structure of the matrix $\bar{B}^O_{\mathrm{N}_i}$, one can categorize the family of fault signatures into the following a subfamilies $FL_j, j \in \mathbf{a}$ such that $FL_j = \{\bar{L}^O_{kj}, k = 1, ..., |\mathrm{N}_i| + 1\}$ satisfies the conditions of Theorem 3.6 with $b_j = |\mathrm{N}_i| + 1$ and $\mu_j = |\mathrm{N}_i| - 1$. If the SFDIP problem has a solution for the *coding scheme 2*, then one needs to generate $a \times C(|\mathrm{N}_i| + 1, |\mathrm{N}_i| - 1) = a \times (|\mathrm{N}_i| + 1) \times |\mathrm{N}_i|/2$ residuals for detecting and isolating $|\mathrm{N}_i| - 1$ multiple faults which is much less than $C(a \times (|\mathrm{N}_i| + 1), |\mathrm{N}_i| - 1)$. Moreover, according to Remark 3.2, vehicles with more than one neighbor are able to detect multiple faults in <u>all</u> their actuators since fault signatures of each vehicle are in different subfamilies.

Remark 3.3. *It should be noted that for the vehicles with only one neighbor ($|\mathrm{N}_i| = 1$), the isolability index is $\mu = 0$, which implies that one cannot isolate any fault in the vehicle and its neighbor. However, since the matrix B is full rank, one can still categorize the fault signatures into a subfamily $FL_j, j \in \mathbf{a}$ such that $FL_j = \{\bar{L}^O_{1j}, -\bar{L}^O_{1j}\}$. In this case according to the coding scheme 2, one needs to design a residual generators such that each one is affected by only one subfamily and is decoupled from others. By utilizing this coding scheme, one can isolate faults among actuators but cannot isolate between the vehicle and its only neighbor.*

The result of this subsection is now summarized in the following theorem.

Theorem 3.9. *The semi-decentralized SFDIP problem has a solution for the* coding scheme 2, *if the fault signatures L_k's are strongly detectable for the system* (3.22).

Proof: Proof is similar to that of Theorem 3.8 and is omitted.

According to Theorems 3.8 and 3.9, the solvability conditions for the FDI problem in the centralized and semi-decentralized architectures are the same. Therefore,

for vehicles with more than one neighbor, the same isolability performance will be achieved by using either scheme. However, in the semi-decentralized scheme the FDI algorithms are distributed among the vehicles and the computational load of each vehicle is much less than that of a centralized FDI unit.

In order to compare the total number of residuals that are necessary in the centralized and the semi-decentralized architectures, let us assume that each vehicle has at most two neighbors. This assumption is based on the fact that a vehicle having two neighbors can detect and isolate its own faults. With this assumption in mind, the total number of residuals in the semi-decentralized architecture is found to be at most $3aN$, which for $N > 7$ is less than the total number of residuals needed in the centralized architecture which is $a \times N \times (N-1)/2$. This shows that for a relatively "large" network of unmanned vehicles, that is for $N > 7$, the total computational load of the semi-decentralized architecture is also much less than the centralized approach.

It should be noted that in the semi-decentralized architecture, these residuals are distributed among all the vehicles. Moreover, by utilizing the semi-decentralized architecture, one can also reduce the practical limitations that are often imposed on the centralized architecture vis-á-vis computational bottlenecks and scarce communication bandwidth resources. Consequently, the semi-decentralized FDI algorithm is more scalable and flexible when compared to the centralized counterpart. Note that in the semi-decentralized architecture the communication overhead per each vehicle is higher than the centralized approach. However, one should also keep in mind that the efforts required (due to the presence of obstacles, limited line of sight, etc.) to maintain the communication links between each vehicle and the central FDI unit in the centralized approach are much higher than those needed to keep the communication links among only the neighboring vehicles in the semi-decentralized architecture.

3.3.3 Simulation Results For Formation Flight of Satellites

In this section, our proposed fault detection and isolation strategy is applied to an application area of significant strategic interest, namely the satellite precision formation flying problem [76,94]. For simulation studies, the relative motion of four satellites are configured with respect to a reference virtual satellite that is following a desired orbit and that can be approximated by linearizing the Keplerian orbital mechanics about this reference trajectory. These equations are known as the Hill-Clohessy-Wiltshire equation [142]. The equations of motion for each satellite about a circular reference orbit are governed by the following dynamics

$$\begin{aligned} \ddot{x} &= 3n^2x + 2n\dot{y} + u_x \\ \ddot{y} &= -2n\dot{x} + u_y \\ \ddot{z} &= -n^2z + u_z \end{aligned} \tag{3.24}$$

where x points in the radial direction, y points along the track, and z points out of the plane. The orbital rate is given by n. The vector $[u_x^\top,\ u_y^\top,\ u_z^\top]^\top$ represents external input accelerations due to the applied actuators thrust. It is assumed that each satellite can measure its relative position with respect to its neighboring satellites where in this example we have assumed $N_1 = \{2\}$, $N_2 = \{1, 3\}$, $N_3 = \{4\}$ and $N_4 = \{1\}$. The satellites are tasked to form a regular square. It is clear from equation (3.24) that the xy-dynamics are decoupled from the z-dynamics. Here, we only consider actuator faults in the xy-dynamics.

A multiple fault scenario is considered for simulations where four faults are injected in both actuators of satellites 2 and 4. Specially, (a) the x-direction and the y-direction actuators of satellite 4 are injected with a lock-in-place fault resulting in the actuators being locked at the values of $u_{41} = 0.1$ and $u_{42} = -0.1$ at $t = 10$ and $t = 15$ seconds, respectively, (b) an 80% loss of effectiveness fault is injected at the x-direction actuator of satellite 2 at $t = 20$ seconds, and (c) the y-direction actuator of satellite 2 is locked at the value of $u_{21} = 0.5$ at $t = 20$ seconds.

One can easily verify that the actuator fault signatures of each satellite are strongly detectable when each satellite has exact position measurements (that is $z_i = Cx_i$). Therefore, according to the Theorem 3.8 the centralized FDI architecture has a solution for the coding scheme 2 and the isolability index of the whole family of signatures is 2. Actuator fault signatures of all the satellites can be categorized into two sets $FL_1 = [\bar{L}^O_{11}, \bar{L}^O_{21}, \bar{L}^O_{31}, \bar{L}^O_{41}]$ and $FL_2 = [\bar{L}^O_{12}, \bar{L}^O_{22}, \bar{L}^O_{32}, \bar{L}^O_{42}]$, where $b_1 = b_2 = 4$, $\mu_1 = \mu_2 = 2$, and $\bar{L}^O_{ki}$ represents the fault signature of the i-th actuator of the k-th satellite in the observable part of the entire network. A total of 12 residuals $r_i, i = 1, ..., 12$ are needed for the coding scheme 2. The family of the coding sets for the above residual set and the family of fault signatures are as follows $\Omega^c_{11} = \{1, 2, 3\}$, $\Omega^c_{21} = \{1, 4, 5\}$, $\Omega^c_{31} = \{2, 5, 6\}$, $\Omega^c_{41} = \{3, 4, 6\}$, $\Omega^c_{12} = \{7, 8, 9\}$, $\Omega^c_{22} = \{7, 10, 11\}$, $\Omega^c_{32} = \{8, 11, 12\}$ and $\Omega^c_{42} = \{9, 10, 12\}$, where Ω^c_{ij} corresponds to the fault signature $\bar{L}^O_{ij}$.

In the semi-decentralized architecture, since satellites 1, 3 and 4 have only one neighbor, according to Remark 3.3 they can isolate faults among actuators but cannot isolate between themselves and their only one neighbor. By utilizing the coding scheme 2, two residuals r_{i1} and r_{i2} are designed for the i-th satellite ($i = 1, 3, 4$) where they are affected by faults in the x-direction actuator and the y-direction actuator of the satellite and its neighbor, respectively. However, since $|N_2| = 2$, satellite 2 not only can detect and isolate multiple faults in its own actuator but also it can detect and isolate faults in satellites 1 and 3. The actuator fault signatures of satellites 1, 2, and 3 can be categorized into two sets $FL_{21} = [\bar{L}^O_{11}, \bar{L}^O_{21}, \bar{L}^O_{31}]$ and $FL_{22} = [\bar{L}^O_{12}, \bar{L}^O_{22}, \bar{L}^O_{32}]$, where $b_1 = b_2 = 3$, $\mu_1 = \mu_2 = 1$, and $\bar{L}^O_{ki}$ represents the fault signature of the i-th actuator of the k-th satellite in the observable part of the nodal model of satellite 2. Based on the coding scheme 2, six residual signals $r_{2j}, j = 1, ..., 6$ are needed for satellite 2. Therefore, in the semi-decentralized architecture, a total of 12 residuals should be generated. Residual

evaluation function for each residual is selected as an instantaneous value of the residual, i.e. $J_{r_i} = r_i$. A uniformly random noise (5%) is added to the relative distance measurements (representing the sensor noise). By considering the worst case analysis of the residuals corresponding to the healthy operation of the satellites that are subject to measurement noise, a threshold value of ± 0.1 is selected for all the residual signals for fault detection and isolation logic evaluation and analysis. The family of the coding sets for satellite 2 is as follows: $\Omega_{11} = \{21, 22\}$, $\Omega_{21} = \{21, 23\}$, $\Omega_{31} = \{22, 23\}$, $\Omega_{12} = \{24, 25\}$, $\Omega_{22} = \{24, 26\}$, and $\Omega_{32} = \{25, 26\}$, where Ω_{ij} corresponds to the fault signature $\bar{L}^{O}_{ij}$.

Figures 3.1 and 3.2 show the residuals corresponding to the considered fault scenario for the centralized architecture. As shown in this figure, faults in the x and y direction actuators of satellite 4 can be detected and isolated using Ω^c_{41} and $\Omega^c_{41} \cup \Omega^c_{42}$ at $t = 10.5$ and $t = 16.4$ seconds, respectively. The occurrence of faults in the x and y direction actuators of satellite 2 can be detected and isolated using $\Omega^c_{21} \cup \Omega^c_{41} \cup \Omega^c_{42}$, and $\Omega^c_{21} \cup \Omega^c_{22} \cup \Omega^c_{41} \cup \Omega^c_{42}$ at $t = 20.5$ and $t = 25.6$ seconds, respectively. Figures 3.3 and 3.3 show the residuals that are generated by using our detection filters associated with the considered fault scenario for the semi-decentralized architecture. As shown in this figure, satellite 2 can detect and isolate the fault in its x-direction actuator at $t = 20.5$ seconds by using the coding set Ω_{21}, and the fault in its y-direction actuator at $t = 25.8$ seconds by using the coding set $\Omega_{21} \cup \Omega_{22}$, but satellites 1, 3, and 4 can only detect the occurrence of faults in both actuators of the satellites and cannot isolate among the satellites. It should be noted that all the residual signals in both centralized and semi-decentralized architectures are generated according to the geometric approach in Chapter 2.

Based on the above results one can conclude that for satellites with more than one neighbor (satellite 2 in the above formation example) the detection and isolation performance of the centralized and the semi-decentralized architectures are

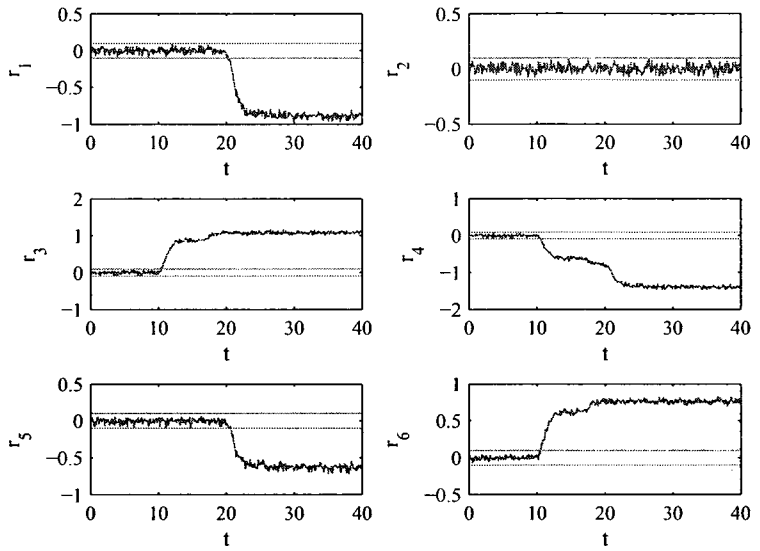

Figure 3.1: The residuals corresponding to multiple fault scenario $r_1, ...r_6$ (centralized architecture).

similar (multiple faults in all their actuators can be detected and isolated). However, in the semi-decentralized architecture the FDI algorithm is distributed among the satellites. This results in an approach that is more robust and fault-tolerant to complete failure of a central FDI unit that is generally placed in one of the satellites (a single point of failure).

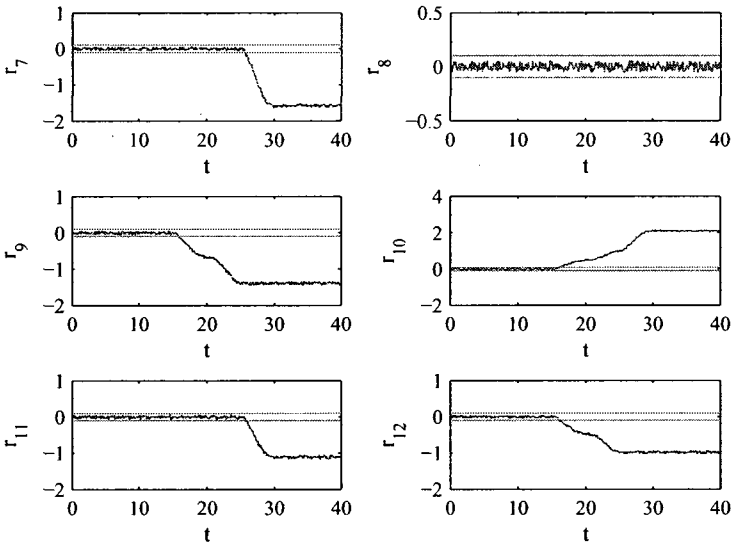

Figure 3.2: The residuals corresponding to multiple fault scenario $r_7, ..., r_{12}$ (centralized architecture).

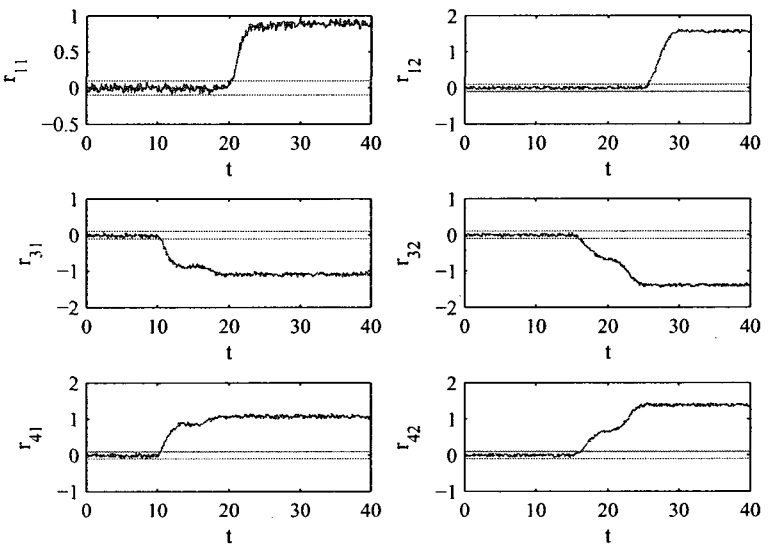

Figure 3.3: The residuals corresponding to multiple fault scenario (semi-decentralized architecture).

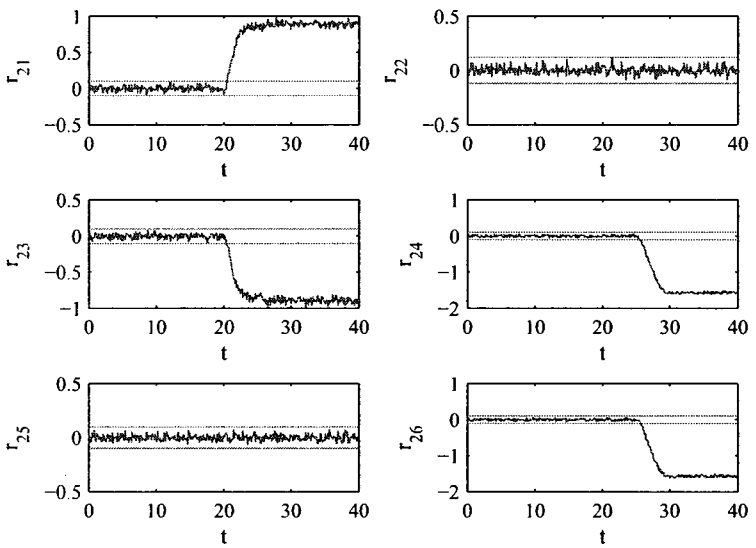

Figure 3.4: The residuals corresponding to multiple fault scenario (semi-decentralized architecture).

3.4 Fault Detection and Isolation of F-18 HARV

To demonstrate the effectiveness of our proposed fault detection and isolation strategy for overactuated systems, we consider actuator faults in an F-18 High Angle of Attack Research Vehicle (HARV) [143]. For simplicity, a linear longitudinal motion is considered. The state vector is defined as $x^{\top} = [v, \alpha, q, \theta]$, where v represents a change in the forward speed of the aircraft, α represents a change in the angle of attack, q represents a change in the pitch rate and θ represents a change in the pitch angle. There are six independent input channels, namely, (1) δ_{TH}: throttle change (2) δ_{TV}: thrust vectoring change (3) δ_{STAB}: change in stabilator, (4) δ_{ASYM}: change in symmetrical aileron, (5) δ_{LEF}: change in leading edge flap deflection and (6) δ_{TEF}: change in trailing edge flap deflection.

The aircraft is assumed to be flying at the Mach number of 0.24 at an altitude of 15000ft which corresponds to a steady forward speed of 239 ft/s. The equilibrium flight path angle is 0° and the angle of attack is 25°. The state equation corresponding to this flight condition is given by :

$$\dot{x} = Ax + Bu, y = x \tag{3.25}$$

where

$$A = \begin{bmatrix} -0.075 & -24.05 & 0 & -32.16 \\ -0.0009 & -0.196 & 0.9896 & 0 \\ -0.0002 & -0.1454 & -0.1677 & 0 \\ 0 & 0 & 1.0 & 0 \end{bmatrix}$$

$$B = \begin{bmatrix} -1.15 & 0 & -2.482 & 0.0393 & -2.466 & 4.32 \\ -0.01 & -0.005 & -0.0136 & 0 & -0.018 & -0.008 \\ -0.335 & -0.035 & -0.408 & -0.0006 & -0.042 & 0.0135 \\ 0 & 0 & 0 & 0 & 0 & 0 \end{bmatrix}$$

and

$$u = \begin{bmatrix} \delta_{TH} & \delta_{TV} & \delta_{STAB} & \delta_{ASYM} & \delta_{LEF} & \delta_{TEF} \end{bmatrix}$$

According to Theorem 3.4, the possible value of isolability index for this system is 2. One can check that the observability subspaces of Theorem 3.3 also exist for $p = 2$, and therefore in addition to detecting faults in each input channel, one can also detect concurrent faults in two input channels. Based on the coding scheme 1, a total of 15 ($C(6,2)$) residuals may be generated such that each is decoupled from 2 input channels. It can be verified that the fault signatures cannot be categorized according to the coding scheme 2.

By considering the maximum value or the worst case scenario of residuals corresponding to the normal mode of the system subject to measurement noise and taking into account some safety margins, a threshold value of 0.1 was considered for all the residuals. The coding sets for the above fault signatures are as follows

$$\Omega_1 = \{6, 7, 8, 9, 10, 11, 12, 13, 14, 15\}$$

$$\Omega_2 = \{2, 3, 4, 5, 10, 11, 12, 13, 14, 15\}$$

$$\Omega_3 = \{1, 3, 4, 5, 7, 8, 9, 13, 14, 15\}$$

$$\Omega_4 = \{1, 2, 4, 5, 6, 8, 9, 11, 12, 15\}$$

$$\Omega_5 = \{1, 2, 3, 5, 6, 7, 9, 10, 12, 14\}$$

$$\Omega_6 = \{1, 2, 3, 4, 6, 7, 8, 10, 11, 13\}$$

where Ω_i corresponds to the fault signatures of the i-th actuator.

First, we consider that there is a hard over fault in the input channel $u_5 = \delta_{LEF}$ at $t = 50$ sec. Figure 3.5 depicts the residual outputs corresponding to this fault scenario. According to these figures, one can detect and isolate this fault using the coding set Ω_5. Next, we consider a 60% loss of effectiveness in the input channel $u_6 = \delta_{TEF}$ at $t = 50$ sec. Figure 3.6 shows the residual outputs corresponding to this

fault scenario. According to this figure one can clearly detect this fault using Ω_6. Finally, we consider concurrent hard over faults in the two input channels, namely $u_2 = \delta_{TH}$ at $t = 50$ and $u_5 = \delta_{LEF}$ at $t = 70$ sec. Figures 3.7 shows the residual outputs corresponding to this scenario. According to these plots, one can detect and isolate these concurrent faults based on the coding set $\Omega_2 \cup \Omega_5$.

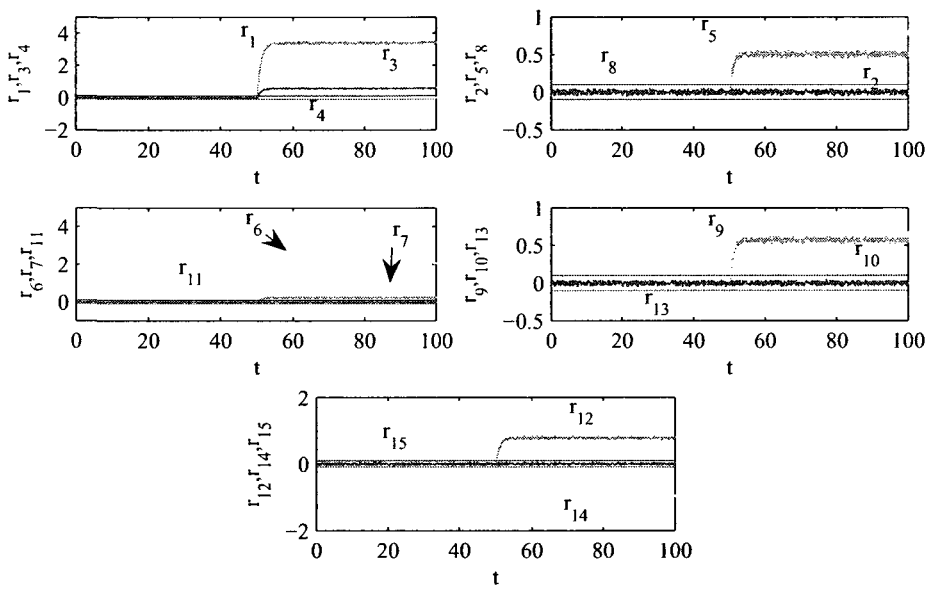

Figure 3.5: Residual outputs corresponding to the hard-over fault in the leading edge flap deflection.

3.5 Fault Detection and Isolation of Redundant Reaction Wheels

Let $\mathcal{F}_o$ denote the inertial frame with origin $O \in \mathcal{R}^3$ and $\mathcal{F}_b$ a moving body frame whose origin O_i is at the mass center of the spacecraft. The attitude kinematics may be described by quaternion $q = (\hat{q}^\top, q_4)$. The attitude and angular velocity of the spacecraft with respect to the inertial frame $\mathcal{F}_o$ can be described by the following

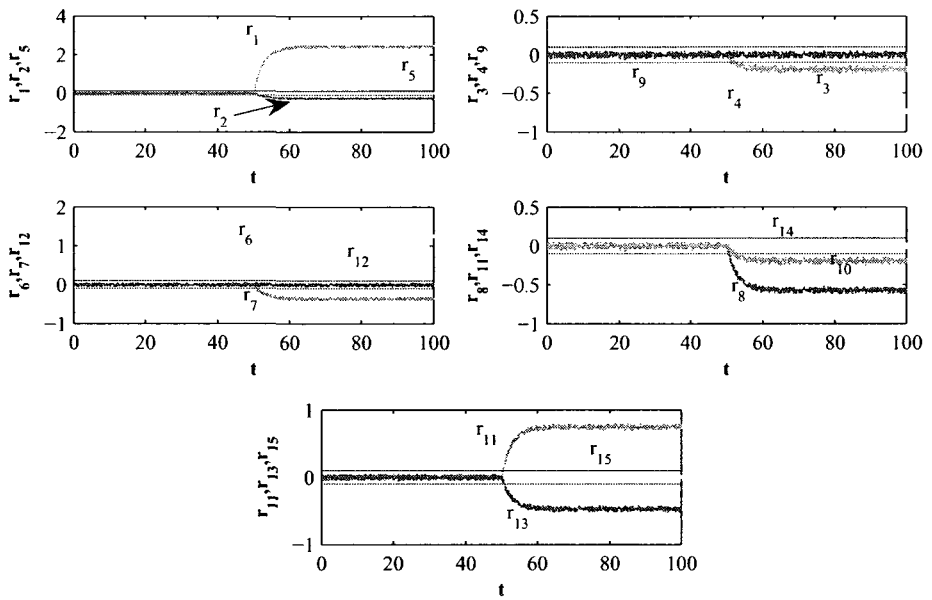

Figure 3.6: Residual outputs corresponding to 60% loss of effectiveness in the trailing edge flap deflection.

quaternion equation [1]

$$\begin{aligned} \frac{{}^{o}d\hat{q}}{dt} &= \frac{q_4\omega - \omega \times \hat{q}}{2} \\ \frac{q_4}{dt} &= -\frac{\omega \cdot \hat{q}}{2} \end{aligned} \tag{3.26}$$

and the Euler equation

$$\begin{aligned} \frac{{}^{o}d(I\omega + h)}{dt} &= \tau_d \\ I\frac{{}^{b}d\omega}{dt} + \omega \times (I\omega + h) &= -\dot{h} + \tau_d \end{aligned} \tag{3.27}$$

where $q^{\top} = (\hat{q}^{\top}, q_4)$ denotes the unit quaternion, I is the tensor of inertia in the body frame $\mathcal{F}_b$, h is the angular momentum of wheels, and τ_d is the external disturbance torque associated with the spacecraft.

Let $h_i, (i = 1, 2, 3, 4)$ denotes the angular momentum of the ith reaction wheel and $h_w = [h_1, h_2, h_3, h_4]^{\top}$, then the relationship between h and h_w is given by

$$h = Ah_w \tag{3.28}$$

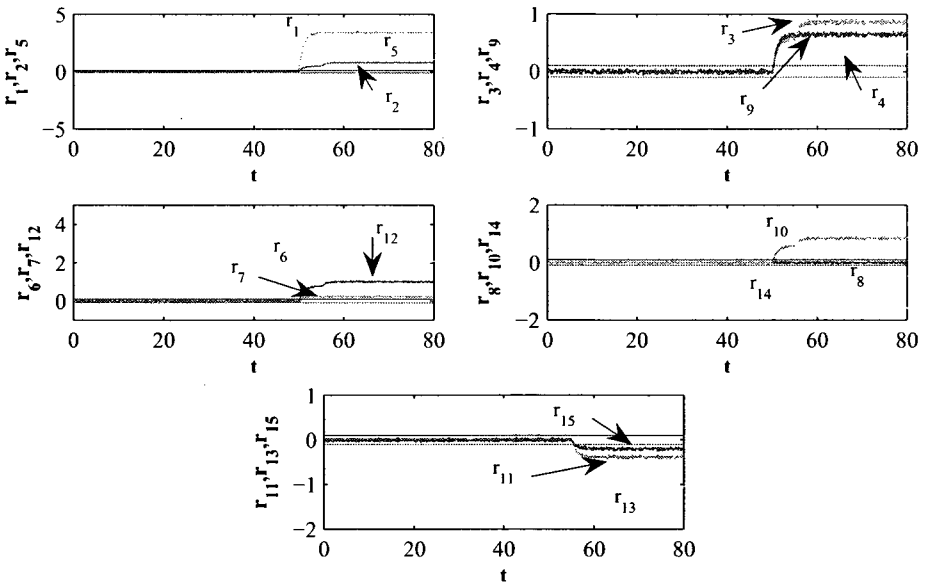

Figure 3.7: Residual outputs corresponding to concurrent hard over faults in the throttle and trailing edge flap deflection.

where $A \in \mathcal{R}^{3\times 4}$ is the configuration matrix of the reaction wheels. As shown in Figure 3.8, four wheels in a tetrahedron configuration were employed where A is given by [1]

$$A = \begin{bmatrix} \sqrt{\frac{1}{3}} & \sqrt{\frac{1}{3}} & -\sqrt{\frac{1}{3}} & -\sqrt{\frac{1}{3}} \\ \sqrt{\frac{2}{3}} & -\sqrt{\frac{2}{3}} & 0 & 0 \\ 0 & 0 & -\sqrt{\frac{2}{3}} & \sqrt{\frac{2}{3}} \end{bmatrix} \tag{3.29}$$

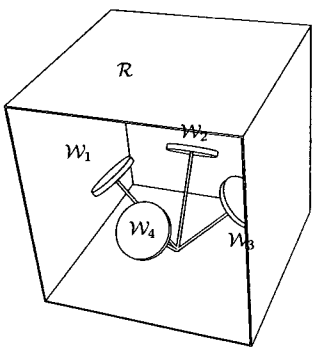

Figure 3.8: Gyrostat with four reaction wheels in a tetrahedron configuration [1].

By substituting equation (3.28) in equation (3.27), we have

$$I\frac{^b d\omega}{dt} + \omega \times (I\omega + Ah_w) = -Au + \tau_d \tag{3.30}$$

where the control input is $u = \dot{h}_w$. We further assume that the following output measurements are available:

$$y = \begin{bmatrix} \omega \\ h_w \end{bmatrix} \tag{3.31}$$

The main problem that we are addressing is how one can detect and isolate faults in the redundant reaction wheels. We can rewrite equation (3.30) as

$$\begin{aligned} \dot{\omega} &= f(\omega) + \sum_{i=1}^{4} g_i u_i + \tau_d \\ y &= \omega \end{aligned} \tag{3.32}$$

where

$$\begin{aligned} f(\omega) &= -I^{-1}(\omega \times (I\omega + Ah_w)), \\ g_1 &= I^{-1}\begin{bmatrix} \sqrt{\frac{1}{3}} \\ \sqrt{\frac{2}{3}} \\ 0 \end{bmatrix}, g_2 = I^{-1}\begin{bmatrix} \sqrt{\frac{1}{3}} \\ -\sqrt{\frac{2}{3}} \\ 0 \end{bmatrix} \\ g_3 &= I^{-1}\begin{bmatrix} -\sqrt{\frac{1}{3}} \\ 0 \\ -\sqrt{\frac{2}{3}} \end{bmatrix}, g_4 = I^{-1}\begin{bmatrix} -\sqrt{\frac{1}{3}} \\ 0 \\ \sqrt{\frac{2}{3}} \end{bmatrix} \end{aligned}$$

According to Theorem 3.4, one can check that the possible value of the isolability index for the above system is 2. Thus one should try to generate $C(4,2) = 6$ residual signals $r_i(t), i = 1, ..., 6$. The sets Γ_i's for having the isolability index of 2 can be found from Theorem 3.3 (coding scheme 1) as $\Gamma_1 = \{3,4\}$, $\Gamma_2 = \{2,4\}$, $\Gamma_3 = \{2,3\}$, $\Gamma_4 = \{1,4\}$, $\Gamma_5 = \{1,3\}$, $\Gamma_6 = \{1,2\}$ and the corresponding coding sets are $\Omega_1 = \{4,5,6\}$, $\Omega_2 = \{2,3,6\}$, $\Omega_3 = \{1,3,5\}$, and $\Omega_4 = \{1,2,3\}$.

Next, the observability codistributions of Theorem 2.6 for the above coding set are obtained by using the algorithm proposed in [60] as follows

$$\Pi^*_{\Gamma_1} = \text{span}\{d\omega_3\}$$

$$\Pi^*_{\Gamma_2} = \text{span}\{d(-0.8165\omega_1 + 0.4619\omega_2 + 0.3464\omega_3\}$$

$$\Pi^*_{\Gamma_3} = \text{span}\{d(0.8165\omega_1 - 0.4619\omega_2 + 0.3464\omega_3\}$$

$$\Pi^*_{\Gamma_4} = \text{span}\{d(-0.8165\omega_1 - 0.4619\omega_2 + 0.3464\omega_3\}$$

$$\Pi^*_{\Gamma_5} = \text{span}\{d(0.8165\omega_1 + 0.4619\omega_2 + 0.3464\omega_3\}$$

$$\Pi^*_{\Gamma_6} = \text{span}\{d(\omega_2)\}$$

where it is assumed that the inertia matrix is $I = \text{diag}\{5, 4, 3\}$. It is easy to verify that the necessary conditions (2.47) of Theorem 2.6 are satisfied and the SFDIP problem has a solution for the above system with a isolability index of 2. According to the above observability codistributions, the following set of new states can be found:

$$z_1 = \omega_3$$

$$z_2 = -0.8165\omega_1 + 0.4619\omega_2 + 0.3464\omega_3$$

$$z_3 = 0.8165\omega_1 - 0.4619\omega_2 + 0.3464\omega_3$$

$$z_4 = -0.8165\omega_1 - 0.4619\omega_2 + 0.3464\omega_3$$

$$z_5 = 0.8165\omega_1 + 0.4619\omega_2 + 0.3464\omega_3$$

$$z_6 = \omega_2$$

The state space representation of the satellite attitude dynamics may now be expressed in the new coordinates as follows:

$$\dot{z}_1 = \frac{1}{3}(\omega_1\omega_2 + \omega_2 h_{w_1} - \omega_1 h_{w_2} + \sqrt{\frac{2}{3}}(u_4 - u_3))$$

$$\dot{z}_2 = -0.8165(\frac{1}{5}(\omega_2\omega_3 + \omega_3 h_{w_2} - \omega_2 h_{w_3})) + 0.4619(\frac{1}{4}(-2\omega_1\omega_3 - \omega_3 h_{w_1} + \omega_1 h_{w_3}))$$
$$+ 0.3464(\frac{1}{3}(\omega_1\omega_2 + \omega_2 h_{w_1} - \omega_1 h_{w_2})) + 0.1886(u_4 - u_2)$$

$$\dot{z}_3 = 0.8165(\frac{1}{5}(\omega_2\omega_3 + \omega_3 h_{w_2} - \omega_2 h_{w_3})) - 0.4619(\frac{1}{4}(-2\omega_1\omega_3 - \omega_3 h_{w_1} + \omega_1 h_{w_3}))$$
$$+ 0.3464(\frac{1}{3}(\omega_1\omega_2 + \omega_2 h_{w_1} - \omega_1 h_{w_2})) + 0.1886(u_2 - u_3)$$
$$\dot{z}_4 = -0.8165(\frac{1}{5}(\omega_2\omega_3 + \omega_3 h_{w_2} - \omega_2 h_{w_3})) - 0.4619(\frac{1}{4}(-2\omega_1\omega_3 - \omega_3 h_{w_1} + \omega_1 h_{w_3}))$$
$$+ 0.3464(\frac{1}{3}(\omega_1\omega_2 + \omega_2 h_{w_1} - \omega_1 h_{w_2})) + 0.1886(u_4 - u_1)$$
$$\dot{z}_5 = 0.8165(\frac{1}{5}(\omega_2\omega_3 + \omega_3 h_{w_2} - \omega_2 h_{w_3})) - 0.4619(\frac{1}{4}(-2\omega_1\omega_3 - \omega_3 h_{w_1} + \omega_1 h_{w_3}))$$
$$+ 0.3464(\frac{1}{3}(\omega_1\omega_2 + \omega_2 h_{w_1} - \omega_1 h_{w_2})) + 0.1886(u_1 - u_3)$$
$$\dot{z}_6 = \frac{1}{4}(-2\omega_2\omega_3 - \omega_3 h_{w_1} + \omega_1 h_{w_3} + \sqrt{\frac{2}{3}}(u_1 - u_2))$$

where

$$\begin{bmatrix} h_{w_1} \\ h_{w_2} \\ h_{w_3} \end{bmatrix} = A h_w \tag{3.33}$$

The next step is to design observers for generating the estimated states $\hat{z}_1$, $\hat{z}_2$, $\hat{z}_3$, $\hat{z}_4$, $\hat{z}_5$, and $\hat{z}_6$, and subsequently define the residuals as $r_i = z_i - \hat{z}_i$, $i \in \{1, ..., 6\}$.

The simulation results of our proposed nonlinear FDI scheme when applied to the attitude dynamics of a satellite are presented below. The circular dawn-dusk sun synchronous orbit with a 6pm ascending node and 650 km altitude has been considered for simulations. The satellite is subjected to four disturbance torques, namely: gravity gradient, solar radiation, the Earth's magnetic field, and aerodynamic torque. Table 3.1 shows the characteristics of these disturbance torques for the selected orbit. The Earth observation mission is considered for the satellite with pointing accuracy of 0.5 degree in all the three axes. According to the mission requirements and disturbances, a PD controller has been designed for the satellite. One of the common faults in the reaction wheel is the loss of effectiveness due to bus voltage drop or friction [68, 69, 73, 144, 145] which can be modeled as:

$$u_{true} = k u_c, \qquad , 0 \leq k < 1 \tag{3.34}$$

where u_{true} and u_c denote the actual output and controller command of the reaction wheel, respectively.

Table 3.1: Orbital Disturbances

Disturbances	Magnitude	Constant/cyclic
Gravity gradient	$3.006e-8$ N.m	Constant
Solar radiation	$5.468e-6$ N.m	Constant
The Earth's magnetic field	$4.568e-5$ N.m	Cyclic
Aerodynamic torque	$7.008e-7$ N.m	Constant

Figure 3.9 shows the residuals corresponding to the normal operation of the satellite. According to this figure, the residuals are cyclic due to disturbances. First, we consider a 20% loss of effectiveness in the reaction wheel #3. Figure 3.10 depicts the residuals corresponding to this fault scenario. As shown in this figure, the residuals are still cyclic, but the magnitude of the residuals is increased due to the fault. This cyclic feature of the residuals will make the fault decision making process more difficult. To remedy this problem, the L_2 norm of the residuals in each orbit was considered for deciding on the fault detection and isolation tasks. Figure 3.11 shows the L_2 norm of the residuals corresponding to the healthy mode where the norm are reset when the satellite passes the perigee of its orbit. According to Figure 3.11 different threshold values have been chosen for each residual as shown in Table 3.2. Figure 3.12 depicts norm of the residuals corresponding to the 20% loss of effectiveness fault in the reaction wheel #3, and one can easily detect and isolate the fault in this reaction wheel using the coding set Ω_3. Finally, a concurrent fault scenario was also considered for the reaction wheels #1 and #3. Figures 3.13 and 3.14 show the residuals and their norms corresponding to this faulty scenario. As shown in Figure 3.14, all residuals except r_2 exceed their threshold and based on the coding set $\Omega_1 \cup \Omega_3$ one can detect and isolate both faults in these reaction wheels.

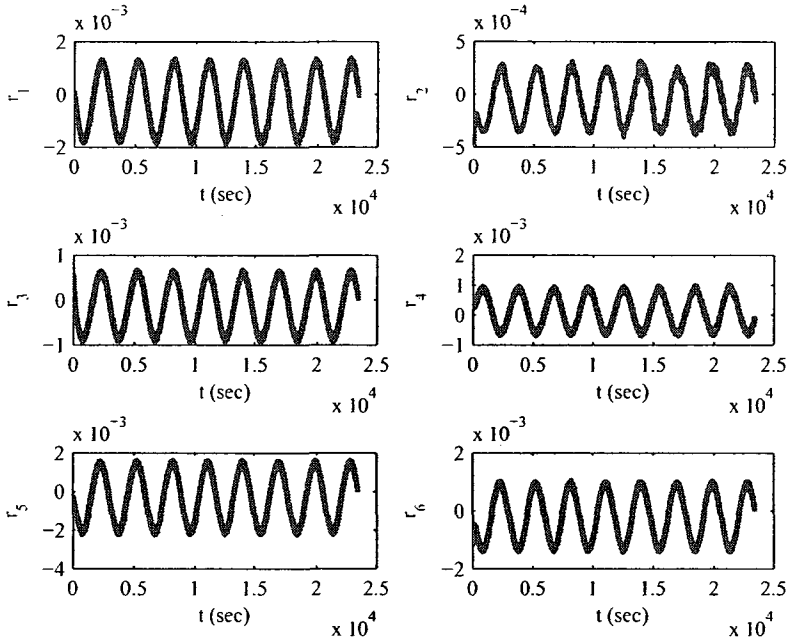

Figure 3.9: Residuals corresponding to the normal mode (Healthy operation).

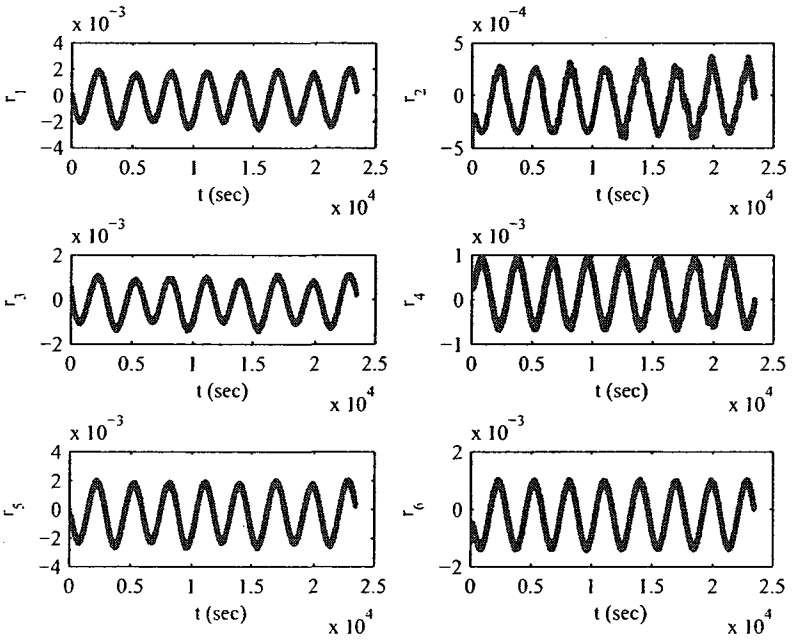

Figure 3.10: Residuals corresponding to a 20% loss of effectiveness in the reaction wheel #3.

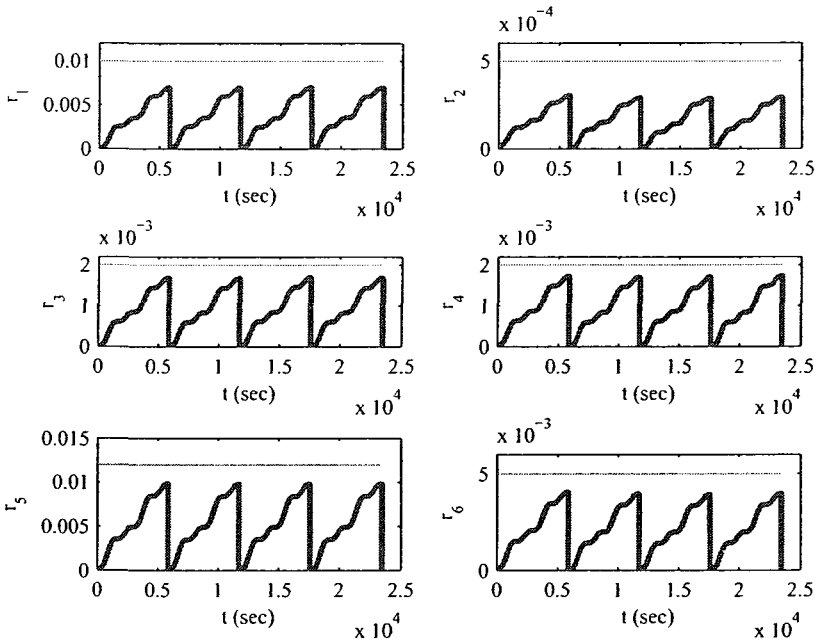

Figure 3.11: Residual L_2 norm corresponding to the normal mode.

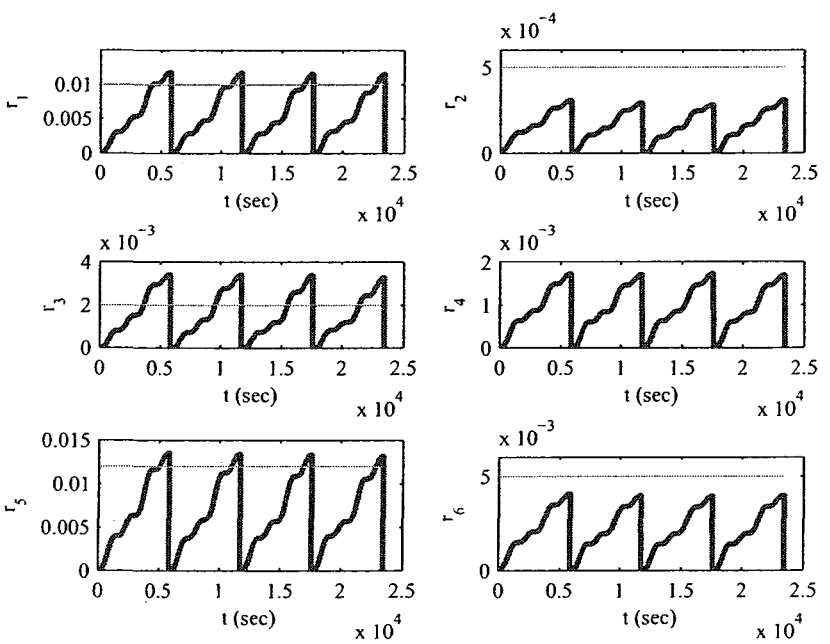

Figure 3.12: Residual L_2 norm corresponding to a 20% loss of effectiveness in the reaction wheel # 3.

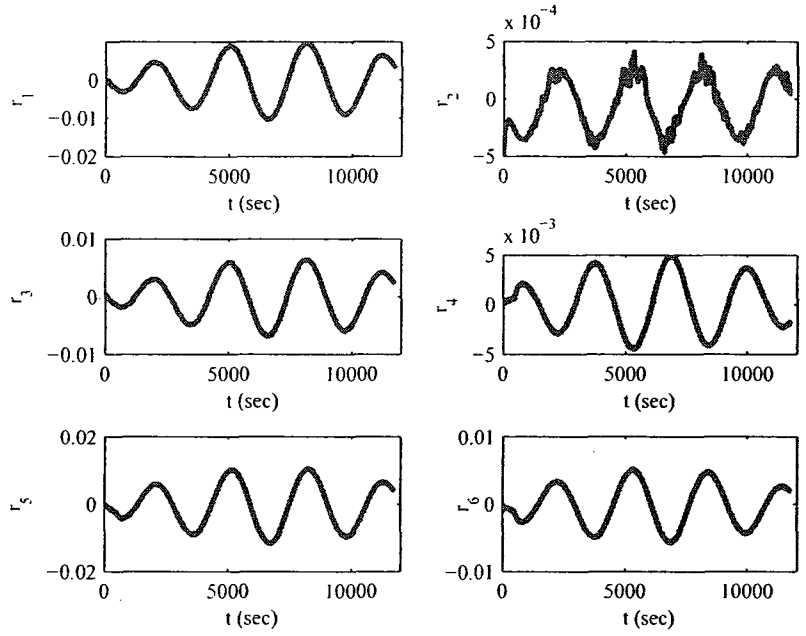

Figure 3.13: Residual corresponding to a 40% loss of effectiveness in the reaction wheel #3 and 50% loss of effectiveness in reaction wheel #1.

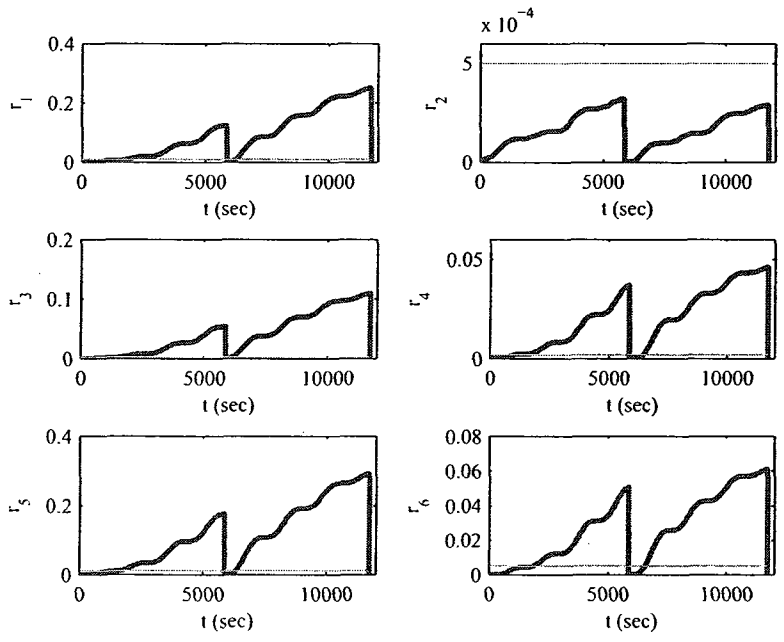

Figure 3.14: Residuals L_2 norm corresponding to 40% loss of effectiveness in the reaction wheel #3 and 50% loss of effectiveness in the reaction wheel #1.

Table 3.2: Residual threshold values

Residuals	Threshold Value
r_1	0.01
r_2	0.0005
r_3	0.002
r_4	0.002
r_5	0.012
r_6	0.005

3.6 Conclusions

In this chapter, new structured residual sets are designed and developed for both linear and nonlinear systems with dependent fault signatures, The notion of a isolability index is formally defined for these systems and necessary and sufficient conditions for the coding sets to achieve a specific isolability index is obtained. Our proposed residual set is applied to three case studies, namely, actuators FDI in F-18 HARV aircraft, actuator FDI in a satellite with redundant reaction wheel and the FDI problem in a network of unmanned vehicles. Three FDI architectures, namely, centralized, decentralized and semi-decentralized, are considered for a network of unmanned vehicles. Simulation results are also presented to illustrate and demonstrate the effectiveness of our proposed approach.

Chapter 4

A Robust Fault Detection and Isolation Scheme with a Disturbance Decoupling Property

In this chapter, the actuator fault detection and isolation problem for a network of unmanned vehicles subject to large input disturbances is considered. One of the main challenges in the design of FDI algorithms is to distinguish the effect of disturbances from faults and develop a robust FDI scheme without compromising the detection of incipient faults in the vehicles. In unmanned vehicles such UAV's, this problem is more challenging due to the small size feature and more sensitivity of them with respect to disturbances such as wind gust. In this chapter, we try to design a robust FDI algorithm by developing a hybrid fault detection and isolation scheme for both linear and nonlinear systems that are subject to large environmental disturbances.

This chapter is organized as follows. We begin with a brief literature review. In Section 4.2, we formulate the FDI problem for both linear and nonlinear systems subject to external disturbances. In Section 4.2.1, a systematic way for generating

a novel set of residuals in the hybrid FDI scheme is presented. In Section 4.2.2, we discuss the residual evaluation functions required for our hybrid FDI scheme. A discrete-event system (DES) fault diagnoser is presented in Section 4.2.3. In Sections 4.3 and 4.4, our proposed hybrid FDI algorithm is applied to actuators fault detection and isolation in a network of unmanned vehicles (linear systems) and an Almost-Lighter-Than-Air-Vehicle (ALTAV) (nonlinear systems), respectively.

Contributions

The main contributions of this chapter are now summarized below:

- A novel hybrid FDI scheme is introduced for designing a robust FDI algorithm for both linear and nonlinear systems subject to large disturbances.
- A robust hybrid FDI algorithm is developed for a network of unmanned vehicles.

4.1 Introduction

One of the important issues in the model-based FDI is robustness against uncertainties and modeling errors. Since a perfectly accurate and complete mathematical model of a physical system is never available and parameters of the system may vary with time in an uncertain manner, there is always a mismatch between the actual process and its mathematical model even when there is no process faults and this discrepancies cause fundamental difficulties in FDI application. Therefore, the effect of modeling uncertainties is the most crucial point in the model-based FDI concepts. Various robust model-based FDI techniques have been developed in the literature. These include Unknown Input Observer (UIO) approach [38, 146–148], eigenstructure assignment [149–151], optimal parity relation for robust FDI [152–154], frequency domain design and H_∞ optimization FDI approach [155–157]. A comprehensive treatment of robust FDI is presented in [6].

In UIO robust FDI approach, disturbances and model uncertainties are modeled as an additive disturbance in the state space representation of the system. Model uncertainties include interconnecting terms in large scale systems, nonlinear terms in system dynamics, terms arising from time-varying system dynamics, linearization and model reduction errors, and parameters variations. In this approach an observer is designed whose estimation error converges to zero regardless of an unknown input (disturbance) in the system. The remaining design degree of freedom is used for fault detection and isolation purposes. In the eigenstructure assignment robust FDI, a direct approach to design disturbance decoupled residuals is developed where the residual signal is decoupled from disturbance while the state estimation error may not be decoupled from it. The existing conditions for an eigenstructure assignment could be relaxed when compared with those required for UIO.

In the optimal parity relation approach, two objective functions for the design of parity relations are defined. The optimization objectives are the minimization of effects due to the modeling uncertainty and the maximization of fault effects. These lead to a multi-objective optimization problem which is solved by forming a mixed objective function optimization problem. In this approach the uncertainty is considered as bounded parameter variations and set of possibilities for system parameters within their bounds is considered to describe multiple models of the system. In an H_∞ optimization approach one tries to keep the sensitivity of the residual signal to unknown inputs (disturbances) less than a specific bound while increase the sensitivity of the residual signal to the fault over a frequency range of the fault. Different methods can be used to achieve the above criteria such as coprime factorization, LMI method, and H_∞ filtering based on algebraic Riccati equation. The main difference between the UIO and the eigenstructure approaches with parity relation and H_∞ approaches is in the first two approaches, one seeks to decouple the effect of unknown inputs from the residual signals. However, in the

second pair of robust approaches, effects of unknown inputs on residual signals are attenuated. Therefore, solvability conditions of the second pair of approaches are generally more relaxed when compared to the first two approaches.

In all the above approaches, the modeling uncertainties and errors are considered as unknown inputs and one seeks to decouple or attenuate the effects of them on residuals. An alternative approach [158, 159] is to consider structured model uncertainty in the system and design a robust fault detection filter for the system with such structured uncertainty. However, in this approach prior choice of a nominal model can lead to suboptimal solutions in all situations in which a nominal plant model is not easily identifiable or is not available. To remedy this problem, recently [160, 161], has developed robust fault detection filters for systems with polytopic model uncertainty based on an H_∞ optimization approach.

In another research direction, discrete-event based fault diagnosis approaches [162–164] attempt to represent the nominal and the faulty-system behaviors in the form of event trajectories, and as a result design fault diagnosers to estimate the current status of the system. This abstraction may result in the loss of information that can be critical to the task of fault isolation. Recently, hybrid fault diagnosis approaches have been investigated for complex dynamical systems whose behavior is modeled as a hybrid system. In [165], fault diagnosis of a continuous-time system with embedded supervisory controllers subject to abrupt, partial and full failure of components is investigated as a model selection problem. Reference [166] presents an online model-based diagnosis methodology for parametric faults in hybrid systems, which is based on tracking hybrid behavior (for both continuous-time and discrete-event behaviors). In [121] a discrete-event system diagnosis approach is presented for abrupt parametric faults in continuous-time systems based on qualitative abstraction of the system behavior.

In this chapter, a novel hybrid FDI algorithm for both linear and nonlinear

systems that are subject to large environmental disturbances is developed. Many modern systems such as aircraft and balloons are expected to operate in harsh environments where large disturbances (wind gust) may be present. One of the main challenges in designing a robust FDI algorithm for these systems is to determine how to distinguish between large environmental disturbances and faults or failures.

Towards the above end, a hybrid architecture for a robust FDI is introduced that is composed of a bank of continuous-time residual generators and a DES fault diagnoser. First a set of residual signals is generated based on the coding set introduced in Chapter 3 for a family of fault signatures with a given detectability index. Two threshold levels are assigned to the residual signals. It is further assumed that the input disturbances can be categorized into two families, namely, the tolerable disturbance inputs and the large and unexpected disturbances. A first level of threshold is selected such that the tolerable disturbance inputs do not generate any false alarms using the residual signals. Next, a complementary set of residual signals is generated by considering the effects of the disturbances on the first set of generated residual signals. A DES fault diagnoser is then designed to invoke an appropriate combination of the residual signals and their sequential features to not only detect and isolate faults and guarantee no false alarms subject to large external disturbance signals but also to detect and identify the occurrence of large external disturbances. It should be emphasized that our proposed FDI approach performs simultaneous robust fault detection and isolation as well as large and unexpected disturbances detection without imposing any limitations on the total number of faults that can be detected and isolated. In contrast, in the previous FDI algorithms developed in [49, 60, 167], robustness against disturbance inputs is achieved by limiting the number of possible faults that can be present in the system. Our proposed hybrid FDI algorithm is subsequently applied to the actuators fault detection and isolation problem in a network of unmanned vehicles as well as an

Almost-Lighter-Than-Air-Vehicle (ALTAV).

4.2 Hybrid FDI approach

Consider the following linear system

$$\begin{aligned} \dot{x}(t) &= Ax(t) + Bu(t) + \sum_{i=1}^{k} L_i m_i(t) + \sum_{j=1}^{P} P_j \omega_j(t) \\ y(t) &= Cx(t) + v(t) \end{aligned} \tag{4.1}$$

and the nonlinear system

$$\begin{aligned} \dot{x} &= f(x) + g(x)u + \sum_{i=1}^{k} l_i(x) m_i + \sum_{j=1}^{P} p_j(x) \omega_j \\ y &= h(x) + v \end{aligned} \tag{4.2}$$

where $\omega_j \in \mathbb{R}^{P_j}$ denotes the disturbance input , v represents the measurement noise and L_i and $l_i(x)$ represent fault signatures. It is assumed that $\omega_j, v \in \mathfrak{L}^p[0, \infty]$ for some $1 \leq p \leq \infty$ where $\mathfrak{L}^p[0, \infty]$ denotes the space of $\mathfrak{L}^p$ norm bounded signals, i.e. $||\omega||_p < \infty$.

Assumption 4.1. *The disturbance inputs are categorized into two types, namely tolerable disturbance signals* $\mathfrak{D}_1 = \{\omega \in \mathfrak{L}^p[0, \infty] \mid ||\omega||_p < \delta_1\}$ *and large and unexpected disturbance signals* $\mathfrak{D}_2 = \{\omega \in \mathfrak{L}^p[0, \infty] \mid \delta_1 \ll ||\omega||_p < \delta_2\}$ *where* $\delta_1 \ll \delta_2$.

Assumption 4.2. *The faults and the large disturbance inputs do not occur simultaneously and there exists a sufficient time separating the occurrence of a fault and the disturbance.*

The objective of this chapter is to design a Hybrid Fault Diagnoser (HFD) for detecting and isolating each fault m_i while guaranteeing that the diagnoser remains robust with respect to both types of disturbances. In other words, no false alarms should be generated due to disturbance signals. The hybrid fault diagnoser

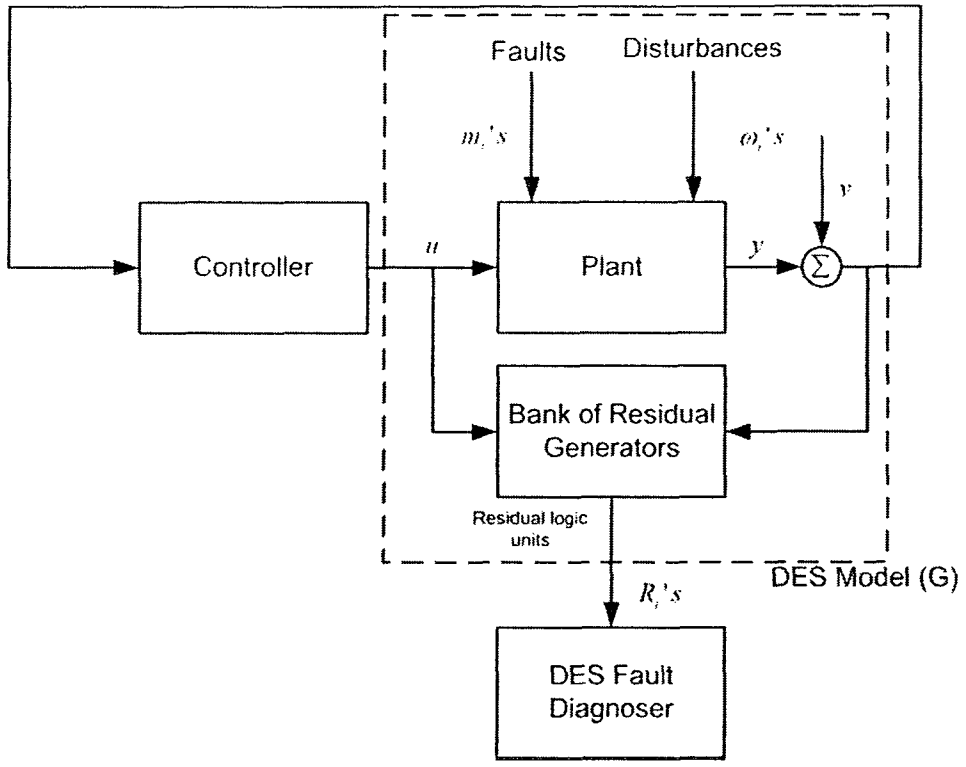

Figure 4.1: General architecture of our proposed hybrid diagnoser.

is composed of two modules, namely, a low-level bank of residual generators and a high level DES diagnoser. The bank of continuous-time residual generators produces first a set of residual signals based on the geometric FDI approach. It then compares, using an evaluation function, each residual signal to its corresponding threshold value, from which a set of residual logic units is generated. Two levels of thresholds are needed for certain residual signals (this will be discussed in more details subsequently). The DES diagnoser module is a finite-state automaton that takes the residual logic units as inputs and estimates the current state of the system. For designing such a DES diagnoser, the combined plant and the bank of residual generators is modeled as a finite state Moore automaton (G). The general architecture of our proposed hybrid fault diagnoser is shown in Figure 4.1.

Remark 4.1. *One possible approach to design a robust FDI algorithm for system* (4.1) *(*(4.2)*) is to generate a set of residual signals [3] ([60]) that each residual*

is affected by only one fault and is decoupled from all other faults and all the disturbances. If such a set of residual signals exist, then one can robustly detect and isolate faults despite the presence of disturbances. Under these circumstances, there will be no need to have a hybrid structure for the fault diagnoser. However, such a set of residual signals may not always exist due to presence of multiple faults that can occur in the system.

In the following sections, the procedure for designing a hybrid fault diagnoser composed of a bank of residual generators and a DES diagnoser is described in details.

4.2.1 Bank of Continuous-Time Residual Generators

In this section, a systematic approach is proposed to design a set of residual generators that provides the necessary information required by the DES diagnoser. Towards this end, two sets of residual signals are developed. The first set is generated according to the coding set that is introduced in Chapter 3 for a family of fault signatures with a given detectability index. The hybrid fault diagnoser (HFD) developed below is guaranteed to remain robust with respect to both tolerable disturbance inputs $\omega_i \in \mathfrak{D}_1$ and measurement noise v by selecting appropriate threshold values associated with this first set of residual signals. To ensure that the HFD is also robust to large disturbance inputs ($\omega_i \in \mathfrak{D}_2$), a second set of complementary residuals is generated so that the DES fault diagnoser, by utilizing the entire set of residual signals, will robustly detect and isolate a fault.

In the following, we assume that the detectability index of L_i's ($l_i(x)$'s) is $\mu \leq k$ (which includes strong detectability). Therefore, the SFDIP problem has a solution for the coding scheme Ω_i's with detectability index of μ, and a set of residuals $r_i, i \in \Xi_1 = \{1, ..., \xi\}$ can be generated ($\xi = C(k, \mu)$ for the coding scheme 1). We denote $\mathfrak{R}_1 = \{r_i, i \in \Xi_1\}$. Let Λ_i denote the set of disturbance signatures

P_j's ($p_j(x)$'s) that affects the residual r_i. In other words, for linear system (4.1),

$$\Lambda_i = \{j \in \mathbf{P} | \mathcal{P}_j \cap \mathcal{S}^*_{\Gamma_i} = 0\}, \quad i \in \Xi_1 \tag{4.3}$$

and for nonlinear system (4.2)

$$\Lambda_i = \{j \in \mathbf{P} | \operatorname{span}\{p_j(x)\} \not\subseteq (\Pi^*_{\Gamma_i})^{\perp}\}, \quad i \in \Xi_1 \tag{4.4}$$

where $\mathcal{S}^*_{\Gamma_i}$ and $\Pi^*_{\Gamma_i}$ are defined in Theorems 2.3 and 2.6, respectively.

Assume that one can generate a set of complementary residuals $\mathfrak{R}_2 = \{r_{\xi+i}, i \in \Xi_1\}$ such that $r_{\xi+i}$ is decoupled from the disturbance inputs specified by Λ_i but is affected by all the faults $m_l, l \in \Gamma_i$ and possibly other fault modes. Necessary and sufficient conditions for generating such complementary residual signals will be derived below in Theorems 4.1 and 4.2.

For each disturbance input $\omega_j \in \mathbf{P}$ and fault mode $m_i, i \in \mathbf{k}$, the coding sets Ω^p_j and Ω^f_i denote a set of residuals that are affected by ω_j and m_i, respectively. It is clear that $\Omega_i \subset \Omega^f_i, i \in \mathbf{k}$. The following two lemmas will be used subsequently to design our proposed DES fault diagnoser.

Lemma 4.1. ***a)*** *The coding sets Ω^p_i and Ω^f_j are distinct, i.e. $\Omega^p_i \neq \Omega^f_j, i \in \boldsymbol{P}, j \in \boldsymbol{k}$, and* ***b)*** *The coding sets Ω^f_i and $\Omega^f_j, i \neq j$ are distinct, i.e. $\Omega^f_i \neq \Omega^f_j, i, j \in \boldsymbol{k}$, $i \neq j$.*

Proof: a) First we consider the disturbances ω_j, $j \in \mathbf{P}$ such that $j \in \Lambda_i$ for some $i \in \Xi_1$ (ω_j affects at least one of the residuals $r_i \in \mathfrak{R}_1$). Since the residual $r_{\xi+i}$ is decoupled from ω_j and is affected by all the faults $m_i, i \in \Gamma_i$, we have $\xi + i \notin \Omega^p_j$ and $\xi + i \in \Omega^f_l$, $l \in \Gamma_i$. Hence, we have $\Omega^p_j \neq \Omega^f_l$, $l \in \Gamma_i$. Moreover, for all m_l, $l \in \mathbf{k}$ such that $l \notin \Gamma_i$, we have $i \in \Omega^p_j$ and $i \notin \Omega^f_l$; hence $\Omega^p_j \neq \Omega^f_l$, $l \notin \Gamma_i$. Therefore, $\Omega^p_j \neq \Omega^f_i, i \in \mathbf{k}$. Next we consider the disturbances ω_j, $j \in \mathbf{P}$ such that $j \notin \cup_{i=1}^{\xi} \Lambda_i$, i.e. disturbance inputs that do not affect any of the residuals $r_i, i \in \Xi_1$. Therefore, we have $i \notin \Omega^p_j, \forall i \in \Xi_1$. However, for any $j \in \mathbf{k}$, there exists at least one residual signal $r_l \in \mathfrak{R}_1$ ($l \in \Xi_1$) such that $l \in \Omega^f_j$; hence $\Omega^p_j \neq \Omega^f_i, i \in \mathbf{k}$.

b) Given the procedure in Chapter 3 for generating the residual signals r_i, $i \in \Xi_1$, we conclude that $\Omega_i \neq \Omega_j$, $i, j \in \mathbf{k}$, $i \neq j$. Let us define a new set Υ_i^f according to $\Upsilon_i^f = \Omega_i^f \cap \{\xi + 1, ..., 2\xi\}$, $i \in \mathbf{k}$. Consequently, we can write $\Omega_i^f = \Omega_i \cup \Upsilon_i^f, i \in \mathbf{k}$. Since $\Omega_i \cap \{\xi + 1, ..., 2\xi\} = 0$, $i \in \mathbf{k}$, it follows that $\Omega_i^f \neq \Omega_j^f$, $i, j \in \mathbf{k}$, $i \neq j$. ■

For each fault $m_i, i \in \mathbf{k}$, the set Υ_i^f represents the complementary residuals $r_i \in \mathfrak{R}_2$ that are affected by m_i, i.e. $\Upsilon_i^f = \{j \in \{\xi + 1, ..., 2\xi\} \mid r_j \in \Omega_i^f\}$. The above lemma ensures that the occurrence of faults and disturbances can be uniquely distinguished.

Assumption 4.3. *For disturbance inputs ω_j such that $j \notin \bigcup_{i=1}^{\xi} \Lambda_i$, it is assumed that $\Omega_j^p = \emptyset$.*

The disturbances which satisfy Assumption 4.3 have no effect on the residuals, and therefore the hybrid diagnoser does not need to be robust to them. In other words, the generated set of residuals are already decoupled from these disturbances and no further invoking of the DES diagnoser is required.

Lemma 4.2. *Consider the sets Υ_i^f as defined above, then $\Omega_j^p \neq \Upsilon_i^f$, $i \in \boldsymbol{k}, j \in \boldsymbol{P}$.*

Proof: For the disturbance inputs $\omega_j \in \mathbf{P}$ such that $j \in \Lambda_i$ for some $i \in \mathbf{k}$, the proof follows along the same lines as that in proof of part a) of Lemma 4.1. According to Assumption 4.3, for the disturbance inputs that do not affect any of the residual signals $r_i \in \mathfrak{R}_1$ we have $\Omega_j^p = \emptyset$. Since $i + k \in \Upsilon_i^f$, then $\Omega_j^p \neq \Upsilon_i^f$. ■

As will be demonstrated in Section 4.2.3, the above lemma guarantees that one can distinguish between the occurrence of low severity faults and the disturbances. Based on the geometric framework presented in Chapter 3 for both linear and nonlinear systems, the next two theorems provide the necessary and sufficient conditions for existence of the residuals $r_i \in \mathfrak{R}_2$ for linear and nonlinear systems, respectively. Note that the necessary and sufficient conditions for generating the residuals $r_i \in \mathfrak{R}_1$ are presented in Theorems 2.3 for linear systems.

Theorem 4.1. *The residual signals $r_i \in \mathfrak{R}_2$ can be generated if and only if*

$$\mathcal{S}^*_{\xi+i} \cap \mathcal{L}_j = 0, \quad j \in \Gamma_i, i \in \Xi_1 \tag{4.5}$$

where $\mathcal{S}^*_{\xi+i} = \inf \underline{\mathcal{S}}(\sum_{j\in\Lambda_i} \mathcal{P}_j)$

Proof: The proof follows from Theorem 2.3 and is omitted. ■

Theorem 4.2. *The residual signals $r_i \in \mathfrak{R}_1 \cup \mathfrak{R}_2$ can be generated if and only if there exist observability codistributions $\Pi^*_{\Gamma_i} = o.c.a.((\Sigma_*^{\mathcal{L}_{\Gamma_i}})^\perp), i = 1, ..., 2\xi$ where*

$$\mathcal{L}_{\Gamma_i} = span\{l_j(x), j \notin \Gamma_i\}, \quad i \in \Xi_1 \tag{4.6}$$

$$\mathcal{L}_{\Gamma_{\xi+i}} = span\{p_j(x), j \in \Lambda_i\}, \quad i \in \Xi_1 \tag{4.7}$$

such that

$$span\{l_j\} \not\subseteq [\Pi^*_{\Gamma_i}]^\perp, \quad i \in \Xi_1 \tag{4.8}$$

$$span\{l_j\} \not\subseteq [\Pi^*_{\Gamma_{\xi+i}}]^\perp, \quad i \in \Xi_1 \tag{4.9}$$

for all $j \in \Gamma_i$.

Proof: The proof follows from Theorem 2.6 and is omitted. ■

Remark 4.2. *For a system where $\Lambda_i = \Lambda, i \in \boldsymbol{k}$, in other words when the set of disturbances that affects all the residuals $r_i \in \mathfrak{R}_1$ are the same, only a single extra residual $r_{\xi+1}$ is sufficient for designing our hybrid FDI scheme. According to Theorem 4.2, the residuals can be generated for the nonlinear system if and only if there exist observability codistributions $\Pi^*_{\Gamma_i} = o.c.a.((\sum_*^{\mathcal{L}_i})^\perp), i = 1, ..., \xi + 1$ where*

$$\mathcal{L}_{\Gamma_i} = span\{l_j(x), j \notin \Gamma_i\}, \quad i \in \Xi_1 \tag{4.10}$$

$$\mathcal{L}_{\Gamma_{\xi+1}} = span\{p_j(x), j \in \Lambda\} \tag{4.11}$$

such that $span\{l_j\} \not\subseteq [\Pi^*_{\Gamma_i}]^\perp$ for $j \in \Gamma_i, i \in \Xi_1$, and $span\{l_j\} \not\subseteq [\Pi^*_{\Gamma_{\xi+1}}]^\perp$ for $j \in \boldsymbol{k}$. The same result can be derived for linear systems.

In the following example, we demonstrate how to construct and generate the above set of residual signals for a given nonlinear system.

Example 4.1. *Consider a nonlinear system that has 3 fault signatures and one disturbance input as governed by the following dynamics*

$$\dot{x}_1 = -x_1x_2 + m_1 + exp(x_2)m_2 + 2m_3 + \omega_1$$
$$\dot{x}_2 = -x_1^2 - 2\frac{x_2}{x_1}m_1 + m_2 + 0.5m_3 - 0.2\omega_1$$

with the output measurement $y = [x_1, x_2]^\top$. *It is clear that the above family of fault signatures does not satisfy the necessary condition* (2.29), *and hence it is* <u>*not*</u> *strongly detectable. Now we show that the detectability index for the above fault signatures is 1, i.e.* $\mu = 1$. *First we generate the coding sets that are required for the family of fault signatures with* $\mu = 1$. *Towards this end, the sets* $\Gamma_i, i = 1, 2, 3$ *are selected as 2 combinations of the set* $\{1, 2, 3\}$, *namely* $\Gamma_1 = \{1, 2\}$, $\Gamma_2 = \{1, 3\}$ *and* $\Gamma_3 = \{2, 3\}$. *The corresponding coding sets* Ω_i, $i = 1, 2, 3$ *are given by* $\Omega_1 = \{1, 2\}$, $\Omega_2 = \{1, 3\}$ *and* $\Omega_3 = \{2, 3\}$ *and the number of residuals is* $\xi = C(3, 1) = 3$. *Our next step involves checking the solvability conditions for the SFDIP problem. According to Theorem 2.6, one needs first to obtain unobservability codistributions* $\Pi^*_{\Gamma_i}, i = 1, 2, 3$. *These codistributions are found by using the algorithm that is presented in [168] and are given as follows*

$$\Pi^*_{\Gamma_1} = span\{d(x_1^2x_2)\}$$
$$\Pi^*_{\Gamma_2} = span\{d(x_1 - exp(x_2))\}$$
$$\Pi^*_{\Gamma_3} = span\{d(x_1 - 4x_2)\}$$

It can be verified that the necessary conditions (2.27) *are satisfied, and hence the detectability index for the above family of fault signatures is 1. We are now ready to design the residual generators. Towards this end, the* z_1*-subsystem* (2.41) *for each*

unobservability codistribution is obtained as follows:

$$\Pi^*_{\Gamma_1}: \begin{cases} \dot{z}_1 = -2\frac{z_1^2}{y_2} - y_2^4 + (2\frac{z_1}{y_2}exp(\frac{z_1}{y_2^2}) + y_2^2)m_2 \\ \qquad + (4\frac{z_1}{y_2} + 0.5y_2^2)m_3 + (2\frac{z_1}{y_2} - 0.2y_2^2)\omega_1 \\ y_1 = z_1 \end{cases}$$

$$\Pi^*_{\Gamma_2}: \begin{cases} \dot{z}_1 = -(z_1 + exp(y_2))y_2 + (1 - 2\frac{y_2}{z_1+exp(y_2)}exp(y_2))m_1 \\ \qquad - exp(y_2)(z_1 + exp(y_2))^2 + (2 - 0.5exp(y_2))m_3 + (1 - 0.2exp(y_2))\omega_1 \\ y_1 = z_1 \end{cases}$$

$$\Pi^*_{\Gamma_3}: \begin{cases} \dot{z}_1 = -(z_1 + 4y_2)y_2 + 4(z_1 + 4z_2)^2 + (1 + 8\frac{y_2}{z_1+4y_2})m_1 \\ \qquad + (exp(y_2) - 4)m_3 + 0.2\omega_1 \\ y_1 = z_1 \end{cases}$$

The residual generators can easily be designed from the above system of equations since the state z_1 is measurable. It follows that $\Lambda_i = \Lambda = \{1\}$ (the disturbance input ω_1 affects all residual signals r_i, $i = 1, 2, 3$) and according to Remark 4.2, only one extra residual signal is required. To generate this residual, one needs to find $\Pi^*_{\Gamma_4}$ that is given by

$$\Pi^*_{\Gamma_4} = span\{d(x_1 + 5x_2)\}$$

The corresponding z_1-subsystem is governed by the dynamics:

$$\Pi^*_{\Gamma_4}: \begin{cases} \dot{z}_1 = -(z_1 - 5y_2)y_2 - 10(z_1 - 5y_2)^2 + (1 - 10\frac{y_2}{z_1-5y_2})m_1 \\ \qquad + (exp(y_2) + 5)m_2 + 4.5m_3 \\ y_1 = z_1 \end{cases}$$

Consequently, by using the above z_1-subsystems, the coding sets Ω_1^p and Ω_i^f, $i = 1, 2, 3$ are determined as follows: $\Omega_1^p = \{1, 2, 3\}$, $\Omega_1^f = \{1, 2, 4\}$, $\Omega_2^f = \{1, 3, 4\}$, and $\Omega_3^f = \{2, 3, 4\}$. It is easy to show that these coding sets satisfy Lemmas 4.1 and 4.2, where $\Upsilon_i^f = \{4\}$, $i = 1, 2, 3$.

It should be noted that since the above family of fault signatures is <u>not</u> strongly detectable, the method proposed in [60] <u>cannot</u> be applied to this system. Moreover, as

a comparison with some methods in the literature that consider disturbances as faults [49, 60, 167], if the disturbance input ω_1 is treated as the fourth fault, the detectability index for the new family of fault signatures (four faults) is 1, implying that one cannot detect the concurrent occurrence of a fault and a disturbance. However, as will be shown subsequently, our proposed hybrid FDI algorithm enables one to detect a single fault in the system while a large disturbance input is applied through ω_1.

In the next section, a residual evaluation criteria is introduced for the generated residuals set $\mathfrak{R}_1 \cup \mathfrak{R}_2$.

4.2.2 Residual Evaluation Criteria

Corresponding to each residual signal $r_i \in \mathfrak{R}_1 \cup \mathfrak{R}_2$, an evaluation function is now assigned. Various evaluation functions have been introduced in the literature [132]. For the residual signals $r_i \in \mathfrak{R}_1$, two different thresholds are needed as specified below

$$J^1_{th_i} = \sup_{v \in \mathfrak{L}_p, \omega \in \mathfrak{D}_1, m_j = 0, j \in \mathbf{k}} (J_{r_i}), \quad i \in \Xi_1 \tag{4.12}$$

$$J^2_{th_i} = \sup_{v \in \mathfrak{L}_p, \omega \in \mathfrak{D}_2, m_j = 0, j \in \mathbf{k}} (J_{r_i}), \quad i \in \Xi_1 \tag{4.13}$$

In determining the first threshold, only tolerable disturbance inputs ($\omega_i \in \mathfrak{D}_1$) are considered. However, the second threshold incorporates all the possible disturbance inputs.

Remark 4.3. *It should be noted that one may choose to only consider the threshold level given by $J^2_{th_i}$ as a worst case scenario associated with large disturbances. In this case, no false alarms will be generated due to disturbances. However, this leads to selection of higher threshold values that would unnecessarily reduce the sensitivity of the FDI algorithm to low severity faults. As will be shown subsequently, by selecting two threshold levels and considering the temporal and sequential characteristics of*

the residual signals, one can not only enhance the fault sensitivity but also design a robust FDI algorithm.

The threshold values for the residual signals $r_i \in \mathfrak{R}_2$ are selected according to

$$J^1_{th_i} = \sup_{v \in \mathfrak{L}_p, \omega_l \in \mathfrak{D}_2, i \in \Omega^p_l, m_j = 0, j \in \mathbf{k}} (J_{r_i}), \quad i = \xi + 1, ..., 2\xi \tag{4.14}$$

For a system, such as in Example 1 and the ALTAV system that is discussed in Section 4.4, where the residual signals $r_i \in \mathfrak{R}_2$ are affected by a few or even no disturbance input channels, one can select lower threshold values for these residuals. In other words, the residual signals $r_i \in \mathfrak{R}_2$ are generally less sensitive to disturbance inputs than residual signals $r_i \in \mathfrak{R}_1$.

For each residual $r_i \in \mathfrak{R}_1$ defined at a given point in time t, we can choose the corresponding two threshold logic units $R^1_i(t)$ and $R^2_i(t)$ according to

$$R^1_i(t) = \begin{cases} 1 & \text{if } J_{r_i}(t) > J^1_{th_i} \\ 0 & \text{otherwise} \end{cases} \quad , i \in \Xi_1 \tag{4.15}$$

$$R^2_i(t) = \begin{cases} 1 & \text{if } J_{r_i}(t) > J^2_{th_i} \\ 0 & \text{otherwise} \end{cases} \quad , i \in \Xi_1 \tag{4.16}$$

Similarly, for each residual $r_i(t) \in \mathfrak{R}_2$, the threshold logic unit is assigned as follows

$$R^1_i(t) = \begin{cases} 1 & \text{if } J_{r_i}(t) > J_{th_i} \\ 0 & \text{otherwise} \end{cases} \quad , i \in \{\xi + 1, ..., 2\xi\} \tag{4.17}$$

For each fault mode $m_i, i \in \mathbf{k}$, let us define Δ_i as

$$\Delta_i = \{R^\beta_j | \beta \in \{1, 2\}, j \in \Omega^f_i\}, \quad i \in \mathbf{k} \tag{4.18}$$

In other words, Δ_i is the set of all residual logic units that may take the value of 1 due to the occurrence of a fault in the i-th actuator. The sets Δ_i's will be used in the next section to define the possible DES model outputs of the system (as shown in Table 4.2).

Definition 4.1. *The fault scenarios are categorized into the following three classes, namely, high severity faults, low severity faults, and non-detectable faults:*

1. *High severity faults correspond to faults that will affect residual logic units* $R_i^1, i \in \{1, ..., 2\xi\}$,

2. *Low severity faults correspond to faults that will affect only* $R_i^1, i \in \{\xi + 1, ..., 2\xi\}$, *and*

3. *Non-detectable faults correspond to faults that do not affect any of the residual logic units* $R_i^1, i \in \{1, ..., 2\xi\}$.

4.2.3 DES Fault Diagnoser

For simplicity, let us assume that multiple faults in two components are possible. Furthermore, let us consider the scenarios where only occurrence of one fault and one large disturbance is allowed concurrently. This assumption will limit the number of all possible operational states of the DES system. However, our proposed algorithm is easily expandable to more general cases.

First the plant (linear/nonlinear) along with a bank of residual generators is modeled as a finite state Moore automaton [163] specified according to $G = (S, \Sigma, \delta, s_0, Y, \lambda)$, where S, Σ, Y are finite state, event and output sets; s_0 is the initial state, $\delta : S \times \Sigma \rightarrow S$ is the transition function and $\lambda : S \rightarrow Y$ is the output map. For both linear and nonlinear systems, the state set S along with its description is given in Table 4.1. The event set is $\Sigma = \{\mathcal{F}_1^o, ..., \mathcal{F}_k^o, \mathcal{F}_1^r, ..., \mathcal{F}_k^r, \mathcal{D}^o, \mathcal{D}^r\}$ where the events $\mathcal{F}_i^o$ and $\mathcal{F}_i^r, i = \mathbf{k}$ correspond to the occurrence and removal of a fault in the i-th component, respectively and the event $\mathcal{D}^o$ corresponds to the occurrence of an large disturbance in one of the ω_j, $j \in \mathbf{P}$ channels and $\mathcal{D}^r$ corresponds to the removal of disturbance from all the channels. The output set is $Y = \{(R_1^1, ..., R_{\xi'}^1, R_1^2, ..., R_\xi^2) \in \mathbb{B}^\kappa\}$ where $\mathbb{B} = \{0, 1\}$ and κ can be either $2\xi + 1$ or 3ξ depending on the property

Table 4.1: Finite states of the plant

	Operational state	Description
s_0	Normal operation	No fault and no large disturbance input
s_1	Fault state 1	Fault in the first actuator
$\vdots$	$\vdots$	$\vdots$
s_k	Fault state k	Fault in the k-th actuator
$s_{1,2}$	Multiple faults state (1,2)	Faults in the first and second actuators
$\vdots$	$\vdots$	$\vdots$
$s_{(k-1),k}$	Multiple faults state (k-1,k)	Faults in the $(k-1)$ and k-th actuators
s_D	Disturbance state	Occurrence of large disturbance input
$s_{1,D}$	Fault/Disturbance state 1	Fault in the first actuator and large disturbance inputs
$\vdots$	$\vdots$	$\vdots$
$s_{k,D}$	Fault/Disturbance state k	Fault in the k-th actuator and large disturbance inputs

of Λ_i's. Based on the above definitions, the transition function δ is now defined formally as follows

$$\delta(s_0, \mathcal{D}^o) = s_D, \delta(s_D, \mathcal{D}^r) = s_0, \delta(s_D, \mathcal{F}_i^o) = s_{i,D}, \ i \in \mathbf{k}$$

$$\delta(s_0, \mathcal{F}_i^o) = s_i, \delta(s_i, \mathcal{D}^o) = s_{i,D}, \delta(s_i, \mathcal{F}_i^r) = s_0, \ i \in \mathbf{k}$$

$$\delta(s_i, \mathcal{F}_j^o) = s_{i,j}, \delta(s_{i,j}, \mathcal{F}_i^r) = s_j, \delta(s_{i,j}, \mathcal{F}_j^r) = s_i, \ i, j \in \mathbf{k}, i \neq j$$

$$\delta(s_{i,D}, \mathcal{F}_i^r) = s_D, \quad \delta(s_{i,D}, \mathcal{D}^r) = s_i, \ i \in \mathbf{k}$$

As an illustration, Figure 4.2 shows the corresponding transition function of the nonlinear system that was considered in Example 4.1. It should be noted that since for this system the detectability index is $\mu = 1$, multiple fault states are not applicable. As shown in Figure 4.2, the DES model of the combined nonlinear system and the bank of residual generators in Example 4.1 has eight states, namely the normal operational state s_0, three faulty states $s_i, i = 1, 2, 3$, three concurrent fault and large disturbance states $s_{i,D}, i = 1, 2, 3$, and the large disturbance input s_D. The event set and the output set for this system are $\Sigma = \{\mathcal{F}_1^o, \mathcal{F}_2^o, \mathcal{F}_3^o, \mathcal{F}_1^r, \mathcal{F}_2^r, \mathcal{F}_3^r, \mathcal{D}^o, \mathcal{D}^r\}$ and $Y = \{(R_1^1, ..., R_4^1, R_1^2, ..., R_3^2) \in \mathbb{B}^7\}$, respectively.

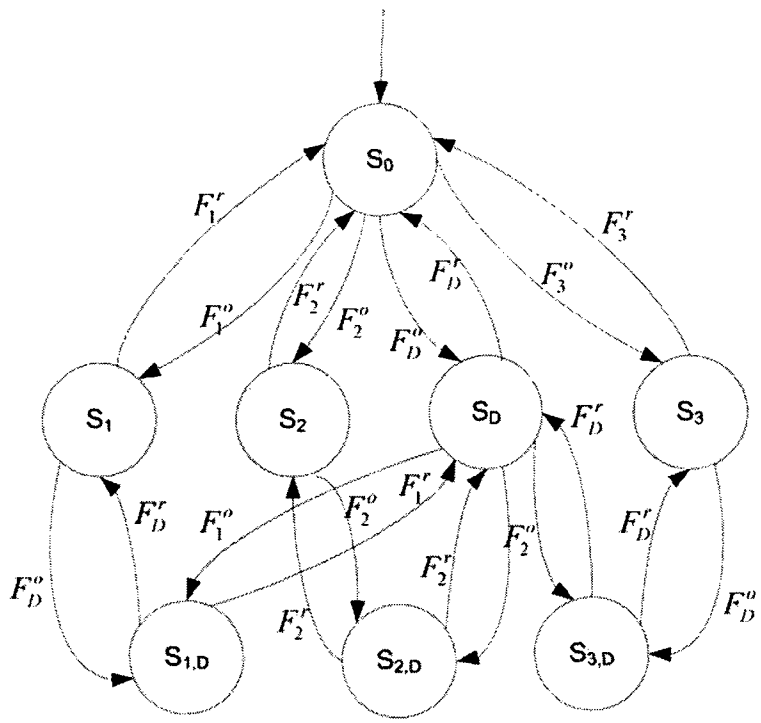

Figure 4.2: The transition function corresponding to Example 1.

The output map λ depends on the severity of a fault and the threshold values for the residual signals. As mentioned in the previous section, threshold values for the residual signals $r_i \in \Re_2$ are usually lower than those of $r_1 \in \Re_1$. Therefore, there could be a low severity fault scenario where the residual logic unit $R^1_{\xi+i}$ becomes one while R^1_i is zero. In defining the output map λ, such scenarios are also incorporated. Table 4.2 shows the corresponding output map λ where $\Xi_2 = \{1, ..., 2\xi\}$. For instance, the outputs of the system which are one at state s_1 are a nonempty subset of the set Δ_1 since some residual signals in Ω^f_1 may not exceed their threshold values. Thus, some states may have different outputs that would depend on the severity of the fault and disturbances. Moreover, non-detectable fault scenarios (refer to Definition 4.1) are not observable from residual logic units, and therefore they cannot be detected and isolated. These types of faults are not considered in λ. In other words, no event is assigned to such faults.

The purpose of the DES diagnoser is to use the output sequence of the system

Table 4.2: Output map of the plant

	Output map λ
s_0	$(0, ..., 0)$
s_D	$\{(R_1^1, ..., R_\xi^2) \in Y \mid \exists l \in \mathbf{P}, \forall j \in \Omega_l^p, R_j^1 = 1\}$
s_i	$\{(R_1^1, ..., R_\xi^2) \in Y \mid \exists \beta \in \{1,2\}, j \in \Xi_2, R_j^\beta \in \Delta_i.\ R_j^\beta = 1\}$
$s_{i,j}$	$\{(R_1^1, ..., R_\xi^2) \in Y \mid \exists \beta \in \{1,2\}, j \in \Xi_2,$ $\exists R_j^\beta \in \Delta_i \cup \Delta_j.\ R_j^\beta = 1\}$
$s_{i,D}$	$\{(R_1^1, ..., R_\xi^2) \in Y \mid \exists \beta \in \{1,2\}, j \in \Xi_2, R_j^\beta \in \Delta_i.\ R_j^\beta = 1\}$ $\cup\{(R_1^1, ..., R_\xi^2) \in Y \mid \exists l \in \mathbf{P}, \forall j \in \Omega_l^p, R_j^1 = 1\}$

(residual logic units) as inputs and to generate an estimate of the state of the system. In this work, a DES diagnoser is modeled as a finite state automaton $H = (S_H, I_H, \delta_H, z_0, Y_H, \lambda_H)$ where S_H, I_H, Y_H denote the finite state, input and output sets; z_0 is the initial state of the diagnoser, $\delta_H : S_H \times I_H \rightarrow S_H$ denotes the transition function and λ_H is the output map. In order to eliminate any possible ambiguity in the DES model (G) output, two additional states with respect to the state set of G are considered for H, namely $S_H = \{S, s_F, s_{F,D}\}$, where s_F corresponds to the faulty state where one cannot isolate the faulty channel and $s_{F,D}$ corresponds to the concurrent occurrence of a fault and a large disturbance in the system when a fault may not be isolated. The input set for the diagnoser is an output set of G (set Y). The output set is the same as the state set of the diagnoser ($Y_H = S_H$) and the output map $\lambda_H : S_H \rightarrow Y_H$ is an identity map.

The main step that is left is the design of a transition map δ_H. First, we consider the case when the system is in a normal operational mode s_0 and try to find the transition function corresponding to this mode. Based on Assumption 4.2, three transitions are possible in the normal operation, namely transition to the state s_i which corresponds to the occurrence of a fault in the i-th actuator (event $\mathcal{F}_i^o$), transition to the state s_D which corresponds to the occurrence of a large disturbance in one of the input disturbance channels (event $\mathcal{D}^o$), and finally the transition to the fault mode s_F which corresponds to the occurrence of a low severity fault in one

Table 4.3: Transition function of state s_0

Current State	Input $(R_1^1, ..., R_{2\xi}^1, R_1^2, ..., R_\xi^2)$	Next state	Corresponding event in G
s_0	$\bigwedge_{j\in\Omega_i^f} R_j^1 = 1$	$s_i, i \in \mathbf{k}$	$\mathcal{F}_i^o$
s_0	$\exists l \in \mathbf{k}$ such that $\bigwedge_{j\in\Upsilon_l^f} R_j^1 = 1$	s_F	$\mathcal{F}_i^o \in \{\mathcal{F}_1^o, ..., \mathcal{F}_k^o\}$
s_0	$\exists l \in \mathbf{P}$ such that $\bigwedge_{j\in\Omega_l^p} R_j^1 = 1$	s_D	$\mathcal{D}_i^o$

of the actuators that may not be isolable. According to Lemma 4.1, the effects of a fault and a disturbance can be distinguished easily by the fault diagnoser using the coding sets Ω_i^f and Ω_j^p, and therefore the sets Ω_i^f and Ω_j^p can be used for the transition to states s_i and s_D, respectively.

The only remaining case of interest is when the occurrence of a low severity fault (refer to Definition 4.1) in the i-th actuator will lead to changes in only $R_{\xi+i}^1$. In this case, according to Lemma 4.2, the diagnoser can *detect* the occurrence of a fault in the system since $\Upsilon_i^f \neq \Omega_j^p$. However, we may have $\Upsilon_i^f = \Upsilon_j^f$ for some $i, j \in \mathbf{k}$, and therefore the fault cannot be *isolated.* In this case, the state of the fault diagnoser will change to s_F. Table 4.3 summarizes the transition function that is initiated from the state s_0 where all the unspecified residual logic units are zero.

The next step is now to consider scenarios when initially a large disturbance is applied to the system followed by a fault that is concurrently present in one of the system actuators. Therefore, it is assumed that the system has a transition from the normal operation state s_0 to the disturbance state s_D where we define a set $\mathcal{D} = \{1 \leq i \leq \xi | R_i^1 = 1\}$. In this state, the second threshold logic units R_i^2 are used for all the residuals $r_i, i \in \mathcal{D}$. The transition function for the state s_D is given in Table 4.4. It is assumed that the effects of the fault is not nullified by a large disturbance input, which is quite a reasonable consideration for practically most situations.

Now let us consider a scenario where a fault is detected in the i-th actuator and the state of the fault diagnoser is s_i. Generally, we should investigate three possible

Table 4.4: Transition function of state s_D

Current state	Input $(R_1^1, ..., R_{2\xi}^1, R_1^2, ..., R_\xi^2)$	Next state	Corresponding event in G
s_D	all inputs become zero	s_0	$\mathcal{D}^r$
s_D	for $(\bigwedge_{j\in\Omega_i^f\cup\mathcal{D}} R_j^2 \bigwedge_{l\in\Upsilon_i^f} R_l^1 = 1)$	$s_{i,D}$	$\mathcal{F}_i^o$
s_D	$\exists l \in \mathbf{k}$ such that $\bigwedge_{j\in\Upsilon_l^f} R_j^1 = 1$	$s_{F,D}$	$\mathcal{F}_i^o \in \{\mathcal{F}_1^o, ..., \mathcal{F}_k^o\}$

Table 4.5: Transition function of state $s_i,\ i \in \mathbf{k}$

Current state	Input $(R_1^1, ..., R_{2\xi}^1, R_1^2, ..., R_\xi^2)$	Next state	Corresponding event in G
s_i	all inputs become zero	s_0	$\mathcal{F}_i^r$
s_i	$\bigwedge_{l\in\Omega_i^f\cup\Omega_j^f} R_l^1 = 1$ for the time interval τ_0	$s_{i,j}$	$\mathcal{F}_j^o$
s_i	$\exists l$ such that $\bigwedge_{j\in\Omega_i^f\cup\Omega_l^p} R_j^1 = 1$	$s_{i,D}$	$\mathcal{D}^o$

cases, namely 1) the removal of a detected fault, 2) the occurrence of a second fault in the j-th actuator, and 3) the occurrence of a disturbance in $\omega_l, l \in \mathbf{P}$. Actually, the main challenge here is to distinguish between cases 2 and 3, since the removal of a fault can be easily detected when all the threshold logic units become zero. The necessary condition for distinguishing between cases 2 and 3 is governed by

$$\Omega_i^f \cup \Omega_j^f \neq \Omega_i^f \cup \Omega_l^p,\ i, j \in \mathbf{k}, ; l \in \mathbf{P} \tag{4.19}$$

The next lemma provides the sufficient condition for satisfying the condition (4.19).

Lemma 4.3. *If the number of residuals $r_i \in \mathfrak{R}_1$ that are affected by each disturbance input is more than $|\Omega_i \cup \Omega_j| = \xi - C(k-2, k-\mu)$, i.e. $|\Omega_l^p \cap \Xi_1| > \xi - C(k-2, k-\mu), \forall l \in \boldsymbol{P}$, then the condition (4.19) is satisfied for all the disturbance inputs $l \in \boldsymbol{P}$ as well as fault modes $m_i, m_j, i \neq j$.*

Proof: If $|\Omega_l^p \cap \Xi_!| > \xi - C(k-2, k-\mu)$, then for any two fault modes $m_i, m_j, i, j \in \mathbf{k}, i \neq j$, there exists at least one residual $r_\alpha \in \mathfrak{R}_1$ such that $r_\alpha \in \Omega_l^p$ and $r_\alpha \notin \Omega_i^f \cup \Omega_j^f$, and therefore it follows that $\Omega_i^f \cup \Omega_j^f \neq \Omega_i^f \cup \Omega_l^p$. ■

It can be easily verified that the system in Remark 4.2 where $\Lambda_i = \Lambda, i \in \mathbf{k}$ satisfies the above sufficient condition if $\mu > 1$ since $|\Omega_l^p \cap \Xi_1| = \xi$ and $|\Omega_i^f \cup \Omega_j^f| < \xi$.

Table 4.6: Transition function of states s_F, $s_{F,D}$, $s_{i,D}$ and $s_{i,j}$

Current state	Input $(R_1^1, ..., R_{2\xi}^1, R_1^2, ..., R_\xi^2)$	Next state	Corresponding event in G
s_F	$\bigwedge_{j\in\Omega_i^f} R_j^1 = 1$	s_i	$\mathcal{F}_i^o$
s_F	$\exists l \in \mathbf{P}$ such that $\bigwedge_{j\in\Omega_l^p} R_j^1 = 1$	$s_{F,D}$	$\mathcal{D}^o$
$s_{F,D}$	$(\bigwedge_{j\in\Omega_i^f\cup\mathcal{D}} R_j^2 \bigwedge_{l\in\Upsilon_i^f} R_l^1 = 1)$	$s_{i,D}$	$\mathcal{F}_i^o$
$s_{F,D}$	$\exists l \in \mathbf{k}$ such that $\bigwedge_{j\in\Upsilon_l^f} R_j^1 = 1$	s_F	$\mathcal{D}^r$
$s_{F,D}$	$\exists l \in \mathbf{P},\ i \in \mathbf{k}$ such that $\bigwedge_{j\in\Omega_l^p} R_j^1 = 1$	s_D	$\mathcal{F}_i^r \in \{\mathcal{F}_1^o, ..., \mathcal{F}_k^o\}$
$s_{i,D}$	$\exists l \in \mathbf{P}$ such that $\bigwedge_{j\in\Omega_l^p} R_j^1 = 1$	s_D	$\mathcal{F}_i^r \in \{\mathcal{F}_1^o, ..., \mathcal{F}_k^o\}$
$s_{i,D}$	$\bigwedge_{j\in\Omega_i^f} R_j^1 = 1$	s_i	$\mathcal{D}^r$
$s_{i,j}$	$\bigwedge_{l\in\Omega_i^f} R_l^1 = 1$	s_i	$\mathcal{F}_j^r$
$s_{i,j}$	$\bigwedge_{l\in\Omega_j^f} R_l^1 = 1$	s_j	$\mathcal{F}_i^r$

Remark 4.4. *In a situation where $\Omega_i^f \cup \Omega_j^f \subset \Omega_i^f \cup \Omega_l^p$ one could potentially have a false alarm associated with the second fault while a large disturbance input is present. To remedy this problem, the DES diagnoser will declare the detection of the second fault after a specific waiting-time interval τ_0, if all the residual threshold logics specified by $\Omega_i^f \cup \Omega_j^f$ are at 1 while the remaining residual threshold logic units specified by $\{\Omega_i^f \cup \Omega_j^f\} - \{\Omega_i^f \cup \Omega_l^p\}$ remain at zero. Table 4.5 illustrates the transition function for the state associated with s_i, $i \in \mathbf{k}$.*

Table 4.6 shows the remaining transitions that should be considered for the DES diagnoser. By specifying these transitions, the design of our proposed hybrid DES diagnoser is completed.

Example 4.1 *(Cont.)* According to the coding sets that were obtained for the nonlinear system in Example 4.1, the DES diagnoser can be designed as follows: the state set is specified by $S_H = \{s_0, s_1, s_2, s_3, s_D, s_F, s_{1,D}, s_{2,D}, s_{3,D}\}$, the input set is defined by $I_H = \{R_1^1, R_2^1, R_3^1, R_4^1, R_1^2, R_2^2, R_3^2\}$ and the transition map λ_H is given in Table 4.7. Therefore, the design of our proposed hybrid diagnoser for the nonlinear system in Example 4.1 is completed.

In the next two sections, our proposed FDI algorithm will be applied to the

Table 4.7: Transition function of Example 4.1

Current State	Input $(R_1^1, ..., R_4^1, R_1^2, ..., R_3^2)$	Next state
s_0	$R_1^1 \bigwedge R_2^1 \bigwedge R_4^1 = 1$	s_1
s_0	$R_1^1 \bigwedge R_3^1 \bigwedge R_4^1 = 1$	s_2
s_0	$R_2^1 \bigwedge R_3^1 \bigwedge R_4^1 = 1$	s_3
s_0	$R_1^1 \bigwedge R_2^1 \bigwedge R_3^1 = 1$	s_D
s_0	$R_4^1 = 1$	s_F
s_i	all zero	s_0
s_D	all zero	s_0
s_D	$R_1^2 \bigwedge R_2^2 \bigwedge R_4^1 = 1$	$s_{1,D}$
s_D	$R_1^2 \bigwedge R_3^2 \bigwedge R_4^1 = 1$	$s_{2,D}$
s_D	$R_2^2 \bigwedge R_3^2 \bigwedge R_4^1 = 1$	$s_{3,D}$
s_F	all zero	s_0
s_F	$R_1^1 \bigwedge R_2^1 \bigwedge R_4^1 = 1$	s_1
s_F	$R_1^1 \bigwedge R_3^1 \bigwedge R_4^1 = 1$	s_2
s_F	$R_2^1 \bigwedge R_3^1 \bigwedge R_4^1 = 1$	s_3
s_F	$R_1^1 \bigwedge R_2^1 \bigwedge R_3^1 \bigwedge R_4^1 = 1$	$s_{F,D}$

actuator FDI problem in a network of unmanned vehicles (linear system) and the ATLAV system (nonlinear system).

4.3 Actuator Fault Detection and Isolation in a Network of Unmanned Vehicles

In this section, our hybrid FDI method is applied to the actuator fault detection and isolation (FDI) problem for a network of N vehicles whose (identical) linear dynamics are governed by

$$\dot{x}_i(t) = Ax_i(t) + Bu_i(t) + \sum_{k=1}^{a} L_k m_{ik}(t) + \sum_{j=1}^{P} P_j \omega_{ij}(t) \tag{4.20}$$

where the fault signature L_k represents a fault in the k-th actuator of the vehicle, i.e, L_k is the k-th column of B. It is assumed that matrix B is full rank (Rank(B)=a). It should be noted that in comparison with the vehicle dynamics considered in Section 3.3, additional disturbance terms are added to the vehicle dynamics. Similar relative

state measurements are considered for each vehicle as

$$z_{ij}(t) = C(x_i(t) - x_j(t)) \qquad j \in \mathrm{N}_i \tag{4.21}$$

where the set $\mathrm{N}_i \subset [1, N]\backslash i$ represents the set of vehicles that vehicle i can sense and is designated as the neighboring set of the vehicle i, and $z_{ij} \in \mathcal{Z}_i, j \in \mathrm{N}_i$ represents the state measurement relative to the other vehicles. It is assumed that the pair (A, C) is observable.

Assumption 4.4. *It is assumed that the family of fault signature L_i's are strongly detectable when each vehicle has an absolute state measurement $y_i = Cx_i$.*

In this section only semi-decentralized FDI architecture (Section 3.3.2) is investigated and hence it is assumed that local communication links exist between each vehicle and its neighbors and the control signals u_i are communicated among them.

Let $\mathrm{N}_i = \{i_1, i_2, ..., i_{|\mathrm{N}_i|}\}$. We have $z_i(t) = [z_{ii_1}^\top(t), z_{ii_2}^\top(t), \cdots, z_{ii_{|\mathrm{N}_i|}}^\top(t)]^\top$, and equation (3.2) can be rewritten as $z_i(t) = C_i x(t)$ where $x(t) = [x_1^\top(t), \cdots, x_N^\top(t)]^\top$. Since the output measurement z_i depends on the state of the neighboring vehicles, the following nodal model should be considered for the i-th vehicle for designing a FDI filter, namely

$$\begin{aligned} \dot{x}_{\mathrm{N}_i}(t) &= A^{|\mathrm{N}_i|+1} x_{\mathrm{N}_i}(t) + B^{|\mathrm{N}_i|+1} u_{\mathrm{N}_i}(t) + \sum_{k=1}^{|\mathrm{N}_i|+1} \sum_{j=1}^{a} \bar{L}_{kj} m_{kj}(t) + \sum_{k=1}^{|\mathrm{N}_i|+1} \sum_{j=1}^{P} \bar{P}_{kj} \omega_{kj}(t) \\ z_i(t) &= \bar{C}_{|\mathrm{N}_i|} x_{\mathrm{N}_i}(t) \end{aligned} \tag{4.22}$$

where $x_{\mathrm{N}_i}^\top(t) = [x_i^\top(t), x_{i_1}^\top(t), \cdots, x_{i_{|\mathrm{N}_i|}}^\top(t)]$, $u_{\mathrm{N}_i}^\top = [u_i^\top(t), u_{i_1}^\top(t), \cdots, u_{i_{|\mathrm{N}_i|}}^\top(t)]$, $\bar{L}_{kj}$ is the $(k-1) \times a + j$ column of $B^{|\mathrm{N}_i|+1}$, $z_i^\top(t) = [z_{ii_1}^\top(t), z_{ii_2}^\top(t), \cdots, z_{ii_{|\mathrm{N}_i|}}^\top(t)]$, It should be noted that $\bar{L}_{1j}$'s represents the fault signatures of the i-th vehicle in the nodal system (4.22). It is clear that the entire state x_{N_i} is not fully observable from the relative state measurements z_i, and the states of the centroid of vehicle i and

its neighbors cannot be determined from z_i. Since the pair $(A^{|\mathrm{N}_i|+1}, \bar{C}_{|\mathrm{N}_i|})$ is not observable, one can first try to obtain the observable part of system (4.22) as

$$\dot{x}^O_{\mathrm{N}_i}(t) = A^{\mathrm{N}_i} x^O_{\mathrm{N}_i}(t) + \bar{B}^O_{|\mathrm{N}_i|} u_{\mathrm{N}_i}(t) + \sum_{k=1}^{|\mathrm{N}_i|+1} \sum_{j=1}^{a} \bar{L}^O_{kj} m_{kj}(t) + \sum_{k=1}^{|\mathrm{N}_i|+1} \sum_{j=1}^{a} \bar{P}^O_{kj} \omega_{kj}(t)$$

$$z_i(t) = C^{\mathrm{N}_i} x^O_{\mathrm{N}_i}(t) \tag{4.23}$$

where $x^O_{\mathrm{N}_i}(t) = [x_i^T(t) - x_{i_1}^T(t), x_i^T(t) - x_{i_2}^T(t), \cdots, x_i^T(t) - x_{i_{|\mathrm{N}_i|}}^T(t)]^T$ and $\bar{L}^O_{kj}$ and $\bar{P}^O_{kj}$ are the $(k-1) \times a + j$ column of $\bar{B}^O_{|\mathrm{N}_i|}$ and $\bar{P}^O_{|\mathrm{N}_i|}$, respectively where $\bar{B}^O_{|\mathrm{N}_i|}$ and $\bar{P}^O_{|\mathrm{N}_i|}$ are defined based on (3.5).

As discussed in Section 3.3.2, the family of $a \times (|\mathrm{N}_i| + 1)$ fault signatures $\bar{L}^O_{kj}, k = 1, ..., |\mathrm{N}_i| + 1,\ j = 1, ..., a$ satisfies the conditions of Theorem 3.6 with the detectability index of $\mu = |\mathrm{N}_i| - 1$. Based on Assumption 4.4, the SFDIP problem has a solution for coding scheme 2 and one needs to generate $C(a \times (|\mathrm{N}_i|+1), |\mathrm{N}_i|-1)$ residuals for detecting and isolating $|\mathrm{N}_i| - 1$ multiple faults.

As pointed out in Remark 4.1, considering the disturbance inputs as faults in the system limits the number of fault that can be detected and isolated, i.e. , it will decrease the detectability index of fault signatures. However, by using our proposed FDI algorithm, one can keep the detectability index of fault signatures as high as possible.

4.3.1 Simulation Results

In this section, our proposed hybrid FDI strategy is applied to a network of four unmanned vehicles, whose dynamics are assumed to be governed by double integrators in a plane and each vehicle can measure its relative position with respect to its neighboring vehicles. Hence, each vehicle is modeled as in equation (4.20) with the

following matrices:

$$A = \begin{bmatrix} 0 & 0 & 1 & 0 \\ 0 & 0 & 0 & 1 \\ 0 & 0 & 0 & 0 \\ 0 & 0 & 0 & 0 \end{bmatrix}, B = \begin{bmatrix} 0 & 0 \\ 0 & 0 \\ 1 & 0 \\ 0 & 1 \end{bmatrix}, P_1 = \begin{bmatrix} 0 \\ 0 \\ 1 \\ 1 \end{bmatrix}$$

with $d = 1$. The neighbor sets for this network are given by $\mathrm{N}_1 = \{2\}$, $\mathrm{N}_2 = \{1, 3\}$, $\mathrm{N}_3 = \{4\}$ and $\mathrm{N}_4 = \{1\}$. Here, we only consider actuator FDI problem for vehicle 2. According to the results in Section 3.3.2, the detectability index for the family of actuator fault signatures in the nodal model of vehicle 2 is 1, i.e. $\mu = 1$. Therefore, $\xi = C(6, 1) = 6$ residual signals $r_1, ..., r_6$ are needed for the fault detection and isolation. The corresponding coding sets are as follows $\Omega_{11} = \{2, 3, 4, 5, 6\}$, $\Omega_{21} = \{1, 3, 4, 5, 6\}$, $\Omega_{31} = \{1, 2, 4, 5, 6\}$, $\Omega_{12} = \{1, 2, 3, 5, 6\}$, $\Omega_{22} = \{1, 2, 3, 4, 6\}$, and $\Omega_{32} = \{1, 2, 3, 4, 5\}$, where Ω_{ij} corresponds to the fault signature $\bar{L}^O_{ij}$. The next step is to find the sets Λ_i's for each residuals. According to (4.3), these sets are as follows $\Lambda_i = \{1, 2, 3\}, i = 1, ..., 6$ which implies that all residuals are affected by disturbance inputs ω_{11}, ω_{21} and ω_{31}. It should be noted that the disturbance input ω_{41} does not affect the nodal model of vehicle 2 since the vehicle 4 is not a neighbor of the vehicle 2. According to Remark 4.2, one extra residual is sufficient for design of the DES diagnoser. The residual signal r_7 should be affected by all the faults and decoupled from all the disturbance inputs. It can be verified that the necessary and sufficient conditions of Theorem 4.1 for generating the residual signal r_7 are satisfied. Hence, the coding sets Ω^f_i's and Ω^p_j's are as follows: $\Omega^f_{11} = \{2, 3, 4, 5, 6, 7\}$, $\Omega^f_{21} = \{1, 3, 4, 5, 6, 7\}$, $\Omega^f_{31} = \{1, 2, 4, 5, 6, 7\}$, $\Omega^f_{12} = \{1, 2, 3, 5, 6, 7\}$, $\Omega^f_{22} = \{1, 2, 3, 4, 6, 7\}$, and $\Omega^f_{32} = \{1, 2, 3, 4, 5, 7\}$ and $\Omega^p_{j1} = \{1, 2, 3, 4, 5, 6\}, j = 1, 2, 3$ where Ω^p_{j1} correspond to disturbance input ω_{j1}.

The evaluation functions are selected as $J_{r_i}(t) = \int_{t-T_0}^{t} r_i^T(t) r_i(t) dt, i = 1, ..., 7$ where $T_0 = 5$ seconds is the length of the evaluation window. By considering the

worst case scenario of residuals corresponding to the healthy mode of the network subject to the measurement noise with uniform distribution $\pm$ 0.005 and tolerable input disturbances ($\omega \in \mathfrak{D}_1$) as a band-limited white noise with power of 0.01, the threshold values are $J^1_{th_i} = 0.3, J^2_{th_i} = 1.2,\ i = 1, ..., 6$ and $J^1_{th_7} = 0.005$. It should be pointed out that since the residual signal r_7 is decoupled from the disturbance inputs, one can select a lower threshold value for it.

The next step is to design a DES fault diagnoser H. The state set is defined as $S_H = \{s_1, ..., s_6, s_{1,D}, ..., s_{6,D}, s_F, s_{F,D}\}$ where cardinality of S is 14. Since the detectability index of actuator fault signatures of vehicle 2 is 1, concurrent faults in two actuators cannot be isolated. Therefore, the states that correspond to concurrent faults in two components are not applicable. Therefore, the only cases that should be considered for the DES diagnoser when it is in the state $s_i, i = 1, ..., 6$ is removal of the fault from the i-th component. The input set of the diagnoser is $I = \{(R^1_1, ..., R^1_7, R^2_1, ...R^2_6) \in \mathbb{B}^{13}\}$ and the output set is equal to S_H. The transition function λ_H can be found by following the results in Section 4.2.3.

Figure 4.3 shows the residual evaluation functions corresponding to a permanent lock in place fault in the first actuator of vehicle 2 at $t = 30$ seconds. A concurrent large disturbance ($\omega_2 \in \mathfrak{D}_2$) represented by a rectangular pulse of a constant amplitude 0.5 between $t = 20$ and $t = 40$ seconds is also applied to the vehicle 2 in this simulation. Figure 4.4 depicts the state of the DES fault diagnoser. As shown in this figure, the diagnoser state first changes to s_D at $t = 23.6$ seconds after the occurrence of the large disturbance with no false alarm generated. Later on when a fault in the first actuator of the vehicle 2 is injected, the diagnoser state switches to $s_{1,D}$ at $t = 33.72$ seconds. Consequently, we can conclude that the diagnoser can perfectly detect and isolate the fault despite the presence of a large concurrent disturbance. Finally, after the disturbance is removed at $t = 40$ seconds, the diagnoser switches to the state s_1 at $t = 48$ seconds. It should be emphasized

that if one *only* uses the first 6 residuals $r_1, ..., r_6$ with threshold values $J^2_{th_i} = 1.2$, although no false alarm will be generated due to the large disturbance but the actual fault at $t = 30$ *cannot* be detected and isolated after $t = 45$ seconds (false negative). However, by using our proposed hybrid FDI methodology, we are able to distinguish the occurrence of a fault as well as large disturbance by designing only one additional residual signal.

Figure 4.5 depicts the residual evaluation functions associated with a permanent 50% loss of effectiveness (LOE) in the second actuator of the vehicle 2 at $t = 40$ seconds, and Figure 4.6 shows the corresponding hybrid fault diagnoser state. A large disturbance that is represented by a rectangular pulse of constant amplitude 0.5 (N) is also injected between $t = 20$ and $t = 30$ seconds in the simulations. As seen from Figure 4.6, the diagnoser first detects the occurrence of a large disturbance between $t = 23.6$ and $t = 34$ seconds and no false alarm is generated due to the presence of this disturbance input. Moreover, in this fault scenario, the residual evaluation functions $J_{r_i}, i = 1, ..., 6$ do not exceed their threshold J_{th_i} whereas the residual evaluation function J_{r_7} does exceed its threshold J_{th_7}. Therefore, in this scenario the fault diagnoser can only detect the occurrence of the fault but cannot isolate it.

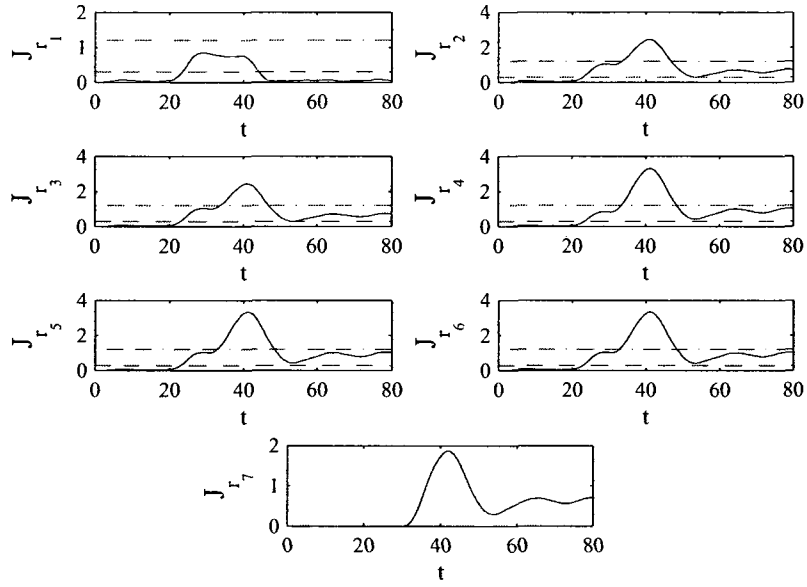

Figure 4.3: Residual evaluation functions corresponding to a fault in the first actuator of the vehicle 2.

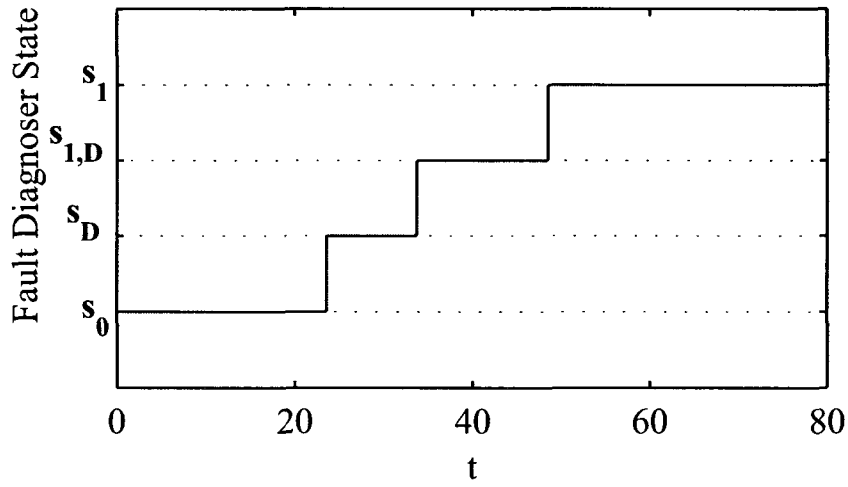

Figure 4.4: Fault diagnoser state corresponding to fault in the first actuator of the vehicle 2.

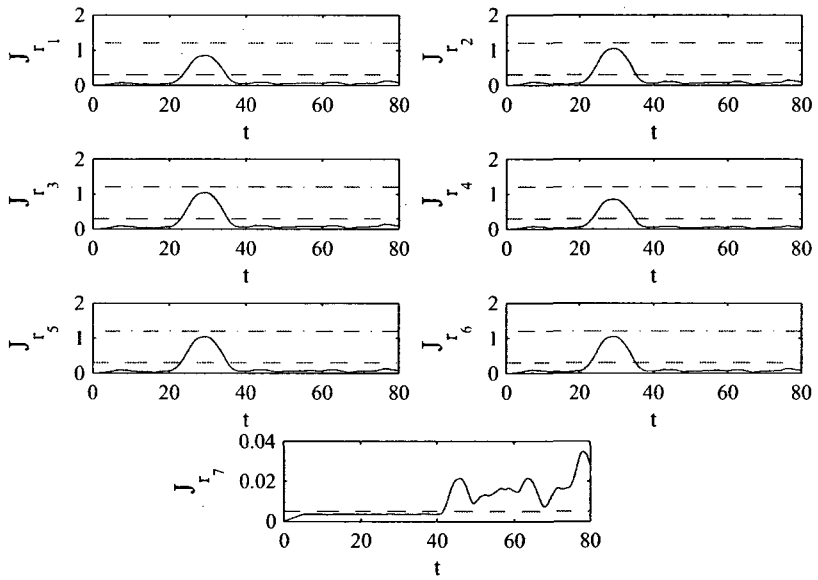

Figure 4.5: Residual evaluation functions corresponding to a 50% loss of effectiveness fault in the second actuator of the vehicle 2.

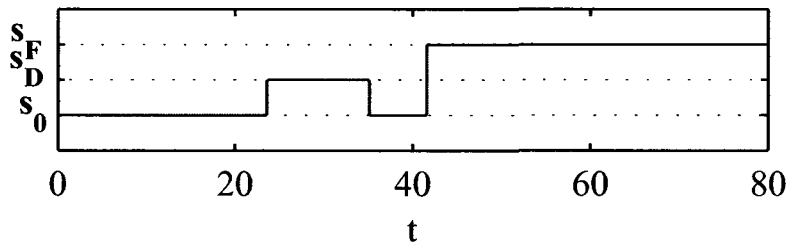

Figure 4.6: Fault diagnoser state corresponding to a 50 % loss of effectiveness fault in the second actuator of the vehicle 2.

4.4 Hybrid FDI Design for the ALTAV System

Example 4.1 and a network of unmanned vehicles worked out in Sections 4.2 and 4.3 belonged to a class of systems with not strongly detectable family of fault signatures. In this section, we consider the application of our proposed FDI methodology to an ALTAV system where the actuator fault signatures are strongly detectable.

4.4.1 ALTAV System

The ALTAV system considered in this section is a six degrees of freedom unmanned aerial vehicle as shown in Figure 4.7. The states/variables describing the motion of the system are x, y, z, θ, γ and ϕ. These states correspond to the translation in the x, y and z directions and rotations about the z, y and x axes (heading, pitch and roll angles) in the local horizontal/local vertical frame, respectively. It is assumed that these states and their first order derivatives are available for measurement. It should be pointed out that the system uses a "right handed" coordinate system with the positive z direction as down. The dynamics of the ALTAV system is governed by the following equations [169]:

$$
\begin{aligned}
M\ddot{x} &= \sum_{i=1}^{4} F_i sin(\gamma) - C_x\dot{x} + W_x \\
M\ddot{y} &= \sum_{i=1}^{4} F_i sin(\phi) - C_y\dot{y} + W_y \\
M\ddot{z} &= -\sum_{i=1}^{4} F_i cos(\gamma)cos(\phi) - F_B + Mg - C_z\dot{z} \\
J_\theta\ddot{\theta} &= (F_1 l - F_2 l + F_3 l - F_4 l)sin(\rho) - C_\theta\dot{\theta} \\
J_\gamma\ddot{\gamma} &= (F_1 l - F_3 l) - F_B L_B sin(\gamma) - C_\gamma\dot{\gamma} \\
J_\phi\ddot{\phi} &= -(F_2 l - F_4 l) - F_B L_B sin(\phi) - C_\phi\dot{\phi}
\end{aligned} \tag{4.24}
$$

where the physical significance and definition of the states and parameters are provided in Table 4.8.

Table 4.8: ALTAV parameters

M	Mass, kg	θ	Heading angle, Radian
J	Moment of inertia, kg m^2	γ	Pitch angle, Radian
x	Translation in x direction, m	ϕ	Roll angle, Radian
y	Translation in y direction, m	W	Wind disturbance, N
z	Translation in z direction, m	F_B	Buoyant force, N
C	Drag coefficient	F_i	Force of propeller, N
l	Perpendicular distance between the motors and vehicle center of gravity, m	ρ	Angular offset from vertical of the motor thrust vectors

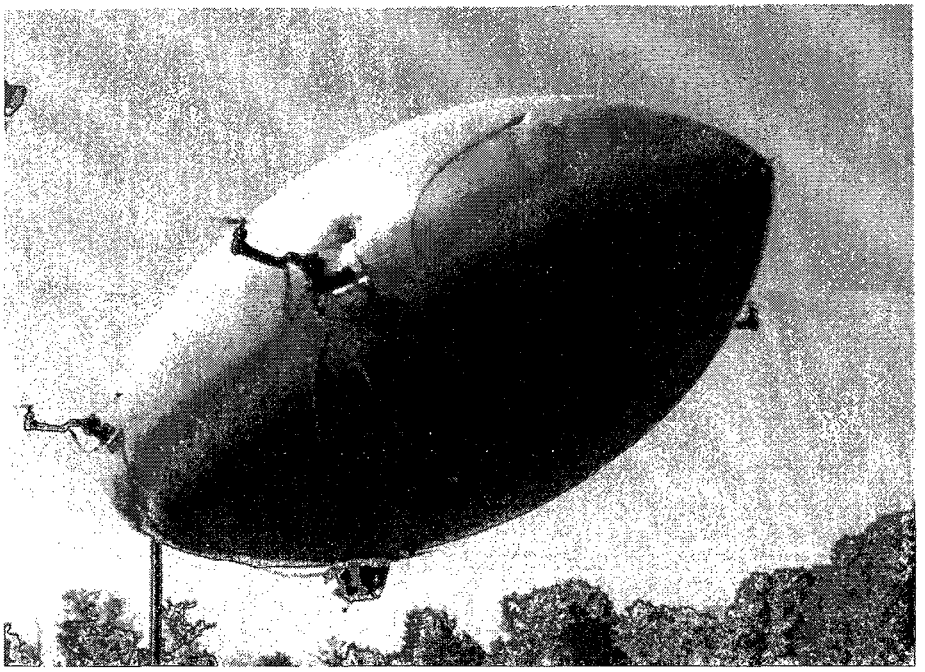

Figure 4.7: Schematic of an Almost-Lighter-Than-Air-Vehicle (ALTAV) [2].

The ALTAV system has four input forces $F_i, i = 1, ..., 4$ that are produced by propellers which are controlled through four vectoring brushless DC motors subject to the constraints $0 \leq F_i \leq F_i^{max}$.

4.4.2 Design of a Hybrid FDI Scheme for the ALTAV System

In this section, a bank of residual generators is first designed for the four input channels of the ALTAV system. The state space representation of the ALTAV system is rewritten as follows:

$$\begin{aligned} \dot{X} &= f(X) + \sum_{i=1}^{4} g_i(X)F_i + \sum_{j=1}^{3} p_j(X)\omega_j \\ Y &= X + v \end{aligned} \tag{4.25}$$

where $F_1, ..., F_4$ are the input force control channels, $X^\top = [x, y, z, \dot{x}, \dot{y}, \dot{z}, \theta, \gamma, \phi, \dot{\theta}, \dot{\gamma}, \dot{\phi}]$, ω_1 and ω_2 represent the wind disturbances in the x and the y directions, respectively, ω_3 represents a change in the buoyant force F_B, v is the measurement noise and

$$p_1(X) = \begin{bmatrix} 0 & 0 & 0 & \frac{1}{M} & 0 & 0 & 0 & 0 & 0 & 0 & 0 & 0 \end{bmatrix}^\top \tag{4.26}$$

$$p_2(X) = \begin{bmatrix} 0 & 0 & 0 & 0 & \frac{1}{M} & 0 & 0 & 0 & 0 & 0 & 0 & 0 \end{bmatrix}^\top \tag{4.27}$$

$$p_2(X) = \begin{bmatrix} 0 & 0 & 0 & 0 & 0 & \frac{1}{M} & 0 & 0 & 0 & 0 & -\frac{L_B sin(X_8)}{J_\gamma} & -\frac{L_B sin(X_9)}{J_\phi} \end{bmatrix}^\top \tag{4.28}$$

where we denote $X = \{X_i\}_{i=1}^{12}$ and $Y = \{Y_i\}_{i=1}^{12}$.

First, we need to generate residual signals $r_i, i = 1, ..., 4$ such that each residual signal r_i is only affected by F_i and is decoupled from all other faults $F_j, j \neq i$. Towards this end, the largest observability codistributions $\Pi_i^* = o.c.a.((\sum_*^{\mathcal{L}_i})^\perp)$ should be found where $\mathcal{L}_1 = span\{g_2(X), g_3(X), g_4(X)\}$, $\mathcal{L}_2 = span\{g_1(X), g_3(X), g_4(X)\}$, $\mathcal{L}_3 = span\{g_1(X), g_2(X), g_4(X)\}$, and $\mathcal{L}_4 = span\{g_1(X), g_2(X), g_3(X)\}$ such that

$$span\{g_i(X)\} \not\subset (\Pi_i^*)^\perp, \quad i = 1, ..., 4 \tag{4.29}$$

Condition (4.29) is the necessary condition for decoupling faults in a nonlinear system. For the ALTAV system since full state measurements $X_i, i = 1, ..., 12$ are assumed to be available, we have $\Pi_i^* = \mathcal{L}_i^{\perp}$.

According to the above observability codistribution, the following set of states can be found such that $z_i, i = 1, ..., 4$ is affected by F_i and is decoupled from the other input channels $F_j, j \neq i$, namely

$$z_1 = 2J_\gamma sin(\rho)sin(X_8)X_{11} + J_\theta sin(X_8)X_{10} + lMsin(\rho)X_4$$

$$z_2 = -2J_\phi sin(\rho)sin(X_8)X_{12} - J_\theta sin(X_8)X_{10} + lMsin(\rho)X_4$$

$$z_3 = -2J_\gamma sin(\rho)sin(X_8)X_{11} + J_\theta sin(X_8)X_{10} + lMsin(\rho)X_4$$

$$z_4 = 2J_\phi sin(\rho)sin(X_8)X_{12} - J_\theta sin(X_8)X_{10} + lMsin(\rho)X_4$$

The state space representation of the ALTAV system corresponding to the above states is now expressed as follows:

$$\dot{z}_1 = -2C_\gamma sin(\rho)sin(X_8)X_{11} - 2F_B L_B sin(\rho)sin^2(X_8) + 2J_\gamma cos(X_8)sin(\rho)X_{11}^2$$
$$- C_\theta X_{10} sin(X_8) + J_\theta X_{10} X_{11} cos(X_8) - C_x X_4 l sin(\rho) + 4l sin(\rho) sin(X_8) F_1$$
$$+ l sin(\rho)\omega_1 - 2L_B sin(\rho) sin^2(X_8)\omega_3$$
$$\dot{z}_2 = 2C_\phi sin(\rho)sin(X_8)X_{12} + 2F_B L_B sin(\rho)sin(X_8)sin(X_9)$$
$$- 2J_\phi cos(X_8)sin(\rho)X_{11}X_{12} + C_\theta X_{10} sin(X_8) - J_\theta X_{10} X_{11} cos(X_8) - C_x X_4 l sin(\rho)$$
$$+ 4l sin(\rho) sin(X_8) F_2 + l sin(\rho)\omega_1 + 2L_B sin(\rho) sin(X_8) sin(X_9)\omega_3$$
$$\dot{z}_3 = 2C_\gamma sin(\rho)sin(X_8)X_{11} + 2F_B L_B sin(\rho)sin^2(X_8) - 2J_\gamma cos(X_8)sin(\rho)X_{11}^2$$
$$- C_\theta X_{10} sin(X_8) + J_\theta X_{10} X_{11} cos(X_8) - C_x X_4 l sin(\rho) + 4l sin(\rho) sin(X_8) F_3$$
$$+ l sin(\rho)\omega_1 + 2L_B sin(\rho) sin^2(X_8)\omega_3$$
$$\dot{z}_4 = -2C_\phi sin(\rho)sin(X_8)X_{12} - 2F_B L_B sin(\rho)sin(X_8)sin(X_9)$$
$$+ 2J_\phi cos(X_8)sin(\rho)X_{11}X_{12} + C_\theta X_{10} sin(X_8) - J_\theta X_{10} X_{11} cos(X_8) - C_x X_4 l sin(\rho)$$
$$+ 4l sin(\rho) sin(X_8) F_4 + l sin(\rho)\omega_1 - 2L_B sin(\rho) sin(X_8) sin(X_9)\omega_3$$

From the above equations, we have $\Lambda_i = \{p_1, p_3\}, i = 1, ..., 4$ and according to Remark 4.2, one needs only to generate one extra residual signal that is decoupled from ω_1 and ω_3. Towards this end, the largest observability codistribution $\Pi_5^* = o.c.a.((\sum_*^{\mathcal{L}_5})^\perp)$ should be found where $\mathcal{L}_5 = \{p_1, p_3\}$ such that

$$span\{g_i(X)\} \not\subset (\Pi_5^*)^\perp, \quad i = 1, ..., 4$$

For the ALTAV model, we have

$$\Pi_5^* = \mathcal{L}_5^\perp$$

Based on Π_5^* the following set of states can be found that are decoupled from p_1 and p_3 and are affected by all control inputs F_i's, namely

$$z_5 = X_{10}$$

$$z_6 = X_5$$

However, only one of the above states is sufficient and in order to satisfy Assumption 4.3, we can only select z_5 for this purpose, since $\Omega_3^p = \{r_6\}$ where r_6 corresponds to the residual signal that is generated by the observer of state z_6. The state space representation and the governing equation corresponding to z_5 is given by:

$$\dot{z}_5 = -\frac{C_\theta}{J_\theta} z_5 - \frac{l sin(\rho)}{J_\theta}(F_1 - F_2 + F_3 - F_4)$$

In the next step, detection filters or nonlinear observers are designed for the complete set of the five states z_1 to z_5. Given our original assumption regarding the availability of all the ALTAV states, the following observers are now constructed.

$$\dot{\hat{z}}_1 = -2C_\gamma sin(\rho)sin(Y_8)Y_{11} - 2F_B L_B sin(\rho)sin^2(Y_8) + 2J_\gamma cos(Y_8)sin(\rho)Y_{11}^2$$

$$- C_\theta Y_{10} sin(Y_8) + J_\theta Y_{10} Y_{11} cos(Y_8) - C_x Y_4 l sin(\rho) + 4l sin(\rho) sin(Y_8) F_1 + k_1(z_1 - \hat{z}_1)$$

$$\dot{\hat{z}}_2 = 2C_\phi sin(\rho)sin(Y_8)Y_{12} + 2F_B L_B sin(\rho)sin(Y_8)sin(Y_9) - 2J_\phi cos(Y_8)sin(\rho)Y_{11}Y_{12}$$

$$+ C_\theta Y_{10} sin(Y_8) - J_\theta Y_{10} Y_{11} cos(Y_8) - C_x Y_4 l sin(\rho)$$

$$+ 4l sin(\rho) sin(Y_8) F_2 + k_2(z_2 - \hat{z}_2)$$

$$\dot{\hat{z}}_3 = 2C_\gamma sin(\rho)sin(Y_8)Y_{11} + 2F_B L_B sin(\rho)sin^2(Y_8)] - 2J_\gamma 7 cos(Y_8)sin(\rho)Y_{11}^2$$

$$- C_\theta Y_{10} sin(Y_8) + J_\theta Y_{10} Y_{11} cos(Y_8) - C_x Y_4 l sin(\rho)$$

$$+ 4l sin(\rho) sin(Y_8) F_3 + k_3(z_3 - \hat{z}_3)$$

$$\dot{\hat{z}}_4 = -2C_\phi sin(\rho)sin(Y_8)Y_{12} - 2F_B L_B sin(\rho)sin(Y_8)sin(Y_9)$$

$$+ 2J_\phi cos(Y_8)sin(\rho)Y_{11}Y_{12} + C_\theta Y_{10} sin(Y_8) - J_\theta Y_{10} Y_{11} cos(Y_8)$$

$$- C_x Y_4 l sin(\rho) + 4l sin(\rho) sin(Y_8) F_4 + k_4(z_4 - \hat{z}_4)$$

$$\dot{\hat{z}}_5 = -\frac{C_\theta}{J_\theta}\hat{z}_5 - \frac{l sin(\rho)}{J_\theta}(F_1 - F_2 + F_3 - F_4) + k_5(z_5 - \hat{z}_5)$$

where $k_i > 0, i = 1, ..., 5$ are the observer gains that can be selected to achieve a tradeoff between ensuring higher robustness to uncertainties and disturbances versus higher sensitivity to faults. By utilizing the above observers, the residual signals $r_i(t) = z_i(t) - \hat{z}_i(t), i = 1, ..., 5$ can now be produced. The coding sets for the fault channels $F_1, ..., F_4$ and the disturbance inputs ω_1 and ω_3 are as follows: $\Omega_1^f = \{1, 5\}$, $\Omega_2^f = \{2, 5\}$, $\Omega_3^f = \{3, 5\}$, $\Omega_4^f = \{4, 5\}$ and $\Omega_1^p = \Omega_3^p = \{1, 2, 3, 4\}$. Moreover, it is clear that the sufficient condition in Lemma 4.3 is also satisfied for the ALTAV system.

Once the residual signals $r_i(t), i = 1, ..., 5$ are constructed, the next step is to determine the threshold J_{th_i} and the evaluation function $J_{r_i}(t)$. In this paper, the following evaluation functions are selected

$$J_{r_i}(t) = \int_{t-T_0}^{t} r_i^\top(t) r_i(t) dt, \quad i = 1, ..., 5 \tag{4.30}$$

where T_0 is the length of the evaluation window. The main advantage of these evaluation functions is that one can detect intermittent faults easily. The threshold values and the corresponding residual logic units $R_i^1, i = 1, ..., 5$ and $R_i^2, i = 1, ..., 4$ are selected according to equations (4.12), (4.14), (4.15) and (4.17), respectively.

Remark 4.5. *The evaluation function $J_{r_i}(t) = r_i(t)$ is not applicable to the ALTAV system since oscillations are present in the residual signals $r_i, i = 1, ..., 4$ when simultaneously there is a fault in one of the input channels F_i and the state γ happens to be also varying about zero. Under these circumstances the corresponding residual signals will also behave similar to that of γ. Refer to Figure 4.11 depicted in the next section for further clarification.*

The next step is to design a DES fault diagnoser H. According to Table 4.1, the state set is defined as $S_H = \{s_0, ..., s_4, s_{1,2}, ..., s_{3,4}, s_{1,D}, ..., s_{4,D}, s_F, s_{F,D}\}$ where cardinality of S is 23. The input set of the diagnoser is $I = \{R_1^1, ..., R_5^1, R_1^2, ...R_4^2\}$ and the output set is equal to S_H. The transition function λ_H can be found following the results in Section 4.4.2, which is shown in Table 4.9.

4.4.3 Simulation Results

In this section, simulation results of our proposed hybrid scheme that is applied to the nonlinear ALTAV system are presented. Various actuator faults are considered in the four input channels of the ALTAV system. Figure 4.8 shows the desired reference trajectory and the actual ALTAV trajectory in the normal or healthy operation of the system. In this surveillance-type maneuvering mission, the ALTAV initiates its motion from the coordinate (0,0,10) (m), follows a rectangular path in the x-y plane, and then changes its altitude to 20 (m) and follows the same pattern in this altitude. Tables 4.10 and 4.11 show the characteristics of the output measurement noise and tolerable disturbance inputs $\mathfrak{D}_1$ that are considered in the simulation results below, respectively. Since large changes in the buoyant force F_B do not produce any changes

Table 4.9: Transition function of the ALTAV DES fault diagnoser

Current State	Input $R_1^1 \ldots R_5^1 \;\; R_1^2 \ldots R_4^2$	Next state
s_0	$R_1^1 \bigwedge R_5^1 = 1$	s_1
s_0	$R_2^1 \bigwedge R_5^1 = 1$	s_2
s_0	$R_3^1 \bigwedge R_5^1 = 1$	s_3
s_0	$R_4^1 \bigwedge R_5^1 = 1$	s_4
s_0	$R_1^1 \bigwedge R_2^1 \bigwedge R_3^1 \bigwedge R_4^1 = 1$	s_D
s_0	$R_5^1 = 1$	s_F
s_1	all zero	s_0
s_1	$R_1^1 \bigwedge R_2^1 \bigwedge R_5^1 = 1$	$s_{1,2}$
s_1	$R_1^1 \bigwedge R_3^1 \bigwedge R_5^1 = 1$	$s_{1,3}$
s_1	$R_1^1 \bigwedge R_4^1 \bigwedge R_5^1 = 1$	$s_{1,4}$
s_1	$\bigwedge_{j=1}^{5} R_j^1 = 1$	$s_{1,D}$
$\vdots$	$\vdots$	$\vdots$
s_4	all zero	s_0
s_4	$R_1^1 \bigwedge R_4^1 \bigwedge R_5^1 = 1$	$s_{1,4}$
s_4	$R_2^1 \bigwedge R_4^1 \bigwedge R_5^1 = 1$	$s_{2,4}$
s_4	$R_3^1 \bigwedge R_4^1 \bigwedge R_5^1 = 1$	$s_{3,4}$
s_4	$\bigwedge_{j=1}^{5} R_j^1 = 1$	$s_{4,D}$
s_D	all zero	s_0
s_D	$R_1^2 \bigwedge R_2^1 \bigwedge R_3^1 \bigwedge R_4^1 \bigwedge R_5^1 = 1$	$s_{1,D}$
s_D	$R_2^2 \bigwedge R_1^1 \bigwedge R_3^1 \bigwedge R_4^1 \bigwedge R_5^1 = 1$	$s_{2,D}$
s_D	$R_3^2 \bigwedge R_1^1 \bigwedge R_2^1 \bigwedge R_4^1 \bigwedge R_5^1 = 1$	$s_{3,D}$
s_D	$R_4^2 \bigwedge R_1^1 \bigwedge R_2^1 \bigwedge R_3^1 \bigwedge R_5^1 = 1$	$s_{4,D}$
s_D	$R_1^1 \bigwedge R_2^1 \bigwedge R_3^1 \bigwedge R_4^1 \bigwedge R_5^1 = 1$	$s_{F,D}$
s_F	all zero	s_0
s_F	$R_1^1 \bigwedge R_5^1 = 1$	s_1
s_F	$R_2^1 \bigwedge R_5^1 = 1$	s_2
s_F	$R_3^1 \bigwedge R_5^1 = 1$	s_3
s_F	$R_4^1 \bigwedge R_5^1 = 1$	s_4
s_F	$R_1^1 \bigwedge R_2^1 \bigwedge R_3^1 \bigwedge R_4^1 \bigwedge R_5^1 = 1$	$s_{F,D}$

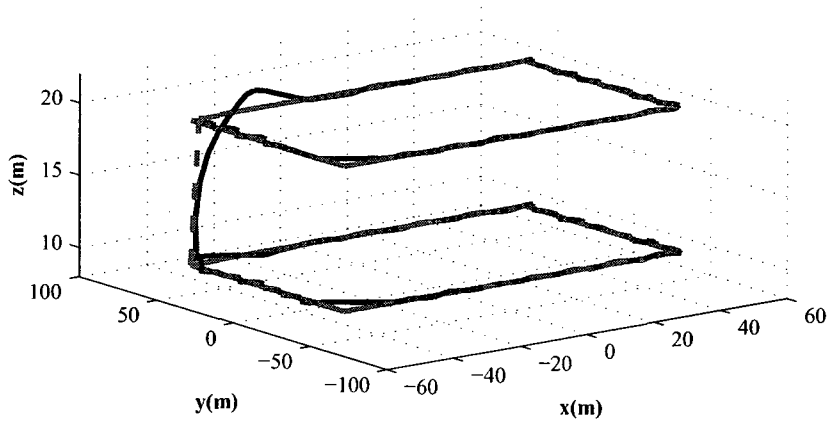

Figure 4.8: The reference trajectory (dashed line) and the ALTAV trajectory (solid line) corresponding to a healthy operation.

in the residuals, only the wind disturbance in the x-direction needs to be considered for simulations (the wind disturbance in the y-direction is unobservable from the residual signals), i.e.

$$\mathfrak{D}_2 = \{W_x | 0.5 \ll W_x < 5(Newton)\}$$

By considering the worst case scenario of residuals corresponding to the healthy mode of the ALTAV system subject to the measurement noise and tolerable input disturbances $\mathfrak{D}_1$ (refer to Table 4.11), the threshold values of $J^1_{th_i} = 6e-4, J^2_{th_i} = 4.5e-3,\ i = 1, ..., 4$ and $J^1_{th_5} = 3e-5$ and the evaluation window $T_0 = 5$ seconds and $T_0 = 10$ seconds were selected for the residual signals $r_1, ..., r_4$ and r_5, respectively. It should be pointed out that since the residual signal r_5 is decoupled from all the disturbance inputs, one can select a lower threshold value for it.

Figure 4.9 shows the residual evaluation functions corresponding to a permanent float fault in the input channel F_1 at $t = 100$ seconds. A concurrent wind disturbance gust represented by a rectangular pulse of a constant amplitude 3 (N) in the x-direction between $t = 80$ and $t = 120$ seconds is also applied to the ALTAV system in this simulation. Figure 4.10 depicts the state of the DES fault diagnoser. As shown in this figure, the diagnoser state first changes to s_D at $t = 83$ seconds

Table 4.10: Output measurement noise characteristics

Output measurement	Noise characteristics
γ	Uniform random variable $\pm$ 1 degree
ϕ	Uniform random variable $\pm$ 1 degree
$\dot{x}$	Uniform random variable $\pm$ 0.1 m/s
$\dot{\theta}$	Uniform random variable $\pm$ 0.5 degree/s
$\dot{\gamma}$	Uniform random variable $\pm$ 0.5 degree/s
$\dot{\phi}$	Uniform random variable $\pm$ 0.5 degree/s

Table 4.11: Tolerable disturbance input $\mathfrak{D}_1$ characteristics

	Disturbance characteristics
W_x	Uniform random variable $\pm$ 0.5 Newton
W_y	Uniform random variable $\pm$ 0.5 Newton
ΔF_B	Uniform random variable $\pm$ 2 Newton

after the occurrence of the large wind disturbance in the x-direction with no false alarm generated. Later when a fault in the input channel F_1 is injected, the diagnoser state first switches to $s_{F,D}$ at $t = 101.3$ seconds and then after about 2 seconds it switches to state $s_{1,D}$ at $t = 103$ seconds. Consequently, we can conclude that the diagnoser can perfectly detect and isolate the fault despite the presence of a large concurrent disturbance. Finally, after the disturbance is removed at $t = 120$ seconds, the diagnoser switches to the state s_1. It should be emphasized that if one *only* uses the first 4 residuals $r_1, ..., r_4$, not only a *false alarm* will be generated due to the wind disturbance but also the actual fault at $t = 100$ *cannot* be detected and isolated. However, by using our proposed hybrid FDI methodology, we are able to distinguish the occurrence of a fault as well as large wind disturbance in the x-direction ($\omega_1 \in \mathfrak{D}_2$) by designing only one additional residual signal.

Figure 4.11 shows the residual signals corresponding to the above fault scenario. According to the points raised in Remark 4.5, it is now evident from Figure 4.11 why one cannot directly evaluate the residual signals using their thresholds, i.e. $J_{r_i} = r_i$ since due to the dynamics of the ALTAV system after the occurrence of the fault, the residuals tends to oscillate in and out of the threshold bounds.

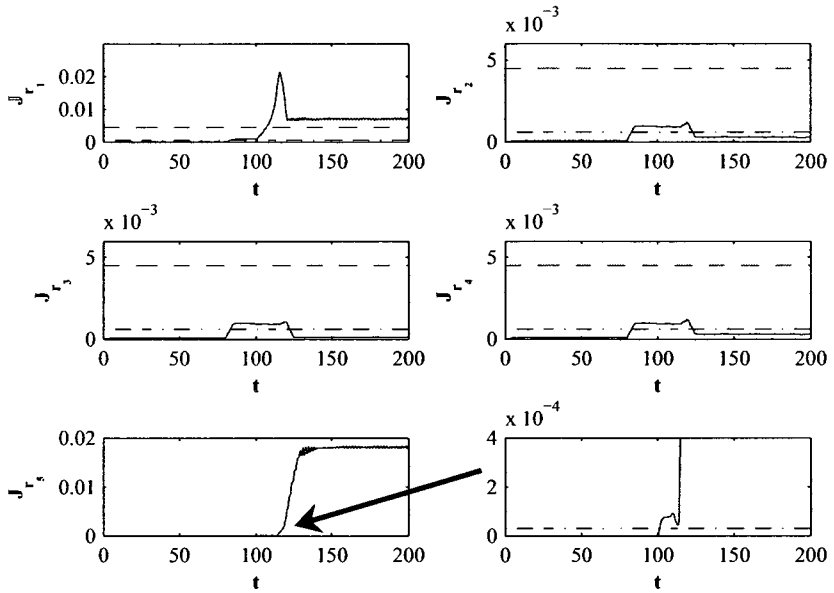

Figure 4.9: Residual evaluation functions corresponding to a float fault in the F_1 actuator (the dashed dots correspond to the threshold values $J^1_{th_i} = 6e{-}4, i = 1, ..., 4$ and $J^1_{th_5} = 3e{-}5$, the dashed lines correspond to the threshold value $J^2_{th_i} = 4.5e{-}3$).

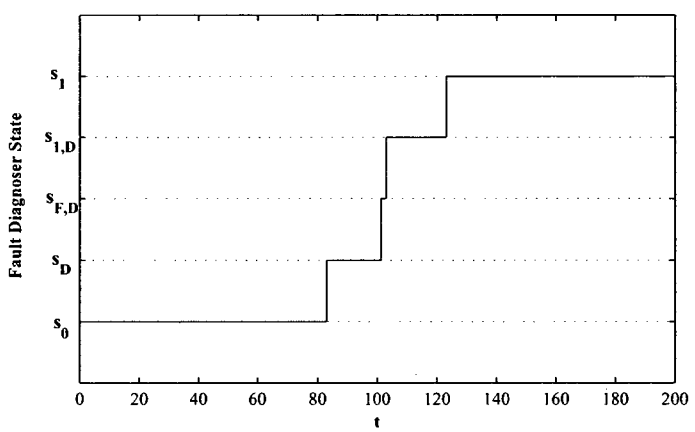

Figure 4.10: Fault diagnoser state corresponding to a float fault in the F_1 actuator.

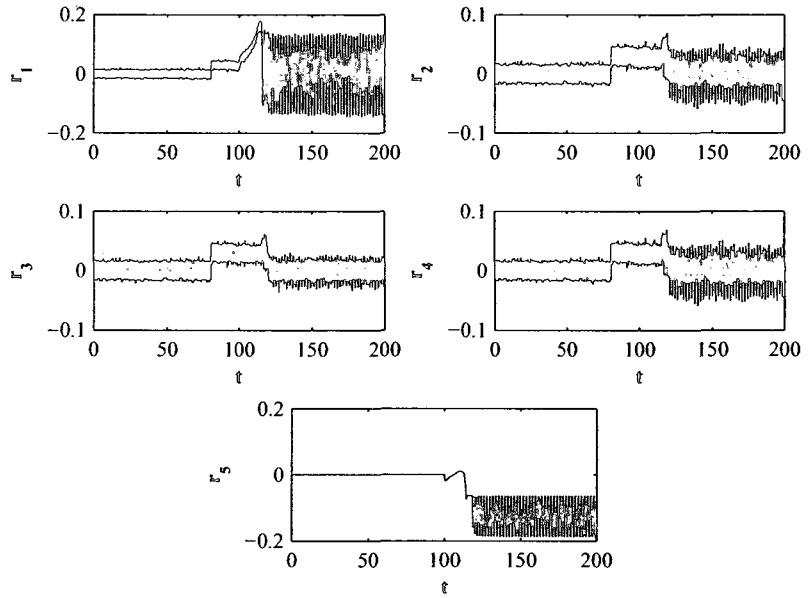

Figure 4.11: Residuals corresponding to a float fault in the F_1 actuator.

Figure 4.12 depicts the residual evaluation functions associated with a permanent hard over fault (HOF) in the input channel F_2 that is applied at $t = 100$ seconds, and Figure 4.13 shows the corresponding fault diagnoser state. A wind disturbance gust that is represented by a rectangular pulse of constant amplitude 3 (N) in the x-direction is also injected between $t = 50$ and $t = 80$ seconds in the simulations. As seen from Figure 4.13, the diagnoser first detects the fault at $t = 100.2$ seconds and also isolates the fault at $t = 107.5$ seconds. Moreover, no false alarm is generated due to the presence of the disturbance input. As shown in Figure 4.12, the residual evaluation function J_{r_2} does not exceed the second threshold values $J^2_{th_i}$. Consequently, if one only uses a conventional FDI method and chooses the threshold values by considering the entire disturbance set, i.e. $\mathfrak{D}_2$, then the hard over fault cannot be detected and isolated. However, by using our proposed approach, this fault can easily be detected and then isolated despite the presence of large wind disturbance.

Figures 4.14 and 4.15 depict the residual evaluation functions and the fault

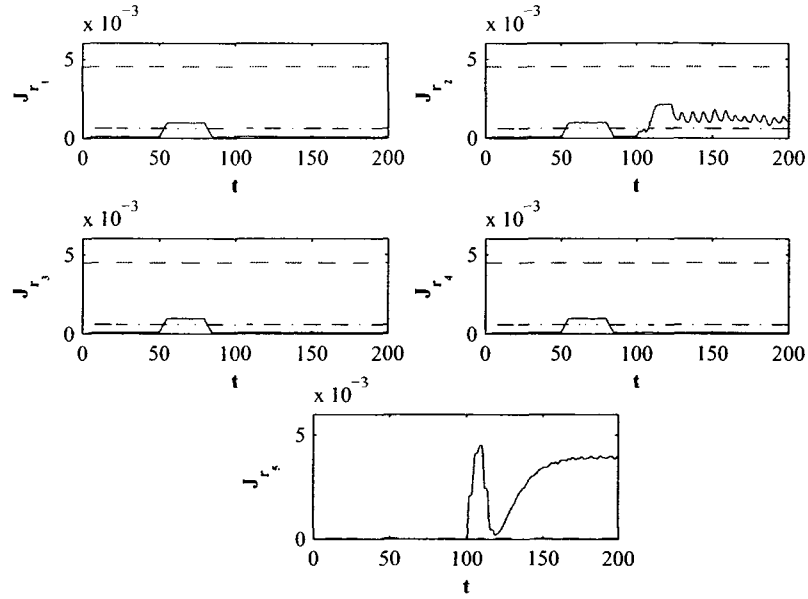

Figure 4.12: Residual evaluation functions corresponding to a hard over fault in the F_2 actuator (the dashed dots correspond to the threshold values $J^1_{th_i} = 6e - 4, i = 1, ..., 4$ and $J^1_{th_5} = 3e - 5$, the dashed lines correspond to the threshold value $J^2_{th_i} = 4.5e - 3$).

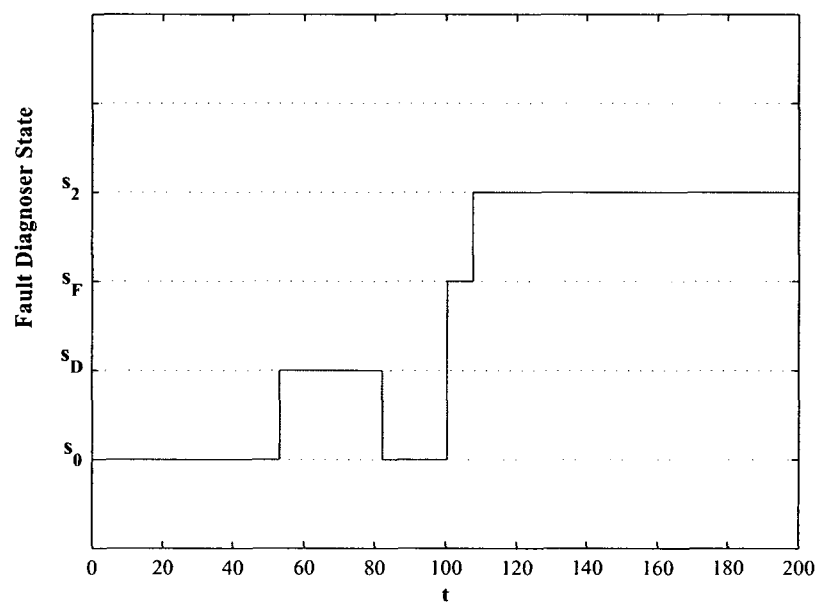

Figure 4.13: Fault diagnoser state corresponding to a hard over fault in the F_2 actuator.

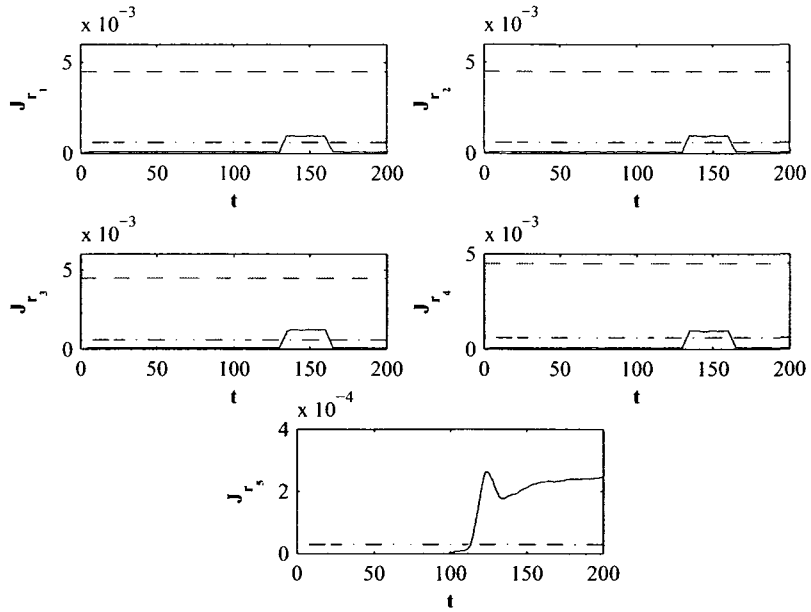

Figure 4.14: Residual evaluation functions corresponding to a 50% loss of effectiveness in the F_3 actuator (the dashed dots correspond to the threshold values $J^1_{th_i} = 6e-4, i = 1, ..., 4$ and $J^1_{th_5} = 3e-5$, the dashed lines correspond to the threshold value $J^2_{th_i} = 4.5e-3$).

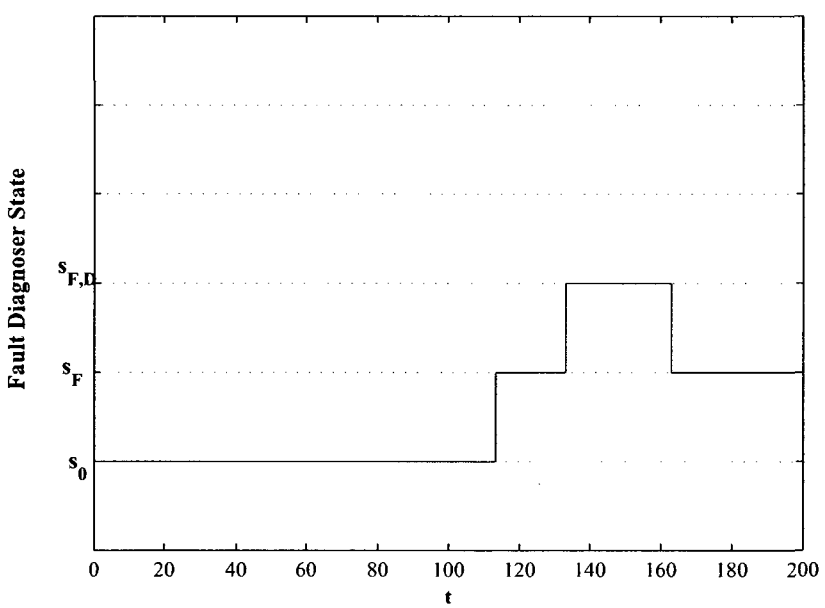

Figure 4.15: Fault diagnoser state corresponding to a 50% loss of effectiveness in the F_3 actuator.

diagnoser state, respectively, corresponding to a permanent 50% loss of effectiveness (LOE) fault in the input channel F_3 injected at $t = 100$ seconds and a wind gust disturbance that is represented by a rectangular pulse of constant amplitude 3 (N) in the x-direction between $t = 130$ and $t = 160$ seconds. As seen from the above figures the residual evaluation function J_{r_3} does not exceed its threshold whereas the residual evaluation function J_{r_5} does exceed its threshold. In this scenario the fault diagnoser can only detect the occurrence of the fault but cannot isolate it. Moreover, the occurrence of a concurrent large disturbance does not cause any false alarms in any of the input channels. This scenario also illustrates another advantage of introducing our set of complementary residuals (the residual r_5 in the case of the ATLAV system), since by incorporating this set of residuals one can also detect the occurrence of a low severity fault.

The last scenario we consider corresponds to presence of multiple faults in the ALTAV actuators. For the generated residual signals, we have $\Omega_i^f \cup \Omega_j^f \subset \Omega_i^f \cup \Omega_1^p$. Therefore, according to Remark 4.4, a waiting time interval of $\tau_0 = 1$ second is considered for detecting the second fault. Figures 4.16 and 4.17 show the corresponding residual evaluation functions and the fault diagnoser, respectively, to an intermittent float fault in the input channel F_1 that is applied between $t = 100$ and $t = 150$ seconds, a permanent 50% loss of effectiveness fault in the input channel F_4 that is applied at $t = 120$ seconds and a wind gust disturbance that is represented by a rectangular pulse of constant amplitude 3 (N) that is injected in the x-direction between $t = 50$ and $t = 80$ seconds. According to these figures one does clearly detect and isolate multiple faults in the ALTAV system.

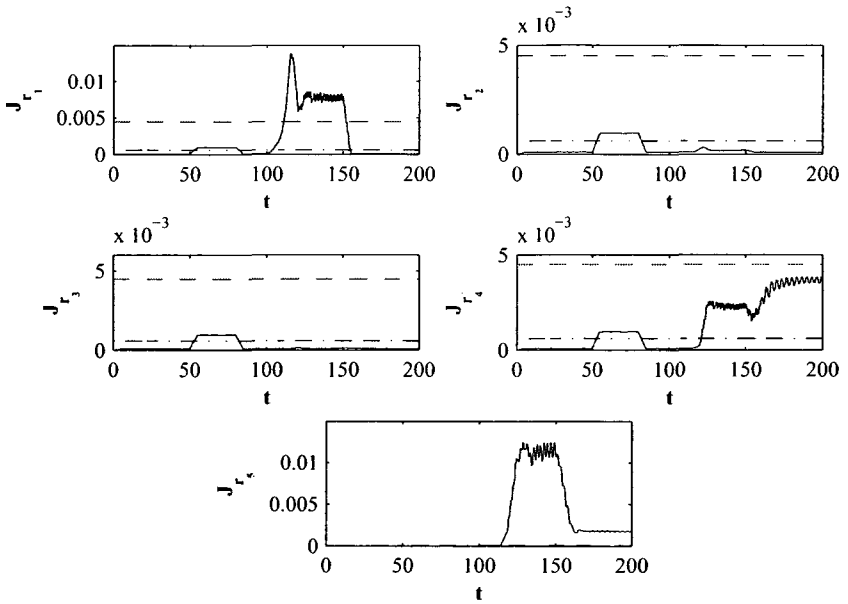

Figure 4.16: Residual evaluation functions corresponding to multiple faults in the F_1 and F_4 actuators (the dashed dot corresponds to the threshold values $J^1_{th_i} = 6e-4, i = 1, ..., 4$ and $J^1_{th_5} = 3e-5$, the dashed lines correspond to the threshold value $J^2_{th_i} = 4.5e-3$).

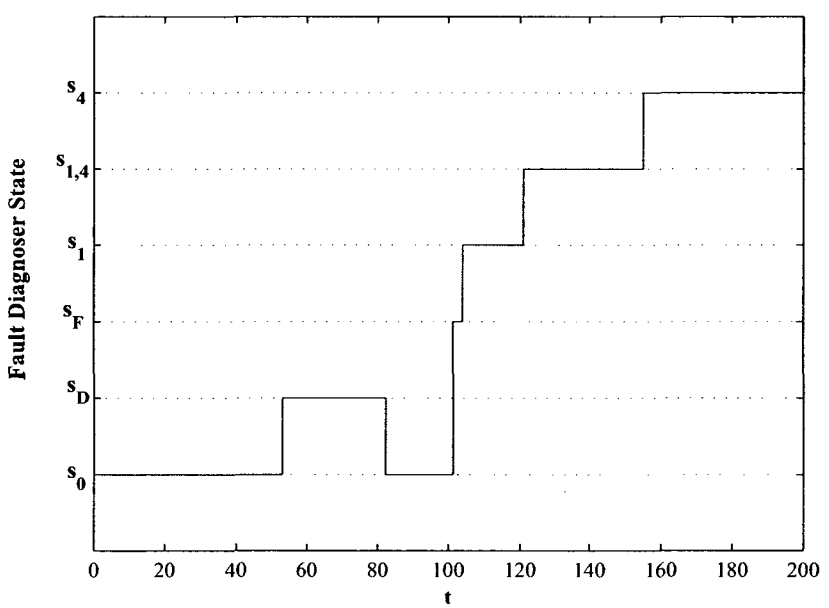

Figure 4.17: Fault diagnoser state corresponding to multiple faults in the F_1 and F_4 actuators.

4.5 Conclusions

A novel hybrid fault detection and isolation scheme is proposed for both linear and nonlinear systems subject to large disturbances. The proposed scheme consists of two modules, namely, a bank of residual generators and a discrete-event system (DES)-based fault diagnoser. A DES diagnoser is developed which uses the residual signals and their temporal behavior to robustly detect and isolate the faulty channels. Our proposed hybrid FDI methodology is applied to the problem of actuators fault detection and isolation for an ALTAV system and a network of unmanned vehicles. Simulation results clearly illustrate and demonstrate the effectiveness and advantages of our proposed approach.

Chapter 5

Compensating for Communication Channels Effects in Fault Detection and Isolation

This chapter deals with the problem of fault detection and isolation in a network of unmanned vehicles when there exist imperfect communication channels among the vehicles. A discrete-time communication link with stochastic packet dropping effect is considered based on Gilbert-Elliott model [170, 171] which is known as packet erasure channel model and the entire network is modeled as a discrete-time Markovian Jump System (MJS). The above problem can be treated in the general framework of Markovian jump systems. This motivates us to develop a geometric FDI framework for both continuous-time and discrete-time Markovian jump systems and apply the developed algorithm to FDI of a network of unmanned vehicles in the presence of imperfect communication channels. The work presented in this chapter has partly appeared in [172].

This chapter is organized as follows. After a summary of the relevant literature, we begin in Section 5.2 with briefly discussing the packet erasure channel model

that we use in this chapter. In Section 5.3, a discrete-time Markovian jump model of a networked of unmanned vehicles combined with the packet erasure channel model is developed in the centralized architecture. In Section 5.4, the FDI problem for discrete-time MJS is investigated in a geometric FDI framework. Toward this end, in Section 5.4.1 a geometric property related to the unobservable subspace of a Markovian jump system is presented. A new approach for determining the conditions for weak-observability of MJS systems is then introduced. The concept of unobservability subspace is presented and an algorithm for obtaining it is described. In Section 5.4.2 the necessary and sufficient conditions for solvability of the fundamental problem of residual generation (FPRG) for MJS systems are obtained by utilizing our introduced unobservability subspace. We also present and develop sufficient conditions for designing H_∞-based FDI algorithms for MJS systems subject to input disturbances in Section 5.4.3. Our proposed algorithm is then applied to the FDI problem in a formation flight of satellites. In Section 5.5 similar results are derived for FDI of continuous-time Markovian jump system. Finally, our proposed algorithm is applied to fault detection and isolation of VTOL (vertical take-off and landing) helicopter actuators in Section 5.5.4.

Contributions

The main contributions of this chapter are now summarized as follows:

- A new geometric property of unobservable subspace for Markovian jump systems (both continuous-time and discrete-time) are derived.
- The geometric concept of unobservability subspaces is introduced for Markovian jump systems (both continuous-time and discrete-time) and an algorithm for obtaining these subspaces is presented.
- The necessary and sufficient conditions for solvability of the fundamental problem of residual generation (FPRG) for MJS systems are derived.

- The problem of actuator fault detection and isolation in a network of unmanned vehicles in the presence of imperfect communication links is tackled in the framework of Markovian jump systems.

5.1 Introduction

Recently, networked control systems (NCS) have become a hot area of research and have found some important applications in a wide variety of engineering systems including manufacturing plants, aircraft, automobiles, etc. Generally speaking, NCS are comprised of a large amount of actuators, sensors, and controllers which are all equipped with network interfaces, and are equal nodes of the network. All the signals, including real-time sensing, controller outputs, commands, coordination and supervision signals are transmitted through shared network channels. New and interesting challenges arise when feedback loops are closed via networks. The network itself is a dynamical system that exhibits characteristics such as networked-induced delay, packet dropout, asynchronous clock among network nodes which could degrade the performance of the closed-loop system and even destabilize the system.

Research on NCS has received increasing attention in recent years, and a large body of work have been produced on the modeling, design and stability analysis. However, few results exist on the fault detection and diagnosis in NCS. In [173], a Kalman filter is designed for fault detection with the assumption that network delay is known but time-varying. In [174], fault detection for NCS with missing measurements is investigated. In this work NCS is modeled as a Markovian jump linear system and an H_∞ optimization technique is used for designing a fault detection filter for the Markovian jump system. In [175], a robust parity space approach is developed for *fault detection* in NCS with unknown and time-varying delays between controller and actuator. In [176], NCS model is transformed into a framework of

linear time-invariant system with modeling uncertainty caused by stochastic changes in the system parameters due to the network induced delay and data loss. A unified approach proposed in [177] is used for residual generation. In [178], the effect of network induced delay is modeled as time-varying disturbance and fault isolation filter for NCS with multiple faults is parameterized based on directional residual generation approach. The remaining degrees of freedom are used to satisfy an H_∞ disturbance attenuation in the framework of Markovian jump systems. In [179], the FDI problem for NCS with large transfer delays is considered. With employing the multirate sampling method together with the augmented state matrix method, the NCS with large transfer delays is modeled as a Markovian jump system and an H_∞ fault detection filter is designed for the developed model.

The packet delivery characteristics of a network can be modeled as a Bernoulli or two-state Markov process [170, 171, 180–185]. The latter is commonly used for modeling the fading communication channels and is also known as *packet erasure channel model.* The combination of a discrete-time plant with these channel models yields a discrete-time Markovian jump system (MJS). A great deal of attention has recently been devoted to the Markovian jump systems [186–191] which comprise an important class of hybrid systems. This family of systems is generally modeled by a set of linear systems with transitions between models that are determined by a Markov chain taking values in a finite set. Markovian jump systems are also popular in modeling many practical systems where one may experience abrupt changes in system structure and parameters. These changes are quite common and do frequently occur in manufacturing systems, economic systems, communication systems, power systems, etc. [192].

In recent years, only a few work on fault detection and isolation of MJS systems have appeared in the literature. In [174, 179, 193], a robust fault detection (and *not an isolation*) filter for discrete-time Markovian jump systems is developed based on

an H_∞ filtering framework, in which the residual generator is also an MJS system. An LMI approach is developed for solving the problem. In [194], a robust fault identification filter for a class of discrete-time Markovian jump systems with mode dependent time-delays and norm bounded uncertainty is developed based on an H_∞ optimization technique. In the approach in [194], the generated residual signal is an estimate of the fault signal. However, the problem of fault isolation for Markovian jump systems has not been completely solved and fully addressed in the above references.

In this chapter, based on the Gilbert-Elliott model [170, 171, 180, 181], a network of unmanned vehicles combined with a two-state Markov process model of communication channels is modeled as a discrete-time Markovian jump system. The FDI problem in a network of unmanned vehicles in the presence of imperfect communication links can be solved in the framework of Markovian jump systems. A geometric approach is adopted for the FDI problem of both discrete-time and continuous-time Markovian jump systems. Towards this end, the first contribution of this chapter is the derivation of a geometric property for the unobservable subspace of MJS systems (Theorems 5.2 and 5.9) and development of a new approach for determining their weak-observability (Algorithm 5.1). The notion of an unobservability subspace is then introduced for MJS systems (Definition 5.6). To construct an algorithm for obtaining this subspace, an alternative definition of an unobservability subspace is presented in Theorem 5.4, which only depends on the matrices of the system. Based on this alternative definition, an algorithm for constructing the smallest unobservability subspace containing a given subspace is proposed (Algorithm 5.3). By utilizing the developed geometric framework, necessary and sufficient solvability conditions are derived for Markovian jump systems (Theorem 5.6). Using the properties of unobservability subspaces, a set of residuals is generated such that each residual is affected by one fault and is decoupled from others. Finally, we investigate the

problem of designing an H_∞-based FDI algorithm for a MJS system that has an unknown transition matrix and is subjected to external disturbances. These results are obtained by applying our proposed geometric approach and H_∞ disturbance attenuation technique (Theorem 5.7).

5.2 The Packet Erasure Channel Model

In this chapter, discrete-time communication links with stochastic packet dropping effects are considered among the vehicles and the FDI unit. Many phenomena are introduced due to the presence of communication links such as [182]:

1. Time delay: Data is usually buffered, quantized and coded before transmission over a channel. After a network delay due to propagation, the data is received and decoded in the receiver end. In the cases where the data is not received properly, the communication protocol may re-transmit the data. Hence, by the time the information is used by the receiver, a delay has been introduced. This delay is usually random with time-varying probability distribution.

2. Data loss: In most communication protocols, if the data is not received within a specific time limit, the packet is assumed to be lost. A variety of reasons can cause this data loss. For instance, simultaneous transmission by two transmitters in a shared multiple access medium such as wireless channels, may lead to loss of both transmitter data. In a network of communication channels, overflow of buffers can also cause the packet loss. Finally, in a network of unmanned vehicles, the presence of obstacles among vehicles and limited line of sight of each vehicle may lead to packet loss.

3. Quantization: In digital communication networks any data needs to be quantized and the number of bits that can be transmitted at every sampling time is usually upper-bounded.

4. Data corruption: Due to noise and attenuation introduced by the channel, the received data may not be identical to the signal that the transmitter sent through the communication channel. Most communication protocols has error detection and error correction algorithms to reduce the data corruption of the communication links.

At every sampling time k, the time line for the operation of a communication link of the i-th vehicle is as follows.

1. The i-the vehicle creates a packet containing the information that are needed to be shared with other vehicles or the FDI unit.

2. The packet is sent across the link.

3. At time step $k+1$ the packet is either received without error or dropped stochastically.

In the above communication links, it is assumed that:

- The channel coding is ignored and it is assumed that the packet will be either received and decoded successfully at the end of the link or totally lost.

- If a packet arrives too late, it is discarded and treated as a dropped packet and the lost packets are not re-sent.

- The number of bits in each packet is relatively large and hence the quantization effect of the channel is ignored.

One of the following models [185] can be considered for modeling the stochastic packet dropout:

- The independent and identically distributed (i.i.d.) Bernoulli model:

  A Bernoulli random variable γ_k is assigned to the communication link such

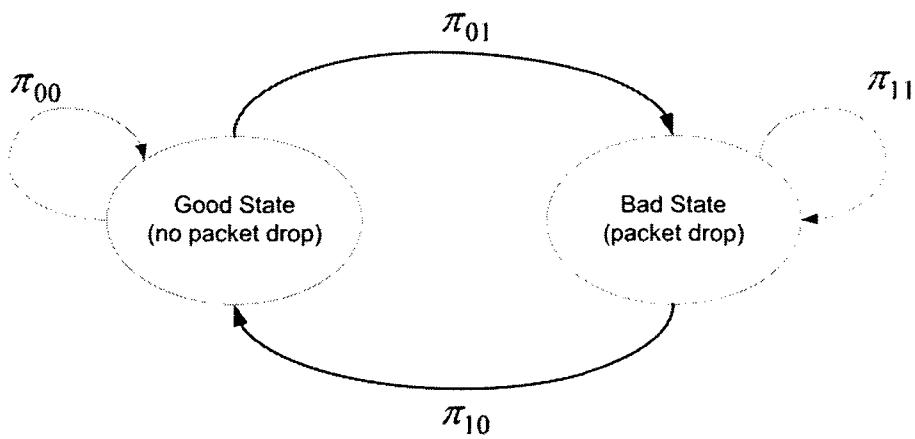

Figure 5.1: The Gilbert-Elliott model

that if the packet k is received correctly, then $\gamma_k = 1$, otherwise $\gamma_k = 0$. A random variable γ_k is i.i.d. with probability distribution $P(\gamma_k = 1) = \lambda$ and $P(\gamma_k = 0) = (1 - \lambda)$.

- The Gilbert-Elliott model [170, 171] shown in Figure 5.1. In this model, the network is considered as a discrete-time Markov chain with two possible states: "good" and "bad". The packet is received correctly in the "good" state and is dropped in the "bad" state. The network jumps between these two states according to a Markov chain with transition probability matrix Π as

$$\begin{bmatrix} \pi_{00} & \pi_{01} \\ \pi_{10} & \pi_{11} \end{bmatrix}$$

  where 1 is the good state, 0 is the bad state, and π_{ij} is the probability from the previous state i to the next state j.

In this thesis, we consider the Gilbert-Elliott model of the communication link since this model is able to capture the dependence between consecutive losses, i.e. bursty packet dropping.

5.3 A Network of Unmanned Vehicles in the Presence of Imperfect Communication Channels

In this section, a network of unmanned vehicles considered with the packet erasure channel model is modeled as a discrete-time MJS. It should be mentioned that a centralized architecture is considered here. Due to the discrete feature of the communication links, the discrete model of each vehicle is considered as

$$\begin{aligned} x_i(k+1) &= Ax_i(k) + Bu_i(k) + \sum_{j=1}^{P} L_j m_{ij}(k) \\ z_{ij}(k) &= C(x_i(k) - x_j(k)) \qquad j \in \mathrm{N}_i \end{aligned} \tag{5.1}$$

with the sampling time T_s where the set $\mathrm{N}_i \subset \mathbf{N} \setminus i$ represents the set of vehicles that vehicle i can sense and is designated as the neighboring set of vehicle i, and $z_{ij} \in \mathcal{Z}_i, j \in \mathrm{N}_i$ represents the state measurement relative to the other vehicles. Let $\mathrm{N}_i = \{i_1, i_2, ..., i_{|\mathrm{N}_i|}\}$. We have $z_i(t) = [z_{ii_1}^\top(t), z_{ii_2}^\top(t), \cdots, z_{ii_{|\mathrm{N}_i|}}^\top(t)]^\top$, and equation (5.1) can be rewritten as $z_i(t) = C_i x(t)$, where $x(t) = [x_1^\top(t), x_2^\top(t), \cdots, x_N^\top(t)]^\top$.

As discussed in Section 3.3.1, in the centralized architecture, all information should be sent to a central FDI unit through the "entire" communication network channels. It is assumed that each vehicle sends its information i.e. u_i and z_i with a sampling time T_d where $T_d \geq T_s$. Therefore, the overall system can be modeled as follows:

$$\begin{aligned} x(k+1) &= A^N x(k) + B^N u(k) + \sum_{k=1}^{N} \sum_{j=1}^{P} \bar{L}_{kj} m_{kj}(k) \\ z(k) &= \bar{C} x(k) \end{aligned} \tag{5.2}$$

with the sampling time T_d where $A_N = I_N \otimes A$, $B_N = I_N \otimes B$, $\otimes$ denotes the Kronecker product, N is a positive integer, I_N is an $N \times N$ identity matrix, $u = [u_1^\top, u_2^\top, \cdots, u_N^\top]^\top$, $\bar{L}_{kj}$ is the $(k-1) \times a + j$ column of B^N, $z = [z_1^\top, z_2^\top, \cdots, z_N^\top]^\top$ and $\bar{C}^\top = \left[C_1^\top, C_2^\top, \cdots, C_N^\top\right]$. The central FDI unit waits for T_d seconds to collect

all the information from all the vehicles. Therefore, a network delay of less than T_d does not affect the performance of the FDI algorithm. If the packet has a delay of more than T_d, then the FDI unit assumes that there is a packet dropout in that specific communication link between the central FDI unit and the vehicle.

In order to model packet dropout of communication network channels, a stochastic variable λ_i is assigned to the channel between the i-th vehicle and the central vehicle and it represents data communication status, i.e., $\lambda_i(k) = 1$ means the measurement u_i and z_i at time k arrives correctly, while $\lambda_i(k) = 0$ means that this measurement is lost. λ_i can be modeled as a discrete-time Markov chain with two state $\Psi_i = \{0, 1\}$ with the transition probability matrix $\Pi_i = (\pi_{ij})_{l,j\in\Psi_i}$ and π_{ij} is defined as

$$\pi_{lj} = Pr\{\lambda(k+1) = j|\lambda(k) = l\}$$

When the current information (u_i and z_i) of the i-th vehicle does not arrive on time ($\lambda_i(k) = 0$), the FDI unit uses the last available measurement of the control signal u_i and available output measurements z_j's, $j \neq i$. In other words, if we denote $u_i^a(k)$ as the i-th vehicle information that is used by the central FDI unit, then

$$u_i^a(k) = \begin{cases} u_i(k) & \text{if } \lambda_i(k) = 1 \\ \text{the last available measurment} & \text{if } \lambda_i(k) = 0 \end{cases}$$

Moreover, the central FDI unit uses available relative state measurements $z(k) =$

$\bar{C}_i x(k)$ where

$$\bar{C}_i = \begin{bmatrix} C_1 \\ \vdots \\ C_{i-1} \\ 0 \\ C_{i+1} \\ \vdots \\ C_N \end{bmatrix} \tag{5.3}$$

Remark 5.1. *It should be pointed out that the available relative state measurements for $\lambda_i(k) = 0$ is $z^i(k) = \bar{C}^i x(k)$ with variable dimension where $\bar{C}^{i^\top} = [C_1^\top, \cdots, C_{i-1}^\top, C_{i+1}^\top, \cdots, C_N^\top]$. However, it can be shown that the geometric properties of a Markovian jump system with measurement matrix $\bar{C}_i$ and $\bar{C}^i$ are identical. Indeed, we have $Ker(\bar{C}_i) = Ker(\bar{C}^i)$. Moreover, let $\mathcal{S} =< KerH^i\bar{C}^i | A + D^i\bar{C}^i >$, where $H^i = [H_1, ..., H_{i-1}, H_{i+1}, ..., H_N]$ and $D^i = [D_1, ..., D_{i-1}, D_{i+1}, ..., D_N]$, then $A + D^i\bar{C}^i = A + D_i\bar{C}_i$ where $KerH^i\bar{C}^i = KerH_i\bar{C}_i$ $H_i = [H_1, ..., H_{i-1}, 0, H_{i+1}, ..., H_N]$ and $D_i = [D_1, ..., D_{i-1}, 0, D_{i+1}, ..., D_N]$ and hence $\mathcal{S} =< KerH_i\bar{C}_i | A + D_i\bar{C}_i >$. Therefore, for keeping the dimension of output constant, the measurement matrix $\bar{C}_i$ is considered here.*

In the next assumption, it is assumed that the change of the control input for each vehicle in each FDI sampling time is bounded.

Assumption 5.1. *It is assumed that for each vehicle $\theta_i^u(k) = u_i^a(k) - u_i(k)$ is an $\mathfrak{L}_2$ bounded signal.*

Therefore, in the case of $\lambda_i(k) = 0$, the overall system can be modeled as

$$\begin{aligned} x(k+1) &= A^N x(k) + B^N u(k) + \sum_{k=1}^{N} \sum_{j=1}^{a} \bar{L}_{kj} m_{kj}(k) + B_i^d \theta_i^u(k) \\ z(k) &= \bar{C}_i x(k) \end{aligned} \tag{5.4}$$

where

$$B_i^d = \begin{bmatrix} 0 \\ \vdots \\ B_i \\ \vdots \\ 0 \end{bmatrix}$$

In the case of $\lambda_i(k) = 1$, the overall system model is as in (5.2). Therefore, disturbance terms $B_i^d \theta_i^u(k)$ is added due to the loss of u_i and different measurement matrix $\bar{C}_i$ is used due to the loss of z_i.

In order to incorporate the data dropout of all the communication channels, a discrete-time Markov chain λ with $N+1$ states with the transition probability matrix $\Pi = (\pi_{ij})_{i,j \in \Psi}$ is introduced. Without loss of generality, it is assumed that only one data dropout is allowable at each sampling time. This assumption only limits the number of modes of the system to $N+1$ and can be easily removed by increasing the number of mode and considering multiple data dropout. The mode 1 corresponds to the case with no packet dropout in all the communication links and the mode $i+1$ corresponds to the packet dropout in the communication link of the i-the vehicle. Therefore, the entire system can be modeled by the following Markovian jump system

$$\begin{aligned} x(k+1) &= A^N x(k) + B^N u(k) + \bar{B}^d_{\lambda(k)} \bar{\theta}^u(k) + \sum_{k=1}^{N} \sum_{j=1}^{a} \bar{L}_{kj} m_{kj}(k) \\ z(k) &= \bar{C}_{\lambda(k)} x(k) \end{aligned} \tag{5.5}$$

where

$$\bar{\theta}^u(k) = \begin{bmatrix} \theta_1^u \\ \vdots \\ \theta_N^u \end{bmatrix}$$

and for $\lambda(k) = i+1$, $i \in \mathbf{N}$ we have

$$\bar{B}^d_{i+1} = \begin{bmatrix} 0 & \cdots & 0 & \cdots \\ \vdots & & & \vdots \\ 0 & \cdots & B_i & \cdots \\ \vdots & & & \vdots \end{bmatrix}$$

where B_i is the i-th row and the i-th column of matrices $\bar{B}^d_{i+1}$. For $\lambda(k) = 1$, we have $\bar{B}^d_1 = 0$ and $\bar{C}_0 = \bar{C}$.

Remark 5.2. *It should be noted that the FDI problem in sensor networks (Figure 5.2) can be treated similarly in the framework of Markovian jump systems. Consider a discrete-time linear system*

$$x(k+1) = Ax(k) + Bu(k) + B_d d(k) \tag{5.6}$$

where $x(k) \in \mathcal{X}$ is the state, $u(k) \in \mathcal{U}$ is the control input and $d(k)$ is the input disturbance. The state of the plant is measured by N sensors where the i-th sensor generates the output measurements according to

$$y_i(k) = C_i x(k) + D_{di} d(k) \tag{5.7}$$

Every sensor sends its own measurement through the communication channel. By combining the packet erasure channel model with each measurement equation, a discrete-time MJS model of the entire sensor network can be obtained as follows:

$$\begin{aligned} x(k+1) &= Ax(k) + Bu(k) + B_d d(k) \\ y(k) &= C_{\lambda(k)} x(k) + D_{\lambda(k)} d(k) \end{aligned} \tag{5.8}$$

Hence, our developed algorithm in the next section will be applicable to both networks of unmanned vehicles and sensor networks.

In the next section, a geometric FDI framework for discrete-time Markovian jump systems is developed.

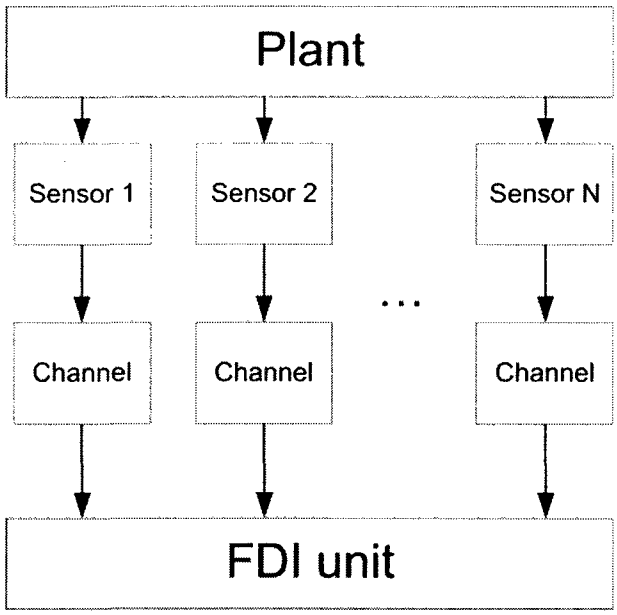

Figure 5.2: FDI in sensor networks

5.4 Discrete-time Markovian Jump Systems

Consider the following discrete-time Markovian jump system

$$\begin{aligned} x(k+1) &= A_{\lambda(k)}x(k) + B_{\lambda(k)}u(k) \\ y(k) &= C_{\lambda(k)}x(k), \quad x(0) = x_0, \quad \lambda(0) = i_0 \end{aligned} \tag{5.9}$$

where $x \in \mathcal{X}$ is the state of the system with dimension n; $u \in \mathcal{U}, y \in \mathcal{Y}$ are input and output signals with dimensions m and q, respectively; and $\{\lambda(k), k \geq 0\}$ is a discrete-time irreducible Markov process taking values in the finite set $\Psi = \{1, ..., N\}$. The Markov process describes the switching between the different system modes and its evolution is governed by the following probability transitions:

$$\pi_{ij} = \mathbb{P}\{\lambda(k+1) = j | \lambda(k) = i\}$$

where $\sum_{j=1}^{N} \pi_{ij} = 1$. The matrices $A_{\lambda(k)}$, $B_{\lambda(k)}$ and $C_{\lambda(k)}$ are known constant matrices for all $\lambda_k = i \in \Psi$. For simplicity, we denote the matrices associated with $\lambda(k) = i$ by $A_{\lambda(k)} = A_i$, $B_{\lambda(k)} = B_i$, $C_{\lambda(k)} = C_i$. Furthermore, the MJS system (5.9) is represented by $(\mathfrak{A}, \mathfrak{B}, \mathfrak{C}, \Pi)$, where $\mathfrak{A} = (A_1, ..., A_N)$, $\mathfrak{B} = (B_1, ..., B_N)$, $\mathfrak{C} = (C_1, ..., C_N)$ and $\Pi = [\pi_{ij}]$, $i, j \in \Psi$.

5.4.1 Unobservable and Unobservability Subspaces

In this section a geometric definition for an unobservable subspace of discrete-time Markovian jump systems (MJS) is introduced. The notion of unobservability subspace is then formalized for discrete-time MJS systems that are governed by (5.9). To develop an algorithm for constructing this subspace, an alternative definition of unobservability subspace is presented, which only depends on the matrices of the system. Based on this alternative definition, an algorithm for constructing the smallest unobservability subspace containing a given subspace is proposed. As shown in the next section, the unobservability subspace for the MJS system plays a central role in solving the fault detection and isolation problem for Markovian jump systems.

We first start with the definition of weak observability for Markovian jump system (5.9) with $B_i = 0, i \in \Psi$.

Definition 5.1 ([195]). *The system* $(\mathfrak{A}, \mathfrak{C}, \Pi)$ *is said to be weakly (W-) observable when there exists* $\gamma > 0$ *such that*

$$W^{n^2N}(x_0, i) = \mathbb{E}\Big\{x_0^\top \Gamma(n^2N)x_0 | x(0) = x_0, \lambda_0 = i_0\Big\} \geq \gamma |x_0|^2, \quad \forall x_0 \in \mathcal{X},\ i_0 \in \Psi \tag{5.10}$$

where the pointwise observability Grammian Γ *is defined as*

$$\Gamma(k) = \sum_{t=0}^{k} \Phi^\top(t) C_{\lambda(t)}^\top C_{\lambda(t)} \Phi(t) \tag{5.11}$$

and Φ *is the state transition matrix of system* $(\mathfrak{A}, \mathfrak{B}, \mathfrak{C}, \Pi)$.

In [195], a collection of matrices $\mathcal{O} = \{\mathcal{O}_1, ..., \mathcal{O}_N\}$ is introduced for testing the W-observability of the Markovian jump systems according to the following procedure. Let $O_i(0) = C_i^\top C_i,\ i \in \Psi$ and define the sequence of matrices as

$$O_i(k) = A_i^\top (\sum_{j=1}^{N} \pi_{ij} O_j(k-1)) A_i \quad k > 0, i \in \Psi \tag{5.12}$$

Then the matrix $\mathcal{O}_i$ is defined according to

$$\mathcal{O}_i = [O_i(0)\ O_i(1) \cdots O_i(n^2N-1)]^\top \tag{5.13}$$

Theorem 5.1 ([195]). *The MJS system* (5.9) *is W-observable if and only if* $\mathcal{O}_i$ *has a full rank for each* $i \in \Psi$.

Definition 5.2. *A state* x *is said to be unobservable if* $W^{n^2N}(x,i) = 0$ *for all* $i \in \Psi$.

Let $\mathcal{Q}$ denotes the unobservable set of the MJS system (5.9), i.e.

$$\mathcal{Q} = \{x | W^{n^2N}(x,i) = 0, \forall i \in \Psi, t \geq 0\} \tag{5.14}$$

It is shown in [195] (Lemma 3) that for irreducible Markov processes, $\mathcal{N}\{\mathcal{O}_i\} = \mathcal{N}\{\mathcal{O}_j\}$, $i,j \in \Psi$, $i \neq j$ and $\mathcal{Q} = \mathcal{N}\{\mathcal{O}_i\}$. Therefore, $\mathcal{Q}$ is the subspace of $\mathcal{X}$ and is called the unobservable subspace of the Markovian jump system (5.9). The theorem introduced below characterizes a geometric property of Q.

Theorem 5.2. *An unobservable subspace* Q *for the system* $(\mathfrak{A}, \mathfrak{C}, \Pi)$ *with irreducible Markov process is the largest* A_i*-invariant* ($i \in \Psi$) *that is contained in* $\mathcal{K} = \bigcap_{i=1}^{N} Ker\ C_i$.

Proof: It follows from the above discussion that $\mathcal{Q} \subseteq \text{Ker } C_i$, $i \in \Psi$, and hence $\mathcal{Q} \subseteq \mathcal{K}$. Let $x \in \mathcal{Q}$. Our goal is to show that $A_i x \in \mathcal{Q}$ for all $i \in \Psi$ (i.e. $\mathcal{Q}$ is A_i-invariant, $i \in \Psi$). Since $x \in \mathcal{N}\{O_i(k-1)\}$ and $x \in \mathcal{N}\{O_i(k)\}$, $i \in \Psi$, then

$$x^\top O_i(k)x = x^\top A_i^\top (\sum_{j=1}^{N} \pi_{ij} O_j(k-1)) A_i x = 0 \Rightarrow \begin{bmatrix} O_1(k-1) \\ \vdots \\ O_N(k-1) \end{bmatrix} Ax_i = 0$$

Hence $A_i x \in \mathcal{N}\{O_i(k-1)\}$ for all $k > 0$ and $A_i x \in \mathcal{N}\{\mathcal{O}_i\}$ for all $i \in \Psi$. This shows that $\mathcal{Q}$ is A_i-invariant for all $i \in \Psi$.

Next we show that Q is the largest A_i-invariant ($i \in \Psi$) that is contained in $\mathcal{K}$. Let $\mathcal{V}$ be an A_i-invariant ($i \in \Psi$) subspace that is contained in $\mathcal{K}$. Clearly,

$\mathcal{V} \subseteq \mathcal{N}\{O_i(0)\}$, $i \in \Psi$. Let $\mathcal{V} \subseteq \mathcal{N}\{O_i(k-1)\}$, $i \in \Psi$ and $x \in \mathcal{V}$, then

$$x^\top O_i(k)x = A_i^\top (\sum_{j=1}^{N} \pi_{ij} O_j(k-1)) A_i x = 0$$

since $A_i x \in \mathcal{V}$ ($\mathcal{V}$ is A_i-invariant). Hence, $\mathcal{V} \subseteq \mathcal{N}\{O_i(k)\}$, $i \in \Psi$ and $\mathcal{V} \subseteq \mathcal{Q}$. This shows that $\mathcal{Q}$ contains all the subspaces that are A_i-invariant ($i \in \Psi$) and is contained in $\mathcal{K}$. ■

Corollary 5.1. *An unobservable subspace Q is contained in $< Ker\ C_i|A_i >, i \in \Psi$.*

Proof: $<$ Ker $C_i|A_i$ $>$ is the largest A_i-invariant that is contained in Ker C_i. Therefore, we have $\mathcal{Q} \subseteq <$ Ker $C_i|A_i >, i \in \Psi$. ■

The above corollary proves that if each pair (A_i, C_i), $i \in \Psi$ is observable then $Q = 0$ and the MJS system (5.9) is W-observable. Based on our proposed Theorem 5.2 above, the following algorithm provides a procedure for constructing the required subspace Q.

Algorithm 5.1. *The subspace Q coincides with and is obtained from the last term of the following sequence*

$$\mathcal{Z}_0 = \mathcal{K}; \quad \mathcal{Z}_i = \mathcal{K} \cap (\bigcap_{k=0}^{N} A_k^{-1} \mathcal{Z}_{i-1}), \quad (i \in \boldsymbol{k}) \tag{5.15}$$

where the value of $k \leq dim(\mathcal{K})$ is determined from the condition $\mathcal{Z}_{k+1} = \mathcal{Z}_k$.

Let us denote the largest A_i-invariant ($i \in \Psi$) subspace that is contained in $\mathcal{K}$ by

$$<< \mathcal{K}|A_i >>_{i \in \Psi} \tag{5.16}$$

Consider the system $(\mathfrak{A}, \mathfrak{C}, \mathfrak{B}, \Pi)$ that is governed by (5.9). Let $\mathcal{Q}$ be A_i-invariant $i \in \Psi$ and $\mathcal{Q} \subseteq$ Ker C_i, and $P : \mathcal{X} \to \mathcal{X}/\mathcal{Q}$ be a canonical projection. The factor system is defined by $(\mathfrak{A} : \mathcal{X}/\mathcal{Q}, \mathfrak{B} : \mathcal{X}/\mathcal{Q}, \mathfrak{C} : \mathcal{X}/\mathcal{Q}, \Pi)$ with $\mathfrak{A} : \mathcal{X}/\mathcal{Q} = (A_1 : \mathcal{X}/\mathcal{Q}, ..., A_N : \mathcal{X}/\mathcal{Q})$, $\mathfrak{B} : \mathcal{X}/\mathcal{Q} = (B_1 : \mathcal{X}/\mathcal{Q}, ..., B_N : \mathcal{X}/\mathcal{Q})$

$\mathfrak{C} : \mathcal{X}/\mathcal{Q} = (C_1 : \mathcal{X}/\mathcal{Q}, ..., C_N : \mathcal{X}/\mathcal{Q})$ where $PA_i = (A_i : \mathcal{X}/\mathcal{Q})P$, $(B_i : \mathcal{X}/\mathcal{Q}) = PB_i, (C_i : \mathcal{X}/\mathcal{Q})P = C_i,\ i \in \Psi$. Therefore, if $\mathcal{Q}$ is the unobservable subspace of the system $(\mathfrak{A}, \mathfrak{C}, \mathfrak{B}, \Pi)$, then $(\mathfrak{A} : \mathcal{X}/\mathcal{Q}, \mathfrak{B} : \mathcal{X}/\mathcal{Q}, \mathfrak{C} : \mathcal{X}/\mathcal{Q}, \Pi)$ is observable since the unobservable subspace is factored out.

Definition 5.3 ([195]). *The system* (5.9) *is mean square (MS) stable if for each* $x_0 \in \mathcal{X}$ *and* $i_0 \in \Psi$,

$$\lim_{k\to\infty} \mathbb{E}\{||x(k)||^2\} = 0 \tag{5.17}$$

Definition 5.4 ([195]). *We say that* $(\mathfrak{A}, \mathfrak{C}, \Pi)$ *is MS-detectable when there exists* $G = \{G_1, ..., G_N\}$ *of appropriate dimension for which* $(\mathfrak{A}_G, \Pi)$ *is MS-stable, where* $\mathfrak{A}_G = \{A_1 + G_1C_1, ..., A_N + G_NC_N\}$.

The following computational linear matrix inequalities can be used for testing the MS-detectability of a discrete-time MJS system [195]. In other words, the MS-detectability of $(\mathfrak{A}, \mathfrak{C}, \Pi)$ is equivalent to the feasibility of the set

$$\begin{bmatrix} A_i^\top X_i A_i + C_i^\top S_i^\top A_i + A^\top S_i C_i & C_i^\top S_i^\top \\ S_i C_i & -X_i \end{bmatrix} < 0 \tag{5.18}$$

$$\sum_{j=1}^{N} \pi_{ij} H_j \leq X_i \tag{5.19}$$

in the unknowns $X_i > 0$, H_i and S_i with appropriate dimensions.

We are now in a position to introduce the notions of conditioned invariant and unobservability subspaces for the Markovian jump systems.

Definition 5.5. *A subspace* $\mathcal{W} \subseteq \mathcal{X}$ *is said to be conditioned invariant for system* $(\mathfrak{A}, \mathfrak{C}, \Pi)$ *if*

$$A_i(\mathcal{W} \cap Ker\ C_i) \subseteq \mathcal{W}, \qquad i \in \Psi \tag{5.20}$$

It is clear that if $\mathcal{W}$ is conditioned invariant for system $(\mathfrak{A}, \mathfrak{C}, \Pi)$, then $\mathcal{W}$ is (C_i, A_i)-invariant for all $i \in \Psi$. Therefore, there exist maps $D_i : \mathcal{Y} \to \mathcal{X}$ such that $(A_i + D_i C_i)\mathcal{W} \subseteq \mathcal{W}, \ i \in \Psi$.

We denote the class of conditioned invariant subspaces of $\mathcal{X}$ for the system $(\mathfrak{A}, \mathfrak{C}, \Pi)$ by $\mathfrak{W}(\mathfrak{A}, \mathfrak{C}, \mathcal{X})$. If $\mathcal{W} \in \mathfrak{W}(\mathfrak{A}, \mathfrak{C}, \mathcal{X})$, we write $\mathfrak{D}(\mathcal{W})$ for the class of maps $D_i : \mathcal{Y} \to \mathcal{X}$ where $(A_i + D_i C_i)\mathcal{W} \subseteq \mathcal{W}, \ i \in \Psi$. The notion of conditioned invariant subspace for system $(\mathfrak{A}, \mathfrak{C}, \Pi)$ is a dual to that of the robust maximal controlled invariant which is introduced in [196]. By duality it can be shown that $\mathfrak{W}(\mathfrak{A}, \mathfrak{C}, \mathcal{X})$ is closed under the operation of subspace intersection, and hence for any given subspace $\mathcal{L} \subseteq \mathcal{X}$, the family of conditioned invariant subspaces that contains $\mathcal{L}$ (denoted by $\mathfrak{W}(\mathfrak{A}, \mathfrak{C}, \mathcal{L})$ or simply $\mathfrak{W}(\mathcal{L})$) has an infimal element which is denoted by $\mathcal{W}^* = \inf \mathfrak{W}(\mathfrak{A}, \mathfrak{C}, \mathcal{L})$. The following algorithm can now be used for constructing $\mathcal{W}^*$:

Algorithm 5.2. *The subspace $\mathcal{W}^*$ coincides with and is obtained from the last term of the following sequence*

$$\mathcal{W}_0 = \mathcal{L}; \qquad \mathcal{W}_k = \mathcal{L} + \sum_{i=1}^{N} A_i(\mathcal{W}_{k-1} \cap Ker\ C_i)$$

Definition 5.6. *A subspace $\mathcal{S}$ is an* unobservability subspace *for system* (5.9) *if there exist output injection maps $D_i : \mathcal{Y} \to \mathcal{X}$ and measurement mixing maps $H_i : \mathcal{Y} \to \mathcal{Y}$ such that $\mathcal{S}$ is an unobservable subspace of system $(\tilde{\mathfrak{A}}, \tilde{\mathfrak{C}}, \Pi)$, where $\tilde{\mathfrak{A}} = \{A_1 + D_1 C_1, ..., A_N + D_N C_N\}$ and $\tilde{\mathfrak{C}} = \{H_1 C_1, ..., H_N C_N\}$.*

We denote the class of all unobservability subspaces in $\mathcal{X}$ for system $(\mathfrak{A}, \mathfrak{C}, \Pi)$ by $\mathfrak{S}(\mathfrak{A}, \mathfrak{C}, \mathcal{X})$. In the following our goal is to derive an alternative characterization for the unobservability subspace which is independent of the maps D_i and H_i as used in Definition 5.6 (the idea is similar to that in Theorem 2.1). As shown subsequently, this alternative definition provides us with means to obtain the unobservability

subspaces more readily. The following lemma presents a result that is necessary for formulating our alternative definition.

Lemma 5.1. *Let $\hat{\mathcal{S}}_j \subset \mathcal{X}$ such that $KerC_j \subseteq \hat{\mathcal{S}}_j, j \in \Psi$ and $<< \bigcap_{j=1}^{N} \hat{\mathcal{S}}_j | A_i >>_{i\in\Psi} = \mathcal{S}$ (refer to equation (5.16)), then*

$$<< \bigcap_{j=1}^{N} (\mathcal{S} + Ker\ C_j)|A_i >>_{i\in\Psi} = \mathcal{S} \tag{5.21}$$

Conversely, if $<< \bigcap_{j=1}^{N} (\mathcal{S} + Ker\ C_j)|A_i >>_{i\in\Psi} = \mathcal{S}$, there exist maps $H_j : \mathcal{Y} \to \mathcal{Y}$, $j \in \Psi$ such that

$$<< \bigcap_{j=1}^{N} Ker\ H_j C_j | A_i >>_{i\in\Psi} = \mathcal{S}$$

Proof: We have $\mathcal{S} \subseteq \bigcap_{j=1}^{N} \hat{\mathcal{S}}_j \subseteq \hat{\mathcal{S}}_j$ and Ker $C_j \subseteq \hat{\mathcal{S}}_j$, $j \in \Psi$, so that $\bigcap_{j=1}^{N} (\mathcal{S} +$ Ker $C_j) \subseteq \bigcap_{j=1}^{N} \hat{\mathcal{S}}_j$. Consequently,

$$<< \bigcap_{j=1}^{N} (\mathcal{S} + \text{Ker } C_j)|A_i >>_{i\in\Psi} \subseteq << \bigcap_{j=1}^{N} \hat{\mathcal{S}}_j | A_i >>_{i\in\Psi} = \mathcal{S}$$

On the other hand, $A_i \mathcal{S} \subseteq \mathcal{S}$ and

$$\bigcap_{j=1}^{N} (\mathcal{S} + \text{Ker } C_j) \supseteq \mathcal{S} + \bigcap_{j=1}^{N} \text{Ker } C_j \supseteq \mathcal{S}$$

Hence $\mathcal{S} \subseteq << \bigcap_{j=1}^{N} (\mathcal{S} + \text{Ker } C_j)|A_i >>_{i\in\Psi}$, and as a result

$$<< \bigcap_{j=1}^{N} (\mathcal{S} + \text{Ker } C_j)|A_i >>_{i\in\Psi} = \mathcal{S}$$

To show the converse part, let $\{c_1^i, ..., c_r^i\}$ be a basis for $\mathcal{S}$ + Ker C_i such that $\{c_{r-p_i}^i, ..., c_r^i\}$ is the basis for Ker C_i (dim(Ker C_i) $= p_i$). Therefore, $y_{ij} = C_i c_j^i$, $j = 1, ..., r - p_i - 1$ are independent. Let $\{y_{i1}, ..., y_{iq}\}$ be a basis for $\mathcal{Y}$, and define

$$H_i y_{ij} = 0, \quad j = 1, ..., r - p_i - 1$$

$$H_i y_{ij} = y_{ij}, \quad j = r - p_i, ..., r$$

Consequently, Ker $C_i + \mathcal{S} =$ Ker $H_i C_i$, and $\bigcap_{i=1}^{N}$ Ker $C_i + \mathcal{S} = \bigcap_{i=1}^{N}$ Ker $H_i C_i$. ■

We are now in a position to state our next result.

Theorem 5.3. *A subspace $\mathcal{S}$ is an unobservability subspace for system* (5.9) *if and only if there exist maps $D_i : \mathcal{Y} \to \mathcal{X}$, such that*

$$\mathcal{S} = << \bigcap_{j=1}^{N} (\mathcal{S} + Ker\ C_j) | A_i + D_i C_i >>_{i \in \Psi} \tag{5.22}$$

Proof: The proof follows readily from Lemma 5.1 by taking $\hat{\mathcal{S}}_j = \text{Ker } H_j C_j$. ■

The above theorem eliminates the need for the maps H_i from the Definition 5.6 (this is similar to equation (2.16) for a system with only a single mode). For a given unobservability subspace $\mathcal{S}$, the measurement mixing maps H_i's can be computed from $\mathcal{S}$ by solving the following equations, namely

$$\text{Ker } H_i C_i = \mathcal{S} + \text{Ker } C_i, \quad i \in \Psi \tag{5.23}$$

Next, we try to characterize the unobservability subspace by means of an algorithm that computes $\mathcal{S}$ without explicitly constructing $(D_1, ..., D_N) \in \mathfrak{D}(\mathcal{S})$. For an arbitrary subspace $\mathcal{S} \subset \mathcal{X}$ let us define a family

$$\mathcal{G}_{(\mathfrak{A},\mathfrak{C})} = \{\mathscr{S} : \mathscr{S} = \bigcap_{i=1}^{N} (\mathcal{S} + (A_i^{-1}\mathscr{S} \cap \text{ Ker } C_i))\} \tag{5.24}$$

Below we first show that $\mathcal{G}_{(\mathfrak{A},\mathfrak{C})}$ has a unique maximal member.

Lemma 5.2. *There exists a unique element $\mathscr{S}^* \in \mathcal{G}_{(\mathfrak{A},\mathfrak{C})}$ such that $\mathscr{S} \subseteq \mathscr{S}^*$ for every $\mathscr{S} \in \mathcal{G}_{(\mathfrak{A},\mathfrak{C})}$.*

Proof: Define a sequence $\mathscr{S}^\mu \subset \mathcal{X}$ according to

$$\mathscr{S}^0 = \mathcal{X}; \qquad \mathscr{S}^\mu = \bigcap_{i=1}^{N} (\mathcal{S} + (A_i^{-1}\mathscr{S}^{\mu-1} \cap \text{ Ker } C_i)), \quad \mu \in \mathbf{n} \tag{5.25}$$

The sequence $\mathscr{S}^\mu$ is non-increasing since $\mathscr{S}^1 \subseteq \mathscr{S}^0$ and if $\mathscr{S}^\mu \subseteq \mathscr{S}^{\mu-1}$, then

$$\mathscr{S}^{\mu+1} = \bigcap_{i=1}^{N} (\mathcal{S} + (A_i^{-1}\mathscr{S}^{\mu} \cap \text{ Ker } C_i)) \subseteq \bigcap_{i=1}^{N} (\mathcal{S} + (A_i^{-1}\mathscr{S}^{\mu-1} \cap \text{ Ker } C_i)) = \mathscr{S}^\mu$$

Therefore, there exists $k \leq n$ such that $\mathscr{S}^{\mu} = \mathscr{S}^{k}$, and we set $\mathscr{S}^{*} = \mathscr{S}^{k}$. Clearly $\mathscr{S}^{*} \in \mathcal{G}_{(\mathfrak{A},\mathfrak{C})}$. Next, we show that $\mathscr{S}^{*}$ is the maximal element. Let $\mathscr{S} \subseteq \mathcal{G}_{(\mathfrak{A},\mathfrak{C})}$, then $\mathscr{S} \subseteq \mathscr{S}^{0}$ and if $\mathscr{S} \subseteq \mathscr{S}^{\mu}$, we have

$$\mathscr{S} = \bigcap_{i=1}^{N}(\mathcal{S} + (A_i^{-1}\mathscr{S} \cap \text{ Ker } C_i)) \subseteq \bigcap_{i=1}^{N}(\mathcal{S} + (A_i^{-1}\mathscr{S}^{\mu} \cap \text{ Ker } C_i)) = \mathscr{S}^{\mu+1}$$

Consequently, $\mathscr{S} \subseteq \mathscr{S}^{\mu}$ for all μ, and hence $\mathscr{S} \subseteq \mathscr{S}^{*}$. ■

The next lemma provides an important property of the maximal element $\mathscr{S}^{*}$ which will be used for introducing our suggested alternative characterization of the unobservability subspace of system $(\mathfrak{A}, \mathfrak{C}, \Pi)$.

Lemma 5.3. *Let $\mathcal{S} \in \mathfrak{W}(\mathfrak{A}, \mathfrak{C}, \mathcal{X})$ and $(D_1, ..., D_N) \in \mathfrak{D}$, then $\mathscr{S}^{*}$ is the largest $(A_i + D_iC_i)$-invariant $(i \in \Psi)$ that is contained in $\bigcap_{j=1}^{N}(\mathcal{S} + ker\ C_j)$, i.e. $\mathscr{S}^{*} =<< \bigcap_{j=1}^{N}(\mathcal{S} + Ker\ C_j)|A_i + D_iC_i >>_{i\in\Psi}$.*

Proof: First we show that any $\mathscr{S} \in \mathcal{G}_{(\mathfrak{A},\mathfrak{C})}$ is $(A_i + D_iC_i)$-invariant $(i \in \Psi)$. We have $\mathscr{S} = \bigcap_{i=1}^{N}(\mathcal{S} + (A_i^{-1}\mathscr{S} \cap \text{ Ker } C_i))$ and

$$\begin{aligned}(A_j + D_jC_j)\mathscr{S} &= (A_j + D_jC_j)\bigcap_{i=1}^{N}(\mathcal{S} + (A_i^{-1}\mathscr{S} \cap \text{ Ker } C_i)) \\ &\subseteq (A_j + D_jC_j)(\mathcal{S} + A_j^{-1}\mathscr{S} \cap \text{ Ker } C_j) \\ &\subseteq (A_j + D_jC_j)\mathcal{S} + A_j(A_j^{-1}\mathscr{S} \cap \text{ Ker } C_j) \\ &\subseteq \mathcal{S} + \mathscr{S} \subseteq \mathscr{S}\end{aligned}$$

where we used the relationship $\mathscr{S} = \bigcap_{i=1}^{N}(\mathcal{S}+(A_i^{-1}\mathscr{S}\cap \text{ Ker } C_i)) \supseteq \mathcal{S}+\bigcap_{i=1}^{N}(A_i^{-1}\mathscr{S}\cap \text{ Ker } C_i) \supset \mathcal{S}$ and $A_j(A_j^{-1}\mathscr{S}) \subseteq \mathscr{S}$. Therefore, $(A_j + D_jC_j)\mathscr{S} \subseteq \mathscr{S}$, $j \in \Psi$; and hence $\mathscr{S} \in \mathfrak{W}(\mathfrak{A}, \mathfrak{C}, \mathcal{X})$ and $(D_1, ..., D_N) \in \mathfrak{D}(\mathscr{S})$.

Consequently, we have $\mathscr{S}^{*} \in \mathfrak{W}(\mathfrak{A}, \mathfrak{C}, \mathcal{X})$. Next we show that for any subspace $\mathcal{W}$ such that it is $(A_i+D_iC_i)$-invariant $(i \in \Psi)$ and is contained in $\bigcap_{j=1}^{N}(\mathcal{S}+\text{ker } C_j)$, we have $\mathcal{W} \subseteq \mathscr{S}^{*}$. If $\mathcal{W} \subseteq \mathcal{S}$ then it follows that $\mathcal{W} \subseteq \mathscr{S}^{*}$, since $\mathcal{S} \subseteq \mathscr{S}^{*}$. Therefore, we consider the case where $\mathcal{S} \subseteq \mathcal{W}$. We have

$$A_i^{-1}\mathcal{W} \cap \text{ Ker } C_i = (A_i + D_iC_i)^{-1}\mathcal{W} \cap \text{ Ker } C_i$$

and as a result

$$\bigcap_{i=1}^{N}(\mathcal{S} + A_i^{-1}\mathcal{W} \cap \text{ Ker } C_i) = \bigcap_{i=1}^{N}(\mathcal{S} + (A_i + D_iC_i)^{-1}\mathcal{W} \cap \text{ Ker } C_i)$$

It is clear that $\mathcal{W} \subseteq \mathscr{S}^0$. If $\mathcal{W} \subseteq \mathscr{S}^{\mu-1}$, then

$$\begin{aligned}\mathscr{S}^{\mu} &= \bigcap_{i=1}^{N}(\mathcal{S} + (A_i^{-1}\mathscr{S}^{\mu-1} \cap \text{ Ker } C_i)) \supset \bigcap_{i=1}^{N}(\mathcal{S} + (A_i^{-1}\mathcal{W} \cap \text{ Ker } C_i)) \\ &= \bigcap_{i=1}^{N}(\mathcal{S} + (A_i + D_iC_i)^{-1}\mathcal{W} \cap \text{ Ker } C_i)) \\ &\supset \bigcap_{i=1}^{N}(\mathcal{S} + (\mathcal{W} \cap \text{Ker } C_i)) = \sum_{i=1}^{N}(\mathcal{W} \cap (\mathcal{S} + \text{Ker } C_i)) = \mathcal{W}\end{aligned}$$

where we used the fact that $\mathcal{W} \subseteq (A_i + D_iC_i)^{-1}\mathcal{W}$ and the modular distributive rule [134] (if $\mathcal{S} \subseteq \mathcal{W}$, then $\mathcal{S} + (\mathcal{W} \cap \text{Ker } C_i) = \mathcal{W} \cap (\mathcal{S} + \text{Ker } C_i)$). As a consequence $\mathscr{S}^{\mu} \supset \mathcal{W}$; and hence $\mathscr{S}^* \supset \mathcal{W}$. This shows that $\mathscr{S}^*$ is the largest $(A_i + D_iC_i)$-invariant ($i \in \Psi$) which is contained in $\bigcap_{i=1}^{N}(\mathcal{S} + \text{Ker } C_i)$. ■

We are in the position to introduce our proposed alternative characterization of an unobservability subspace for system $(\mathfrak{A}, \mathfrak{C}, \Pi)$.

Theorem 5.4. *Let $\mathcal{S} \subset \mathcal{X}$ and define $\mathcal{G}_{(\mathfrak{A},\mathfrak{C})}$ as in* (5.24). *Then $\mathcal{S} \in \mathfrak{S}(\mathfrak{A}, \mathfrak{C}, \Pi)$ if and only if*

$$\mathcal{S} \in \mathfrak{W}(\mathfrak{A}, \mathfrak{C}, \Pi) \quad (\mathcal{S} \textit{ is conditioned invariant}) \tag{5.26}$$

and

$$\mathcal{S} = \mathscr{S}^* \tag{5.27}$$

where $\mathscr{S}^*$ is the maximal element of $\mathcal{G}_{(\mathfrak{A},\mathfrak{C})}$.

Proof: **(If part)** If (5.26) and (5.27) hold, then according to Lemma 5.3, we have $\mathcal{S} =<< \bigcap_{j=1}^{N}(\mathcal{S} + \text{Ker } C_j)|A_i >>_{i\in\Psi}$, and hence using Theorem 5.3, we have $\mathcal{S} \in \mathfrak{S}(\mathfrak{A}, \mathfrak{C}, \Pi)$.

(Only if part) If $\mathcal{S} \in \mathfrak{S}(\mathfrak{A}, \mathfrak{C}, \Pi)$, it follows that $\mathcal{S} \in \mathfrak{W}(\mathfrak{A}, \mathfrak{C}, \Pi)$ and according to Lemma 5.3, we have $\mathcal{S} = \mathscr{S}^*$. ■

The above theorem provides a similar characteristic for the unobservability subspace of the Markovian jump system as the one that Theorem 2.1 provides for unobservability subspace of a system having only a single mode. Next, we show that the class of unobservability subspace of system $(\mathfrak{A}, \mathfrak{C}, \Pi)$ is a semilattice with respect to inclusion and subspace addition, and hence the class of unobservability subspace which contains a given subspace has an infimal element. This property is crucial for the application of unobservability subspace to the problem of fault detection and isolation of MJS systems.

Lemma 5.4. *The class of subspaces $\mathfrak{S}(\mathfrak{A}, \mathfrak{C}, \Pi)$ is closed under the operation of subspace intersection.*

Proof: The proof is based on the characterization of unobservability subspace in Theorem 5.4. Let $\mathcal{S}_1, \mathcal{S}_2 \in \mathfrak{S}(\mathfrak{A}, \mathfrak{C}, \Pi)$. It is clear that $\mathcal{S}_1 \cap \mathcal{S}_2 \in \mathfrak{W}(\mathfrak{A}, \mathfrak{C}, \Pi)$. Furthermore, $\mathcal{S}_j = \mathscr{S}_j^n, j = 1, 2$, where

$$\mathscr{S}_j^0 = \mathcal{X}; \qquad \mathscr{S}_j^\mu = \bigcap_{i=1}^{N} (\mathcal{S}_j + (A_i^{-1}\mathscr{S}^{\mu-1} \cap \text{ Ker } C_i)), \quad \mu \in \mathbf{n}$$

Define $\mathscr{S}$ according to

$$\mathscr{S}^0 = \mathcal{X}; \qquad \mathscr{S}^\mu = \bigcap_{i=1}^{N} ((\mathcal{S}_1 \cap \mathcal{S}_2) + (A_i^{-1}\mathscr{S}^{\mu-1} \cap \text{ Ker } C_i)), \quad \mu \in \mathbf{n}$$

We have $\mathscr{S}_1^0 = \mathscr{S}_2^0 = \mathscr{S}^0$ and if $\mathscr{S}^{\mu-1} \subseteq \mathscr{S}_j^{\mu-1}, j = 1, 2$, then

$$\begin{aligned}\mathscr{S}^\mu &= \bigcap_{i=1}^{N} ((\mathcal{S}_1 \cap \mathcal{S}_2) + (A_i^{-1}\mathscr{S}^{\mu-1} \cap \text{ Ker } C_i)) \subseteq \bigcap_{i=1}^{N} (\mathcal{S}_j + (A_i^{-1}\mathscr{S}^{\mu-1} \cap \text{ Ker } C_i)) \\ &\subseteq \bigcap_{i=1}^{N} (\mathcal{S}_j + (A_i^{-1}\mathscr{S}_j^{\mu-1} \cap \text{ Ker } C_i) = \mathscr{S}_j^\mu, \quad j = 1, 2\end{aligned}$$

Therefore, $\mathscr{S}^n \subseteq \mathscr{S}_1^n \cap \mathscr{S}_2^n$, and consequently

$$\mathcal{S}_1 \cap \mathcal{S}_2 \subseteq \mathscr{S}^n \subseteq \mathscr{S}_1^n \cap \mathscr{S}_2^n = \mathcal{S}_1 \cap \mathcal{S}_2$$

and $\mathcal{S}_1 \cap \mathcal{S}_2 = \mathscr{S}^n$, so that the result follows from Theorem 5.4. ■

Let $\mathcal{L} \subseteq \mathcal{X}$ be an arbitrary subspace and denote $\mathfrak{S}(\mathfrak{A}, \mathfrak{C}, \mathcal{L})$ (or simply $\mathfrak{S}(\mathcal{L})$) as the family of u.o.s. that contains $\mathcal{L}$, i.e.

$$\mathfrak{S}(\mathfrak{A}, \mathfrak{C}, \mathcal{L}) = \{\mathcal{S} : \mathcal{S} \in \mathfrak{S}(\mathfrak{A}, \mathfrak{C}, \mathcal{X}) \ \& \ \mathcal{L} \subseteq \mathcal{S}\}$$

As indicated previously, $\mathfrak{S}(\mathfrak{A}, \mathfrak{C}, \mathcal{X})$ refers to the class of all unobservability subspaces in $\mathcal{X}$.

Lemma 5.5. *For any given subspace $\mathcal{L} \subseteq \mathcal{X}$, $\mathfrak{S}(\mathfrak{A}, \mathfrak{C}, \mathcal{L})$ has an infimal element (denoted by $\mathcal{S}^* = \inf \mathfrak{S}(\mathfrak{A}, \mathfrak{C}, \mathcal{L})$).*

Proof: It follows that $\mathcal{X} \in \mathfrak{S}(\mathfrak{A}, \mathfrak{C}, \mathcal{L})$ and $\mathfrak{S}(\mathfrak{A}, \mathfrak{C}, \mathcal{L})$ is closed under intersection (Lemma 5.4). Therefore, it has an infimal element. ■

The next algorithm provides a procedure for constructing $\mathcal{S}^*$.

Algorithm 5.3. *Let $\mathcal{W}^* = \inf \mathfrak{W}(\mathfrak{A}, \mathfrak{C}, \mathcal{L})$ and define the sequence $\mathcal{Z}^\mu$ according to*

$$\mathcal{Z}^0 = \mathcal{X}; \quad \mathcal{Z}^\mu = \bigcap_{i=1}^{N} (\mathcal{W}^* + (A_i^{-1}\mathcal{Z}^{\mu-1} \cap Ker\ C_i)) \tag{5.28}$$

Then $\mathcal{S}^* = \mathcal{Z}^k$, whenever $\mathcal{Z}^{k+1} = \mathcal{Z}^k$.

To analyze the above algorithm note that the sequence $\mathcal{Z}^\mu$ is non-increasing and $\mathcal{Z}^{k+1} = \mathcal{Z}^k$ for $k \geq n - \dim(\mathcal{W}^*)$. Let $\mathcal{Z}^* = \mathcal{Z}^k$. According to Lemma 5.3, $\mathcal{Z}^* =<< \bigcap_{i=1}^{N}(\mathcal{W}^* + \mathrm{Ker}C_j)|A_i + D_iC_i >>_{i\in\Psi}$ for some $(D_1, ..., D_N) \in \mathfrak{D}(\mathcal{W}^*)$. Using the same approach as in Lemma 5.1, one can obtain the maps H_j's such that

$$\mathcal{Z}^* =<< \bigcap_{i=1}^{N}(\mathcal{W}^* + \mathrm{Ker}C_j)|A_i + D_iC_i >>_{i\in\Psi} =<< \bigcap_{i=1}^{N} \mathrm{Ker}H_jC_j|A_i + D_iC_i >>_{i\in\Psi} \tag{5.29}$$

and therefore $\mathcal{Z}^*$ is an unobservability subspace according to Definition 5.6. Moreover, it follows that $\mathcal{L} \subseteq \mathcal{W}^* \subseteq \mathcal{Z}^*$ ($\mathcal{Z}^* \in \mathfrak{W}(\mathcal{L})$ and $\mathcal{W} = \inf \mathfrak{W}(\mathcal{L})$); hence $\mathcal{Z}^* \in \mathfrak{S}(\mathcal{L})$, and consequently $\mathcal{S}^* \subseteq \mathcal{Z}^*$.

On the other hand, according to Theorem 5.4 we have $\mathcal{S}^* = \mathcal{S}^n$ where

$$\mathcal{S}^0 = \mathcal{X}; \qquad \mathcal{S}^\mu = \bigcap_{i=1}^{N}(\mathcal{S}^* + (A_i^{-1}\mathcal{S}^{\mu-1} \cap \text{Ker } C_i)), \quad \mu \in \mathbf{n}$$

Since $\mathcal{W}^* \subseteq \mathcal{S}^*$, it can be shown by induction that $\mathcal{Z}^\mu \subseteq \mathcal{S}^\mu$, $\mu \in \mathbf{n}$. Indeed, $\mathcal{Z}^0 = \mathcal{S}^0$, and if $\mathcal{Z}^{\mu-1} \subseteq \mathcal{S}^{\mu-1}$, then

$$\mathcal{Z}^\mu = \bigcap_{i=1}^{N}(\mathcal{W}^* + (A_i^{-1}\mathcal{Z}^{\mu-1} \cap \text{Ker } C_i)) \subseteq \bigcap_{i=1}^{N}(\mathcal{S}^* + (A_i^{-1}\mathcal{S}^{\mu-1} \cap \text{Ker } C_i)) = \mathcal{S}^\mu$$

Consequently $\mathcal{Z}^* \subseteq \mathcal{S}^*$.

It follows from the above algorithm and Lemma 5.3 that $\mathfrak{D}(\mathcal{W}^*) \subseteq \mathfrak{D}(\mathcal{S}^*)$. Therefore, the maps D_i's for $\mathcal{S}^*$ can be found from $\mathcal{W}^*$ and once $\mathcal{S}^*$ is found from Algorithm 5.3, the maps H_i's can also be computed from $\mathcal{S}^*$ and equation (5.23).

The next lemma characterizes the relationship between $\mathcal{S}^*$ and $\mathcal{W}^*$ (similar to that for single mode systems as governed by equation (2.21)).

Lemma 5.6. *Given* $\mathcal{W}^* = \inf \mathfrak{W}(\mathfrak{A}, \mathfrak{C}, \mathcal{L})$, $\mathcal{S}^* = \inf \mathfrak{S}(\mathfrak{A}, \mathfrak{C}, \mathcal{L})$ *and* $(D_1, ..., D_N) \in \mathfrak{D}(\mathcal{W}^*)$, *we have*

$$\mathcal{S}^* = << \bigcap_{i=1}^{N}(\mathcal{W}^* + Ker\ C_j)|A_i + D_iC_i >>_{i\in\Psi}$$

Proof: The proof is immediate from (5.29) and the fact that $\mathcal{Z}^* = \mathcal{S}^*$. ■

Finally, we introduce the notion of outer MS-detectability of an unobservability subspace. As shown in the next section, outer MS-detectability is a necessary condition for designing a stable residual generator for the FDI problem.

Definition 5.7. *A subspace* $\mathcal{S} \in \mathfrak{S}(\mathfrak{A}, \mathfrak{C}, \mathcal{X})$ *is said to be outer MS-detectable if the factor system* $(\mathfrak{A} + \mathfrak{D}\mathfrak{C} : \mathcal{X}/\mathcal{S}, \mathfrak{H}\mathfrak{C} : \mathcal{X}/\mathcal{S}, \Pi)$ *is MS-detectable where* $\mathfrak{H}\mathfrak{C} = \{H_1C_1, ..., H_NC_N\}$ *and* $\mathfrak{A} + \mathfrak{D}\mathfrak{C} = \{A_1 + D_1C_1, ..., A_N + D_NC_N\}$.

The next example illustrates how one can find $\mathcal{S}^*$ for a given Markovian jump system and it also summarizes our proposed result.

Example 5.1. *Let $N = 2$ and*

$$A_1 = \begin{bmatrix} 0 & 3 & 4 \\ 1 & 2 & 3 \\ 0 & 2 & 5 \end{bmatrix}, \quad A_2 = \begin{bmatrix} 1 & 2 & 4 \\ 2 & -1 & 2 \\ 0 & 1 & 4 \end{bmatrix}, C_1 = \begin{bmatrix} 0 & 1 & 0 \\ 0 & 0 & 1 \end{bmatrix}, C_2 = \begin{bmatrix} 1 & 1 & 0 \\ 0 & 0 & 1 \end{bmatrix}$$

, $L = [-3, 1, 0]^{\mathrm{T}}$ and Π as in Example 1. First $\mathcal{W}^*$ can be found from Algorithm 5.2 as

$$\mathcal{W}^* = \begin{bmatrix} -3 \\ 1 \\ 0 \end{bmatrix}$$

The unobservability subspace $\mathcal{S}^*$ is found from Algorithm 5.3 which is equal to $\mathcal{W}^*$. It should be noted that

$$\mathcal{S}_1^* = \begin{bmatrix} -3 & 1 \\ 1 & 0 \\ 0 & 0 \end{bmatrix}, \mathcal{S}_2^* = \begin{bmatrix} -3 \\ 1 \\ 0 \end{bmatrix}$$

where $\mathcal{S}_j^*$, $j = 1, 2$ is the infimal (C_j, A_j) unobservability subspace that contains $\mathcal{L} = Im\ L$ and $\mathcal{S}^* \subset \mathcal{S}_1^*$ and $\mathcal{S}^* \subset \mathcal{S}_2^*$.

5.4.2 Fault Detection and Isolation Based on Geometric Approach

In this section the Fundamental Problem in Residual Generation (FPRG) is investigated for the discrete-time Markovian jump systems. This problem was originally considered for linear systems in [3] and was extended to nonlinear systems in [60]. The objective in this section is to generalize these results to Markovian jump systems (MJS). Consider the following discrete-time Markovian jump system

$$\begin{aligned} x(k+1) &= A_{\lambda(k)}x(k) + B_{\lambda(k)}u(k) + L^1_{\lambda(k)}m_1(k) + L^2_{\lambda(k)}m_2(k) \\ y(k) &= C_{\lambda(k)}x(k), \quad x(0) = x_0, \quad \lambda(0) = i_0 \end{aligned} \tag{5.30}$$

where it is assumed that all the matrices are the same as in (5.9) and the Markov process $\lambda(k)$ is irreducible. The matrices $L^1_{\lambda(k)}$, $L^2_{\lambda(k)}$ represent the fault signatures and are monic and $m_i(k) \in \mathcal{M}_i \subset \mathcal{X}$, $i = 1, 2$ denote the fault modes. For sake of simplicity in analysis and derivation of our results, we first consider the case with two faults. The more general case of multiple faults is considered at the end of this section. We denote the fault signatures associated with $\lambda(k) = i$ by L^1_i and L^2_i. The fault modes together with the fault signatures can be used to model the effects of actuator faults, sensor faults and system faults on the dynamics of the system. For example, the effect of a fault in the i-th actuator may be represented by L^1_i as the i-th column of B_i and if an actuator fails, then $m_1(k) = -u_i(k)$.

The FPRG problem is concerned with the design of a Markovian jump residual generator that is governed by the filter dynamics of the form

$$\begin{aligned} w(k+1) &= F_{\lambda(k)}w(k) - E_{\lambda(k)}y(k) + K_{\lambda(k)}u(k) \\ r(k) &= M_{\lambda(k)}w(k) - H_{\lambda(k)}y(k) \end{aligned} \tag{5.31}$$

where $w(k) \in \mathcal{F} \subset \mathcal{X}$ such that the response of $r(k)$ is affected by the fault mode $m_1(k)$ and is decoupled from $m_2(k)$ and if m_1 is identically zero then

$$\lim_{k\to\infty} \mathbb{E}||r(k)||^2 = 0$$

for any input signal $u(k)$. We can rewrite equations (5.30) and (5.31) as follows:

$$\begin{aligned} \begin{bmatrix} x(k+1) \\ w(k+1) \end{bmatrix} &= \begin{bmatrix} A_{\lambda(k)} & 0 \\ -E_{\lambda(k)}C_{\lambda(k)} & F_{\lambda(k)} \end{bmatrix} \begin{bmatrix} x(k) \\ w(k) \end{bmatrix} \\ &\quad + \begin{bmatrix} B_{\lambda(k)} & L^2_{\lambda(k)} \\ K_{\lambda(k)} & 0 \end{bmatrix} \begin{bmatrix} u(k) \\ m_2(k) \end{bmatrix} + \begin{bmatrix} L^1_{\lambda(k)} \\ 0 \end{bmatrix} m_1(k) \\ r(k) &= \begin{bmatrix} -H_{\lambda(k)}C_{\lambda(k)} & M_{\lambda(k)} \end{bmatrix} \begin{bmatrix} x(k) \\ w(k) \end{bmatrix} \end{aligned} \tag{5.32}$$

Define the extended space $\mathcal{X}^e = \mathcal{X} \oplus \mathcal{F}$ and $\mathcal{U}^e = \mathcal{U} \oplus \mathcal{M}_2$, so that equation

(5.32) can be expressed as

$$\begin{aligned} x^e(k+1) &= A^e_{\lambda(k)}x^e(k) + B^e_{\lambda(k)}u^e(k) + L^{e1}_{\lambda(k)}m_1(k) \\ r(k) &= H^e_{\lambda(k)}x^e(k) \end{aligned} \tag{5.33}$$

with $x^e(t) \in \mathcal{X}^e$ and $u^e \in \mathcal{U}^e$. In order to investigate the criteria for determining whether a nonzero $m_1(k)$ affects the residual signal $r(k)$, the notion of an input observability for the Markovian jump system is defined and formalized below.

Definition 5.8. *The Markovian jump system* (5.9) *is said to be input observable if* B_i, $i \in \Psi$ *is monic and the image of* B_i*'s does not intersect with the unobservable subspace of system* (5.9).

Based on the above definition, the FPRG problem for system (5.30) can now be formally stated as the problem of designing the dynamical filter (5.31) such that

(a) r is decoupled from u^e, (5.34)

(b) m_1 is input observable in the augmented system (5.33), and (5.35)

(c) $\lim_{k\to 0} \mathbb{E}\{||r(k)||^2\} = 0$, for $m_1(k) = 0, \forall\, i_0 \in \Psi$ and $\forall x^e_0 \in \mathcal{X}^e$. (5.36)

We need to first derive a preliminary result for obtaining the solvability condition for the FPRG problem. The following embedding map $Q : \mathcal{X} \to \mathcal{X}^e$ is defined according to [3]:

$$Qx = \begin{bmatrix} x \\ 0 \end{bmatrix} \tag{5.37}$$

where if $\mathcal{V} \subset \mathcal{X}^e$, we have

$$Q^{-1}\mathcal{V} = \{x | x \in \mathcal{X}, \quad \begin{bmatrix} x \\ 0 \end{bmatrix} \in \mathcal{V}\}$$

Our first result is the generalization of the Proposition 1 that was obtained in [3] to the Markovian jump systems.

Lemma 5.7. *Let $\mathcal{S}^e$ be the unobservable subspace of system* (5.33). *The unobservability subspace for system* $(\mathfrak{A}, \mathfrak{C}, \Pi)$ *is given by* $Q^{-1}\mathcal{S}^e$.

Proof: First we show that $\mathcal{S} = Q^{-1}\mathcal{S}^e$ is conditioned invariant. Let $x \in \mathcal{S} \cap \text{Ker } C_i$, we need to show that $A_i x \in \mathcal{S}$. This follows by noting that

$$\begin{bmatrix} A_i x \\ 0 \end{bmatrix} = \begin{bmatrix} A_i & 0 \\ -E_i C_i & F_i \end{bmatrix} \begin{bmatrix} x \\ 0 \end{bmatrix} \in \mathcal{S}^e$$

since $\mathcal{S}^e$ is A_i^e-invariant $i \in \Psi$. Therefore, $A_i x \in \mathcal{S}$ and $\mathcal{S}$ is conditioned invariant. Next if $x \in \mathcal{S}$, then $Qx \in \mathcal{S}^e$ and therefore

$$\begin{bmatrix} x \\ 0 \end{bmatrix} \in \bigcap_{i=1}^{N} \text{Ker } H_i^e$$

This shows that $H_i C_i x = 0$; and hence $x \in \cap_{i=1}^{N} \text{Ker } H_i C_i$ and $\mathcal{S} \subseteq \cap_{i=1}^{N} \text{Ker } H_i C_i$. Finally, according to the definition of the unobservable subspace $\mathcal{S}^e$ (the largest A^e-invariant subspace in $\cap \text{Ker } H_i^e$), $\mathcal{S}$ is the largest conditioned invariant contained in $\cap_{i=1}^{N} \text{Ker } H_i C_i$, and therefore $\mathcal{S} \in \mathfrak{S}(\mathfrak{A}, \mathfrak{C}, \Pi)$. ■

We are now in a position to derive the solvability condition for the FPRG problem corresponding to the Markovian jump system (5.30).

Theorem 5.5. *The FPRG problem has a solution for the augmented MJS system* (5.33) *only if*

$$\mathcal{S}^* \bigcap \mathcal{L}_j^1 = 0, \quad j \in \Psi \tag{5.38}$$

where $\mathcal{S}^* = \inf \mathfrak{S}(\mathfrak{A}, \mathfrak{C}, \sum_{i=1}^{N} \mathcal{L}_i^2)$. *On the other hand, if the above* $\mathcal{S}^*$ *exists such that it is also outer MS-detectable, then the FPRG problem is then guaranteed to have a solution.*

Proof: **(Only if part)** Let $\mathcal{S}^e$ be an unobservable subspace of system (5.33). To satisfy the condition (5.34), we should have $\mathcal{B}_i^e \subset \mathcal{S}^e, i \in \Psi$. Hence, $\mathcal{L}_{i2} \subset Q^{-1}\mathcal{B}_i^e \subset$

$Q^{-1}\mathcal{S}^e = \mathcal{S}$ and by invoking Lemma 5.7, we obtain

$$\mathcal{S} \in \mathfrak{S}(\mathfrak{A}, \mathfrak{C}, \sum_{i=1}^{N} \mathcal{L}_{i2}) \tag{5.39}$$

For condition (5.35) to hold, according to the Definition 5.8, L_{i1}^e should be monic (which is already assumed to hold) and $\mathcal{L}_{i1}^e \cap \mathcal{S}^e = 0,\ i \in \Psi$. Thus

$$Q^{-1}(\mathcal{L}_{i1}^e \cap \mathcal{S}^e) = \mathcal{L}_{i1} \cap \mathcal{S} = 0, \quad i \in \Psi \tag{5.40}$$

Therefore, equations (5.39) and (5.40) hold only if equation (5.38) is true.

(if part): Given the unobservability subspace $\mathcal{S}^*$ which is outer MS-detectable, there exist output injection maps D_i's and measurement mixing maps H_i's such that $\mathcal{S}^* =<< \bigcap_{j=1}^{N} \text{Ker } H_j C_j | A_i + D_i C_i >>_{i\in\Psi}$ where H_j is the solution to equation (5.23). Let P be the canonical projection of $\mathcal{X}$ on $\mathcal{X}/\mathcal{S}^*$ and $M_i, i \in \Psi$ be a unique solution to $M_i P = H_i C_i$ and $A_{0i} = (A_i + D_i C_i : \mathcal{X}/\mathcal{S}^*)$ where $P(A_i + D_i C_i) = A_{0i} P,\ i \in \Psi$. Due to the fact that $\mathcal{S}^*$ is assumed to be outer MS-detectable, there exist $G_i,\ i \in \Psi$ such that $(\mathfrak{A}_{0_G}, \Pi)$ is MS-stable where $\mathfrak{A}_{0_G} = \{A_{01} + G_1 M_1, ..., A_{0N} + G_N M_N\}$. Let us define $F_i = A_{0i} + G_i M_i$, $E_i = P(D_i + P^{-r} G_i H_i)$, $K_i = PB_i,\ i \in \Psi$, and $e(k) = w(k) - Px(k)$. By using equation (5.31) we obtain

$$\begin{aligned}
\dot{e}(k+1) =& F_i w(k) - E_i y(k) + K_i u(k) - P(A_i x(k) + B_i u(k) + L_{i1} m_1(k) + L_{i2} m_2(k)) \\
=& F_i w(k) - P L_{i1} m_1(k) - P(A_i + D_i C_i) x(k) - G_i H_i C_i x(k) \\
=& F_i w(k) - P L_{i1} m_1(k) - A_{0i} P x(k) - G_i M_i P x(k) = F_i e(k) - P L_{i1} m_1(k)
\end{aligned}$$

Note that $PL_{i2} = 0, i \in \Psi$, since $\mathcal{L}_{i2} \in \mathcal{S}^*, i \in \Psi$. Also

$$r(k) = M_i w(k) - H_i y(k) = M_i w(k) - H_i C_i x(k) = M_i e(k)$$

Consequently, the error dynamics can be written according to

$$\begin{aligned}
\dot{e}(k) &= F_{\lambda(k)} e(k) - P L_{\lambda(k)}^1 m_1(k) \\
r(k) &= M(\lambda) e(k)
\end{aligned} \tag{5.41}$$

It is clear that the fault mode $m_2(k)$ does not affect the residual signal $r(k)$ and since the dynamics (5.41) is observable, condition (5.35) also holds. Moreover, for $m_1(k) = 0$ the system is MS-stable and condition (5.36) holds. ■

To conclude this section, we now consider a discrete-time Markovian jump system that has multiple faults and that is governed by the following dynamical system

$$\begin{aligned} x(k+1) &= A_{\lambda(k)}x(k) + B_{\lambda(k)}u(k) + \sum_{j=1}^{P} L^j_{\lambda(k)} m_j(k) \\ y(k) &= C_{\lambda(k)}x(k) \qquad x(0) = x_0, \quad \lambda(0) = i_0 \end{aligned} \tag{5.42}$$

where all the matrices are the same as in the dynamical model (5.30), $L^j_{\lambda(k)}$, $j \in \mathbf{k}$ are the fault signatures, and $m_j(k) \in \mathcal{M}_j$, $j \in \mathbf{P}$ are the fault modes. We denote the fault signatures associated with $\lambda(k) = i$ by $L^j_i, i \in \Psi, j \in \mathbf{P}$.

The Structured Fault Detection and Isolation Problem (SFDIP) (Section 2.1) for the Markovian jump system (5.42) is now defined as the problem of generating p residual signals $r_l(k), l \in \mathbf{p}$ based on a given coding set $\Omega_i, i \in \mathbf{P}$, from the following Markovian jump detection filters

$$\begin{aligned} w_l(k+1) &= F^l_{\lambda(k)} w_l(k) - E^l_{\lambda(k)} y(k) + K^l_{\lambda(k)} u(k) \\ r_l(k) &= M^l_{\lambda(k)} w_l(k) - H^l_{\lambda(k)} y(k), \qquad l \in \mathbf{p} \end{aligned} \tag{5.43}$$

such that the residuals $r_l(k)$ for $l \in \Omega_i$ are sensitive to a fault of the i-th component, and the other residuals $r_\alpha(k)$ for $\alpha \in \mathbf{p} - \Omega_i$ are insensitive to this fault. The solvability condition for the SFDIP problem is obtained by invoking the solvability condition that was developed earlier for the FPRG problem as follows:

Theorem 5.6. *The SFDIP problem has a solution for system* (5.42) *only if*

$$\mathcal{S}^*_{\Gamma_j} \bigcap \mathcal{L}^l_i = 0, \quad i \in \Psi, l \in \Gamma_j \tag{5.44}$$

where $\mathcal{S}^*_{\Gamma_j} = \inf \mathfrak{S}(\mathfrak{A}, \mathfrak{C}, \sum_{v=1}^{N} \sum_{l \notin \Gamma_j} \mathcal{L}^l_v)$, $j \in \boldsymbol{p}$. *On the other hand, if the above* $\mathcal{S}^*_{\Gamma_j}, j \in \boldsymbol{p}$ *exist such that they are outer MS-detectable, the EFPRG problem is then guaranteed to have a solution.*

Proof: The proof is immediate by following the same steps as in the proof of Theorems 5.5 and 2.3. ■

5.4.3 H_∞-based Fault Detection and Isolation Design

In this section, we consider a discrete-time Markovian jump system that are subjected to both external input and output measurement disturbances and noise and that is governed by

$$\begin{aligned} x(k+1) &= A_{\lambda(k)}x(k) + B_{\lambda(k)}u(k) + \sum_{j=1}^{P} L^j_{\lambda(k)}m_j(k) + B^d_{\lambda(k)}d(k) \\ y(k) &= C_{\lambda(k)}x(k) + D^d_{\lambda(k)}d(k) \end{aligned} \tag{5.45}$$

where all the matrices are defined as in (5.42). The signal $d(k) \in \mathbb{R}^p$ represents an unknown disturbance input and output measurement noise. We denote the disturbance matrices $B^d_{\lambda(k)}$ and $D^d_{\lambda(k)}$ associated with $\lambda(k) = i$ by B^d_i and D^d_i, $i \in \Psi$. It is further assumed that the disturbance input $d(t)$ belongs to $\mathscr{L}_2$, i.e.

$$||d||_2 = \Big(\sum_{k=0}^{\infty} d^\top(k)d(k)\Big)^{1/2} < \infty$$

Based on the above formulation of the Markovian jump system (5.45), an H_∞-based Structured Fault Detection and Isolation Problem (H_∞-SFDIP) is introduced which is concerned with the design of a set of detection filters (5.43) that generate p residuals $r_j(k)$ based on given coding sets $\Omega_i, i \in \mathbf{P}$ such that the residuals $r_j(t)$ for $j \in \Omega_i$ are sensitive to a fault of the i-th component, and the other residuals $r_\alpha(t)$ for $\alpha \in \mathbf{p} - \Omega_i$ are insensitive to this fault and

$$||r_l||^2_{2,E} = \mathbb{E}\Big\{\sum_{k=0}^{\infty} r_l^\top(k)r_l(k)|(x_0, i_0)\Big\} < \gamma^2||d||_2, \quad l \in \mathbf{p} \tag{5.46}$$

for all $d(k) \in \mathscr{L}_2$, where $\gamma > 0$ is the prescribed level of disturbance attenuation.

Below we first present preliminary results on disturbance attenuation of Markovian jump systems.

Lemma 5.8 ([197]). *Consider the system* (5.45) *with* $u(k) = 0$ *and* $m_j(k) = 0, j \in \boldsymbol{P}$. *Let* $\gamma > 0$ *be a given scalar, then the system is mean square stable when* $d = 0$ *and under zero initial conditions satisfies*

$$||y||_{2,E} < \gamma ||d||_2 \tag{5.47}$$

if there exist matrices $R_i > 0, i \in \Psi$ *such that the following LMIs:*

$$\begin{bmatrix} A_i^\top \bar{R}_i A_i - R_i & A_i^\top \bar{R}_i B_i^d & C_i^\top \\ * & -\gamma^2 I + B_i^{d^\top} \bar{R}_i B_i^d & D_i^{d^\top} \\ * & * & -I \end{bmatrix} < 0 \tag{5.48}$$

hold for $i \in \Psi$ *where* $\bar{R}_i = \sum_{j=1}^{N} \pi_{ij} R_j$. *Moreover, LMI* (5.48) *is equivalent to*

$$\begin{bmatrix} -R_i & A_i^\top \bar{R}_i & 0 & C_i^\top \\ * & -\bar{R}_i & \bar{R}_i B_i^d & 0 \\ * & * & -\gamma^2 I & D_i^{d^\top} \\ * & * & * & -I \end{bmatrix} < 0 \tag{5.49}$$

for $i \in \Psi$.

Lemma 5.9 ([198]). *The LMI* (5.49) *with* $R_i > 0$, $i \in \Psi$ *is feasible if and only if there exist matrices* $R_i > 0$ *and* $\mathscr{G}_i$, $i \in \Psi$ *such that*

$$\begin{bmatrix} -R_i & A_i^\top \mathscr{G}_i^\top & 0 & C_i^\top \\ * & -\mathscr{G}_i^\top - \mathscr{G}_i + \bar{R}_i & \mathscr{G}_i B_i^d & 0 \\ * & * & -\gamma^2 I & D_i^{d^\top} \\ * & * & * & -I \end{bmatrix} < 0$$

We are now in a position to derive our sufficient conditions for determining the solvability of the H_∞-SFDIP problem for discrete-time MJS systems.

Theorem 5.7. *The* H_∞*-SFDIP problem defined by expressions* (5.46) *and* (5.43) *has a solution for the Markovian jump system* (5.45) *if there exist unobservability*

subspaces

$$\mathcal{S}^*_{\Gamma_l} = \inf \mathfrak{S}(\mathfrak{A}, \mathfrak{C}, \sum_{v=1}^{N} \sum_{j \notin \Gamma_l} \mathcal{L}^j_v), \quad l \in \boldsymbol{p} \tag{5.50}$$

such that $\mathcal{S}^*_{\Gamma_l} \bigcap \mathcal{L}^j_i = 0,\ i \in \Psi, j \in \Gamma_l$ *as well as the matrices* T^l_i, $\mathscr{G}^l_i$ *and positive-definite matrices* R^l_i, $i \in \Psi$, $l \in \boldsymbol{p}$ *such that*

$$\begin{bmatrix} -R^l_i & A^{l^\top}_i \mathscr{G}^l_i + M^{l^\top}_i T^{l^\top}_i & 0 & M^{l^\top}_i \\ * & -\mathscr{G}^{l^\top}_i - \mathscr{G}^l_i + \bar{R}^l_i & \mathscr{G}^l_i B^d_{li} - T^l_i H^l_i D^d_i & 0 \\ * & * & -\gamma^2 I & D^{d^\top}_{li} \\ * & * & * & -I \end{bmatrix} < 0 \tag{5.51}$$

where $\bar{R}^l_i = \sum_{j=1}^{N} \pi_{ij} R^l_j$ *and* P_l *is the canonical projection of* $\mathcal{X}$ *on* $\mathcal{X}/\mathcal{S}^*_{\Gamma_l}$, $B^d_{li} = -P_l B^d_i - P_l D^l_i D^d_i$, $D^d_{li} = -H^l_i D^d_i$, *the pairs* (M^l_i, A^l_i), $i \in \Psi$, $l \in \boldsymbol{p}$ *are the factor system of the pairs* $(C_i, A_i), i \in \Psi$ *on* $\mathcal{X}/\mathcal{S}^*_{\Gamma_l}$ *and* H^l_i *is the solution to Ker* $H^l_i C_i = \mathcal{S}^*_{\Gamma_l} + Ker\ C_i$.

Proof: Given the common unobservability subspaces $\mathcal{S}^*_{\Gamma_l}$, there exist output injection maps D^l_i and measurement mixing maps H^l_i $i \in \Psi$, $l \in \mathbf{p}$ such that

$$\mathcal{S}^*_{\Gamma_l} = << \text{Ker } H^l_i C_i | A_i + D^l_i C_i >>_{i \in \Psi}$$

where H^l_i is the solution to Ker $H^l_i C_i = \mathcal{S}^*_l + \text{Ker } C_i$. Let M^l_i be a unique solution to $M^l_i P_l = H^l_i C_i$ and

$$A^l_i = (A_i + D^l_i C_i : \mathcal{X}/\mathcal{S}^*_{\Gamma_l})$$

where $P_l(A_i + D^l_i C_i) = A^l_i P_l$. Let T^l_i and $\mathscr{G}^l_i$ be the solution to the inequality (5.51) and define $G^l_i = \mathscr{G}^{l^{-1}}_i T^l_i$ and $F^l_i = A^l_i + G^l_i M^l_i$, $E^l_i = P_l(D^l_i + P^{-r}_l G^l_i H^l_i)$. Let

$K_i^l = P_l B_i$. Define $e_l(k) = w_l(k) - P_l x(k)$, then using (5.31) we have

$$
\begin{aligned}
e_l(k+1) &= F_i^l w_l(k) - E_i^l y(k) + K_i^l u(k) \\
&- P_l(A_i x(k) + B_i u(k) + B_i^d d(k) + \sum_{j=1}^{L} L_i^j m_j(k)) \\
&= F_i^l w_l(k) - \sum_{j\in\Gamma_l} P_l L_i^j m_j(k) - P_l B_i^d d(k) \\
&- P_l(A_i + D_i^l C_i)x(k) - G_i^l H_i^l C_i x(k) - E_i^l D_i^d d(k) \\
&= F_i^l w_l(k) - \sum_{j\in\Gamma_l} P_l L_i^j m_j(k) + (B_{li}^d - G_i^l H_i^l D_i^d)d(k) - A_i^l P_l x(k) - G_i^l M_i^l P_l x(k) \\
&= (A_i^l + G_i^l M_i^l)e_l(k) - \sum_{j\in\Gamma_l} P_l L_i^j m_j(k) + (B_{li}^d - G_i^l H_i^l D_i^d)d(k)
\end{aligned}
$$

Note that $P_l L_i^j = 0, i \in \Psi, j \notin \Gamma_l$, since $\mathcal{L}_i^j \in \mathcal{S}_{\Gamma_l}^*, j \notin \Gamma_l$. Also

$$
r_l(t) = M_i^l w_l(k) - H_i^l y(k) = M_i^l w_l(k) - H_i^l C_i x(k) - H_i^l D_i^d d(k) = M_i^l e_l(k) + D_{li}^d d(k)
$$

Consequently, the error dynamics can be written as

$$
\begin{aligned}
e_l(k+1) =& (A_i^l + G_i^l M_i^l)e_l(k) - \sum_{j\in\Gamma_l} P_l L_i^j m_j(k) + (B_{li}^d - G_i^l H_i^l D_i^d)d(k) \\
r_l(k) =& M_i^l e_l(k) + D_{li}^d d(k)
\end{aligned}
\tag{5.52}
$$

Using Lemma 5.8 and the inequality (5.49), it follows that the inequality (5.46) holds. Moreover, from the error dynamics (5.52), it follows that $r_l(k)$ is only affected by $L_{\lambda(k)}^j, j \in \Gamma_l$ and is decoupled from other fault signatures. ■

After constructing the residual signals $r_l(k), l \in \mathbf{p}$, the last step for a successful fault detection and isolation is the residual evaluation stage which includes determining evaluation functions J_{r_l} and thresholds J_{th_l}. In this paper, evaluation functions and thresholds are selected as

$$
J_{r_l}(k) = \sum_{k-k_0}^{k} r_l^\top(k) r_l(k), \quad l \in \mathbf{p} \tag{5.53}
$$

$$
J_{th_l} = \sup_{d\in\mathfrak{L}_2, m_j=0, j\in\Gamma_l} E(J_{r_l}), \quad l \in \mathbf{p} \tag{5.54}
$$

where k_0 is the length of the evaluation window. Based on the above thresholds and evaluation functions, the occurrence of a fault can be detected and isolated by using the following decision logics

$$J_{r_l} > J_{th_l} \quad \forall l \in \Omega_j \Longrightarrow m_j \neq 0, \quad j \in \mathbf{P} \tag{5.55}$$

5.4.4 FDI of a Formation Flight of Satellites

In order to investigate the effect of packet dropout on the FDI of formation flight of four satellites (Section 3.3.3), two different topologies (neighboring sets) are considered here. The first one is the same as the network topology that is considered in Section 3.3.3, namely $N_1 = \{2\}$, $N_2 = \{1, 3\}$, $N_3 = \{4\}$ and $N_4 = \{1\}$. It can be verified that the SFDIP problem has a solution for the same coding sets as in Section 3.3.3 and hence the packet dropout does not change the detectability index of the actuator fault signatures of the vehicles. This is due to the fact that the graph of the network remains weakly connected when all the arcs that leave node i are deleted for each $i \in \mathbf{N}$.

The second topology that is considered here is as $N_1 = \{2\}$, $N_2 = \{3\}$, $N_3 = \{4\}$ and $N_4 = \{2\}$. It can be verified that the SFDIP problem has a solution with the same coding sets as in the first topology when the communication links are considered to be ideal (without time-delay and packet dropout, i.e. system (5.2)). However, in the presence of imperfect communication links (system (5.5)), the SFDIP problem does not have a solution for this coding sets and hence the detectability index of the actuator fault signatures is less than the ideal case. This is due to the fact that when the graph of the network does not remain weakly connected when the arc leaving node 1 to node 2 is deleted. In other words, when the measurement from the vehicle 1 is lost, there exists no way to recover this information.

Next, we try to find a suitable coding sets for the above network. Due to

the lack of measurement from satellite 1 when there is a packet dropout in the communication link between this satellite and central FDI unit, actuator faults in satellite 1 cannot be decoupled. In other words, we have $\mathcal{L}_{11} \subset \mathcal{S}^*(\mathcal{L}_{12})$ and $\mathcal{L}_{12} \subset \mathcal{S}^*(\mathcal{L}_{11})$. Hence, these two fault signatures are considered together as a subfamily $FL_1 = \{\mathcal{L}_{11}, \mathcal{L}_{12}\}$. Now, we consider the generalized residual set for the 7 fault signatures FL_1 and $\mathcal{L}_{kj}$, $k \in \{2,3,4\}$, $j \in \{1,2\}$. In other words, we consider the following coding sets $\Omega_{FL_1} = \{2,3,4,5,6,7\}$, $\Omega_{21} = \{1,3,4,5,6,7\}$, $\Omega_{22} = \{1,2,4,5,6,7\}$, $\Omega_{31} = \{1,2,3,5,6,7\}$, $\Omega_{32} = \{1,2,3,4,6,7\}$, $\Omega_{41} = \{1,2,3,4,5,7\}$ and $\Omega_{41} = \{1,2,3,4,5,6\}$. It can be verified that the SFDIP problem has a solution for these coding sets, and hence one can detect and isolate single fault in the actuators of satellites 2,3 and 4 but actuator faults of satellite 1 cannot be isolated and only occurrence of a fault in this satellite can be detected and isolated.

For simulations a 10% packet dropout rate is considered for all the communication links and hence the following transition probability is considered for the Markovian jump model of the satellite formation

$$\Pi = \begin{bmatrix} 0.5 & 0.1 & 0.1 & 0.1 & 0.1 \\ 0.95 & 0.05 & 0 & 0 & 0 \\ 0.95 & 0 & 0.05 & 0 & 0 \\ 0.95 & 0 & 0 & 0.05 & 0 \\ 0.95 & 0 & 0 & 0 & 0.05 \end{bmatrix}$$

The length of the evaluation window is selected as $k_0 = 50$ (5 seconds). By considering the worst case analysis of the residuals corresponding to the healthy operation of the satellites that are subject to measurement noise, threshold values $J_{th_1} = J_{th_2} = 0.002$, $J_{th_3} = 0.001$, $J_{th_4} = J_{th_5} = J_{th_6} = J_{th_7} = 0.0006$ are selected for the residual signals for fault detection and isolation logic evaluation and analysis.

Two fault scenarios are considered here for simulations. In the first one, a Lock-in-place fault is injected at the first actuator of satellite 1 at $t = 20$ where

$u_{11} = -1$. Figure 5.3 shows the residual evaluation functions that are generated by using our detection filters associated with the considered fault scenario. As shown in this figure, the injected fault can be detected and isolated among the satellites based on the coding set Ω_{FL_1}. However, one cannot isolate between the actuators of satellite 1. In the second fault scenario, a Lock-in-place fault is injected at the second actuator of satellite 2 at $t = 25$ where $u_{22} = 0.5$. Figure 5.4 depicts the residual evaluation functions corresponding to this fault scenario. Based on this figure and the coding sets Ω_{22}, this fault can be detected and isolated.

5.5 Continuous-time Markovian Jump Systems

Consider the following Markovian jump system

$$\begin{aligned} \dot{x}(t) &= A(\lambda(t))x(t) + B(\lambda(t))u(t) \\ y(t) &= C(\lambda(t))x(t), \quad x(0) = x_0, \quad \lambda(0) = i_0 \end{aligned} \tag{5.56}$$

where $x \in \mathcal{X}$ is the state of the system with dimension n; $u \in \mathcal{U}, y \in \mathcal{Y}$ are input and output signals with dimensions m and q, respectively; and $\{\lambda(t), t \geq 0\}$ is a continuous-time irreducible Markov process taking values in the finite set $\Psi = \{1, ..., N\}$. The Markov process describes the switching between the different system modes and its evolution is governed by the following probability transitions:

$$\mathbb{P}\diagdown\{\lambda(t+h) = j|\lambda(t) = i\} = \begin{cases} \pi_{ij}h + o(h) & \text{when } \lambda(t) \text{ jumps from } i \text{ to } j \\ 1 + \pi_{ii}h + o(h), & \text{otherwise} \end{cases}$$

where π_{ij} is the transition rate from mode i to mode j with $\pi_{ij} \geq 0$ when $i \neq j$, $\pi_{ii} = -\sum_{j=1, j\neq i}^{N} \pi_{ij}$, and $o(h)$ is a function that satisfies $lim_{h\to 0}\frac{o(h)}{h} = 0$. The matrices $A(\lambda(t))$, $B(\lambda(t))$ and $C(\lambda(t))$ are known constant matrices for all $\lambda(t) = i \in \Psi$. For simplicity, we denote the matrices associated with $\lambda(t) = i$ by $A(\lambda(t)) = A_i$, $B(\lambda(t)) = B_i$, $C(\lambda(t)) = C_i$. Furthermore, the MJS system (5.56) is represented

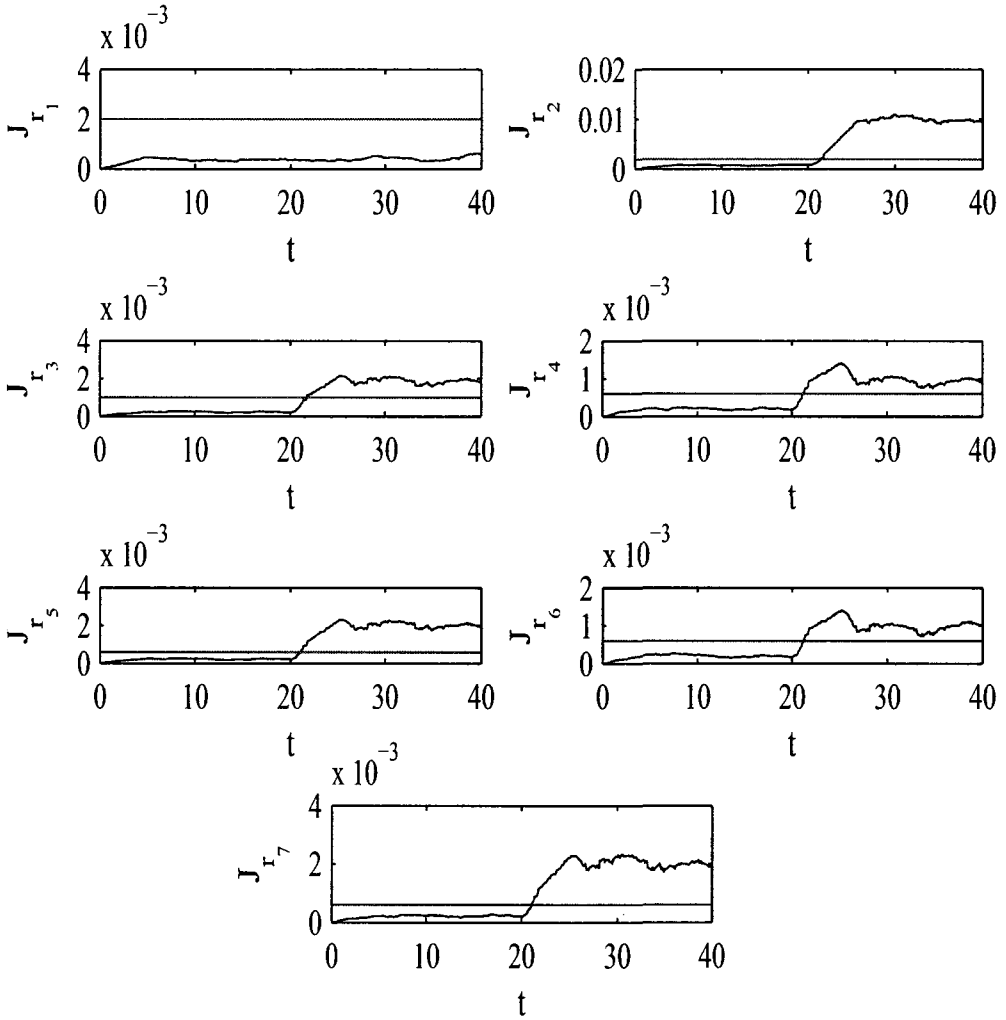

Figure 5.3: Residual evaluation functions corresponding to a fault in the first actuator of satellite 1.

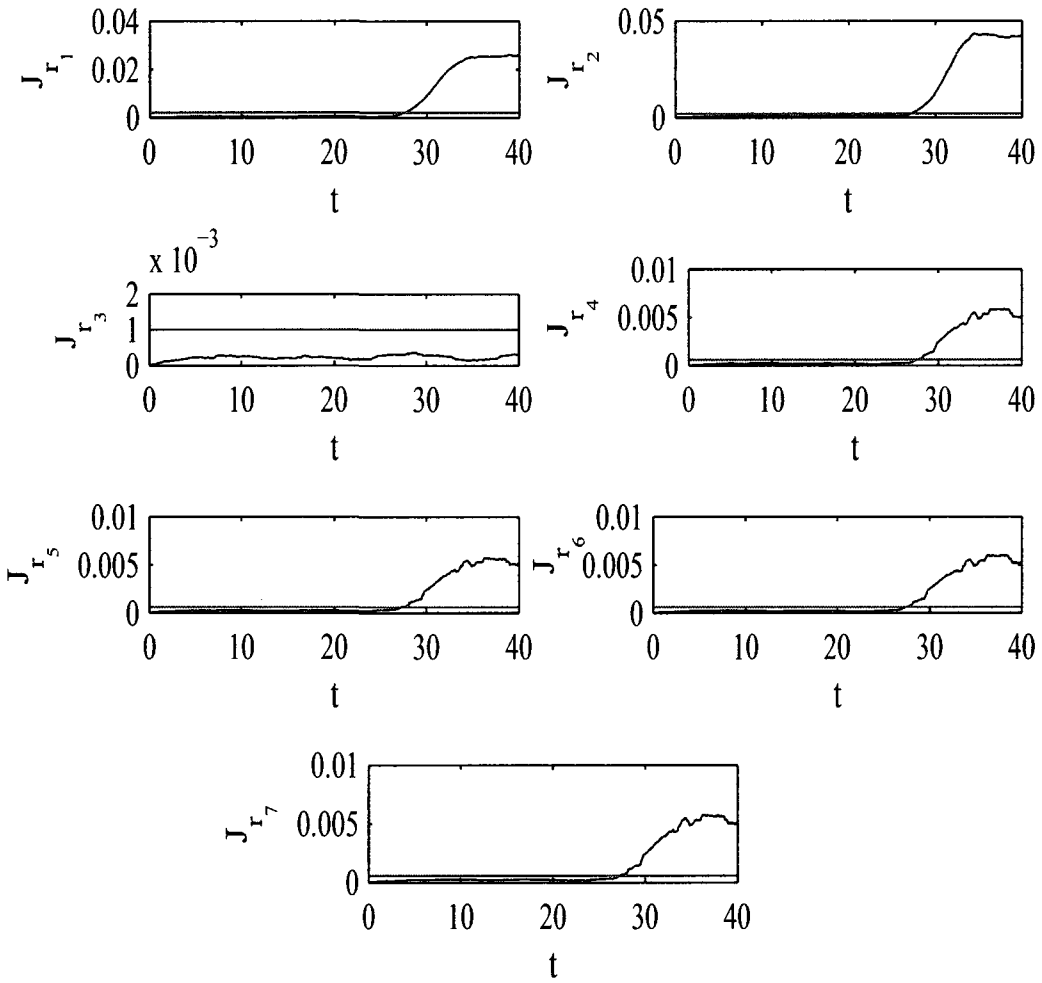

Figure 5.4: Residual evaluation functions corresponding a fault in the second actuator of satellite 2.

by $(\mathfrak{A}, \mathfrak{B}, \mathfrak{C}, \Pi)$, where $\mathfrak{A} = (A_1, ..., A_N)$, $\mathfrak{B} = (B_1, ..., B_N)$, $\mathfrak{C} = (C_1, ..., C_N)$ and $\Pi = [\pi_{ij}]$, $i, j \in \Psi$.

5.5.1 Unobservable and Unobservability Subspaces

Similar to Section 5.4.1, in this section a geometric definition for unobservable subspace of continuous-time Markovian jump systems (MJS) is introduced. The notion of unobservability subspace is then formalized for continuous-time MJS systems that are governed by (5.56). We first start with the definition of weak observability for Markovian jump system (5.56) with $B_i = 0, i \in \Psi$.

Definition 5.9 ([199]). *The system* $(\mathfrak{A}, \mathfrak{C}, \Pi)$ *is said to be weakly (W-) observable when there exist* $t_d \geq 0$ *and* $\gamma > 0$ *such that* $W^{t_d}(x, i) \geq \gamma |x|^2$ *for each* $x \in \mathcal{X}$ *and* $i \in \Psi$ *where*

$$W^{\top}(x, i) = \mathbb{E}\Big\{ \int_0^{\top} x^{\top}(\tau) C_{\lambda(\tau)}^{\top} C_{\lambda(\tau)} x(\tau) d\tau | x(0) = x, \lambda_0 = i \Big\} \tag{5.57}$$

In [199], a collection of matrices $\mathcal{O} = \{\mathcal{O}_1, ..., \mathcal{O}_N\}$ is introduced for testing the W-observability of the Markovian jump systems according to the following procedure. Let $O_i(0) = C_i^{\top} C_i$, $i \in \Psi$ and define the sequence of matrices as

$$O_i(k) = A_i^{\top} O_i(k-1) + O_i(k-1) A_i + \sum_{j=1}^{N} \pi_{ij} O_j(k-1), \quad k > 0, i \in \Psi \tag{5.58}$$

The matrix $\mathcal{O}_i$ is defined according to

$$\mathcal{O}_i = [O_i(0)\ O_i(1) \cdots O_i(n^2 N - 1)]^{\top} \tag{5.59}$$

Theorem 5.8 ([199]). *The MJS system* (5.56) *is W-observable if and only if* $\mathcal{O}_i$ *has a full rank for each* $i \in \Psi$.

It is also known that system (5.56) is W-observable if each pair $(A_i, C_i), i \in \Psi$ is observable. However, this condition is not necessary [199]. By considering the above definition of W-observability, one can define the set of unobservable states as follows.

Definition 5.10. *A state x is said to be unobservable if $W^\top(x,i) = 0$ for all $t \geq 0$ and $i \in \Psi$.*

Let $\mathcal{Q}$ denotes the unobservable set of the MJS system (5.56), i.e.

$$\mathcal{Q} = \{x | W^\top(x,i) = 0, \forall i \in \Psi, t \geq 0\} \tag{5.60}$$

It is shown in [199] that for an irreducible Markov processes, $\mathcal{N}\{\mathcal{O}_i\} = \mathcal{N}\{\mathcal{O}_j\}$, $i,j \in \Psi$, $i \neq j$ and $\mathcal{Q} = \mathcal{N}\{\mathcal{O}_i\}$. Therefore, $\mathcal{Q}$ is the subspace of $\mathcal{X}$ and is called the unobservable subspace of the Markovian jump system (5.56). The theorem introduced below characterizes a geometric property of Q.

Theorem 5.9. *An unobservable subspace Q for the system $(\mathfrak{A}, \mathfrak{C}, \Pi)$ with irreducible Markov process is the largest A_i-invariant ($i \in \Psi$) that is contained in $\mathcal{K} = \bigcap_{i=1}^{N} Ker\ C_i$.*

Proof: It follows from the above discussion that $\mathcal{Q} \subseteq \text{Ker } C_i$, $i \in \Psi$, and hence $\mathcal{Q} \subseteq \mathcal{K}$. Let $x \in \mathcal{Q}$. Our goal is to show that $A_i x \in \mathcal{Q}$ for all $i \in \Psi$ (i.e. $\mathcal{Q}$ is A_i-invariant, $i \in \Psi$). Since $x \in \mathcal{N}\{O_i(k-1)\}$ and $x \in \mathcal{N}\{O_i(k)\}$, $i \in \Psi$, then

$$O_i(k)x = A_i^\top O_i(k-1)x + O_i(k-1)A_i x + \sum_{j=1}^{N} \pi_{ij} O_j(k-1)x = O_i(k-1)A_i x = 0$$

Hence $A_i x \in \mathcal{N}\{\mathcal{O}_i(k-1)\}$ and $\mathcal{Q}$ is A_i-invariant for all $i \in \Psi$.

Next we show that Q is the largest A_i-invariant ($i \in \Psi$) that is contained in $\mathcal{K}$. Let $\mathcal{V}$ be an A_i-invariant ($i \in \Psi$) subspace that is contained in $\mathcal{K}$. Clearly, $\mathcal{V} \subseteq \mathcal{N}\{O_i(0)\}$, $i \in \Psi$. Let $\mathcal{V} \subseteq \mathcal{N}\{O_i(k-1)\}$, $i \in \Psi$ and $x \in \mathcal{V}$, then

$$O_i(k)x = A_i^\top O_i(k-1)x + O_i(k-1)A_i x + \sum_{j=1}^{N} \pi_{ij} O_j(k-1)x = 0$$

since $O_i(k-1)x = 0, i \in \Psi$ and $A_i x \in \mathcal{V}$ ($\mathcal{V}$ is A_i-invariant). Hence, $\mathcal{V} \subseteq \mathcal{N}\{O_i(k)\}$, $i \in \Psi$ and $\mathcal{V} \subseteq \mathcal{Q}$. This shows that $\mathcal{Q}$ contains all the subspaces that are A_i-invariant ($i \in \Psi$) and is contained in $\mathcal{K}$. ■

The same algorithm as in Algorithm 5.1 can be used for obtaining an unobservable subspace of continuous-time Markovian jump system (5.56). Moreover, similar definition of conditioned invariant and unobservability subspaces for discrete-time MJS can be applied to continuous-time MJS (Definitions 5.5 and 5.6, respectively) and the same algorithm can be used for obtaining such subspaces (Algorithms 5.2 and 5.3, respectively).

Next, we present definitions for stability and detectability of MJS systems.

Definition 5.11 ([199]). *The system* $(\mathfrak{A}, \Pi)$ *is mean square (MS) stable if for each* $x_0 \in \mathcal{X}$ *and* $i_0 \in \Psi$,

$$\lim_{t\to\infty} \mathbb{E}\{||x(t)||^2\} = 0 \tag{5.61}$$

MS-detectability of continuous-time MJS is defined similarly to discrete-time MJS as follows

Definition 5.12 ([199]). *We say that* $(\mathfrak{A}, \mathfrak{C}, \Pi)$ *is MS-detectable when there exists* $G = \{G_1, ..., G_N\}$ *of appropriate dimension for which* $(\mathfrak{A}_G, \Pi)$ *is MS-stable, where* $\mathfrak{A}_G = \{A_1 + G_1C_1, ..., A_N + G_NC_N\}$.

The following computational linear matrix inequalities can be used for testing the MS-detectability of a continuous-time MJS system [199]. In other words, the MS-detectability of $(\mathfrak{A}, \mathfrak{C}, \Pi)$ is equivalent to the feasibility of the set

$$A_i^\top X_i + X_iA_i + C_i^\top L_i^\top + L_iC_i + \sum_{j=1}^{N} \pi_{ij}X(j) < 0, \quad i = 1, ..., N \tag{5.62}$$

in the unknowns $X_i > 0$ and L_i with appropriate dimensions. In [199] an example is given that is W-observable but not MS-detectable. The example below illustrates the results that we have developed so far for the MJS systems. It also shows that an MJS system could be MS-detectable or not depending on the mode transition matrix.

Example 5.2. *Let $N = 2$ and set*

$$A_1 = \begin{bmatrix} 1 & 0 \\ 0 & 1 \end{bmatrix}, A_2 = \begin{bmatrix} 2 & 3 \\ 0 & 5 \end{bmatrix}, C_1 = \begin{bmatrix} 0 & 0 \end{bmatrix}, C_2 = \begin{bmatrix} 0 & 1 \end{bmatrix}; \Pi = \begin{bmatrix} -1 & 1 \\ 1 & -1 \end{bmatrix}$$

From (5.59), one can evaluate rank($\mathcal{O}_1$)=rank($\mathcal{O}_2$)=1 and Theorem 5.8 ensures that this system is not W-observable. Using Algorithm 5.1, the unobservable subspace $\mathcal{Q}$ is found to be

$$\mathcal{Q} = \begin{bmatrix} 1 \\ 0 \end{bmatrix}$$

The factor system for the above system can be found as $(A_1 : \mathcal{X}/\mathcal{S}) = 1$, $(A_2 : \mathcal{X}/\mathcal{S}) = 5$, $(C_1 : \mathcal{X}/\mathcal{S}) = 0$, and $(C_2 : \mathcal{X}/\mathcal{S}) = 1$, which is clearly W-observable, but according to (5.62) it is not MS-detectable. However, corresponding to the probability transition matrix

$$\Pi = \begin{bmatrix} -10 & 10 \\ 3 & -3 \end{bmatrix}$$

the above factor system is both W-observable and MS-detectable.

The above example shows that W-observability is a structural property of the MJS system with irreducible Markov processes which depends on only the matrices A_i's and C_i's (this also follows from Theorem 5.9), but the MS-detectability depends furthermore on the mode transition matrix Π.

Remark 5.3. *It should be emphasized that our proposed Theorem 5.9 and Algorithm 5.1 do indeed provide a less computationally intensive method for verifying the W-observability of the Markovian jump systems in comparison with the results in [199], where one needs to obtain the N matrices $\mathcal{O}_i \in \mathcal{R}^{n(n^2N)\times n}$.*

We are now in a position to formally introduce the fundamental problem in residual generation (FPRG) for the Markovian jump systems.

5.5.2 Fault Detection and Isolation Based on Geometric Approach

Similar to Section 5.4.2, in this section the Fundamental Problem in Residual Generation is now investigated for the continuous-time Markovian jump systems. Consider the following Markovian jump system

$$\begin{aligned} \dot{x}(t) &= A(\lambda(t))x(t) + B(\lambda(t))u(t) + L_1(\lambda(t))m_1(t) + L_2(\lambda(t))m_2(t) \\ y(t) &= C(\lambda(t))x(t), \quad x(0) = x_0, \quad \lambda(0) = i_0 \end{aligned} \tag{5.63}$$

where it is assumed that all the matrices are the same as in (5.56) and the Markov process $\lambda(t)$ is irreducible. The matrices $L_1(\lambda(t))$, $L_2(\lambda(t))$ represent the fault signatures and are monic and $m_i(t) \in \mathcal{M}_i \subset \mathcal{X}$, $i = 1, 2$ denote the fault modes. We denote the fault signatures associated with $\lambda(t) = i$ by L_{i1} and L_{i2}. The fault modes together with the fault signatures can be used to model the effects of actuator faults, sensor faults and system faults on the dynamics of the system. For example, the effect of a fault in the i-th actuator may be represented by L_{i1} as the i-th column of B_i and if an actuator fails, then $m_1(t) = -u_i(t)$.

The FPRG problem is concerned with the design of a Markovian jump residual generator that is governed by the filter dynamics of the form

$$\begin{aligned} \dot{w}(t) &= F(\lambda(t))w(t) - E(\lambda(t))y(t) + K(\lambda(t))u(t) \\ r(t) &= M(\lambda(t))w(t) - H(\lambda(t))y(t) \end{aligned} \tag{5.64}$$

where $w(t) \in \mathcal{F} \subset \mathcal{X}$ such that the response of $r(t)$ is affected by the fault mode $m_1(t)$ and is decoupled from $m_2(t)$ and if m_1 is identically zero then

$$\lim_{t \to \infty} \mathbb{E}||r(t)||^2 = 0$$

for any input signal $u(t)$.

We can rewrite equations (5.63) and (5.64) as follows:

$$\begin{bmatrix} \dot{x}(t) \\ \dot{w}(t) \end{bmatrix} = \begin{bmatrix} A(\lambda(t)) & 0 \\ -E(\lambda(t))C(\lambda(t)) & F(\lambda(t)) \end{bmatrix} \begin{bmatrix} x(t) \\ w(t) \end{bmatrix}$$
$$+ \begin{bmatrix} B(\lambda(t)) & L_2(\lambda(t)) \\ K(\lambda(t)) & 0 \end{bmatrix} \begin{bmatrix} u(t) \\ m_2(t) \end{bmatrix} + \begin{bmatrix} L_1(\lambda(t)) \\ 0 \end{bmatrix} m_1(t)$$
$$r(t) = \begin{bmatrix} -H(\lambda(t))C(\lambda(t)) & M(\lambda(t)) \end{bmatrix} \begin{bmatrix} x(t) \\ w(t) \end{bmatrix} \tag{5.65}$$

Define the extended space $\mathcal{X}^e = \mathcal{X} \oplus \mathcal{F}$ and $\mathcal{U}^e = \mathcal{U} \oplus \mathcal{M}_2$, so that equation (5.65) can be expressed as

$$\begin{aligned} \dot{x}^e(t) &= A^e(\lambda(t))x^e(t) + B^e(\lambda(t))u^e(t) + L_1^e(\lambda(t))m_1(t) \\ r(t) &= H^e(\lambda(t))x^e(t) \end{aligned} \tag{5.66}$$

with $x^e(t) \in \mathcal{X}^e$ and $u^e \in \mathcal{U}^e$. Similar to input observability for the discrete-time Markovian jump systems, the same notion the continuous-time Markovian jump system is defined below.

Definition 5.13. *The Markovian jump system* (5.56) *is said to be input observable if B_i, $i \in \Psi$ is monic and the image of B_i's does not intersect with the unobservable subspace of system* (5.56).

Based on the above definition, the FPRG problem can now be formally stated as the problem of designing the dynamical filter (5.64) such that

(a) r is decoupled from u^e, (5.67)

(b) m_1 is input observable in the augmented system (5.66), and (5.68)

(c) $\lim_{t \to 0} \mathbb{E}\{||r(t)||^2\} = 0$, for $m_1(t) = 0, \forall\, i_0 \in \Psi$ and $\forall x_0^e \in \mathcal{X}^e$. (5.69)

It is easy to show that Lemma 5.7 holds also for continuous-time MJS with the embedding map defined in (5.37). We are now in a position to derive the

solvability condition for the FPRG problem corresponding to the Markovian jump system (5.63).

Theorem 5.10. *The FPRG problem has a solution for the augmented MJS system* (5.66) *only if*

$$\mathcal{S}^* \bigcap \mathcal{L}_{j1} = 0, \quad j \in \Psi \tag{5.70}$$

where $\mathcal{S}^* = \inf \mathfrak{S}(\mathfrak{A}, \mathfrak{C}, \sum_{i=1}^{N} \mathcal{L}_{i2})$. *On the other hand, if the above* $\mathcal{S}^*$ *exists such that it is also outer MS-detectable, then the FPRG problem is then guaranteed to have a solution.*

Proof: The proof is similar to the proof of Theorem 5.5. ■

The next example illustrates through a detailed derivation steps how to design the detection filter (5.64) for a given Markovian jump system.

Example 5.3. *Consider the Markovian jump system* (5.63) *with* $N = 2$ *and matrices* $A_i, C_i,\ i = 1, 2$ *as follows*

$$A_1 = \begin{bmatrix} 0 & 3 & 4 \\ 1 & 2 & 3 \\ 0 & 2 & 5 \end{bmatrix}, \quad A_2 = \begin{bmatrix} 1 & 2 & 4 \\ 2 & -1 & 2 \\ 0 & 1 & 4 \end{bmatrix}, C_1 = \begin{bmatrix} 0 & 1 & 0 \\ 0 & 0 & 1 \end{bmatrix}, C_2 = \begin{bmatrix} 1 & 1 & 0 \\ 0 & 0 & 1 \end{bmatrix}$$

and $B_i = 0$. *The mode transition matrix and the fault signatures as given by*

$$\Pi = \begin{bmatrix} -8 & 8 \\ 3 & -3 \end{bmatrix}, L_{i1} = \begin{bmatrix} 1 \\ 0 \\ 0 \end{bmatrix}, L_{i2} = \begin{bmatrix} -3 \\ 1 \\ 0 \end{bmatrix}, \quad i \in \Psi$$

respectively. The unobservability subspace $\mathcal{S}^*(\mathcal{L}_{i2})$ *is found from Algorithm 5.3 which is given by*

$$\mathcal{S}^*(\mathcal{L}_{i2}) = \begin{bmatrix} -3 \\ 1 \\ 0 \end{bmatrix}$$

It is clear that $\mathcal{S}^*(\mathcal{L}_{i2}) \cap \mathcal{L}_{i1} = 0$. *It can be checked that* $\mathcal{S}^*(\mathcal{L}_{i2})$ *is outer MS-detectable and hence the FPRG problem has a solution. According to Theorem 5.10, the matrices that specify the governing dynamics of the detection filter in* (5.64) *are found through the following steps (all the geometric manipulations are performed by using the "geometric approach toolbox" [200]) :*

1. *The output injection maps* $D_i, i = 1, 2$ *are obtained from* $\mathcal{S}^*(\mathcal{L}_{i2})$ *as*

$$D_1 = \begin{bmatrix} 0 & -0.65 \\ 0 & -1.95 \\ -2 & -2.5 \end{bmatrix}, D_2 = \begin{bmatrix} -1.1 & -0.5 \\ -3.3 & -1.5 \\ 0.5 & -2.0 \end{bmatrix}$$

2. *The measurement maps* H_i *are found from equation* (5.23) *as* $H_1 = H_2 = \begin{bmatrix} 0 & 1 \end{bmatrix}$

3. *The canonical projection map* P *for* $\mathcal{S}^*(\mathcal{L}_{i2})$ *is given by*

$$P = \begin{bmatrix} 1 & -3 & 0 \\ 0 & 0 & 1 \end{bmatrix}$$

4. *The maps* $M_1 = M_2 = \begin{bmatrix} 0 & 1 \end{bmatrix}$ *are the unique solutions to* $M_i P = H_i C_i$, $i = 1, 2$

5. *The induced maps* A_{0i} *are found from* (2.23) *as follows*

$$A_{01} = \begin{bmatrix} 3 & -2.055 \\ 0 & 2.5 \end{bmatrix}, A_{02} = \begin{bmatrix} -4 & -1.581 \\ -1.581 & 2 \end{bmatrix}$$

6. *The maps* G_i *are obtained by solving the corresponding LMI's by using the YALMIP LMI Toolbox [201] which yields*

$$G_1 = \begin{bmatrix} 4.12 \\ -3.29 \end{bmatrix}, G_2 = \begin{bmatrix} 2.77 \\ -4.99 \end{bmatrix}$$

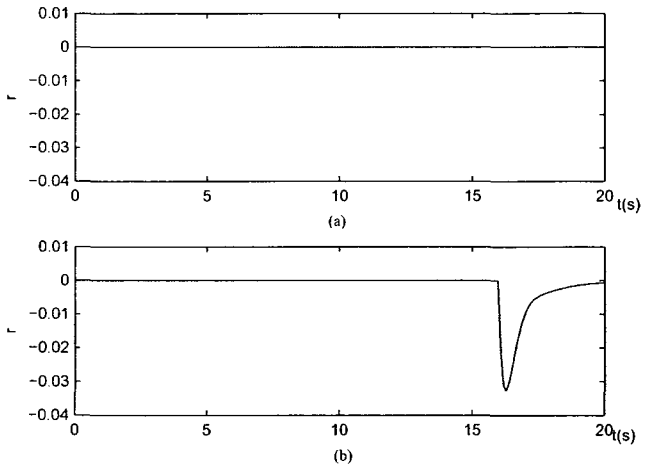

Figure 5.5: Residual signal: (a) $m_2(t) = 0.1, t > 10sec$; (b) $m_1(t) = 0.1, t > 15sec$

7. Finally, the maps F_i and E_i are found according to Theorem 5.10 as follows:

$$F_1 = \begin{bmatrix} 3 & -2.0716 \\ 0 & -0.798 \end{bmatrix}, F_2 = \begin{bmatrix} -4 & 1.1941 \\ -1.581 & -2.99 \end{bmatrix},$$

$$E_1 = \begin{bmatrix} 0 & 6.18 \\ -2 & -5.798 \end{bmatrix}, E_2 = \begin{bmatrix} 3.47 & 4.35 \\ 0.5 & -6.99 \end{bmatrix}$$

It is interesting to note that the FPRG problem for the mode 1 by itself does not have a solution since $\mathcal{L}_{i1} \subset \mathcal{S}_1^*$. However, when there is a jump in the system, one can solve the FPRG problem. Figure 5.5 shows the residual signal $r(t)$ that is obtained for the above system by constructing the detection filter (5.64)*. Two fault scenarios are considered: (a) $m_2(t) = 0.1, t > 10$ seconds, and (b) $m_1(t) = 0.1, t > 15$ seconds. As shown in Figure 5.5 the residual signal is only affected by $m_1(t)$ and the fault mode $m_2(t)$ does not have any effect on it.*

To conclude this section, we now consider a Markovian jump system that has multiple faults and that is governed by the following dynamical system

$$\begin{aligned} \dot{x}(t) &= A(\lambda(t))x(t) + B(\lambda(t))u(t) + \sum_{j=1}^{k} L_j(\lambda(t))m_j(t) \\ y(t) &= C(\lambda(t))x(t) \qquad x(0) = x_0, \quad \lambda(0) = i_0 \end{aligned} \tag{5.71}$$

where all the matrices are the same as in the dynamical model (5.63), $L_j(\lambda(k))$, $j \in \mathbf{k}$ are the fault signatures, and $m_j(t) \in \mathcal{M}_j$, $j \in \mathbf{k}$ are the fault modes. We denote the fault signatures associated with $\lambda(t) = i$ by $L_{ij}, i \in \Psi, j \in \mathbf{k}$.

The SFDIP problem for the Markovian jump system (5.71) is now defined as the problem of generating p residual signals $r_j(t), j \in \mathbf{p}$ from the following Markovian jump detection filters

$$\begin{aligned} \dot{w}_j(t) &= F_j(\lambda(t))w_j(t) - E_j(\lambda(t))y(t) + K_j(\lambda(t))u(t) \\ r_j(t) &= M_j(\lambda(t))w_j(t) - H_j(\lambda(t))y(t), \qquad j \in \mathbf{k} \end{aligned} \tag{5.72}$$

such that the residuals $r_j(t)$ for $j \in \Omega_i$ are sensitive to a fault of the i-th component, and the other residuals $r_\alpha(t)$ for $\alpha \in \mathbf{p} - \Omega_i$ are insensitive to this fault. The solvability condition for the SFDIP problem is obtained by invoking the solvability condition that was developed earlier for the FPRG problem as follows:

Theorem 5.11. *The SFDIP problem has a solution for system* (5.71) *only if*

$$\mathcal{S}^*_{\Gamma_j} \bigcap \mathcal{L}^l_i = 0, \quad i \in \Psi, l \in \Gamma_j \tag{5.73}$$

where

$$\mathcal{S}^*_{\Gamma_j} = \inf \mathfrak{S}(\mathfrak{A}, \mathfrak{C}, \sum_{v=1}^{N} \sum_{l \notin \Gamma_j} \mathcal{L}^l_v), \quad j \in \boldsymbol{p} \tag{5.74}$$

On the other hand, if the above $\mathcal{S}^*_j, j \in \boldsymbol{k}$ exist such that they are outer MS-detectable, the EFPRG problem is then guaranteed to have a solution.

Proof: The proof is immediate by following along the lines that we developed for the proof of Theorems 5.10 and 2.3. ■

5.5.3 H_∞-based Fault Detection and Isolation Design

In this section, we consider Markovian jump systems that are subjected to both external input and output measurement disturbances and noise and that are governed

by

$$\begin{aligned}\dot{x}(t) &= A(\lambda(t))x(t) + B(\lambda(t))u(t) + \sum_{j=1}^{k} L_j(\lambda(t))m_j(t) + B_d(\lambda(t))d(t) \\ y(t) &= C(\lambda(t))x(t) + D_d(\lambda(t))d(t)\end{aligned} \tag{5.75}$$

where all the matrices are defined as in (5.71). The signal $d(t) \in \mathbb{R}^p$ represents an unknown disturbance input and output measurement noise. We denote the disturbance matrices $B_d(\lambda(t))$ and $D_d(\lambda(t))$ associated with $\lambda(t) = i$ by B_{di} and D_{di}, $i \in \Psi$. It is further assumed that the disturbance input $d(t)$ belongs to $\mathscr{L}_2[0, \infty]$, i.e.

$$||d(t)||_2 = \int_0^\infty d^\top(t)d(t)dt < \infty$$

Moreover, it is assumed that the mode transition matrix Π is <u>not</u> known precisely. In other words, it belongs to the following admissible uncertainty domain [202]:

$$\mathscr{D}_\Pi = \{\bar{\Pi} + \Delta\Pi : |\Delta\Pi_{ij}| \leq \epsilon_{ij}, \epsilon_{ij} \geq 0, \quad \forall i, j \in \Psi, \ i \neq j\} \tag{5.76}$$

where $\bar{\Pi} = [\bar{\pi}_{ij}]$ is a known constant matrix and denotes the estimated value of Π and $\Delta\Pi = [\Delta\pi_{ij}]$ denotes the uncertainty in the mode transition rate matrix.

Based on the above formulation of the Markovian jump system (5.75), an H_∞-based Extended Fundamental Problem in Residual Generation (HEFPRG) is introduced which is concerned with the design of a set of detection filters (5.72) that generate k residuals $r_j(t)$ such that a fault in the l-th component $m_l(t) \neq 0$ can only affect the residual $r_l(t)$ and no other residual $r_j(t)(j \neq l)$ and

$$||r_l||_{2,E}^2 = \mathbb{E}\Big\{ \int_0^\infty r_l^\top(t)r_l(t)dt|(x_0, i_0)\Big\} < \gamma^2||d||_2, \quad l \in \mathbf{k} \tag{5.77}$$

for all $d(t) \in \mathscr{L}_2$ and $\Pi \in \mathscr{D}_\Pi$, where $\gamma > 0$ is the prescribed level of disturbance attenuation.

Below we first present a preliminary result on disturbance attenuation of Markovian jump systems.

Lemma 5.10. *[190] Let γ be a given positive constant. If there exists a set of symmetric and positive-definite matrices $\mathfrak{R} = (R_1, ..., R_N) > 0$ such that the following set of coupled LMIs hold for every $i \in \Psi$:*

$$\begin{bmatrix} J_i & C_i^\top D_{di} + R_i B_{di} \\ * & D_{di}^\top D_{di} - \gamma^2 I \end{bmatrix} < 0 \tag{5.78}$$

where $J_i = A_i^\top R_i + R_i A_i + \sum_{j=1}^N \pi_{ij} R_j + C_i^\top C_i$, then system (5.75) with $u(t) = 0$ and $m_j(t) = 0, j \in \boldsymbol{k}$ is stochastically stable and for zero initial conditions satisfies the inequality

$$||y||_{2,E}^2 = \mathbb{E}\Big\{ \int_0^\infty y^\top(t) y(t) dt | (x_0, i_0) \Big\} < \gamma^2 ||d||_2, \quad l \in \boldsymbol{k} \tag{5.79}$$

A system that satisfies the above conditions is said to be stochastically stable with a γ-disturbance attenuation.

In the next lemma we consider the effects of uncertainties in the mode transition matrix Π for analyzing the stochastic stability properties of system (5.75).

Lemma 5.11. *Let γ be a given positive constant. If there exists a set of symmetric and positive-definite matrices $\mathfrak{R} = (R_1, ..., R_N) > 0$ and $\{\xi_{ij} > 0, i, j \in \Psi, i \neq j\}$ such that the following set of coupled LMIs holds for every $i \in \Psi$:*

$$\begin{bmatrix} Q_i & C_i^\top D_{di} + R_i B_{di} & M_i \\ * & D_{di}^\top D_{di} - \gamma^2 I & 0 \\ * & * & -\Xi_i \end{bmatrix} < 0 \tag{5.80}$$

where

$$Q_i = A_i^\top R_i + R_i A_i + \sum_{j=1}^N \bar{\pi}_{ij} R_j + C_i^\top C_i + \sum_{j=1, j\neq i}^N \frac{\xi_{ij}}{4} \epsilon_{ij}^2 I$$

$$M_i = \begin{bmatrix} R_i - R_1 & \cdots & R_i - R_{i-1} & R_i - R_{i+1} & \cdots & R_i - R_N \end{bmatrix}$$

$$\Xi_i = diag(\xi_{i1} I, ..., \xi_{i(i-1)} I, \xi_{i(i+1)} I, ..., \xi_{iN} I)$$

then the uncertain system (5.75) *with* $u(t) = 0$ *and* $m_j(t) = 0, j \in \boldsymbol{k}$ *is stochastically stable. Moreover, for zero initial conditions the system satisfies the inequality* (5.79) *for all* $\Pi \in \mathscr{D}_{\Pi}$.

Proof: According to Lemma 5.10, the uncertain system (5.75) with $u(t) = 0$ and $m_j(t) = 0, j \in \mathbf{k}$ is stochastically stable with γ-disturbance attenuation if

$$A_i^\top R_i + R_i A_i + \sum_{j=1}^{N}((\bar{\pi}_{ij} + \Delta\pi_{ij})R_j + C_i^\top C_i$$
$$- (C_i^\top D_{di} + R_i B_{di})(D_{di}^\top D_{di} - \gamma^2 I)^{-1}(C_i^\top D_{di} + R_i B_{di})^\top < 0$$

for all $i \in \Psi$. The above inequality can be rewritten as [202]

$$A_i^\top R_i + R_i A_i + \sum_{j=1}^{N} \bar{\pi}_{ij} R_j + C_i^\top C_i + \sum_{j=1, j\neq i}^{N} [\frac{1}{2}\Delta\pi_{ij}(R_j - R_i) + \frac{1}{2}\Delta\pi_{ij}(R_j - R_i)]$$
$$- (C_i^\top D_{di} + R_i B_{di})(D_{di}^\top D_{di} - \gamma^2 I)^{-1}(C_i^\top D_{di} + R_i B_{di})^\top < 0$$

The above inequality holds for all $|\Delta\pi_{ij}| \leq \epsilon_{ij}$ if there exist $\xi_{ij} > 0, i, j \in \Psi, i \neq j$ such that

$$A_i^\top R_i + R_i A_i + \sum_{j=1}^{N} \bar{\pi}_{ij} R_j + C_i^\top C_i + \sum_{j=1, j\neq i}^{N} [\frac{\xi_{ij}}{4}\epsilon_{ij}^2 I + \frac{1}{\xi_{ij}}(R_j - R_i)^2]$$
$$- (C_i^\top D_{di} + R_i B_{di})(D_{di}^\top D_{di} - \gamma^2 I)^{-1}(C_i^\top D_{di} + R_i B_{di})^\top < 0$$

It can be shown easily that the above is equivalent to the inequality (5.80) by using the Schur complement. ■

We are now in a position to derive our sufficient conditions for determining the solvability of the HEFPRG problem for an uncertain MJS system.

Theorem 5.12. *The HEFPRG problem has a solution for the Markovian jump system* (5.75) *with uncertain mode transition matrix if there exist* k *outer MS-detectable unobservability subspaces* $\mathcal{S}_j^* = \inf \mathfrak{S}(\mathfrak{A}, \mathfrak{C}, \sum_{v=1}^{N} \sum_{l=1, l\neq j}^{k} \mathcal{L}_{vl}), j \in \boldsymbol{k}$ *such that*

$$\mathcal{S}_j^* \bigcap \mathcal{L}_{ij} = 0, \quad i \in \Psi, j \in \boldsymbol{k} \tag{5.81}$$

as well as the matrices T_{ij}, positive-definite matrices R_{ij}, $i \in \Psi$, $j \in \boldsymbol{k}$, and $\{\xi_{il}^j > 0, i, l \in \Psi, i \neq l, j \in \boldsymbol{k}\}$ such that

$$\begin{bmatrix} Q_{ij} & -M_{ij}^\top H_{ij} D_{di} - R_{ij} P_j D_{ij} D_{di} - R_{ij} P_j B_{di} - T_{ij} H_{ij} D_{di} & \Theta_{ij} \\ * & D_{di}^\top H_{ij}^\top H_{ij} D_{di} - \gamma^2 I & 0 \\ * & * & -\Xi_{ij} \end{bmatrix} < 0 \quad (5.82)$$

for all $i \in \Psi, j \in \boldsymbol{k}$ with

$$Q_{ij} = A_{ij}^\top R_{ij} + M_{ij}^\top T_{ij}^\top + R_{ij} A_{ij} + T_{ij} M_{ij} + \sum_{l=1}^{N} \bar{\pi}_{il} R_{lj} + M_{ij}^\top M_{ij} + \sum_{l=1, l\neq i}^{N} \frac{\xi_{il}^j}{4} \epsilon_{il}^2 I$$

$$\Theta_{ij} = \begin{bmatrix} R_{ij} - R_{1j} & \cdots & R_{ij} - R_{(i-1)j} & R_{ij} - R_{(i+1)j} & \cdots & R_{ij} - R_{Nj} \end{bmatrix}$$

$$\Xi_{ij} = diag(\xi_{i1}^j I, ..., \xi_{i(i-1)}^j I, \xi_{i(i+1)}^j I, ..., \xi_{iN}^j I)$$

and where P_j is the canonical projection of $\mathcal{X}$ on $\mathcal{X}/\mathcal{S}_j^*$, the pairs (M_{ij}, A_{ij}), $i \in \Psi$, $j \in \boldsymbol{k}$ are the factor system of the pairs $(C_i, A_i), i \in \Psi$ on $\mathcal{X}/\mathcal{S}_j^*$, H_{ij} is the solution to $Ker\ H_{ij} C_i = \mathcal{S}_j^* + Ker\ C_i$ and $\mathcal{S}_j^* =<< \bigcap_{l=1}^N Ker\ H_{lj} C_l | A_i + D_{ij} C_i >>_{i \in \Psi}$, $j \in \boldsymbol{k}$.

Proof: Given P_j as the canonical projection of $\mathcal{X}$ on $\mathcal{X}/\mathcal{S}_j^*$, let $M_{ij}, i \in \Psi$ be a unique solution to $M_{ij} P_j = H_{ij} C_i$ and define $A_{ij} = (A_i + D_{ij} C_i : \mathcal{X}/\mathcal{S}_j^*), i \in \Psi$. Let $G_{ij} = R_{ij}^{-1} T_{ij}$, $i \in \Psi, j \in \mathbf{k}$ where T_{ij} and R_{ij} are solutions to the inequality (5.82). Define $F_{ij} = A_{ij} + G_{ij} M_{ij}$, $E_{ij} = P_j(D_{ij} + P_j^{-r} G_{ij} H_{ij})$ and $K_{ij} = P_j B_i$ for $i \in \Psi, j \in \mathbf{k}$. Furthermore, define $e_j(t) = w_j(t) - P_j x(t)$, so that by using (5.72) we have

$$\dot{e}_j(t) = F_{ij} w_j(t) - E_{ij} y(t) + K_{ij} u(t) - P_j(A_i x(k) + B_i u(k) + \sum_{l=1}^{k} L_{il} m_l(t) + B_{di} d(t))$$

$$=(A_{ij} + G_{ij} M_{ij}) e_j(t) - P_j L_{ij} m_j(t) - P_j D_{ij} D_{di} d(t) - P_j B_{di} d(t) - G_{ij} H_{ij} D_{di} d(t)$$

Also

$$\begin{aligned} r_j(t) &= M_{ij} w_j(t) - H_{ij} y(t) = M_{ij} w_j(t) - H_{ij} C_i x(t) - H_{ij} D_{di} d(t) \\ &= M_i e_j(t) - H_{ij} D_{di} d(t) \end{aligned}$$

Consequently, the error dynamics associated with the detection filters can be expressed as

$$\begin{aligned}\dot{e}_j(t) =&(A_{ij} + G_{ij}M_{ij})e_j(t) - P_jL_{ij}m_j(t)\\ &- P_jD_{ij}D_{di}d(t) - P_jB_{di}d(t) - G_{ij}H_{ij}D_{di}d(t)\\ r_j(t) =&M_{ij}e_j(t) - H_{ij}D_{di}d(t)\end{aligned} \tag{5.83}$$

Therefore, the residual r_j is only affected by the fault m_j and according to Lemma 5.11 and inequality (5.82), the disturbance attenuation inequality (5.77) holds for all the residuals $r_j(t),\ j \in \mathbf{k}$. ■

Remark 5.4. *It should be noted in the above theorem that since we only considered the sufficient solvability conditions for the HEFPRG problem, there was no need to consider an augmented system for the purpose of analysis and proof.*

Once the residual signals $r_j(t), j \in \mathbf{k}$ are constructed and generated, the final step in developing a reliable fault detection and isolation strategy deals with the residual evaluation process which involves determining the evaluation functions J_{r_j} and their associated thresholds J_{th_j}. In this paper, the evaluation functions and the thresholds are selected, respectively according to the following formal criteria, namely

$$J_{r_j}(t) = \int_{t-T_0}^{\mathrm{T}} r_j^{\mathrm{T}}(\tau)r_j(\tau)d\tau, \quad j \in \mathbf{k} \tag{5.84}$$

$$J_{th_j} = \sup_{d\in\mathfrak{L}_2, m_j=0} \mathbb{E}(J_{r_j}), \quad j \in \mathbf{k} \tag{5.85}$$

where T_0 is the length of the evaluation window. According to the above thresholds and evaluation functions, the occurrence of a fault can be detected and isolated by using the following decision logics

$$J_{r_j} > J_{th_j} \Longrightarrow m_j \neq 0, \quad j \in \mathbf{k} \tag{5.86}$$

5.5.4 A Case Study

In this section, our proposed H_∞-based FDI algorithm is applied to a VTOL (vertical take-off and landing) helicopter [190, 203]. The dynamics of the VTOL system can be written as

$$\begin{aligned} \dot{x}(t) &= A(\lambda(t))x(t) + B(\lambda(t))u(t) + L_1(\lambda(t))m_1(t) + L_2(\lambda(t))m_2(t) + B_d d(t) \\ y(t) &= Cx(t) + D_d d(t) \end{aligned} \tag{5.87}$$

where $\lambda(t)$ is a continuous time Markov process with three different modes that correspond to the airspeeds 135 (nominal value), 60 and 170 knots. The state variables corresponding to the system are taken as the horizontal velocity (x_1), the vertical velocity (x_2), the pitch rate (x_3), and the pitch angle (x_4). The input signals u_1 and u_2 are the collective pitch control and the longitudinal cyclic pitch control, respectively. The input signal $d(t)$ represents the external disturbances and uncertainties. The matrices associated with the VTOL system are given by

$$A(\lambda(t)) = \begin{bmatrix} -0.04 & 0.04 & 0.02 & -0.5 \\ 0.05 & -1.01 & 0.0 & -4.0 \\ 0.1 & a_{32}(\lambda(t)) & -0.71 & a_{34}(\lambda(t)) \\ 0.0 & 0.0 & 1.0 & 0.0 \end{bmatrix}, B(\lambda(t)) = \begin{bmatrix} 0.44 & 0.18 \\ b_{21}(\lambda(t)) & -7.6 \\ -5.52 & 4.49 \\ 0 & 0 \end{bmatrix}$$

$$C = \begin{bmatrix} 1 & 0 & 0 & 0 \\ 0 & 1 & 0 & 0 \\ 0 & 0 & 1 & 0 \end{bmatrix}, B_d = \begin{bmatrix} 0.1 & 0.0 \\ 0.0 & 0.1 \\ 0.1 & 0.0 \\ 0.0 & 0.1 \end{bmatrix}, D_d = \begin{bmatrix} 0.0 & 0.1 \\ 0.1 & 0.1 \\ 0.0 & 0.0 \end{bmatrix}$$

where the values of the parameters $a_{32}(\lambda(t))$, $a_{34}(\lambda(t))$, and $b_{21}(\lambda(t))$ are given in Table 5.1. The fault signatures $L_1(\lambda(t))$ and $L_2(\lambda(t))$ represent the actuator faults, and hence are selected as the first and the second columns of $B(\lambda(t))$. Different fault modes can be considered for actuators in general [204], namely, i) lock-in-place

Table 5.1: The specific values for the parameters of the VTOL helicopter

Airspeed (knots)	$a_{32}(\lambda(t))$	$a_{34}(\lambda(t))$	$b_{21}(\lambda(t))$
135	0.37	1.42	3.55
60	0.07	0.12	1.0
170	0.51	2.52	5.11

(LIP), ii) loss of effectiveness, iii) float, and iv) hard over. For this application and due to space limitations we consider LIP, loss of effectiveness , and float faults. The mode transition matrix is taken as

$$\Pi = \begin{bmatrix} -2.09 & 1.07 & 1.02 \\ 0.07 & -0.07 & 0.0 \\ 0.02 & 0.0 & -0.02 \end{bmatrix}$$

with an uncertainty level of $\epsilon_{ij} = 0.1, i, j \in \Psi i \neq j$ as specified in equation (5.76).

The FDI problem that is considered here for the VTOL is to design two residual signals $r_1(t)$ and $r_2(t)$ such that $r_1(t)$ is only affected by the first actuator fault $(m_1(t))$ and $r_2(t)$ is only affected by the second actuator fault $(m_2(t))$. Moreover, the effect of the disturbance input $d(t)$ on these residuals is attenuated with a factor of γ. According to the results of Theorem 5.12, we first need to construct the unobservability subspaces $\mathcal{S}_1^* = \inf(\mathfrak{A}, \mathfrak{C}, \mathcal{L}_2)$ and $\mathcal{S}_2^* = \inf(\mathfrak{A}, \mathfrak{C}, \sum_{i=1}^{3} \mathcal{L}_{i1})$. These unobservability subspaces are obtained by using Algorithm 5.3 as follows:

$$\mathcal{S}_1^* = \begin{bmatrix} 0.0204 \\ -0.8608 \\ 0.5085 \\ 0 \end{bmatrix}, \mathcal{S}_2^* = \begin{bmatrix} -0.0795 & 0 \\ 0 & 1 \\ 0.9968 & 0 \\ 0 & 0 \end{bmatrix}$$

It can be easily verified that the necessary conditions $\mathcal{S}_1^* \cap \mathcal{L}_{i1} = 0, i = 1, 2, 3$ and $\mathcal{S}_2^* \cap \mathcal{L}_2 = 0$ are both satisfied. Next we need to verify the feasibility of the inequality (5.82) corresponding to a given disturbance attenuation level γ. Using the LMI toolbox, inequality (5.82) is solved for $\gamma = 0.1$. Subsequently, all the maps

and matrices that are defined in Theorem 5.12 are obtained. It should be noted that from equation (5.72), $r_1 \in \mathbb{R}^2$ and $r_2 \in \mathbb{R}$.

The disturbance inputs $d_1(t)$ and $d_2(t)$ are assumed to be independent and band-limited white-noises with the power of 0.1 and 0.2, respectively. The length of the evaluation window is selected as $T_0 = 2$ seconds. The calculated thresholds are found to be $J_{th_1} = J_{th_2} = 5e - 3$. Figure 5.6 shows both the residuals and the evaluation functions corresponding to a float fault that is injected in the first actuator (u_1) at $t = 25$ seconds (float fault implies that the actuator is frozen at zero output). This fault can be modeled as $m_1(t) = -u_1(t)$, where $m_1(t)$ is the fault mode of the first actuator. As shown in Figure 5.6, the fault is detected and isolated at $t = 34$ seconds and the evaluation function of r_2 (i.e. J_{r_2}) remains below its corresponding threshold. Figure 5.7 shows the residuals and the evaluation functions corresponding to an intermittent fault that is injected in the second actuator where the actuator is locked (LIP fault) at a value of 0.1 between $t = 20$ and $t = 30$ seconds. This fault can be modeled as $m_2(t) = -u_2(t) + 0.1$, where $m_2(t)$ is the fault mode of the second actuator. As shown in Figure 5.7, this fault is detected and isolated at $t = 22.5$ seconds and the evaluation function of r_1 (i.e. J_{r_1}) remains below its associated threshold. Figure 5.8 shows the residuals and the evaluation functions corresponding to simultaneous faults that are injected in both actuators where a 50% loss of effectiveness (gain) fault is occurred in the first actuator at $t = 25$ seconds and the second actuator is locked at the output value of 0.1 between $t = 20$ and $t = 30$ seconds. According to Figure 5.8, both faults are properly detected and isolated at time $t = 25$ seconds and $t = 26$ seconds, respectively.

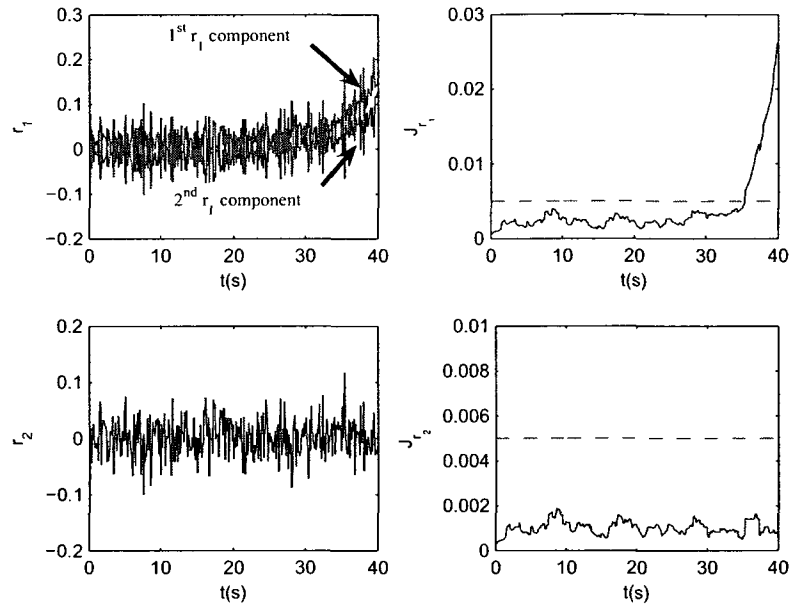

Figure 5.6: Residual signals and their evaluation functions corresponding to a float fault in the first actuator $m_1 = -u_1$ (the dashed line in J_{r_i} denotes the threshold).

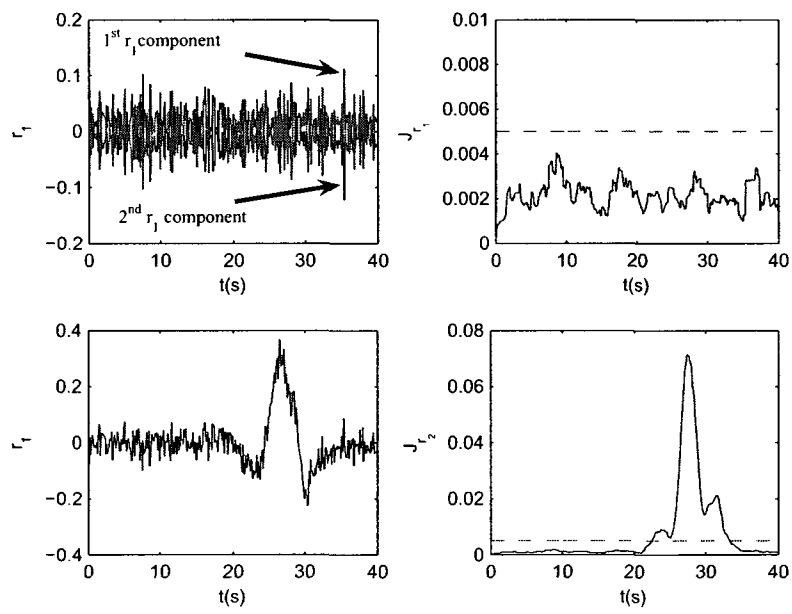

Figure 5.7: Residual signals and their evaluation functions corresponding to a lock-in-place (LIP) fault in the second actuator $m_2 = -u_2 + 0.1$ (the dashed line in J_{r_i} denotes the threshold).

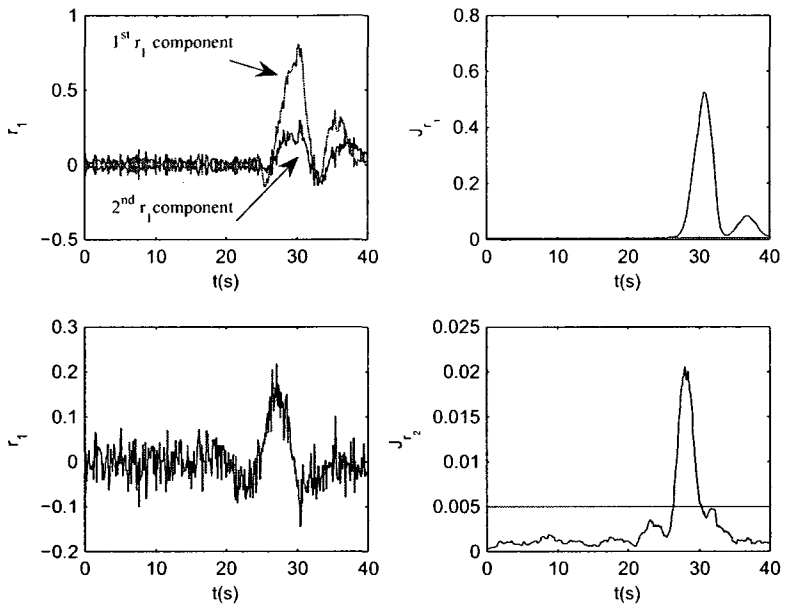

Figure 5.8: Residual signals and their evaluation functions corresponding to multiple faults in actuators, namely a 50% loss of effectiveness fault in the first actuator and a lock in place fault in the second actuator (the dashed line in J_{r_i} denotes the threshold).

5.6 Conclusions

The problem of fault detection and isolation in a network of unmanned vehicles in the presence of imperfect communication links is investigated in this chapter in the framework of Markovian jump systems. A geometric approach to the problem of fault detection and isolation of both continuous-time and discrete-time linear Markovian jump systems is developed. Starting with a new geometric characterization of the unobservable subspace of a Markovian jump system, the concept of unobservability subspaces is formalized and an algorithm for constructing these subspaces is presented. By invoking the notion of unobservability subspace, the necessary and sufficient conditions for solving the fundamental problem of residual generation for Markovian jump systems is formally investigated. For uncertain Markovian jump systems, an H_∞-based fault detection and isolation strategy is proposed and developed where a set of residual signals are constructed such that each residual is

only affected by one fault and is decoupled from the others while the H_∞ norm of the transfer function between the unknown input (external disturbances and output measurement noise) and the residual signals is guaranteed to be less than a prescribed desired value. Simulation results for application of our proposed novel methodologies to a VTOL (vertical take-off and landing) helicopter and network of unmanned vehicles are also presented to demonstrate and illustrate their effectiveness and capabilities.

Chapter 6

Robust Fault Detection and Isolation of Time-Delay Systems

This chapter investigates the development of fault detection and isolation filters for retarded, neutral, distributed and stochastic time-delay systems. The notion of a finite unobservability subspace is introduced for time-delay systems and it is shown that this subspace can be considered as an unobservability subspace for Makovian jump systems where all modes of MJS system have identical measurement matrix. Hence, the same algorithm that we developed for the Markovian jump systems in previous chapter can be invoked here for constructing finite unobservability subspaces for time-delay systems. A bank of residual generators is then designed so that each residual is affected by one fault and is decoupled from the others while the H_∞ norm of the transfer function between the disturbances and the uncertainties in delays and the residual signals are guaranteed to remain less than a prescribed value. The work presented in this chapter has partly appeared in [205, 206, 208].

This chapter is organized as follows. After a summary of the relevant literature, we first begin in Section 6.2 by considering retarded and neutral time-delay systems. The notion of finite unobservability is introduced in Section 6.2.1 for these time-delay

systems. By utilizing the developed geometric framework, H_∞-based FDI algorithms are developed for retarded and neutral time-delay systems in Sections 6.2.2 and 6.2.3, respectively. We then proceed by considering systems with distributed delay in Section 6.3 and the notion of finite unobservability is also introduced for these systems in Section 6.3.1. In Section 6.3.2, an H_∞-based FDI strategy of distributed delay systems is presented. The FDI problem for Markovian jump system with mode dependent delay is investigated in Section 6.4. Fault detection and isolation decision criteria is presented in Section 6.5 and numerical examples for retarded, neutral, distributed and stochastic time-delay systems are provided in Section 6.6.

Contributions

The main contributions of this chapter are now summarized as follows:

- The geometric concept of finite unobservability subspaces is introduced for retarded, neutral, distributed and stochastic time-delay systems and algorithms for obtaining these subspaces are presented.
- H_∞-based fault detection and isolation problem for the above systems are formulated and the sufficient conditions for solvability of this problem is derived based on the LMI method.

6.1 Introduction

Time-delay is an inherent characteristic of many physical systems, such as rolling mills, chemical processes, water resources, biological, economical, communication, and traffic control systems, to name a few. Only a few results on FDI of time-delay systems have been developed in recent years in the literature. In [123], an unknown input observer (UIO) is designed for fault detection of retarded systems with <u>known</u> delays, and [122] proposed a robust UIO approach for uncertain retarded time-delay systems with bounded uncertainty. In [122, 123], some restrictive assumptions on

the system structures have also been assumed. Parity space approach is developed in [209] for fault detection of retarded time-delay systems. In [124], [125], [126], [127, 128], [129] a robust fault detection problem for linear retarded time-delay systems with known delays is investigated by solving an H_∞ optimization problem. In this approach one attempts to keep the sensitivity of the residual signal to unknown inputs (disturbances) less than a specific bound while to increase the sensitivity of the residual signal to the fault over its frequency range. In [210], [211], [212], an adaptive observer approach is developed for estimating the fault signal in retarded time-delay systems. In [213], a robust fault detection and isolation observer for uncertain singular retarded time-delay systems is developed. In [194], a robust fault identification filter for a class of discrete-time Markovian jump systems with mode dependent time-delays and norm bounded uncertainty is developed based on an H_∞ optimization technique. In this approach, the generated residual signal is an estimate of the fault signal.

The fault diagnosis problem for neutral time-delay systems has only been investigated in [214] where the H_∞ filter approach is used for robust fault detection of neutral time-delay systems. However, the problem of fault isolation for general retarded and neutral time-delay systems with unknown delays has *not* been completely addressed in the above references. Moreover, it is worth pointing out that all the above FDI approaches were for pointwise, single or multiple time-delay systems and, the fault detection and isolation problem for distributed time-delay systems has not yet been investigated in the literature.

In this chapter, a set of residuals that are based on the dedicated residual scheme [3, 6] is generated for retarded, neutral, distributed and stochastic time-delay systems. The notion of a finite unobservability subspace is introduced for time-delay systems and an algorithm for constructing it is presented. By utilizing the developed geometric framework, a set of residuals is generated such that each

residual is affected by one fault and is partially decoupled from others. Furthermore, the effects of the disturbances and uncertainties due to the unknown delays on the residuals are attenuated by using the H_∞ optimization technique and by utilizing the LMI approach.

6.2 Retarded and Neutral Time-Delay Systems

6.2.1 Finite Unobservability Subspaces for Time-delay Systems

In this section, the notion of a finite unobservability subspace is introduced for both retarded and neutral time-delay systems and an algorithm for constructing such subspace is provided. As shown subsequently in Sections 6.2.2 and 6.2.3, the finite unobservability subspace plays a central role in the *geometrical approach* to fault detection and isolation of both retarded and neutral time-delay systems. Consider a linear time-delay system

$$\begin{aligned} \dot{x}(t) &= A_0 x(t) + \sum_{i=1}^{N} A_i x(t-\tau_{xi}(t)) + A_{N+1}\dot{x}(t-\tau_d(t)) \\ y(t) &= Cx(t), \quad x(\theta) = \phi(\theta), \quad \theta \in [-\tau, 0] \end{aligned} \tag{6.1}$$

where $x \in \mathcal{X}$ is the state of the system with dimension n, $y \in \mathcal{Y}$ is output signal with dimensions q, and $\tau = \max_i\{\tau_{xi}(0), \tau_d(0)\}$.

Lemma 6.1. *Let $\mathcal{V} \subset \mathcal{X}$ be A_i-invariant for all $i \in (\boldsymbol{N}+1)_0$, i.e. $A_i\mathcal{V} \subset \mathcal{V}$, $i \in (\boldsymbol{N}+1)_0$. If $\phi(\theta) \in \mathcal{V}$, $\forall\theta \in [-\tau, 0]$, then $x(t) \in \mathcal{V}, \forall t \geq 0$.*

Proof: Based on the variation-of-constant formula, we have

$$x(t) = e^{A_0 t}\phi(0) + \int_0^t e^{A_0(t-s)} \sum_{i=1}^{N} A_i x(s-\tau_{xi}(s))ds + \int_0^t e^{A_0(t-s)} A_{N+1}\dot{x}(s-\tau_d(s))ds \tag{6.2}$$

for $t \geq 0$ and $x(t) = \phi(t)$ for $t \in [-\tau, 0]$. Since $\phi(\theta) \in \mathcal{V}$, $\forall\theta \in [-\tau, 0]$, then $\dot{\phi}(\theta) \in \mathcal{V}$, $\forall\theta \in [-\tau, 0]$. Hence, $x(t) \in \mathcal{V}, \forall t \in [0, \tau_0]$ where $\tau_0 = \min\{\tau_{xi}(0), \tau_d(0)\}$ ($\mathcal{V}$ is A_i-invariant for all $i \in (\mathbf{N}+1)_0$). Since $x(t) \in \mathcal{V}, \forall t \in [0, \tau_0]$, equation (6.2) can be used again to show that $x(t) \in \mathcal{V}$ on $[\tau_0, \tau_0+\tau_1]$, where $\tau_1 = \min\{\tau_{xi}(\tau_0), \tau_d(\tau_0)\}$. Similarly, it can be shown by successive application of this process that $x(t) \in \mathcal{V}, \forall t \geq 0$. ■

Next consider the following time-delay system

$$\begin{aligned}\dot{x}(t) &= (A_0 + D_0C)x(t) + \sum_{i=1}^{N}(A_i + D_iC)x(t - \tau_{xi}(t)) \\ &\quad + (A_{N+1} + D_{N+1}C)\dot{x}(t - \tau_d(t)) \\ \tilde{y}(t) &= HCx(t), \qquad x(\theta) = \phi(\theta) \;\; \theta \in [-\tau, 0]\end{aligned}$$

for given maps $D_i : \mathcal{Y} \to \mathcal{X}$ and $H : \mathcal{Y} \to \mathcal{Y}$. Let us define the subspace $\mathcal{S} \subset \mathcal{X}$ as the largest $A_i + D_iC$-invariant that is contained in Ker HC. According to Lemma 6.1, for any initial condition $\phi(\theta) \in \mathcal{S}$, $\forall\theta \in [-\tau, 0]$, we have $\tilde{y}(t) = 0$, $\forall t > 0$. Let us denote the largest A_i-invariant $i \in (\mathbf{N}+1)_0$ subspace that is contained in $\mathcal{K} \subset \mathcal{X}$ by $<< \mathcal{K}|A_i >>_{i\in(\mathbf{N}+1)_0}$. Based on the above discussion and the assumption that $\mathcal{S} \subset \mathcal{X}$ ($\mathcal{S}$ is a finite subspace), we define the notion of a finite unobservability subspace for the time-delay system (6.1) as follows.

Definition 6.1. *A subspace $\mathcal{S}$ is called a finite unobservability subspace for system* (6.1) *if for some output injection maps $D_i : \mathcal{Y} \to \mathcal{X}$ and measurement mixing map $H : \mathcal{Y} \to \mathcal{Y}$, we have*

$$\mathcal{S} =<< Ker\ HC|A_i + D_iC >>_{i\in(N+1)_0} \tag{6.3}$$

It should be noted that the above definition of the finite unobservability subspace coincides with the unobservability subspace of the Markovian jump systems with identical matrices C_i's, i.e. $C_i = C$, $i \in \Psi$. Hence, based on Algorithm 5.3, the following algorithm can also be used for obtaining the smallest finite unobservability subspace $\mathcal{S}^*$.

Algorithm 6.1. *Let $\mathcal{W}^* = \inf \mathfrak{W}(\mathfrak{A}, \mathcal{L})$ (obtained from Algorithm 5.2) and define the sequence $\mathcal{Z}^\mu$ according to*

$$\mathcal{Z}^0 = \mathcal{X}; \quad \mathcal{Z}^\mu = \bigcap_{i=0}^{N+1} (\mathcal{W}^* + (A_i^{-1}\mathcal{Z}^{\mu-1} \cap Ker\, C)) \tag{6.4}$$

Then $\mathcal{S}^* = \mathcal{Z}^k$, whenever $\mathcal{Z}^{k+1} = \mathcal{Z}^k$.

This implies that the developed algorithm for Markovian jump system is more general and can be used also for obtaining the smallest finite unobservability subspace.

Remark 6.1. *The concept of unobservability subspaces for bilinear and LPV systems have been introduced in [62] and [215], respectively. It is shown in [215] that an unobservability subspace for the following LPV system*

$$\begin{aligned} \dot{x}(t) &= (A_0 + \rho_1(t)A_1 + \cdots + \rho_{N+1}(t)A_{N+1})x(t) \\ y(t) &= Cx(t) \end{aligned}$$

is the largest $A_i + D_iC$-invariant ($i \in (\boldsymbol{N}+1)_0$) that is contained in $Ker\, HC$. A similar fact is also shown in [62] for bilinear systems. The following algorithm [62, 215] can be invoked for obtaining the minimal element $\mathcal{S}^*$,

Algorithm 6.2. *The subspace $\mathcal{S}^*$ coincides with the last term of the following sequence*

$$\mathcal{Z}^0 = \mathcal{X}; \quad \mathcal{Z}^\mu = \mathcal{W}^* + \Big(\bigcap_{i=0}^{N+1} A_i^{-1}\mathcal{Z}^{\mu-1}\Big) \cap Ker\, C \tag{6.5}$$

where $\mathcal{W}^*$ is computed from Algorithm 5.2. In [62, 215], the authors do not provide the detail derivation of the above algorithm. Hence, we present our own derivation of Algorithm 6.2 in Appendix A.

We are now in a position to introduce an H_∞-based fault detection and isolation problem for retarded and neutral time-delay systems.

6.2.2 H_∞-based FDI for Retarded Time-Delay Systems

Consider the following linear retarded time-delay system (with $A_{N+1} \equiv 0$ in (6.1))

$$\begin{aligned}\dot{x}(t) =& A_0 x(t) + \sum_{i=1}^{N} A_i x(t - \tau_{xi}(t)) + B_0 u(t) + \sum_{j=1}^{L} B_j u(t - \tau_{uj}(t)) \\ &+ \sum_{l=1}^{k} L_l m_l(t) + B_d d(t) \\ y(t) =& Cx(t) + D_d d(t)\end{aligned} \tag{6.6}$$

with the continuous initial condition $x(\theta) = \phi(\theta), \theta \in [-\tau, 0]$, where $x \in \mathcal{X}$ is the state of the system with dimension n, $u \in \mathcal{U}, y \in \mathcal{Y}$ are input and output signals with dimensions m and q, respectively, $d(t)$ represents an unknown input vector that could include modeling errors and uncertain disturbances, $m_i \in \mathcal{M}_i, i \in \mathbf{k}$ are the fault modes with dimension k_i, and L_i's are the fault signatures, where $\tau = \max_i \tau_{xi}(0)$.

The fault modes together with the fault signatures may be used to model the effects of actuator faults, sensor faults and system faults on the dynamics of the system. For modeling a fault in the i-th actuator, $L_i = [b_{0i}, b_{1i}, ..., b_{Li}]$ and the fault mode m_i is chosen to model the type of a fault where $b_{ji}, j = 0, ..., L$ denote the i-th column of matrices $B_j, j = 0, ..., L$. For example a complete failure of an actuator can be represented and modeled by $m_i(t) = [-u_i(t), -u_i(t-\tau_{u1}(t)), ..., -u_i(t-\tau_{uL}(t))]^\top$. A system fault can be represented by a potential variation in the parameters of the A_i's matrices as shown below:

$$\begin{aligned}\dot{x}(t) =& (A_0 + \Delta A_0)x(t) + \sum_{i=1}^{N}(A_i + \Delta A_i)x(t - \tau_{xi}(t)) + B_0 u(t) + \sum_{j=1}^{L} B_j u(t - \tau_{uj}(t)) \\ y(t) =& Cx(t)\end{aligned}$$

As an example, a change in the i-th row and j-th column of matrix A_1 can be modeled as $\Delta A_1 x(t - \tau_{x1}(t)) = I_i \Delta a_{1_{ij}} x_j(t - \tau_{x1}(t))$ where x_j is the j-th element of the vector x and I_i is an n-dimensional vector with all zero elements except one in

the i-th element. Define the signal $m_i(t) \triangleq \Delta a_{1_{ij}} x_j(t - \tau_{x1}(t))$ as an external input and fault signature $L_i = I_i$, then this fault can be modeled as in equation (6.6).

It should be noted that sensor faults can initially be modeled as additive inputs in the measurement equation $y = Cx + \sum_{j=1}^{q} E_j n_j$ where E_j is an $q \times 1$ unit vector with a one at the j-th position and $n_j \in \mathbb{R}$ is a sensor fault mode, which corresponds to a fault in the j-th sensor. For example, a complete failure of the j-th sensor can be represented and modeled by $n_j = -c_j x$ where c_j is the j-th row of the matrix C. The sensor fault signature can also be modeled as an input to the system [3,18,130]. Following [18], let f_j be the solution to $E_j = Cf_j$. The new states can be defined according to $\bar{x}(t) = x(t) + \sum_{j=1}^{q} f_j n_j(t)$, where the state space representation for the new states can be written as

$$\dot{\bar{x}}(t) = A_0\bar{x}(t) + \sum_{i=1}^{N} A_i\bar{x}(t - \tau_{xi}(t)) + B_0 u(t) + \sum_{j=1}^{L} B_j u(t - \tau_{uj}(t)) + \sum_{j=1}^{q} L_j m_j(t)$$

$$y(t) = C\bar{x}(t)$$

where $L_j = \begin{bmatrix} f_j & A_0 f_j & A_1 f_j & \cdots & A_N f_j \end{bmatrix}$ and $m_j(t) = [\dot{n}_j(t), -n_j(t), -n_j(t - \tau_{x1}(t)), \cdots, -n_j(t - \tau_{xN}(t))]^\top$.

We now state the main assumptions needed for the development of our proposed FDI scheme for retarded time-delay system (6.6).

Assumption 6.1. *The disturbance signal $d(t)$ is $\mathfrak{L}_2$-norm bounded.*

Although accurate values for the delays $\tau_{xi}(t), i \in \mathbf{N}$ and $\tau_{ui}(t), i \in \mathbf{L}$ are difficult to obtain and are not necessary in our work, the following reasonable assumptions can be made.

Assumption 6.2. *The upper bounds on the delay functions $\tau_{xi}(t)$ and $\tau_{ui}(t)$ are assumed to be known, that is $\tau_{xi}(t) \leq \tau_i^x < \infty$, $\dot{\tau}_{xi}(t) \leq \bar{\tau}_i \leq 1$, and $\tau_{ui}(t) \leq \tau_i^u < \infty$.*

Assumption 6.3. *The error signals $\tilde{x}^\top(t) = [x^\top(t - \tau_{x1}(t)) - x^\top(t - \tau_1^x), ..., x^\top(t - \tau_{xN}(t)) - x^\top(t - \tau_N^x)]$ and $\tilde{u}^\top(t) = [u^\top(t - \tau_{u1}(t)) - u^\top(t - \tau_1^u), ..., u^\top(t - \tau_{uN}(t)) - u^\top(t - \tau_L^u)]$ are $\mathfrak{L}_2$ norm bounded.*

Remark 6.2. *It should be noted that for any system where the states are required to track a constant setpoint or a slowly time-varying trajectory $x_d(t)$ by a proper controller design, Assumption 6.3 will hold without loss of any generality. Moreover, when an H_∞-based controller is designed for the healthy (fault free) closed-loop system guaranteeing that the state x is $\mathfrak{L}_2$ norm bounded, then the error signals $\tilde{x}$ and $\tilde{u}$ also belong to the $\mathfrak{L}_2$ space.*

The class of finite unobservability subspaces containing a given subspace $\mathcal{L}$ for the above retarded time delay system is denoted by $\underline{\mathcal{S}}_R(\mathcal{L})$, i.e.

$$\underline{\mathcal{S}}_R(\mathcal{L}) = \{\mathcal{S} \in \mathcal{X} | \mathcal{S} =<< \mathrm{Ker} HC | A_i + D_i C >>_{i \in \mathbf{N}} \quad \text{and} \quad \mathcal{L} \in \mathcal{S}\} \tag{6.7}$$

The smallest element of $\underline{\mathcal{S}}_R(\mathcal{L})$ is denoted by $\mathcal{S}_R^*$ and can be obtained based on Algorithm 6.2.

Before presenting the main result of this section, the next lemma provides a sufficient condition for asymptotic stability of system (6.6). This result guarantees simultaneously that the H_∞ norm of the transfer function between the disturbance d and the output signal y is less than a prescribed positive value γ when no fault in the system is present, i.e. $m_l(t) = 0,\ l \in \mathbf{k}$.

Lemma 6.2 ([216]). *Given $\gamma > 0$, if there exist positive-definite matrices R and Q such that the following Riccati inequality is satisfied*

$$A_0^\top R + RA_0 + C^\top C + Q + (RB_d + C^\top D_d)(\gamma^2 I - D_d^\top D_d)^{-1}(RB_d + C^\top D_d)^\top$$
$$+ N \sum_{i=1}^{N} c_i R A_i Q^{-1} A_i^\top R < 0$$

with $\gamma^2 I - D_d^\top D_d > 0$ and $c_i = \frac{1}{1-\bar{\tau}_i}$, then system (6.6) is asymptotically stable and its $\mathfrak{L}_2$ gain is not greater than γ, i.e.

$$\int_0^\infty y^\top(t) y(t) dt \leq \gamma^2 \int_0^\infty d^\top(t) d(t) dt \tag{6.8}$$

We are now in a position to introduce our main result in this section. The H_∞-based Extended Fundamental Problem in Residual Generation (HEFPRG) for the retarded time-delay system (6.6) is defined as the design of a set of filters that generate k residuals such that each residual $r_i(t)$ is affected by a fault in the i-th component L_i and is partially decoupled from all other faults $L_j, j \neq i$ and

$$\int_0^\infty r_i^\top(t) r_i(t) dt \leq \gamma^2 \Big(\int_0^\infty \bar{d}^\top(t)\bar{d}(t)dt + \int_0^\infty \tilde{x}^\top(t)\tilde{x}(t)dt + \int_0^\infty \tilde{u}^\top(t)\tilde{u}(t)dt \Big) \tag{6.9}$$

where $\bar{d}^\top(t) = [d^\top(t), d^\top(t-\tau_1^x), ..., d^\top(t-\tau_N^x)]$. By utilizing the residual set $\{r_i\}, i \in \mathbf{k}$, one can detect and isolate multiple faults in all the channels. The residual signals $r_i(t)$ are generated according to the following filters structure:

$$\begin{aligned} \dot{w}_i(t) =& F_{i0} w_i(t) + \sum_{l=1}^{N} F_{il} w_i(t-\tau_l^x) - E_{i0} y(t) + K_{i0} u(t) \\ & - \sum_{l=1}^{N} E_{il} y(t-\tau_l^x) + \sum_{j=1}^{L} K_{ij} u(t-\tau_j^u) \\ r_i(t) =& M_i w_i(t) - H_i y(t), \qquad i \in \mathbf{k} \end{aligned} \tag{6.10}$$

where the matrices are defined and selected according to the conditions in the next theorem which summarizes our proposed fault detection and isolation (FDI) strategy.

Theorem 6.1. *The HEFPRG problem specified by expressions* (6.9) *and* (6.10) *has a solution for the linear retarded time-delay system* (6.6) *if the following finite unobservability subspaces*

$$\mathcal{S}_i^* = \inf \underline{\mathcal{S}}_R(\sum_{j \neq i} \mathcal{L}_j), \quad i \in \boldsymbol{k} \tag{6.11}$$

exist such that $\mathcal{L}_i \cap \mathcal{S}_i^* = 0, i \in \boldsymbol{k}$ *and gain matrices* $T_{ij}, j \in \boldsymbol{N}_0, i \in \boldsymbol{k}$ *and positive-definite matrices* R_i *and* $Q_i, i \in \boldsymbol{k}$ *exist such that*

$$\begin{bmatrix} \Psi_i & \Gamma_{i1} & \cdots & \Gamma_{iN} & \Theta_i & R_iK_i & R_i\bar{A} \\ * & -\frac{1}{N}Q_i & \cdots & 0 & 0 & 0 & 0 \\ \vdots & \vdots & \ddots & \vdots & \vdots & \vdots & \vdots \\ * & * & \cdots & -\frac{1}{N}Q_i & 0 & 0 & 0 \\ * & * & \cdots & * & \Upsilon_i & 0 & 0 \\ * & * & \cdots & * & * & -\gamma^2 I & 0 \\ * & * & \cdots & * & * & * & -\gamma^2 I \end{bmatrix} < 0 \tag{6.12}$$

where $\Psi_i = A_{0_{\mathcal{S}_i^*}}^\top R_i + R_i A_{0_{\mathcal{S}_i^*}} + M_i^\top T_{i0}^\top + T_{i0}M_i + M_i^\top M_i + Q_i$, $\Theta_i = R_i\bar{B}_{di} - T_i + M_i^\top \bar{D}_{di}$, $\Gamma_{ij} = R_i A_{j_{\mathcal{S}_i^*}} + T_{ij}M_i$, $\Upsilon_i = -\gamma^2 I + \bar{D}_{di}^\top \bar{D}_{di}$, $T_i = [T_{i0}H_iD_d, ..., T_{iN}H_iD_d]$, P_i *is the canonical projection of* $\mathcal{X}$ *on* $\mathcal{X}/\mathcal{S}_i^*$, $\bar{B}_{id} = -[P_iB_d + P_iD_{i0}D_d, ..., P_iD_{iN}D_d]$, $\bar{D}_{di} = [-H_iD_d, 0, ..., 0]$, $K_i = [K_{i1}, ..., K_{iL}]$, $\bar{A} = [P_iA_1, ..., P_iA_N]$ *and* $K_{ij} = P_iB_j, j \in \boldsymbol{L}$, $D_{ij}, j \in \boldsymbol{N}_0$ *and* H_i *are the output injection and the measurement mixing maps, respectively, such that* $\mathcal{S}_i^* =<< Ker\ H_iC|A_j + D_{ij}C >>_{j\in \boldsymbol{N}_0}$ *and the pairs* $(M_i, A_{l_{\mathcal{S}_i^*}})$, $l \in \boldsymbol{N}_0$ *are the factor system of the pairs* $(C, A_l), l \in \boldsymbol{N}_0$ *on* $\mathcal{X}/\mathcal{S}_i^*$, *respectively.*

Proof: Given the unobservability subspaces $\mathcal{S}_i^*, i \in \mathbf{k}$, there exist output map injections $D_{i0}, D_{i1}, ..., D_{iN}$ and measurement mixing map H_i such that $\mathcal{S}_i^* =<<$ Ker $H_iC|A_j + D_{ij}C >>_{j\in\mathbf{N}_0}$, where H_i is the solution to Ker $H_iC = \mathcal{S}_i^* +$ Ker C. Let M_i be a unique solution to $M_iP_i = H_iC$ and $A_{j_{\mathcal{S}_i^*}} = (A_j + D_{ij}C : \mathcal{X}/\mathcal{S}_i^*), j \in \mathbf{N}_0$ where

$$P_i(A_j + D_{ij}C) = A_{j_{\mathcal{S}_i^*}}P_i, \quad j \in \mathbf{N}_0 \tag{6.13}$$

Let $G_{ij} = R_i^{-1}T_{ij}$ where R_i and $T_{ij}, j \in \mathbf{N}_0$ are the solution to the inequality (6.12), $F_{ij} = A_{j_{\mathcal{S}_i^*}} + G_{ij}M_i$, $E_{ij} = P_i(D_{ij} + P_i^{-r}G_{ij}H_i), j \in \mathbf{N}_0$ and $K_{i0} = P_iB_0$. Define

$e_i(t) = w_i(t) - P_i x(t)$, then using (6.10), we have

$$\begin{aligned}
\dot{e}_i(t) &= F_{i0} w_i(t) + \sum_{l=1}^{N} F_{il} w_i(t-\tau_l^x) - P_i(A_0 + D_{i0}C)x(t) - G_{i0} M_i P_i x(t) \\
&- \sum_{l=1}^{N} P_i(A_l + D_{il}C)x(t-\tau_l^x) - P_i B_d d(t) - P_i D_{i0} D_d d(t) - G_{i0} H_i D_d d(t) \\
&- \sum_{l=1}^{N} G_{il} M_i P_i x(t-\tau_l^x) - P_i L_i m_i(t) - \sum_{l=1}^{N} (P_i D_{il} + G_{il} H_i) D_d d(t-\tau_l^x) \\
&+ \sum_{j=1}^{L} K_{ij}(u(t-\tau_j^u) - u(t-\tau_{uj}(t))) + \sum_{l=1}^{N} P_i A_l (x(t-\tau_l^x) - x(t-\tau_{xl}(t))) \\
&= F_{i0} e_i(t) + \sum_{l=1}^{N} F_{il} e_i(t-\tau_l^x) - P_i L_i m_i(t) + (\bar{B}_{id} - G_i)\bar{d}(t) + K_i \tilde{u}(t) + \bar{A}\tilde{x}(t)
\end{aligned}$$

where $G_i = [G_{i0} H_i D_d, ..., G_{iN} H_i D_d]$. Note that $P_i L_j = 0, j \neq i$, since $\mathcal{L}_j \in \mathcal{S}_i^*, j \neq i$. Also

$$r_i(t) = M_i w_i(t) - H_i C x(t) - H_i D_d d(t) = M_i e_i(t) - H_i D_d d(t), \quad i \in \mathbf{k}$$

Consequently, the error dynamics can be written as

$$\begin{aligned}
\dot{e}_i(t) =& F_{i0} e_i(t) + \sum_{l=1}^{N} F_{il} e_i(t-\tau_l^x) - P_i L_i m_i(t) + (\bar{B}_{id} - G_i)\bar{d}(t) + K_i \tilde{u}(t) + \bar{A}\tilde{x}(t) \\
r_i(t) =& M_i e_i(t) + \bar{D}_{di}\bar{d}(t), \qquad i \in \mathbf{k}
\end{aligned} \tag{6.14}$$

Using Lemma 6.2 by setting $c_i = 1$ (constant delay) and the Schur complement of the inequality (6.12), it follows that the inequality (6.9) holds. Moreover, from the error dynamics (6.14), it follows that $r_i(t)$ is only affected directly by L_i. This implies when the delays are known perfect decoupling among faults can be accomplished.

■

It should be noted that the faults $L_j, j \neq i$ have indirect effects on the residual signal $r_i(t)$ through $\tilde{x}$ due to uncertainties in the delay values. However, according to Assumption 6.3, the term $\tilde{x}$ in equation (6.14) is bounded and based on our proposed FDI algorithm of Theorem 6.1 the residual indirect effects are attenuated

by the factor γ. In other words, by using the upper bounds of the delays in the residual generation, the effects of the faults $L_j, j \neq i$ on the residual signal $r_i(t)$ are attenuated from two aspects. First, the direct effects of faults are forced to be zero ($P_i L_j = 0$) using the properties of the finite unobservability subspace $\mathcal{S}_i^*$ of Theorem 6.1. Second, the indirect effects of faults on the residual signal $r_i(t)$ through $\tilde{x}$ are attenuated through the use of the H_∞ approach. As pointed out above if the exact values of the delays are known, the terms $\tilde{x}$ and $\tilde{u}$ will become zero and a perfect or an exact decoupling can be achieved.

6.2.3 H_∞-based FDI for Neutral Time-Delay Systems

Consider the following linear neutral time-delay system (with $N \equiv 1$ in (6.1))

$$\dot{x}(t) = A_0 x(t) + A_1 x(t - \tau(t)) + A_2 \dot{x}(t - \tau_d(t)) + B_0 u(t) + \sum_{l=1}^{k} L_l m_l(t) + B_d d(t)$$

$$y(t) = Cx(t) + D_d d(t) \tag{6.15}$$

with the continuous initial condition $x(\theta) = \phi(\theta), \theta \in [-\tau_m, 0]$, where $x \in \mathcal{X}$ is the state of the system with dimension n, $u \in \mathcal{U}, y \in \mathcal{Y}$ are input and output signals with dimensions m and q, respectively, $d(t)$ represents an unknown input vector that could include modeling errors and uncertain disturbances, $m_i \in \mathcal{M}_i$ are the fault modes with dimension k_i, L_i's are the fault signatures and $\tau_m = \max\{\tau(0), \tau_d(0)\}$.

The fault modes together with the fault signatures can be used to model the effects of actuator faults, sensor faults and system faults on the dynamics of the system. For modeling a fault in the i-th actuator, $L_i = [b_{0i}, b_{1i}, ..., b_{Li}]$ and the fault mode m_i is chosen to model the type of a fault where $b_{ji}, j = 0, ..., L$ denote the i-th column of matrices $B_j, j = 0, ..., L$. For example a complete failure of an actuator can be represented and modeled by $m_i(t) = [-u_i(t), -u_i(t - \tau_{u1}), ..., -u_i(t - \tau_{uL})]^\top$. A system fault can be represented by a potential variation in the parameters of the

A_0, A_1 and A_2 matrices as shown below:

$$\begin{aligned}\dot{x}(t) =&(A_0 + \Delta A_0)x(t) + (A_1 + \Delta A_1)x(t-h)\\ &+ (A_2 + \Delta A_2)\dot{x}(t-d) + B_0u(t) + \sum_{j=1}^{L} B_j u(t-\tau_{uj})\\ y(t) =&Cx(t)\end{aligned}$$

As an example, a change in the i-th row and j-th column of matrix A_2 can be modeled as $\Delta A_2\dot{x}(t-d) = I_i\Delta a_{2_{ij}}\dot{x}_j(t-d)$ where x_j is the j-th element of the vector x and I_i is an n-dimensional vector with all zero elements except one in the i-th element. Define the signal $m_i(t) \triangleq \Delta a_{2_{ij}}\dot{x}_j(t-d)$ as an external input and fault signature $L_i = I_i$, then this fault can be modeled as in equation (6.15).

It should be noted that sensor faults can initially be modeled as additive inputs in the measurement equation $y = Cx + \sum_{j=1}^{q} E_j n_j$ where E_j is an $q \times 1$ unit vector with a one at the j-th position and $n_j \in \mathbb{R}$ is a sensor fault mode, which corresponds to a fault in the j-th sensor. For example, a complete failure of the j-th sensor can be represented and modeled by $n_j = -c_j x$ where c_j is the j-th row of the matrix C. The sensor fault signature can also be modeled as an input to the system [3, 18] and [130]. Following [18], let f_j be the solution to $E_j = Cf_j$. The new states can be defined according to $\bar{x}(t) = x(t) + \sum_{j=1}^{q} f_j n_j(t)$, where the state space representation for the new states can be written as

$$\begin{aligned}\dot{\bar{x}}(t) =&A_0\bar{x}(t) + A_1\bar{x}(t-h) + A_2\bar{x}(t-d) + B_0u(t) + \sum_{j=1}^{L} B_j u(t-\tau_{uj}) + \sum_{j=1}^{q} L_j m_j(t)\\ y(t) =&C\bar{x}(t)\end{aligned}$$

where $L_j = [f_j, A_0 f_j, A_1 f_j, A_2 f_j]$ and $m_j(t) = [\dot{n}_j(t), -n_j(t), -n_j(t-h) - \dot{n}_j(t-d)]^\top$.

We now state the main assumptions needed for the development of our proposed FDI scheme for the neutral time-delay system (6.15).

Assumption 6.4. *The upper bound on the delay functions $\tau(t)$ and $\tau_d(t)$ are assumed to be known. i.e. $\tau(t) < \bar{\tau} < \infty$ and $\tau_d(t) < \bar{\tau}_d < \infty$.*

Assumption 6.5. *The error signal* $\tilde{x}^\top(t) = [x^\top(t-\tau(t)) - x^\top(t-\bar{\tau}), \dot{x}^\top(t-\tau_d(t)) - \dot{x}^\top(t-\bar{\tau}_d)]$ *is* $\mathfrak{L}_2$ *norm bounded.*

Remark 6.3. *The same observations and statements that are made in Remark 6.2 do also apply and can be repeated for the neutral time-delay system* (6.15).

The class of finite unobservability subspaces containing a given subspace $\mathcal{L}$ for the above neutral time delay system is denoted by $\underline{\mathcal{S}}_N(\mathcal{L})$, i.e.

$$\underline{\mathcal{S}}_N(\mathcal{L}) = \{\mathcal{S} \in \mathcal{X} | \mathcal{S} =<< \mathrm{Ker} HC | A_i + D_i C >>_{i \in \mathbf{2}=\{0,1,2\}} \quad \text{and} \quad \mathcal{L} \in \mathcal{S}\} \tag{6.16}$$

The smallest element of $\underline{\mathcal{S}}_N(\mathcal{L})$ is denoted by $\mathcal{S}_N^*$ and can be obtained based on Algorithm 6.2.

We are now in a position to introduce our main result in this section. The H_∞-based Extended Fundamental Problem in Residual Generation (HEFPRG) for the neutral time-delay system (6.15) is defined as the design of a set of filters that generate k residuals such that each residual $r_i(t)$ is affected by a fault in the i-th component L_i and is partially decoupled from all other faults $L_j, j \neq i$ and

$$\int_0^\infty r_i^\top(t) r_i(t) dt \leq \gamma^2 \int_0^\infty (\bar{d}^\top(t)\bar{d}(t) + \tilde{x}^\top(t)\tilde{x}(t)) dt \tag{6.17}$$

where $\bar{d}^\top(t) = [d^\top(t), d^\top(t-\bar{\tau}), \dot{d}^\top(t-\bar{\tau}_d)]$. As mentioned earlier, the residual set $\{r_i\}, i \in \mathbf{k}$ enables one to detect and isolate multiple faults in all the channels. The residual signals $r_i(t)$ are generated according to the following filters:

$$\begin{aligned} \dot{w}_i(t) &= F_{i0} w_i(t) + F_{i1} w_i(t-\bar{\tau}) + F_{i2} \dot{w}_i(t-\bar{\tau}_d) \\ &\quad - E_{i0} y(t) - E_{i1} y(t-\bar{\tau}) - E_{i2} \dot{y}(t-\bar{\tau}_d) + K_i u(t) \\ r_i(t) &= M_i w_i(t) - H_i y(t), \qquad i \in \mathbf{k} \end{aligned} \tag{6.18}$$

which have similar structures as the observers that are considered in [217]. As will be shown in Theorem 6.2, the associated error dynamics corresponding to the residual generators have constant delays. This is due to the fact that the upper bounds of the

delays are used in the detection filters that are given in (6.18). Lemma 6.3 provides a sufficient condition for the asymptotic stability of system (6.15) having constant delay values $\tau(t) = \bar{\tau}$ and $\tau_d(t) = \bar{\tau}_d$ while guaranteeing that the H_∞ norm of the transfer function between the disturbance d and the output signal y is less than a given positive value γ.

Lemma 6.3. *Given $\gamma > 0$ and the neutral time-delay system* (6.15) *having constant delay values $\tau(t) = \bar{\tau}$ and $\tau_d(t) = \bar{\tau}_d$, if there exist positive-definite matrices R, Q_1 and Q_2 such that the inequality* (6.19) *is satisfied where $\Phi_1 = RA_0 + A_0^\top R + A_0^\top Q_1 A_0 + Q_2 + C^\top C$, $\Phi_2 = RB_d + A_0^\top Q_1 B_d + C^\top D_d$ and $\Phi_3 = -\gamma^2 I + B_d^\top Q_1 B_d + D_d^\top D_d$, then system* (6.15) *with all the fault modes set to zero (i.e., $m_i(t) = 0$) is asymptotically stable and its $\mathfrak{L}_2$ gain is not greater than γ, with*

$$\begin{bmatrix} \Phi_1 & RA_1 + A_0^\top Q_1 A_1 & RA_2 + A_0^\top Q_1 A_2 & \Phi_2 \\ * & A_1^\top Q_1 A_1 - Q_2 & A_1^\top Q_1 A_2 & A_1^\top Q_1 B_d \\ * & * & A_2^\top Q_1 A_2 - Q_1 & A_2^\top Q_1 B_d \\ * & * & * & \Phi_3 \end{bmatrix} < 0 \qquad (6.19)$$

Proof: Define a difference operator $\mathbb{D}$ as $\mathbb{D}(\phi) = \phi(0) - A_2\phi(-\bar{\tau}_d)$, then according to the inequality (6.19), we have $A_2^\top Q_1 A_2 - Q_1 < 0$. Hence the operator $\mathbb{D}$ is stable. Let $V(t)$ be a Lyapunov-Krasovskii functional of the form $V(t) = V_1(t) + V_2(t) + V_3(t)$ [217] where

$$V_1(t) = x^\top(t)Rx(t),\ V_2(t) = \int_{t-\bar{\tau}_d}^{t} \dot{x}^\top(s)Q_1\dot{x}(s)ds,\ V_3(t) = \int_{t-\bar{\tau}}^{t} x^\top(s)Q_2x(s)ds$$

The asymptotic stability of system (6.15) can be shown following the results of Theorem 2 in [217]. The $\mathfrak{L}_2$ stability result is now shown according to the following procedure. Define an associated Hamiltonian $H(x, d(t), t) = \dot{V}(t) + y^\top(t)y(t) - \gamma^2 d^\top(t)d(t)$. It is sufficient to show that under zero initial conditions $H(x, d(t), t) \leq 0$. The Hamiltonian can be written as $H(x, d(t), t) \leq \eta^\top(t)\Phi\eta(t)$, where $\eta^\top(t) = [x(t)^\top, x(t-\bar{\tau})^\top, \dot{x}^\top(t-\bar{\tau}_d), d^\top(t)]$ and Φ is the matrix defined in the inequality

(6.19). Therefore, $\Phi < 0$ leads to $H(x, d(t), t) \leq 0$, and hence the inequality (6.8) holds. ■

The following theorem summarizes our proposed FDI strategy for the neutral time-delay system (6.15).

Theorem 6.2. *The HEFPRG problem specified by expressions* (6.17) *and* (6.18) *has a solution for the linear neutral time-delay system* (6.15) *if (a) the following finite unobservability subspaces*

$$\mathcal{S}_i^* = \inf \underline{\mathcal{S}}_N(\sum_{j \neq i} \mathcal{L}_j), \ i \in \boldsymbol{k}, \mathcal{2}_0 = \{0, 1, 2\} \tag{6.20}$$

exist such that $\mathcal{L}_i \cap \mathcal{S}_i^* = 0, i \in \boldsymbol{k}$, *and (b) the matrices* $T_{i0}, T_{i1}, T_{i2}, i \in \boldsymbol{k}$ *and the positive-definite matrices* R_i, *and* $Q_i, i \in \boldsymbol{k}$ *exist such that the inequality* (6.21) *is satisfied where* $\Phi_i = R_i A_{0_{\mathcal{S}_i^*}} + A_{0_{\mathcal{S}_i^*}}^\top R_i + T_{i0} M_i + M_i^\top T_{i0}^\top + M_i^\top M_i + Q_i$, $\Gamma_{ij} = R_i A_{j_{\mathcal{S}_i^*}} + T_{ij} M_i$, $\Theta_i = R_i \bar{B}_{di} - T_i + M_i^\top \bar{D}_{di}$, $\Upsilon_i = -\gamma^2 I + \bar{D}_{di}^\top \bar{D}_{di}$, P_i *is the canonical projection of* $\mathcal{X}$ *on* $\mathcal{X}/\mathcal{S}_i^*$, $\bar{D}_{di} = [-H_i D_d, 0, 0]$, $B_{di} = P_i[-B_d - D_{i0} D_d, -D_{i1} D_d, -D_{i2} D_d]$, $\bar{A} = P_i[-A_1, -A_2]$, $T_i = [T_{i0} H_i D_d, T_{i1} H_i D_d, T_{i2} H_i D_d]$, $D_{ij}, j = 0, 1, 2$ *and* H_i *are the output injection and the measurement mixing maps, respectively, such that* $\mathcal{S}_i^* =<< \text{Ker } H_i C | A_j + D_{ij} C >>_{j \in \mathcal{2}_0}$ *and the pairs* $(M_i, A_{0_{\mathcal{S}_i^*}})$, $(M_i, A_{1_{\mathcal{S}_i^*}})$, $(M_i, A_{2_{\mathcal{S}_i^*}})$ *are the factor system of the pairs* (C, A_0), (C, A_1) *and* (C, A_2) *on* $\mathcal{X}/\mathcal{S}_i^*$, *respectively.*

$$\begin{bmatrix} \Phi_i & \Gamma_{i1} & \Gamma_{i2} & \Theta_i & R_i \bar{A} & A_{0_{\mathcal{S}_i^*}}^\top R_i + M_i^\top T_{i0}^\top \\ * & -Q_i & 0 & 0 & 0 & A_{1_{\mathcal{S}_i^*}}^\top R_i + M_i^\top T_{i1}^\top \\ * & * & -R_i & 0 & 0 & A_{2_{\mathcal{S}_i^*}}^\top R_i + M_i^\top T_{i2}^\top \\ * & * & * & \Upsilon_i & 0 & \bar{B}_{di}^\top R_i - T_i^\top \\ * & * & * & * & -\gamma^2 I & \bar{A}^\top R_i \\ * & * & * & * & * & -R_i \end{bmatrix} < 0 \tag{6.21}$$

Proof: Given the finite unobservability subspaces $\mathcal{S}_i^*$, there exist output injection maps D_{i0}, D_{i1}, D_{i2} and measurement mixing map H_i such that

$$\mathcal{S}_i^* =<< \text{Ker } H_i C | A_j + D_{ij} C >>_{j \in \mathbf{2}_0}$$

where H_i is the solution to Ker $H_iC = \mathcal{S}_i^* +$ Ker C. Let M_i be a unique solution to $M_iP_i = H_iC$ and $A_{j_{\mathcal{S}_i^*}} = (A_j + D_{ij}C : \mathcal{X}/\mathcal{S}_i^*), j = 0, 1, 2$, where $P_i(A_j + D_{ij}C) = A_{j_{\mathcal{S}_i^*}}P_i$. Define $G_{i0} = R_i^{-1}T_{i0}$, $G_{i1} = R_i^{-1}T_{i1}$,$G_{i2} = R_i^{-1}T_{i2}$ where T_{i0}, T_{i1}, T_{i2} and R_i are the solution to the inequality (6.21). Let $F_{ij} = A_{j_{\mathcal{S}_i^*}} + G_{ij}M_i$, $E_{ij} = P_i(D_{ij} + P_i^{-r}G_{ij}H_i), j = 0, 1, 2$, and $K_i = P_iB_0$. Define $e_i(t) = w_i(t) - P_ix(t)$, then using equation (6.18) and following along the same lines as in the proof of Theorem 6.1, the error dynamics can be written as

$$\begin{aligned}
\dot{e}_i(t) =& F_{i0}e_i(t) + F_{i1}e_i(t-\bar{\tau}) + F_{i2}\dot{e}_i(t-\bar{\tau}_d) \\
& - P_iL_im_i(t) + (\bar{B}_{di} - G_i)\bar{d}(t) + \bar{A}\tilde{x}(t) \\
r_i(t) =& M_ie_i(t) + \bar{D}_{di}\bar{d}(t), \qquad i \in \mathbf{k}
\end{aligned} \tag{6.22}$$

By invoking Lemma 6.3 and setting $Q_1 = R$ and using the Schur complement it follows that inequality (6.17) holds. Moreover, from the error dynamics (6.22) it follows that $r_i(t)$ is only affected directly by L_i. ■

Remark 6.4. *It should be noted again that in [214] only the problem of fault detection for neutral time-delay systems is investigated. However, by utilizing our proposed approach a set of residuals are generated to simultaneously perform both fault detection and fault isolation in the neutral time-delay systems.*

6.3 Distributed Delay Systems

In this section, the problem of fault detection and isolation for distributed delay systems is investigated.

6.3.1 Finite Unobservability Subspace for Distributed Delay Systems

Consider a linear system with distributed delay

$$\begin{aligned} \dot{x}(t) &= A_0x(t) + A_1x(t-\tau_1) + A_2\int_{t-\tau_2}^{t} x(s)ds \\ y_0(t) &= C_0x(t), \quad y_1(t) = C_1x(t-\tau_1), \quad y_2(t) = C_2\int_{t-\tau_2}^{t} x(s)ds \\ x(\theta) &= \phi(\theta) \quad \theta \in [-\tau, 0] \end{aligned} \tag{6.23}$$

where $x \in \mathcal{X}$ is the state of the system with dimension n, $y_i \in \mathcal{Y}$ is the output measurement with dimension q_i and $\tau = \max\{\tau_1, \tau_2\}$. The following lemma is needed for finding a finite invariant subspace for the above distributed time-delay.

Lemma 6.4 ([133]). *(the fundamental lemma of the geometric approach) Any trajectory $x(t)$, $t \in [t_0, t_1]$ belongs to a subspace $\mathcal{L} \in \mathcal{X}$ if and only if $x(t_0) \in \mathcal{L}$ and $\dot{x}(t) \in \mathcal{L}$ almost everywhere (a.e.) in $[t_0, t_1]$.*

Based on the above lemma, we have the following result:

Lemma 6.5. *Let $\mathcal{V} \subset \mathcal{X}$ be A_i-invariant for all $i \in \{0,1,2\}$, i.e. $A_i\mathcal{V} \subset \mathcal{V}$, $i \in \{0,1,2\}$. If $\phi(\theta) \in \mathcal{V}$, $\forall\theta \in [-\tau, 0]$, then $x(t) \in \mathcal{V}$ a.e. for $t \geq 0$..*

Proof: Since $\phi(\theta) \in \mathcal{V}$, $\forall\theta \in [-\tau, 0]$, then $\int_{-\tau_2}^{0} \phi(\theta)d\theta \in \mathcal{V}$ a.e. . Indeed, recall that a Lebesgue measurable and integrable function is zero a.e. in $[t_0, t_1]$ if and only if its integral in any subinterval of $[t_0, t_1]$ is zero. Applying this property to function $Y^\top \int_{-\tau_2}^{t} \phi(\theta)d\theta$, $-\tau_2 \leq t \leq 0$, where Y denote a basis matrix of $\mathcal{V}$, we have $\int_{-\tau_2}^{0} \phi(\theta)d\theta \in \mathcal{V}$ almost everywhere. Hence $\dot{x}(t_0^+) \in \mathcal{V}$ and based on Lemma 6.4, we have $x(t_0^+) \in \mathcal{V}$. Similarly, it can be shown by successive application of this process that $x(t) \in \mathcal{V}, \forall t \geq 0$. ■

Next consider the following time-delay system

$$\dot{x}(t) = (A_0 + D_0C_0)x(t) + (A_1 + D_1C_1)x(t-\tau_1) + (A_2 + D_2C_2)\int_{t-\tau_2}^{t} x(s)ds$$

$$\tilde{y}_0(t) = H_0C_0x(t), \quad y_1(t) = H_1C_1x(t-\tau_1), \quad y_2(t) = H_2C_2\int_{t-\tau_2}^{t} x(s)ds$$

$$x(\theta) = \phi(\theta) \quad \theta \in [-\tau, 0]$$

for given maps $D_i : \mathcal{Y} \to \mathcal{X}$ and $H_i : \mathcal{Y} \to \mathcal{Y}$. Let us define the subspace $\mathcal{S} \subset \mathcal{X}$ as the largest $A_i + D_iC_i$-invariant that is contained in Ker H_iC_i for $i \in \{0,1,2\}$. According to Lemma 6.5, for any initial condition $\phi(\theta) \in \mathcal{S}$, $\forall\theta \in [-\tau, 0]$, we have $\tilde{y}_i(t) = 0$, $\forall t > 0$, $i \in \{0,1,2\}$. Based on the above discussion and the assumption that $\mathcal{S} \subset \mathcal{X}$ ($\mathcal{S}$ is a finite subspace), we define the notion of a finite unobservability subspace for the distributed time-delay system (6.23) as follows.

Definition 6.2. *A subspace $\mathcal{S}$ is called a finite unobservability subspace for system (6.23) if for some output injection maps $D_i : \mathcal{Y} \to \mathcal{X}$ and measurement mixing map $H_i : \mathcal{Y} \to \mathcal{Y}$, we have*

$$\mathcal{S} = << \bigcap_{j=0}^{2} Ker\ H_jC_j | A_i + D_iC >>_{i\in\{0,1,2\}} \tag{6.24}$$

It should be noted that the above definition coincides with the definition of unobservability subspace for the Markovian jump system (Definition 5.6) for $\Psi = \{0,1,2\}$. Hence, Algorithm 5.3 can be used for finding the smallest finite unobservability subspace containing a given subspace.

The class of finite unobservability subspaces containing a given subspace $\mathcal{L}$ for the above distributed delay system is denoted by $\underline{\mathcal{S}}_D(\mathcal{L})$, i.e.

$$\underline{\mathcal{S}}_D(\mathcal{L}) = \{\mathcal{S} \in \mathcal{X} | \mathcal{S} = << \bigcap_{j=0}^{2} \mathrm{Ker} H_jC_j | A_i + D_iC_i >>_{i\in\mathbf{2}=\{0,1,2\}} \quad \text{and} \quad \mathcal{L} \in \mathcal{S}\}$$

The smallest element of $\underline{\mathcal{S}}_D(\mathcal{L})$ is denoted by $\mathcal{S}_D^*$ and can be obtained based on Algorithm 5.3.

6.3.2 H_∞-based FDI Strategy of Distributed Delay Systems

Consider the following linear system with distributed time delays

$$\begin{aligned}
\dot{x}(t) &= A_0x(t) + A_1x(t-\tau_1) + A_2\int_{t-\tau_2}^{t} x(s)ds + Bu(t) + \sum_{i=1}^{k} L_im_i(t) + B_dd(t) \\
y_0(t) &= C_0x(t) + D_{d0}d(t), \quad y_1(t) = C_1x(t-\tau_1) + D_{d1}d(t) \\
y_2(t) &= C_2\int_{t-\tau_2}^{t} x(s)ds + D_{d2}d(t)
\end{aligned} \tag{6.25}$$

with continuous initial condition $x(\theta) = \phi(\theta), \theta \in [-\tau, 0]$, where $x \in \mathcal{X}$ is the state of the system with dimension n, $u \in \mathcal{U}, y \in \mathcal{Y}$ are the input and the output signals with dimensions m and q, respectively, and $d(t) \in \mathbb{R}^p$ is the disturbance input. Without loss of generality, it is assumed that d is L_2-norm bounded, i.e. $d(t) \in \mathfrak{L}_2[0,\infty]$. Moreover, $m_i \in \mathcal{M}_i$ are the fault modes with dimension k_i, L_i's are fault signatures and $\tau = \max\{\tau_1, \tau_2\}$. The fault modes together with the fault signatures may be used to model the effects of actuator faults, sensor faults and system faults on the dynamics of the system.

The H_∞-based Extended Fundamental Problem in Residual Generation (HEF-PRG) for the time-delay system (6.25) is stated as that of designing a set of filters that generate k residuals $r_i(t)$ such that a fault in the i-th component L_i can only affect the residual $r_i(t)$ and no other residual $r_j(t)(i \neq j)$ and

$$\int_0^\infty r_i^\top(t)r_i(t)dt \leq \gamma^2 \int_0^\infty d^\top(t)d(t)dt, \quad i \in \mathbf{k} \tag{6.26}$$

Specifically, the residual signals $r_i(t)$ are generated according to the following filters:

$$\begin{aligned}
\dot{w}_i(t) =& F_{i0}w_i(t) + F_{i1}w_i(t-\tau_1) + F_{i2}\int_{t-\tau_2}^{t} w_i(s)ds \\
& - E_{i0}y_0(t) - E_{i1}y_1(t) - E_{i2}y_2(t) + K_iu(t) \\
r_i(t) =& M_{i0}w_i(t) - H_{i0}y_0(t)
\end{aligned} \tag{6.27}$$

The next lemma provides a sufficient condition for asymptotic stability of system (6.25) with $m_i(t) = 0$ while the H_∞ norm of the transfer function between the disturbance d and the output signal y is less that a given positive value γ. This lemma will be used in the proof of Theorem 6.2 for guaranteeing both the stability of detection filters and γ-disturbance attenuation condition (6.26).

Lemma 6.6 ([218]). *Given $\gamma > 0$ and the distributed time-delay system* (6.23), *if there exist positive-definite matrices R, Q_1 and Q_2 such that the following LMI condition holds*

$$\begin{bmatrix} RA_0 + A_0^\top R + Q_1 + \tau_2^2 Q_2 + C_0^\top C_0 & RA_1 & RA_2 & RB_d + C_0^\top D_d \\ A_1^\top R & -Q_1 & 0 & 0 \\ A_2^\top R & 0 & -Q_2 & 0 \\ B_d^\top R + D_d^\top C_0 & 0 & 0 & D_d^\top D_d - \gamma^2 I \end{bmatrix} < 0$$

then system (6.23) *is asymptotically stable and*

$$\int_0^\infty y_0^\top(t) y_0(t) dt \leq \gamma^2 \int_0^\infty d^\top(t) d(t) dt \tag{6.28}$$

for all $d(t) \in \mathfrak{L}_2[0, \infty]$.

The following theorem summarizes our proposed robust FDI strategy.

Theorem 6.3. *The HEFPRG problem defined by expressions* (6.26) *and* (6.27) *has a solution for the linear time-delay system* (6.25) *if there exist the following unobservability subspaces*

$$\mathcal{S}_i^* = \inf \underline{\mathcal{S}}_D(\sum_{j \neq i} \mathcal{L}_j), \quad i \in \boldsymbol{k} \tag{6.29}$$

such that $\mathcal{L}_i \cap \mathcal{S}_i^* = 0, i \in \boldsymbol{k}$ as well as positive-definite matrices R_i, Q_{i1} and Q_{i2},

$i \in \boldsymbol{k}$ *and matrices* T_{ij}, $i \in \boldsymbol{k}, j = 0,1,2$ *such that*

$$\begin{bmatrix} \Upsilon_i + Q_{i1} + \tau_2^2 Q_{i2} & * & * & * \\ \bar{A}_{i1}^\top R_i + M_{i1}^\top T_{i1} & -Q_{i1} & * & * \\ \bar{A}_{i2}^\top R_i + M_{i2}^\top T_{i2} & 0 & -Q_{i2} & * \\ \Phi_i^\top R_i + \Psi_i^\top - D_{d0}^\top H_{i0}^\top M_{i0} & 0 & 0 & D_{d0}^\top H_{i0}^\top H_{i0} D_{d0} - \gamma^2 I \end{bmatrix} < 0 \quad (6.30)$$

where $\Upsilon_i = R_i \bar{A}_{i0} + T_{i0} M_{i0} + \bar{A}_{i0}^\top R + M_{i0}^\top T_{i0}^\top + M_{i0}^\top M_{i0}$, $\Phi_i = -P_i(B_d + D_{i0} D_{d0} + D_{i1} D_{d1} + D_{i2} D_{d2})$, $\Psi_i = -(T_{i0} H_{i0} D_{d0} + T_{i1} H_{i1} D_{d1} + T_{i2} H_{i2} D_{d2})$, P_i *is the canonical projection of* $\mathcal{X}$ *on* $\mathcal{X}/\mathcal{S}_i^*$ *and the pairs* $(M_{ij}, \bar{A}_{ij}), j = 0,1,2$ *are the factor system of the pairs* $(C_j, A_j), j = 0,1,2$ *on* $\mathcal{X}/\mathcal{S}_i^*$, *respectively.*

Proof: Given the unobservability subspaces $\mathcal{S}_i^*$, there exist output map injections D_{i0}, D_{i1}, D_{i2} and measurement mixing map H_{i0}, H_{i1}, H_{i2} such that $\mathcal{S}_i^* =<$ Ker $H_{ij} C_j | A_j + D_{ij} C_j >$, $j = 0,1,2$ where $H_{ij}, j = 0,1,2$ are the solution to Ker $H_{ij} C_j = \mathcal{S}_i^* +$ Ker C_j. Let $\bar{A}_{ij}$ and $M_{ij}, j = 0,1,2$ be the matrices of the factor system of (6.25) on $\mathcal{S}_i^*$, i.e. $M_{ij} P_i = H_{ij} C_j$ and $\bar{A}_{ij} = (A_j + D_{ij} C_j : \mathcal{X}/\mathcal{S}_i^*)$, $j = 0,1,2$. Let R_i and T_{ij}, $i \in \mathbf{k}$, $j = 0,1,2$ be the solution to the inequality (6.30). Define the gain matrices $G_{ij} = R_i^{-1} T_{ij}, i \in \mathbf{k}$, $j = 0,1,2$ and let $F_{ij} = \bar{A}_{ij} + G_{ij} M_{ij}$, $E_{ij} = P_i(D_{ij} + P_i^{-\tau} G_{ij} H_{ij})$, $j = 0,1,2$, and $K_i = P_i B$, $i \in \mathbf{k}$. Define the state errors as $e_i(t) = w_i(t) - P_i x(t)$, so that by using (6.27) we have

$$\begin{aligned} \dot{e}_i(t) &= F_{i0} w_i(t) + F_{i1} w_i(t - \tau_1) + F_{i2} \int_{t-\tau_2}^{t} w_i(s) ds - E_{i0} y_0(t) - E_{i1} y_1(t) \\ &- E_{i2} y_2(t) + K_i u(t) - P_i(A_0 x(t) + A_1 x(t - \tau_1) + A_2 \int_{t-\tau_2}^{t} x(s) ds + B u(t) \\ &+ \sum_{i=1}^{k} L_i m_i(t) + B_d d(t)) \end{aligned}$$

$$
\begin{aligned}
&= F_{i0}w_i(t) + F_{i1}w_i(t-\tau_1) + F_{i2}\int_{t-\tau_2}^{t} w_i(s)ds - P_i(A_0 + D_{i0}C_0)x(t) \\
&- G_{i0}M_{i0}P_ix(t) - P_iL_im_i(t) - P_i(A_1 + D_{i1}C_1)x(t-\tau_1) - G_{i1}M_{i1}P_ix(t-\tau_1) \\
&- P_i(A_2 + D_{i2}C_2)\int_{t-\tau_2}^{t} x(s)ds - G_{i2}M_{i2}P_i\int_{t-\tau_2}^{t} x(s)ds - P_iB_dd(t) - E_{i0}D_{d0}d(t) \\
&- E_{i1}D_{d1}d(t) - E_{i2}D_{d2}d(t) \\
&= (\bar{A}_{i0} + G_{i0}M_{i0})e_i(t) + (\bar{A}_{i1} + G_{i1}M_{i1})e_i(t-\tau_1) \\
&+ (\bar{A}_{i2} + G_{i2}M_{i2})\int_{t-\tau_2}^{t} e_i(s)ds - P_iL_im_i(t) \\
&- P_i(B_d + D_{i0}D_{d0} + D_{i1}D_{d1} + D_{i2}D_{d2})d(t) \\
&- (G_{i0}H_{i0}D_{d0} + G_{i1}H_{i1}D_{d1} + G_{i2}H_{i2}D_{d2})d(t)
\end{aligned}
$$

Note that $P_iL_j = 0, j \neq i$, since $\mathcal{L}_j \in \mathcal{S}_i, j \neq i$. Also

$$
\begin{aligned}
r_i(t) &= M_{i0}w_i(t) - H_{i0}y_0(t) = M_{i0}w_i(t) - H_{i0}C_0x(t) - H_{i0}D_{d0}d(t) \\
&= M_{i0}e_i(t) - H_{i0}D_{d0}d(t)
\end{aligned}
$$

Consequently, the error dynamics can be written as

$$
\begin{aligned}
\dot{e}_i(t) =& (\bar{A}_{i0} + G_{i0}M_{i0})e_i(t) + (\bar{A}_{i1} + G_{i1}M_{i1})e_i(t-\tau_1) + (\bar{A}_{i2} + G_{i2}M_{i2})\int_{t-\tau_2}^{t} e_i(s)ds \\
&- P_iL_im_i(t) - P_i(B_d + D_{i0}D_{d0} + D_{i1}D_{d1} + D_{i2}D_{d2})d(t) \\
&- (G_{i0}H_{i0}D_{d0} + G_{i1}H_{i1}D_{d1} + G_{i2}H_{i2}D_{d2})d(t) \\
r_i(t) =& M_{i0}e_i(t) - H_{i0}D_{d0}d(t)
\end{aligned} \tag{6.31}
$$

Using Lemma 6.6 and the inequality (6.30), it follows that the inequality (6.26) holds. Moreover, from the error dynamics (6.31), it follows that $r_i(t)$ is only affected by L_i and is decoupled from other fault signatures. This completes the proof of Theorem 6.3. ■

6.4 FDI of Markovian Jump Systems with Time-delays

This section investigates development of fault detection and isolation filters for Markovian jump systems with mode-dependent time-delays and uncertain switching probability. Based on our developed results from Chapter 5 and Section 6.2.1, the notion of a finite unobservability subspace is introduced for these systems and an algorithm for finding this subspace is presented. Based on the introduced unobservability subspace, sufficient conditions for solving the fault detection and isolation problem are obtained. A bank of residual generators is designed such that each residual is affected by one fault and is decoupled from the others while the H_∞ norm of the transfer function between the disturbance and the residual signals are less that a prespecified value for all uncertainties in the switching probabilities.

6.4.1 Background and Preliminary Results

In this section, background results on H_∞ disturbance attenuation of Markovian jump systems with mode-dependent time-delays with uncertain mode transition matrix are presented. Consider the following Markovian jump system with time-delay (MJSD)

$$\dot{x}(t) = A(\lambda_t)x(t) + A_\tau(\lambda_t)x(t-\tau_{\lambda_t}(t)) + B(\lambda_t)u(t) + B_d(\lambda_t)d(t) + \sum_{l=1}^{L} L_l(\lambda_t)m_l(t)$$

$$y(t) = C(\lambda_t)x(t) + D_d(\lambda_t)d(t) \qquad x(\theta) = \phi(\theta), \quad \theta \in [-\mu, 0] \tag{6.32}$$

where $x \in \mathcal{X}$ is the state of the system with dimension n; $u \in \mathcal{U}, y \in \mathcal{Y}$ are the input and the output signals with dimensions m and q, respectively; $d(t) \in \mathbb{R}^p$ is the unknown disturbance input; $m_i \in \mathcal{M}_i$ are the fault modes with dimension k_i, and L_i's are the fault signatures. The fault modes together with the fault signatures may be used to model the effects of actuator faults, sensor faults and system faults on the

dynamics of the system. It is assumed that $d(t)$ is $\mathfrak{L}_2$-norm bounded, and $\{\lambda_t, t \geq 0\}$ is a continuous-time Markov process taking values in the finite set $\Psi = \{1, ..., N\}$. The Markov process describes the switching between the different system modes and its evolution is governed by the following transition probabilities:

$$\mathbb{P}\{\lambda_{t+h} = j | \lambda_t = i\} = \begin{cases} \pi_{ij}h + o(h) & \text{when } \lambda_t \text{ jumps from } i \text{ to } j \\ 1 + \pi_{ii}h + o(h), & \text{otherwise} \end{cases}$$

where π_{ij} is the transition rate from mode i to mode j with $\pi_{ij} \geq 0$ when $i \neq j$, $\pi_{ii} = -\sum_{j=1, j\neq i}^{N} \pi_{ij}$, and $o(h)$ is a function that satisfies $lim_{h\to 0}\frac{o(h)}{h} = 0$ and $\Pi := [\pi_{ij}]$. The matrices $A(\lambda_t)$, $B(\lambda_t)$, $C(\lambda_t)$, $B_d(\lambda_t)$, $L_l(\lambda_t)$ and $D_d(\lambda_t)$ are known constant matrices for all $\lambda_t = i \in \Psi$. For simplicity, we denote the matrices associated with $\lambda_t = i$ by

$$A(\lambda_t) = A_i, \; A_\tau(\lambda_t) = A_{\tau i}, \; B(\lambda_t) = B_i, \; B_d(\lambda_t) = B_{di},$$
$$C(\lambda_t) = C_i, \quad D_d(\lambda_t) = D_{di}, \quad L_l(\lambda_t) = L_{li}, \quad l \in \mathbf{L}$$

In system (6.32), $\tau_{\lambda_t}(t)$ denotes the time-varying delay when the mode is in λ_t and satisfies

$$0 < \tau_i(t) \leq \mu_i < \infty \quad \dot{\tau}_i(t) \leq h_i < 1 \quad \forall\, i \in \Psi$$

where μ_i and h_i are real constant scalars for any $i \in \Psi$ and $\mu := \max\{\mu_i, i \in \Psi\}$.

Moreover, it is assumed that the mode transition matrix Π is <u>not</u> known precisely. In other words, it belongs to the following admissible uncertainty domain [202]:

$$\mathscr{D}_\Pi = \{\bar{\Pi} + \Delta\Pi : |\Delta\pi_{ij}| \leq \epsilon_{ij}, \epsilon_{ij} \geq 0, \;\; \forall i, j \in \Psi, \; i \neq j\} \tag{6.33}$$

where $\bar{\Pi} = [\bar{\pi}_{ij}]$ is a known constant matrix and denotes the estimated value of Π and $\Delta\Pi = [\Delta\pi_{ij}]$ denotes the uncertainty in the mode transition rate matrix.

First, a sufficient condition for H_∞ disturbance attenuation of a Markovian jump system with time delay is introduced.

Definition 6.3 ([219]). *System* (6.32) *with* $u(t) = 0$, $d(t) = 0$, $m_l(t) = 0, l \in \boldsymbol{L}$ *is said to be exponentially mean square stable if for any finite* $\phi(t) \in \mathbb{R}^n$ *defined on* $[-\mu, 0]$, *and initial mode* $i_0 \in \Psi$, *there exist constant scalars* $b \geq 0$ *and* $c \geq 0$ *such that*

$$\mathbb{E}\{|x(t, \phi, i_0)|^2\} \leq b \sup_{-\mu \leq \theta \leq 0} |\phi(\theta)|^2 e^{-ct}$$

where $x(t, \phi, i_0)$ *denotes the solution of system* (6.32) *at time* t *with the initial conditions* $\phi(t)$ *and* i_0.

Lemma 6.7 ([219]). *Let* γ *be a given positive constant. If there exists a set of symmetric and positive-definite matrices* $R_i > 0, i \in \Psi$ *and* $Q > 0$ *such that the following set of coupled LMIs holds for every* $i \in \Psi$:

$$\begin{bmatrix} \Phi_i & R_i A_{\tau_i} & C_i^\top D_{di} + R_i B_{di} \\ * & -(1-h_i)Q & 0 \\ * & * & D_{di}^\top D_{di} - \gamma^2 I \end{bmatrix} < 0 \tag{6.34}$$

where $\Phi_i = \sum_{j=1}^N \pi_{ij} R_j + A_i^\top R_i + R_i A_i + (1 + \mu\eta)Q + C_i^\top C_i$ *and*

$$\eta = \max\{|\pi_{ii}|, i \in \Psi\}$$

then system (6.32) *with* $u(t) = 0$ *and* $m_j(t) = 0, j \in \boldsymbol{k}$ *is exponentially mean square stable and for zero initial conditions the system satisfies the inequality*

$$||y||_{2,E}^2 = \mathbb{E}\Big\{ \int_0^\infty y^\top(t) y(t) dt | (x_0, i_0) \Big\} < \gamma^2 ||d||_2 \tag{6.35}$$

Proof: The proof follows along the same lines as in proof of Theorem 1 in [219]. ■

A system that satisfies the above conditions is said to be stochastically exponentially stable with a γ-disturbance attenuation. In the next lemma we consider the effects of uncertainties in the mode transition matrix Π for analyzing the stochastic exponential stability of system (6.32) with a γ-disturbance attenuation.

Lemma 6.8. *Let γ be a given positive constant. If there exists a set of symmetric and positive-definite matrices $R_i > 0, i \in \Psi$, $Q > 0$ and scalars $\{\xi_{ij} > 0, i, j \in \Psi, i \neq j\}$ such that the following set of coupled LMIs holds for every $i \in \Psi$:*

$$\begin{bmatrix} \Theta_i & R_i A_{\tau_i} & C_i^\top D_{di} + R_i B_{di} & \Lambda_i \\ * & -(1-h_i)Q & 0 & 0 \\ * & * & D_{di}^\top D_{di} - \gamma^2 I & 0 \\ * & * & * & -\Xi_i \end{bmatrix} < 0 \tag{6.36}$$

where

$$\Theta_i = A_i^\top R_i + R_i A_i + \sum_{j=1}^{N} \bar{\pi}_{ij} R_j + C_i^\top C_i + \sum_{j=1, j\neq i}^{N} \frac{\xi_{ij}}{4} \epsilon_{ij}^2 I + (1+\eta\mu)Q$$

$$\Lambda_i = \begin{bmatrix} R_i - R_1 & \cdots & R_i - R_{i-1} & R_i - R_{i+1} & \cdots & R_i - R_N \end{bmatrix}$$

$$\Xi_i = diag(\xi_{i1} I, ..., \xi_{i(i-1)} I, \xi_{i(i+1)} I, ..., \xi_{iN} I)$$

then system (6.32) *with $u(t) = 0$ and $m_j(t) = 0, j \in \boldsymbol{L}$ is exponentially mean square stable. Moreover, for zero initial conditions the system satisfies the inequality* (6.35) *for all $\Pi \in \mathscr{D}_\Pi$.*

Proof: According to Lemma 6.7, the uncertain system (6.32) with $u(t) = 0$ and $m_j(t) = 0, j \in \mathbf{L}$ is stochastically exponentially mean square stable with a γ-disturbance attenuation if

$$A_i^\top R_i + R_i A_i + \sum_{j=1}^{N} ((\bar{\pi}_{ij} + \Delta\pi_{ij}) R_j + (1+\mu\eta)Q + (1-h_i)^{-1} R_i A_{\tau_i} Q^{-1} A_{\tau_i}^\top R_i$$
$$+ C_i^\top C_i - (C_i^\top D_{di} + R_i B_{di})(D_{di}^\top D_{di} - \gamma^2 I)^{-1} (C_i^\top D_{di} + R_i B_{di})^\top < 0$$

for all $i \in \Psi$. The above inequality can be rewritten as [202]

$$A_i^\top R_i + R_i A_i + \sum_{j=1}^{N} \bar{\pi}_{ij} R_j + (1+\mu\eta)Q + (1-h_i)^{-1} R_i A_{\tau_i} Q^{-1} A_{\tau_i}^\top R_i$$
$$+ \sum_{j=1, j\neq i}^{N} [\frac{1}{2}\Delta\pi_{ij}(R_j - R_i) + \frac{1}{2}\Delta\pi_{ij}(R_j - R_i)]$$
$$- (C_i^\top D_{di} + R_i B_{di})(D_{di}^\top D_{di} - \gamma^2 I)^{-1} (C_i^\top D_{di} + R_i B_{di})^\top < 0$$

The above inequality holds for all $|\Delta\pi_{ij}| \leq \epsilon_{ij}$ if there exist $\xi_{ij} > 0, i, j \in \Psi, i \neq j$ such that

$$A_i^\top R_i + R_i A_i + \sum_{j=1}^{N} \bar{\pi}_{ij} R_j + C_i^\top C_i + (1+\mu\eta)Q + (1-h_i)^{-1} R_i A_{\tau_i}^\top Q^{-1} A_{\tau_i} R_i$$
$$+ \sum_{j=1, j\neq i}^{N} [\frac{\xi_{ij}}{4}\epsilon_{ij}^2 I + \frac{1}{\xi_{ij}}(R_j - R_i)^2]$$
$$- (C_i^\top D_{di} + R_i B_{di})(D_{di}^\top D_{di} - \gamma^2 I)^{-1}(C_i^\top D_{di} + R_i B_{di})^\top < 0$$

It can be shown easily that the above is equivalent to the inequality (6.36) by using the Schur complement. ■

6.4.2 Unobservability Subspace for Markovian Jump Systems with Time-delay (MJSD)

In this section, the notion of an unobservability subspace is introduced for the Markovian jump system with time-delay (6.32). Since the behavior of system (6.32) in each mode is governed by the retarded time-delay equation, we need to first define an unobservability subspace for each mode of the system. The following notion of finite unobservability subspace is introduced in [205] for retarded time-delay systems.

Definition 6.4. *Given the matrices $A_i, A_{\tau i}$ and C_i for each mode of system* (6.32), *a subspace $\mathcal{S}_i^\tau$ is called a finite unobservability subspace if*

$$\mathcal{S}_i^\tau =< Ker\ H_i C_i | A_i + D_i C_i, A_{\tau i} + D_{\tau i} C_i > \tag{6.37}$$

for some output injection maps $D_i, D_{\tau i} : \mathcal{Y} \to \mathcal{X}$ and measurement mixing map $H_i : \mathcal{Y} \to \mathcal{Y}$ where $< Ker\ H_i C_i | A_i + D_i C_i, A_{\tau i} + D_{\tau i} C_i >$ denotes the largest $A_i + D_i C_i$ and $A_{\tau i} + D_{\tau i} C_i$- invariant subspace contained in $Ker\ H_i C_i$.

Based on Definition 6.4 and definition of unobservability subspaces for the Markovian jump systems (Definition 5.6), we introduce the notion of an finite unobservability subspace for the Markovian jump system with time-delay.

Definition 6.5. *A subspace $\mathcal{S}$ is an* unobservability subspace *for system* (6.32) *if*

$$\mathcal{S} = << \mathcal{K} | A_i + D_i C_i, A_{\tau i} + D_{\tau i} C_i >>_{i \in \Psi} \tag{6.38}$$

for some output injection maps $D_i, D_{\tau i} : \mathcal{Y} \to \mathcal{X}$ and measurement mixing map $H_i : \mathcal{Y} \to \mathcal{Y}$, $i \in \Psi$ where $\mathcal{K} = \bigcap_{i=1}^{N} H_i C_i$.

The notation $\underline{\mathcal{S}}(\mathcal{L})$ refers to the class of unobservability subspace for the MJSD system (6.32) containing $\mathcal{L} \subseteq \mathcal{X}$. Based on Algorithm 5.3, the following algorithm can be used for obtaining the smallest element of $\underline{\mathcal{S}}(\mathcal{L})$ denoted by $\mathcal{S}^*(\mathcal{L})$.

Algorithm 6.3. *The subspace $\mathcal{S}^*(\mathcal{L})$ coincides with the last term of the following sequence*

$$\mathcal{Z}^0 = \mathcal{X}; \quad \mathcal{Z}^\mu = \bigcap_{i=1}^{N} (\mathcal{W}^* + (A_i^{-1} \mathcal{Z}^{\mu-1} \cap Ker\ C_i)) \bigcap_{i=1}^{N} (\mathcal{W}^* + (A_{\tau_i}^{-1} \mathcal{Z}^{\mu-1} \cap Ker\ C_i)) \tag{6.39}$$

The subspace $\mathcal{W}_i^{\tau^*} = \lim\ \mathcal{W}_k$, where $\mathcal{W}_k$ can be obtained from the following algorithm.

Algorithm 6.4. *The subspace $\mathcal{W}_i^{\tau^*}$ coincides with and is obtained from the last term of the following sequence*

$$\mathcal{W}_0 = \mathcal{L}$$

$$\mathcal{W}_k = \mathcal{W}_{k-1} + \sum_{i=1}^{N} A_i (\mathcal{W}_{k-1} \cap Ker\ C_i) + \sum_{i=1}^{N} A_{\tau i} (\mathcal{W}_{k-1} \cap Ker\ C_i)$$

We are now in the position to formally introduce the H_∞-based fault detection and isolation problem for the MJSD system (6.32).

6.4.3 H_∞-based Fault Detection and Isolation Strategy for Markovian Jump Systems with Mode-dependent Time delays

The H_∞-based Extended Fundamental Problem in Residual Generation (HEFPRG) for the Markovian jump system with mode-dependent time-delays is to design a set of filters for (6.32) that generates L residuals $r_j(t)$ such that a fault in the l-th component $L_l(\lambda_t)$ can only affect the residual $r_l(t)$ and no other residual $r_j(t)(j \neq l)$ and

$$||r_l||_{2,E}^2 = \mathbb{E}\Big\{ \int_0^\infty r_l^\top(t) r_l(t) dt | (x_0, i_0) \Big\} < \gamma^2 \int_0^\infty d^\top(t) d(t) dt, \quad l \in \mathbf{k} \tag{6.40}$$

for all $\Pi \in \mathscr{D}_\Pi$. Specifically, the residual signals $r_l(t)$ are generated according to the following Markovian jump filters:

$$\begin{aligned} \dot{w}_l(t) =& F_l(\lambda_t) w_l(t) + F_l^\tau(\lambda_t) w_l(t - \tau_{\lambda_t}(t)) - E_l(\lambda_t) y(t) \\ & - E_l^\tau(\lambda_t) y(t - \tau_{\lambda_t}(t)) + K_l(\lambda_t) u(t) \end{aligned} \tag{6.41}$$

$$r_l(t) = M_l(\lambda_t) w_l(t) - H_l(\lambda_t) y(t) \tag{6.42}$$

The following theorem summarizes our proposed fault detection and isolation strategy.

Theorem 6.4. *The H_∞-EFPRG problem defined by* (6.40) *and* (6.42) *has a solution for the Markovian jump system with mode-dependent time-delays* (6.32) *if there exist unobservability subspaces*

$$\mathcal{S}_l^* = \inf \underline{\mathcal{S}}(\sum_{v=1}^{N} \sum_{j=1, j\neq l}^{L} \mathcal{L}_{jv}), \qquad l \in \boldsymbol{L} \tag{6.43}$$

such that

$$\mathcal{S}_l^* \cap \mathcal{L}_{li} = 0, \quad i \in \Psi, l \in \boldsymbol{L} \tag{6.44}$$

as well as the matrices T_{li}, T_{li}^{τ}, positive-definite matrices R_{li}, $i \in \Psi$, $l \in \boldsymbol{L}$, $Q > 0$ and scalars $\{\xi_{ij} > 0, i, j \in \Psi, i \neq j\}$ such that

$$\begin{bmatrix} \Theta_i & \Theta_i^{\tau} & -M_{li}^{\top} H_{li} D_{di} + R_i B_{dli} - T_{li} H_{li} D_{di} & -P_l D_{li}^{\tau} D_{di} - T_{li}^{\tau} H_{li} D_{di} & \Lambda_i \\ * & -(1-h_i)Q & 0 & 0 & 0 \\ * & * & D_{di}^{\top} H_{li}^{\top} H_{li} D_{di} - \gamma^2 I & 0 & 0 \\ * & * & * & -\gamma^2 I & 0 \\ * & * & * & 0 & -\Xi_i \end{bmatrix} < 0 \tag{6.45}$$

where

$$\begin{aligned} \Theta_i &= A_{li}^{\top} R_i + R_i A_{li} + T_{li} M_{li} + M_{li}^{\top} T_{li} \\ &\quad + \sum_{j=1}^{N} \bar{\pi}_{ij} R_j + M_{li}^{\top} M_{li} + \sum_{j=1, j\neq i}^{N} \frac{\xi_{ij}}{4} \epsilon_{ij}^2 I + (1+\eta\mu) Q \\ \Theta_i^{\tau} &= R_i A_{\tau_i} + T_{li}^{\tau} M_{li} \\ \Lambda_i &= \begin{bmatrix} R_i - R_1 & \cdots & R_i - R_{i-1} & R_i - R_{i+1} & \cdots & R_i - R_N \end{bmatrix} \\ \Xi_i &= diag(\xi_{i1} I, ..., \xi_{i(i-1)} I, \xi_{i(i+1)} I, ..., \xi_{iN} I) \end{aligned}$$

and P_l is the canonical projection of $\mathcal{X}$ on $\mathcal{X}/\mathcal{S}_l^*$, $B_{dli} = -P_l B_{di} - P_l D_{li} D_{di}$, the pairs (M_{li}, A_{li}) and (M_{li}, A_{li}^{τ}), $i \in \Psi$, $l \in \boldsymbol{L}$ are the factor system of the pairs (C_i, A_i) and $(C_i, A_{\tau i})$, $i \in \Psi$ on $\mathcal{X}/\mathcal{S}_l^*$, respectively, and H_{li} is the solution to Ker $H_{li} C_i = \mathcal{S}_l^* +$ Ker C_i.

Proof: Given the unobservability subspaces $\mathcal{S}_l^*$, there exist output injection maps D_{li} and D_{li}^{τ} and measurement mixing map H_{li}, $i \in \Psi$, $l \in \mathbf{L}$ such that

$$\mathcal{S}_l^* = << \bigcap \text{Ker } H_{li} C_i | A_i + D_{li} C_i, A_{\tau i} + D_{li}^{\tau} C_i >>_{i \in \Psi}$$

where H_{li} is the solution to Ker $H_{li}C_i = \mathcal{S}_l^* +$ Ker C_i. Let M_{li} be a unique solution to $M_{li}P_l = H_{li}C_i$ and $A_{li} = (A_i + D_{li}C_i : \mathcal{X}/\mathcal{S}_l^*)$, $A_{li}^\tau = (A_{\tau i} + D_{li}^\tau C_i : \mathcal{X}/\mathcal{S}_l^*)$ where

$$\begin{aligned} P_l(A_i + D_{li}C_i) &= A_{li}P_l \\ P_l(A_{\tau i} + D_{li}^\tau C_i) &= A_{li}^\tau P_l \end{aligned} \tag{6.46}$$

Let T_{li}, T_{li}^τ and R_{li} be the solution to the inequality (6.45) and define $G_{li} = R_{li}^{-1}T_{li}$, $G_{li}^\tau = R_{li}^{-1}T_{li}^\tau$, $F_{li} = A_{li} + G_{li}M_{li}$, $F_{li}^\tau = A_{li} + G_{li}^\tau M_{li}$, $E_{li} = P_l(D_{li} + P_l^{-r}G_{li}H_{li})$, $E_{li}^\tau = P_l(D_{li}^\tau + P_l^{-r}G_{li}^\tau H_{li})$. Let $K_{li} = P_lB_i$. Define $e_l(t) = w_l(t) - P_lx(t)$, then using (6.42) we have

$$\begin{aligned} \dot{e}_l(t) &= F_{li}w_l(t) + F_{li}^\tau w_l(t-\tau_i(t)) - E_{li}y(t) - E_{li}^\tau y(t-\tau_i(t)) + K_{li}u(t) \\ &\quad - P_l(A_ix(t) + A_{\tau i}x(t-\tau_i(t)) + B_iu(t) + B_{di}d(t) + \sum_{l=1}^{L} L_{li}m_l(t)) \\ &= F_{li}w_l(t) + F_{li}^\tau w_l(t-\tau_i(t)) - P_lL_{li}m_l(t) - P_lB_{di}d(t) \\ &\quad - P_l(A_i + D_{li}C_i)x(t) - G_{li}H_{li}C_ix(t) - P_l(A_{\tau i} + D_{li}^\tau C_i)x(t-\tau_i(t)) \\ &\quad - G_{li}^\tau H_{li}C_ix(t-\tau_i(t)) - E_{li}D_{di}d(t) - E_{li}^\tau D_{di}d(t-\tau_i(t)) \\ &= F_{li}w_l(t) + F_{li}^\tau w_l(t-\tau_i(t)) - P_lL_{li}m_l(t) - A_{li}P_lx(t) \\ &\quad - G_{li}M_{li}P_lx(t) - A_{li}^\tau P_lx(t-\tau_i(t)) - G_{li}^\tau M_{li}P_lx(t-\tau_i(t)) \\ &\quad + (B_{dli} - G_{li}H_{li}D_{di})d(t) - (P_lD_{li}^\tau D_{di} - G_{li}^\tau H_{li}D_{di})d(t-\tau_i(t)) \\ &= (A_{li} + G_{li}M_{li})e_l(t) + (A_{li}^\tau + G_{li}^\tau M_{li})e_l(t-\tau_i(t)) - P_lL_{li}m_l(t) \\ &\quad + (B_{dli} - G_{li}H_{li}D_{di})d(t) - (P_lD_{li}^\tau D_{di} + G_{li}^\tau H_{li}D_{di})d(t-\tau_i(t)) \end{aligned}$$

Note that $P_lL_{ji} = 0, j \neq l, j \in \mathbf{L}, i \in \Psi$, since $\mathcal{L}_{ji} \in \mathcal{S}_l^*, j \neq l$. Also

$$\begin{aligned} r_l(t) &= M_{li}w_l(t) - H_{li}y(t) = M_{li}w_l(t) - H_{li}C_ix(t) - H_{li}D_{di}d(t) \\ &= M_{li}e_l(t) - H_{li}D_{di}d(t) \end{aligned}$$

Consequently, the error dynamics can be written as

$$\begin{aligned}
\dot{e}_l(t) &= (A_l(\lambda_t) + G_l(\lambda_t)M_l(\lambda_t))e_l(t) + (A_l^\tau(\lambda_t) + G_l^\tau(\lambda_t)M_l(\lambda_t))e_l(t-\tau_{\lambda_t}(t)) \\
&\quad - P_l L_l(\lambda_t)m_l(t) + [B_{dl}(\lambda_t), -P_l D_l^\tau(\lambda_t)D_d(\lambda_t)]\bar{d}(\lambda_t) \\
&\quad + [-G_l(\lambda_t)H_l(\lambda_t)D_d(\lambda_t), -G_l^\tau(\lambda_t)H_l(\lambda_t)D_d(\lambda_t)]\bar{d}(\lambda_t) \\
r_l(t) &= M_l(\lambda_t)e_l(t) + [-H_l(\lambda_t)D_d(\lambda_t), 0]\bar{d}(\lambda_t)
\end{aligned} \tag{6.47}$$

where $\bar{d}(\lambda_t) = [d(t)^\top, d(t-\tau_{\lambda_t}(t)^\top]^\top$. Using Lemma 6.8 and the inequality (6.45), it follows that the error dynamics is exponentially mean square stable and the inequality (6.40) holds. Moreover, from the error dynamics (6.47), it follows that $r_l(t)$ is only affected by $L_l(\lambda_t)$ and is decoupled from other fault signatures. ■

Corollary 6.1. *The necessary condition for the existence of a solution to the H_∞-EFPRG problem is that*

$$\mathcal{L}_{li} \bigcap (\sum_{x=1}^{N} \sum_{j=1, j\neq l}^{L} \mathcal{L}_{jx}) = 0, \quad i \in \Psi, \quad l \in \boldsymbol{L} \tag{6.48}$$

Proof: Clearly if $\mathcal{L}_{li} \subset (\sum_{x=1}^{N} \sum_{j=1,j\neq l}^{L} \mathcal{L}_{xj})$, then

$$\mathcal{L}_{li} \subset \mathcal{S}_l^* = \inf \underline{\mathcal{S}}(\sum_{x=1}^{N} \sum_{j=1, j\neq l}^{L} \mathcal{L}_{jx})$$

and hence the necessary condition (6.44) in Theorem 6.4 does not hold. ■

6.5 Fault Detection and Isolation Decision Criteria

Once the residual signals $r_i(t), i \in \mathbf{k}$ are constructed, the final step for performing fault detection and isolation is to determine the threshold values J_{th_i} and the evaluation functions $J_{r_i}(t)$. For retarded and neutral time-delay systems the following

thresholds and evaluation functions are selected

$$J_{r_i}(t) = \frac{1}{T_0}\int_{t-T_0}^{t} r_i^\top(t) r_i(t) dt, \quad i \in \mathbf{k} \tag{6.49}$$

$$J_{th_i} = \sup_{d,\tilde{u},\tilde{x}\in\mathfrak{L}_2, m_j=0, j\in\mathbf{k}} (J_{r_i}), \quad i \in \mathbf{k} \tag{6.50}$$

where T_0 is the length of the evaluation window. Similarly, the following thresholds and evaluation functions are selected for distributed delay systems and Markovian jump systems with time-delay:

$$J_{r_i}(t) = \frac{1}{T_0}\int_{t-T_0}^{t} r_i^\top(t) r_i(t) dt, \quad i \in \mathbf{k} \tag{6.51}$$

$$J_{th_i} = \sup_{d\in L_2, m_j=0, j\in\mathbf{k}} (J_{r_i}), \quad i \in \mathbf{k} \tag{6.52}$$

The main advantage of using the evaluation functions proposed above is that one can also easily detect intermittent faults . The evaluation function $J_{r_i}(t) = r_i(t)$ *is not* applicable for time-delay systems since often there exist oscillations in the residual signals of time-delay systems. By selecting a variable window size $T_0 = t$, the evaluation function becomes a truncated $\mathfrak{L}_2$ norm of the residual, however one may then not be able to detect a removal of the fault from the system. According to Assumptions 6.1, 6.3 and 6.5 for retarded and neutral time-delay system, there exist positive numbers σ_d, σ_x and σ_u such that $||d||_2 \leq \sigma_d$, $||\tilde{x}||_2 \leq \sigma_x$ and $||\tilde{u}||_2 \leq \sigma_u$. Therefore, during the healthy operation of the system the threshold is selected as $J_{th_i} = \gamma^2(\sigma_d^2 + \sigma_x^2 + \sigma_u^2)$. Based on the thresholds and the evaluation functions, the occurrence of a fault can then be detected and isolated by using the following decision logics

$$J_{r_i}(t) > J_{th_i} \Longrightarrow m_i \neq 0, \quad i \in \mathbf{k} \tag{6.53}$$

6.6 Numerical Examples

To illustrate the effectiveness and capabilities of our proposed FDI algorithms, a couple of numerical examples are provided in this section for retarded, neutral,

distributed and stochastic time-delay systems.

6.6.1 Retarded Time-Delay System

A dynamic model for a water-quality system corresponding to a representative reach of the River Nile as presented in [220] is considered for the retarded time-delay system (6.6). The model is specified according to the following matrices:

$$A_0 = \begin{bmatrix} -1 & 1 \\ -2 & -3 \end{bmatrix}, A_1 = \begin{bmatrix} 0 & -0.1 \\ 0.5 & 1 \end{bmatrix}, B_0 = \begin{bmatrix} 1 & 0 \\ 0.2 & 0.5 \end{bmatrix}$$

$$C = \begin{bmatrix} 0.5 & 0 \\ 0 & 0.1 \end{bmatrix}, \Delta A_0 = \begin{bmatrix} 0.1sin(2t) & -0.3sin(2t) \\ -0.1sin(t) & 0.075sin(3t) \end{bmatrix}$$

$$\Delta A_1 = \begin{bmatrix} -0.2sin(2t) & 0.1sin(3t) \\ 0.1sin(t) & -0.175sin(t) \end{bmatrix}$$

$$\Delta B_0 = \begin{bmatrix} 0.25sin(t) & -0.15sin(2t) \\ -0.15sin(t) & 0.05sin(3t) \end{bmatrix}$$

where ΔA_0, ΔA_1 and ΔB_0 represent uncertainties in the matrices A_0, A_1 and B_0, respectively. The value of the delay is given as $\tau_{x1}(t) = 0.1|cos(6t)|$, $N = 1$, $k = 2$, and $L = 0$. The state variables are the concentrations of pollutants A (a mixture of the low levels in the bio-strata) and pollutant B (a mixture of the other level in the bio-strata). The control inputs are the relative changes in the effluent waste discharge and in-stream aeration rate. The fault signatures L_1 and L_2 are selected as the first and the second columns of the matrix B_0 so that they represent actuator faults. The input disturbance $v(t) = B_d d(t)$ and the output measurement noise $w(t) = D_d d(t)$ are given by

$$v(t) = \begin{bmatrix} 0.2 + 0.6sin(t) \\ 0.1 + 0.09sin(3t) \end{bmatrix}, w(t) = \begin{bmatrix} 0.1sin(3t) \\ 0.2sin(t) \end{bmatrix}$$

where the disturbance signal $d(t)$ is selected as $d(t) = [1, sin(t), sin(3t)]^{\mathsf{T}}$.

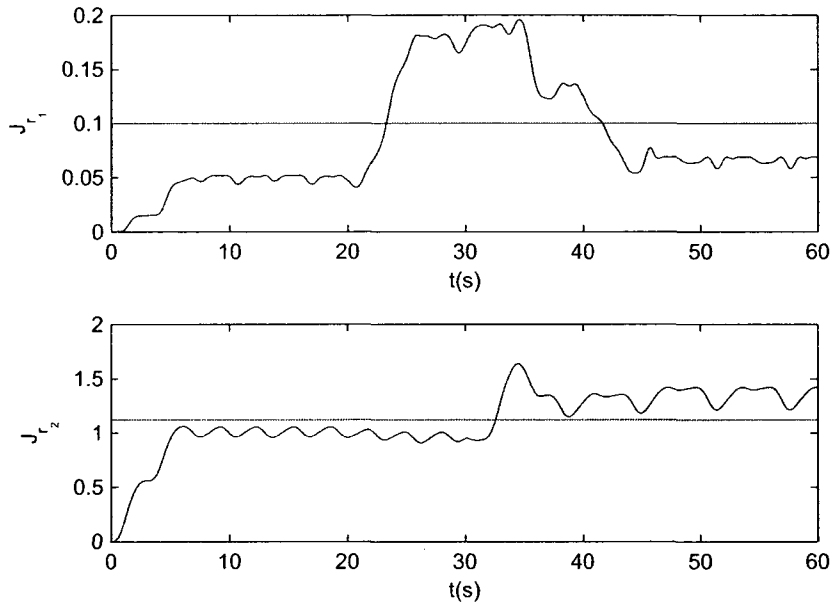

Figure 6.1: Evaluation functions corresponding to multiple faults that are injected in both actuators.

The subspaces that are needed in Theorem 6.1 for the above retarded time-delay system are determined according to Algorithm 6.2, and are obtained as $\mathcal{S}_1^* = \mathcal{L}_1$ and $\mathcal{S}_2^* = \mathcal{L}_2$. After determining the subspaces $\mathcal{S}_1$ and $\mathcal{S}_2$, the maps D_{i0}, $D_{i1}, H_i, M_i, i = 1, 2$ and matrices $A_{0_{\mathcal{S}_1^*}}, A_{1_{\mathcal{S}_1^*}}, A_{0_{\mathcal{S}_2^*}}, A_{1_{\mathcal{S}_2^*}}$ can be found according to Theorem 6.1. The gain matrices G_{10}, G_{11}, G_{20} and G_{21} are computed by solving the LMI inequality (6.12) for $\gamma = 5$ and $\tau_1^x = 0.1$. The thresholds are calculated as $J_{th_1} = 0.1$ and $J_{th_2} = 1.12$ for $T_0 = 6$ seconds.

Figure 6.1 shows the residual evaluation functions corresponding to multiple faults in both actuators where a lock in place fault ($m_1 = -u_1 + 1$) is injected in the first actuator between $t = 20$ and $t = 40$ seconds and a hard over fault ($m_2 = -u_2 + 5$) is injected in the second actuator at $t \geq 30$ seconds. According to this figure, the fault in the first actuator is detected between $t = 23.1$ and $t = 41.2$ seconds and the fault in the second actuator is detected at $t = 32$ seconds. As shown in Figure 6.2 the time-delay system states remain stable in the above fault scenario

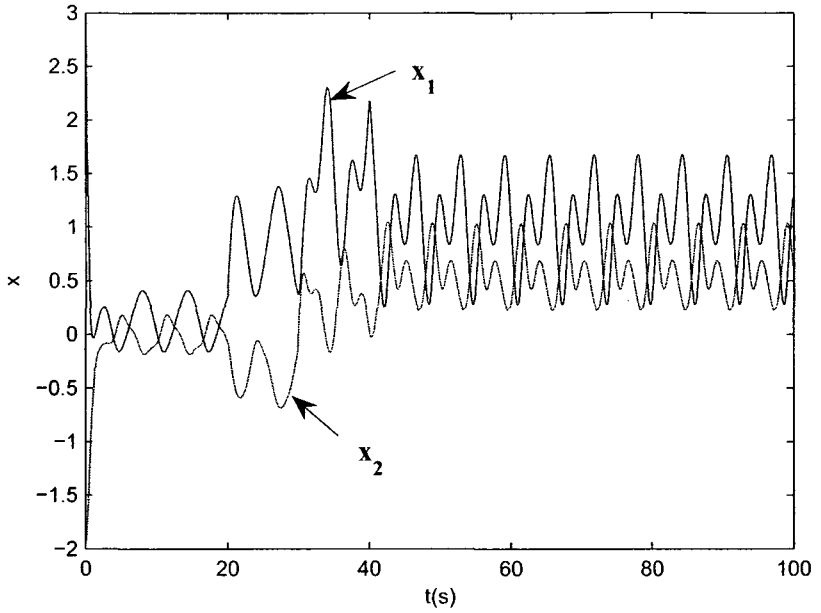

Figure 6.2: System states corresponding to multiple faults scenario.

which not only makes the task of the FDI scheme more challenging, but also ensures that Assumption 3 holds .

6.6.2 Neutral Time-Delay System

Consider the time-delay system (6.15) that is specified according to the following matrices

$$A_0 = \begin{bmatrix} 1 & 2.5 & -1 & 2 \\ 0 & -1 & 1.5 & 1 \\ 1 & 3 & -2 & 0 \\ 2 & 0 & -1 & 2 \end{bmatrix}, A_1 = \begin{bmatrix} -1 & 1 & 0.1 & 0 \\ -0.2 & 2.3 & 0.4 & 1 \\ 0.3 & -2 & 4 & 0.2 \\ 1 & 0.2 & 3 & 2 \end{bmatrix}$$

$$A_2 = \begin{bmatrix} -0.1 & 0 & 0.0 & 0.1 \\ 0.2 & -0.1 & 0.2 & 0.3 \\ 0.4 & 0.3 & 0.4 & 0.1 \\ -0.1 & 0 & 0.2 & 0.3 \end{bmatrix}, C = \begin{bmatrix} 0.2 & 0.3 & 0 & 0 \\ 0 & 0.2 & 0.8 & 0 \\ 0 & 0 & 0 & 1 \end{bmatrix}$$

$$B_0 = \begin{bmatrix} 0.5 & 0 \\ 1 & 2 \\ 0.7 & 1 \\ 0 & 2 \end{bmatrix}, B_d = \begin{bmatrix} 0.2 \\ 0.3 \\ 0.1 \\ 0.4 \end{bmatrix}, D_d = \begin{bmatrix} 0.1 \\ 0.1 \\ 0.2 \end{bmatrix}$$

and $\tau(t) = 1 + 0.1cos(0.1t)$ and $\tau_d(t) = 0.9 + 0.1cos(0.2t)$. The fault signatures L_1 and L_2 are selected as the first and the second columns of the matrix B_0, and hence they represent actuator faults.

The subspaces that are needed in Theorem 6.2 for the above time-delay system are determined according Algorithm 6.2 and are obtained as $\mathcal{S}_1^* = \mathcal{L}_1$ and $\mathcal{S}_2^* = \mathcal{L}_2$. After determining the subspaces $\mathcal{S}_1^*$ and $\mathcal{S}_2^*$, the maps D_{i0}, $D_{i1}, D_{i2}, H_i, M_i, i = 1, 2$ and matrices $A_{0_{\mathcal{S}_1^*}}, A_{1_{\mathcal{S}_1^*}}, A_{2_{\mathcal{S}_1^*}}$, $A_{0_{\mathcal{S}_2^*}}, A_{1^*_{\mathcal{S}_2}}, A_{2^*_{\mathcal{S}_2}}$ can be found according to Theorem 6.2. The gain matrices $G_{10}, G_{11}, G_{12}, G_{20}, G_{21}$ and G_{22} are computed by solving the LMI inequality (6.21) for $\gamma = 1$. An H_∞ robust state feedback control $u(t) = Kx(t)$ is also designed to ensure the stability of the closed-loop system.

A disturbance input signal $d(t)$ is assumed to be a band-limited white-noise with the power of 0.01. Constant upper bounds for the delays $\bar{\tau} = 1.1$ and $\bar{\tau}_d = 1$ are considered in the residual generator (6.18). The thresholds are calculated as $J_{th_1} = 0.05$ and $J_{th_2} = 0.11$ for $T_0 = 5$ seconds. Figure 6.3 shows the residual evaluation functions corresponding to multiple faults in both actuators where a 90% loss of effectiveness (gain) fault is injected in the first actuator at $t = 20$ seconds ($m_1 = -0.9u_1$) and an 80% loss of effectiveness (gain) fault is injected in the second actuator ($m_2 = -0.8u_2$) between $t = 20$ and $t = 40$ seconds. According to this figure, the fault in the first actuator is detected at $t = 26.1$ seconds and the fault in

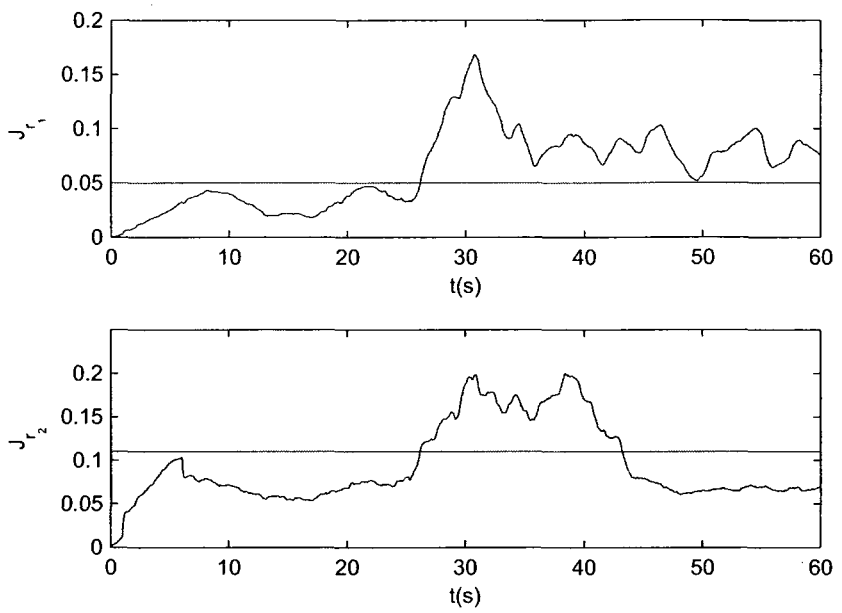

Figure 6.3: Evaluation functions corresponding to multiple faults that are injected in both actuators.

the second actuator is detected between $t = 26.2$ and $t = 43.2$ seconds. It can be observed that the time-delay system states also remain stable for all time.

Remark 6.5. *It should be pointed out that the fault detection time is independent from the choice of T_0. This is due to presence of the term $\frac{1}{T_0}$ in the evaluation function* (6.49). *However for small evaluation window time (typically $T_0 < 4$ seconds), the evaluation function may show excessive and rapid oscillatory behavior in and out of the threshold region after the occurrence of a fault, and this will make the FDI decision making logic quite challenging. However, for sufficiently large evaluation window time (i.e., $T_0 \geq 6$ seconds), the evaluation functions are observed to have indeed a smooth and stable behavior.*

In conclusion, it should be emphasized that the presently available algorithms in the literature for both retarded and neutral time-delay systems cannot generate residual signals that enjoy the above FDI decoupling properties. For example, by using the UIO approach [123], and the associated restrictions that are imposed on

the system structure, the class of retarded time-delay systems that one can generate the decoupled residuals are made significantly limited. In the algorithms developed in [124], [125], [126], [127, 128], [129] for retarded time-delay systems with known delays, faults that one needs to decouple are considered as unknown inputs and the algorithms seek to attenuate the effects of both faults and disturbances on the residual. Therefore, these types of algorithms cannot decouple fault effects from the residuals. Also, in the adaptive fault identification approach that is developed in [210], [211], [212], the delays are assumed to be known *a priori*. However, by using our proposed detection filters approach the residual signals partially decouple the faults from each other and remain robust to disturbances and uncertainties that arise due to unknown delays. Consequently, one can successfully apply these residuals for both fault detection and isolation.

6.6.3 Distributed Time-delay systems

To illustrate the effectiveness and capabilities of our proposed FDI algorithm, two examples are provided in this section for systems with distributed delay. Consider the distributed time-delay system (6.25) that is specified according to the following parameters

$$A_0 = \begin{bmatrix} 2 & -1.5 & 1 & 1 \\ 1 & -1 & 0.5 & 2 \\ 1 & 2 & -3 & 0 \\ 2 & 0 & -1 & 1 \end{bmatrix}, B = \begin{bmatrix} 1 & 0 \\ 1 & 1 \\ 1 & 1 \\ 0 & 1 \end{bmatrix}, A_1 = \begin{bmatrix} -1 & 2 & 0.2 & 0 \\ -0.1 & 1.3 & 0.5 & 1 \\ 0.1 & -1 & 2 & 0.1 \\ 1 & 0.1 & 1 & 2 \end{bmatrix}$$

$$A_2 = \begin{bmatrix} 0.1 & 0 & 0.0 & 0.1 \\ 0.2 & -0.1 & 0.2 & 0.3 \\ 0.4 & 0.3 & 0.4 & 0.1 \\ -0.1 & 0 & 0.2 & 0.3 \end{bmatrix}, C_0 = \begin{bmatrix} 1 & 1 & 0 & 0 \\ 0 & 0.2 & 1 & 0 \\ 0 & 0 & 0 & 1 \end{bmatrix}, D_{d0} = \begin{bmatrix} 0.01 \\ 0.02 \\ 0 \end{bmatrix}$$

$$C_1 = \begin{bmatrix} 1 & 0 & 1 & 0 \\ 0 & 0.1 & 0 & 0.5 \\ 0 & 0 & 0 & 1 \end{bmatrix}, D_{d1} = \begin{bmatrix} 0.02 \\ -0.01 \\ 0.01 \end{bmatrix}, C_2 = \begin{bmatrix} 0 & 0 & 1 & 0 \\ 1 & 0.1 & 0 & 0.5 \\ 0 & 1 & 0 & 1 \end{bmatrix},$$

$$B_d = \begin{bmatrix} 0.3 \\ 0.2 \\ 0 \\ 0.6 \end{bmatrix}, D_{d2} = \begin{bmatrix} 0.03 \\ 0.0 \\ 0.02 \end{bmatrix}$$

and $\tau_1 = 1$ and $\tau_2 = 2$. The fault signatures L_1 and L_2 are selected as the first and the second columns of the matrix B, and hence they represent actuator faults for the distributed time-delay system (6.25).

The subspaces defined in Theorem 6.3 for the above time-delay system can be determined by using Algorithm 5.3 and are given by $\mathcal{S}_1^* = \mathcal{L}_2$, and $\mathcal{S}_2^* = \mathcal{L}_1$. According to Theorem 6.3, the matrices that specify the governing dynamics of the first detection filter r_1 in (6.27) are found through the following steps (all the geometric manipulations are performed by using the "geometric approach toolbox" [200]) :

1. The output injection maps $D_{1j}, j = 0, 1, 2$ are obtained from $\mathcal{S}_1^*$ as

$$D_{10} = \begin{bmatrix} -0.0359 & -0.1233 & -0.3161 \\ 0.4955 & -0.9529 & -0.6854 \\ -0.4518 & 0.8688 & 0.5759 \\ -0.0437 & 0.0841 & 0.1095 \end{bmatrix}, D_{11} = \begin{bmatrix} -0.5850 & -0.9641 & -1.0365 \\ 0.0775 & -0.3630 & -0.3264 \\ 0.1045 & 0.5871 & 0.7766 \\ -0.1820 & -0.2241 & -0.4502 \end{bmatrix}$$

$$D_{12} = \begin{bmatrix} -0.0057 & -0.0618 & -0.0286 \\ 0.0531 & -0.0290 & 0.0655 \\ -0.0894 & -0.0837 & -0.0469 \\ 0.0363 & 0.1127 & -0.0186 \end{bmatrix}$$

2. The measurement maps $H_{1j}, j = 0, 1, 2$ are found by solving $\mathrm{Ker} H_{1j} C_j = \mathrm{Ker} C_j + \mathcal{S}_1^*$ as

$$H_{10} = \begin{bmatrix} -0.6727 & 0.3798 & 0.2170 \\ -0.0000 & -0.6350 & 0.7620 \end{bmatrix}, H_{11} = \begin{bmatrix} 0.6325 & -3.1623 & 1.2649 \\ -0.0000 & -7.0711 & 4.2426 \end{bmatrix}$$

$$H_{12} = \begin{bmatrix} 0.0000 & -0.9623 & 0.2887 \\ -0.8165 & 0.0000 & 0.4082 \end{bmatrix}$$

3. The canonical projection map P_1 for $\mathcal{S}_1^*$ is given by

$$P_1 = \begin{bmatrix} -1.0000 & -0.0000 & -0.0000 & -0.0000 \\ 0.0000 & -0.8165 & 0.4082 & 0.4082 \\ 0.0000 & -0.0000 & -0.7071 & 0.7071 \end{bmatrix}$$

4. The M_{1j} maps are the unique solutions to $M_{1j} P_1 = H_{1j} C_j,\ j = 0, 1, 2$ as

$$M_{10} = \begin{bmatrix} 0.6727 & 0.7309 & -0.1151 \\ 0.0000 & 0.1555 & 0.9878 \end{bmatrix}, M_{11} = \begin{bmatrix} -0.6325 & 0.3873 & -0.6708 \\ 0.0000 & 0.8660 & 0.5000 \end{bmatrix}$$

$$M_{12} = \begin{bmatrix} 0.9623 & -0.2357 & -0.1361 \\ -0.0000 & -0.5000 & 0.8660 \end{bmatrix}$$

5. The induced maps $\bar{A}_{1j}, j = 0, 1, 2$ are found as follows

$$\bar{A}_{10} = \begin{bmatrix} 1.9641 & -1.9113 & 0.1363 \\ 0.1986 & -1.5426 & 0.3456 \\ -0.9957 & 1.5146 & -0.3408 \end{bmatrix}, \bar{A}_{11} = \begin{bmatrix} -1.5850 & 2.3314 & 0.8015 \\ -0.4358 & 1.6956 & -0.0416 \\ -0.4339 & -0.8824 & 0.7770 \end{bmatrix}$$

$$\bar{A}_{12} = \begin{bmatrix} 0.0382 & -0.0426 & -0.0327 \\ 0.0053 & -0.1561 & -0.1136 \\ 0.2147 & 0.2183 & 0.2004 \end{bmatrix}$$

6. The maps $G_{1j}, j = 0, 1, 2$ are obtained by solving the LMI (6.30) for $\gamma = 1$ using the YALMIP LMI Toolbox [201] which yields

$$G_{10} = \begin{bmatrix} -66.3671 & -58.2271 \\ 38.2785 & -2.7080 \\ 76.8216 & 9.5632 \end{bmatrix}, G_{11} = \begin{bmatrix} -1.7245 & -4.2608 \\ -0.8243 & -0.6796 \\ 0.4630 & 0.1002 \end{bmatrix}$$

$$G_{12} = \begin{bmatrix} -0.1569 & 0.1878 \\ -0.0496 & -0.0866 \\ -0.0592 & -0.0412 \end{bmatrix}$$

7. Finally, the maps $F_{1j}, E_{1j},\ j = 0, 1, 2$ and K_1 are found according to Theorem 6.3.

The matrices for the second detection filer r_2 can be found by following the same steps as above. A disturbance input $d(t)$ is assumed to be a band-limited white-noise with power of 0.05. The thresholds are calculated as $J_{th_1} = 0.01$ and $J_{th_2} = 0.015$ for $T_0 = 5$ seconds. Figure 6.4 shows the residuals and the evaluation functions corresponding to a permanent fault in the first actuator (u_1) of the system where the gain of the actuator is decreased by 60% at $t = 10$ seconds. This type of fault can be modeled as $m_1(t) = -0.60u_1(t)$, where $m_1(t)$ is the fault mode of the first actuator. As shown in this figure, the fault is detected and isolated at

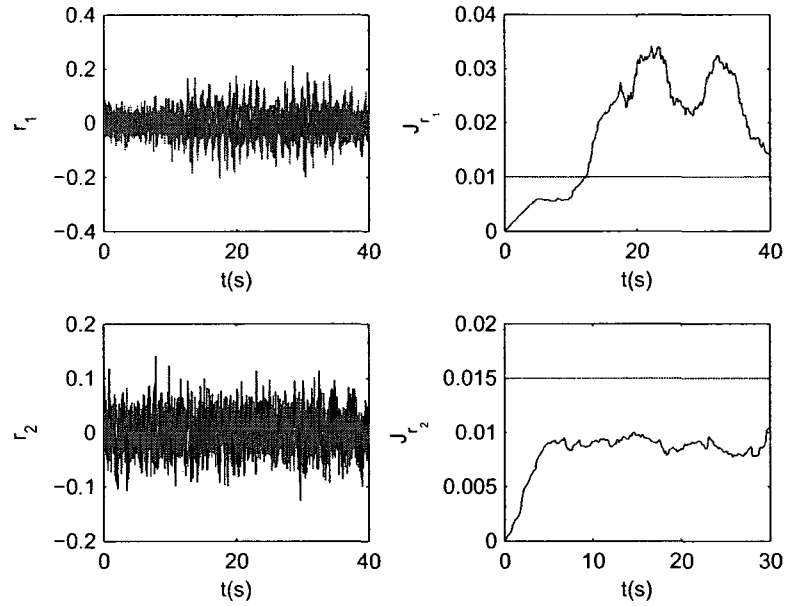

Figure 6.4: Residual signals and their evaluation functions corresponding to a fault in the first actuator.

$t = 12.3$ seconds and the evaluation function of the residual r_2 (i.e. $J(r_2)$) remains below its corresponding threshold. Figure 6.5 shows the residuals and the evaluation functions corresponding to simultaneous faults in both actuators where a permanent 60% loss of effectiveness (gain) fault is injected in the first actuator at $t = 10$ seconds and an intermittent 55% loss of effectiveness fault is injected in the second actuator between $t = 15$ and $t = 25$ seconds. According to this figure, the fault in the first actuator is detected at $t = 12.3$ seconds and the fault in the second actuator is detected at $t = 15.6$ seconds. It should be noted that in all the above scenarios the time-delay system remains stable and well-behaved, which makes the FDI problem more challenging.

6.6.4 Combustion System in a Rocket Motor Chamber

In this section, our proposed FDI algorithm is applied to a combustion system in a rocket motor chamber [221]. A liquid monopropellant rocket motor with a

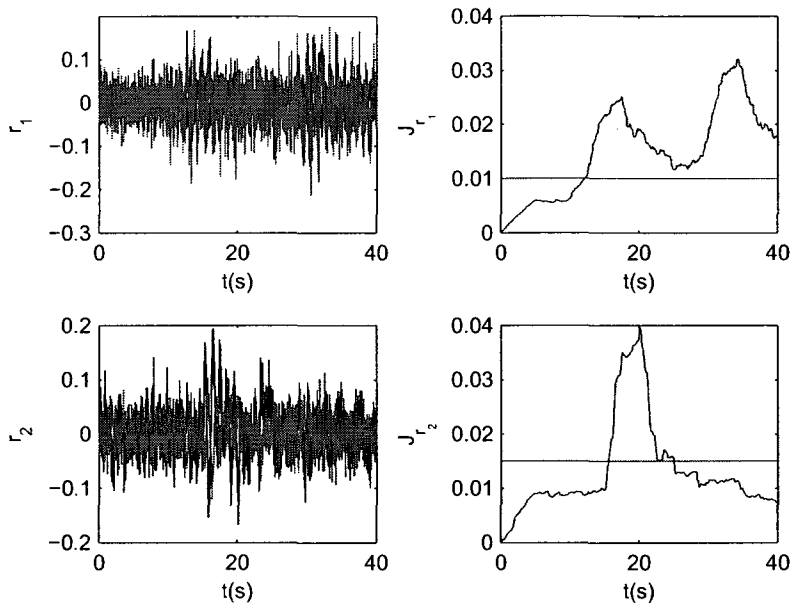

Figure 6.5: Residual signals and their evaluation functions corresponding to concurrent faults in both actuators.

pressure feeding system is considered. A linearized model of the feeding system and the combustion chamber process has been obtained in [222] and [223]. The linearized model has four states $x(t) = [x_1(t), x_2(t), x_3(t), x_4(t)]^\top$ where x_1 is the relative deviations of the instantaneous combustion chamber pressure, x_2 is the instantaneous mass flow upstream of the capacitance, x_3 is the instantaneous mass rate of the injected propellant from its steady value, and x_4 is the ratio between the deviation of the instantaneous pressure in a special place in the feeding line from its value in steady state operation and twice the injector pressure drop in steady

operation. The corresponding matrices of system (6.25) are governed by

$$A_0 = \begin{bmatrix} \rho - 1 & 0 & 0 & 0 \\ 0 & 0 & 0 & -\frac{1}{\zeta J} \\ -0.5\frac{p}{(1-\zeta)J} & 0 & -\frac{1}{(1-\zeta)J} & \frac{1}{(1-\zeta)J} \\ 0 & \frac{1}{E_e} & -\frac{1}{E_e} & 0 \end{bmatrix}, B = \begin{bmatrix} 0 \\ \frac{1}{\zeta J} \\ 0 \\ 0 \end{bmatrix}, A_2 = \begin{bmatrix} \frac{\rho}{\tau_2} & 0 & \frac{1}{\tau_2} & 0 \\ 0 & 0 & 0 & 0 \\ 0 & 0 & 0 & 0 \\ 0 & 0 & 0 & 0 \end{bmatrix}$$

$$C_0 = C_2 = \begin{bmatrix} 1 & 0 & 0 & 0 \\ 0 & 1 & 0 & 0 \\ 0 & 0 & 0 & 1 \end{bmatrix}, D_{d0} = D_{d2} = \begin{bmatrix} 0.1 \\ 0.2 \\ -0.3 \end{bmatrix}, A_1 = 0, C_1 = 0, B_d = \begin{bmatrix} 0 \\ 0 \\ 1 \\ 0 \end{bmatrix}$$

where $\zeta = 0.1$ is the fractional length for the pressure supply, $J = 2$ is the line inertia, $E_e = 1$ is the line elasticity parameter, $p = 1$ is the ratio of steady-state pressure over the steady-state injector pressure drop, $\tau_2 = 1$, and ρ is the pressure exponent of the combustion with a nominal value of 1. The uncertainty in the system is represented in ρ as $\rho = \rho_0 + \Delta\rho$ with $\Delta\rho \in [-\delta\rho_{max}, +\delta\rho_{max}]$.

The FDI problem for the combustion chamber is to generate a residual signal $r_1(t)$ such that a) it is only affected by the actuator fault, b) the effect of the uncertainty in ρ on the residual r_1 is zero, (that is $r_1(t)$ is completely decoupled from $\Delta\rho$), and c) the effect of the disturbance input on $r_1(t)$ is attenuated with a factor γ. Towards this end, the fault signature L_1 is selected as B and the effect of uncertainty in ρ is modeled with the term $L_2 m_2(t)$ where $L_2 = \left[\begin{smallmatrix} 1 & 1 \\ 0 & 0 \\ 0 & 0 \\ 0 & 0 \end{smallmatrix}\right]$ and $m_2(t) = \left[\begin{smallmatrix} \Delta\rho x_1(t) \\ -\Delta\rho \int_{t-\tau_2}^{t} x_1(s)ds \end{smallmatrix}\right]$. The subspace $\mathcal{S}_1^* = \inf \underline{\mathcal{S}}_D(\mathcal{L}_2)$ in Theorem 6.3 for the combustion chamber system is determined by using Algorithm 5.3 and given by

$$\mathcal{S}_1^* = \begin{bmatrix} 1 & 0 & 0 \\ 0 & 0.9939 & 0 \\ 0 & -0.1105 & 0 \\ 0 & 0 & -1 \end{bmatrix} \tag{6.54}$$

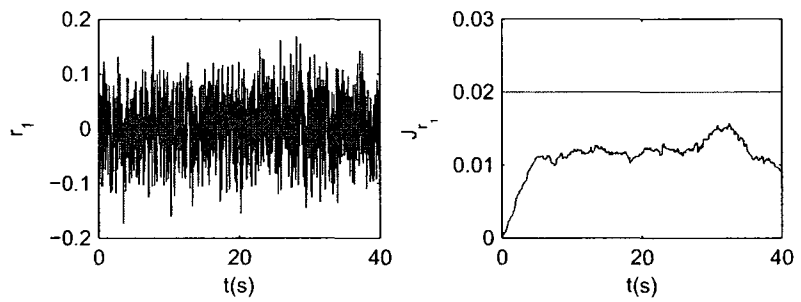

Figure 6.6: Residual signal and its evaluation function corresponding to the normal mode (healthy operation).

It is clear that $\mathcal{S}_1^* \cap L_1 = 0$ and hence decoupling between the actuator fault and the uncertainty term is possible. After determining the subspace $\mathcal{S}_1^*$, the maps D_{1j}, H_{1j}, M_{1j}, $j = 0, 2$ and matrices $\bar{A}_{1j}$, $j = 0, 2$ can be found according to Theorem 6.3. The maps $G_{1j}, j = 0, 2$ are obtained by solving the LMI condition (6.30) by using the YALMIP LMI Toolbox [201] for $\gamma = 0.1$.

A disturbance input $d(t)$ is assumed to be a band-limited white-noise with a power of 0.1. The threshold is calculated as $J_{th_1} = 0.02$ for $T_0 = 5$ seconds. It is assumed that the uncertainty in ρ is characterized by $\Delta\rho = 0.3sin(t)$. Figure 6.6 shows the residual and its evaluation function corresponding to the healthy operation of the system. As shown in this figure no false alarm is generated during the normal operation of the system due to the uncertainty in ρ and the residual signal is completely decoupled from $\Delta\rho$. Figure 6.7 shows the residual and the evaluation function corresponding to a permanent fault in the actuator of the system where the gain of the actuator is decreased by 50% at $t = 20$ seconds. This type of fault can be modeled as $m_1(t) = -0.50u_1(t)$, where $m_1(t)$ is the fault mode of the first actuator. As shown in this figure, the fault is detected at $t = 29.6$ seconds.

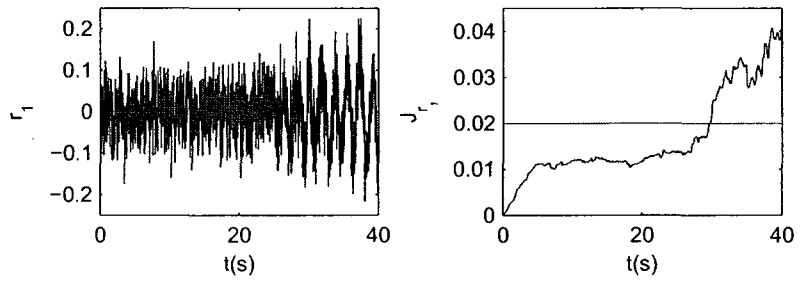

Figure 6.7: Residual signal and its evaluation function corresponding to a fault in the actuator.

6.6.5 Markovian Jump Systems with Mode-dependent Delay

To illustrate the effectiveness and capabilities of our proposed FDI algorithm, a numerical example is provided in this section. Consider the Markovian jump system with mode dependent time-delays (6.32) that is specified with the following parameters [219],

$$A_1 = \begin{bmatrix} -3 & 1 & 0 \\ 0.3 & -2.5 & 1 \\ -0.1 & 0.3 & -3.8 \end{bmatrix}, A_{\tau 1} = \begin{bmatrix} -0.2 & 0.1 & 0.6 \\ 0.5 & -1 & -0.8 \\ 0 & 1 & -2.5 \end{bmatrix}$$

$$A_2 = \begin{bmatrix} -2.5 & 0.5 & -0.1 \\ 0.1 & -3.5 & 0.3 \\ -0.1 & 1 & -2 \end{bmatrix}, A_{\tau 2} = \begin{bmatrix} 0 & -0.3 & 0.6 \\ 0.1 & 0.5 & 0 \\ -0.6 & 1 & -0.8 \end{bmatrix}$$

$$B_1 = B_2 = \begin{bmatrix} 1 & 0 \\ 2 & 1 \\ 0 & -2 \end{bmatrix}, B_{d1} = \begin{bmatrix} 1 \\ 0 \\ 1 \end{bmatrix}, B_{d2} = \begin{bmatrix} -0.6 \\ 0.5 \\ 0 \end{bmatrix}$$

$$C_1 = \begin{bmatrix} 1 & 1 & 0 \\ 0 & 1 & 2 \end{bmatrix}, C_2 = \begin{bmatrix} 0 & 1 & 1 \\ 2 & 0 & 1 \end{bmatrix}, D_{d1} = \begin{bmatrix} 0.2 \\ 0.1 \end{bmatrix}, D_{d2} = \begin{bmatrix} 0.5 \\ -0.1 \end{bmatrix}$$

where $\tau_1(t) = 1+0.2sin(t)$ and $\tau_2(t) = 0.2+0.3sin(t)$ and the transition probabilities are given by

$$\Pi = \begin{bmatrix} -0.5 & 0.5 \\ 0.3 & -0.3 \end{bmatrix}$$

with uncertainty levels $\epsilon_{12} = 0.1$ and $\epsilon_{21} = 0.2$. The fault signatures L_1 and L_2 are selected as the first and the second columns of the matrix B_1, and hence represent actuator faults for the MJSD system.

According to the results of Theorem 5.12, first one needs to construct unobservability subspaces $\mathcal{S}_1^* = \inf \underline{\mathcal{S}}(\mathcal{L}_2)$ and $\mathcal{S}_2^* = \inf \underline{\mathcal{S}}(\mathcal{L}_1)$. These unobservability subspaces are obtained by using Algorithm 5.3 as $\mathcal{S}_1^* = \mathcal{L}_2$ and $\mathcal{S}_2^* = \mathcal{L}_1$. It can be verified that these two unobservability subspaces satisfy the necessary condition (6.44).

According to Theorem 5.12, the matrices that specify the governing dynamics of the detection filter in (6.42) for $l = 1$ (residual r_1) are found through the following steps (all the geometric manipulations are performed by using the "geometric approach toolbox" [200]) :

1. The output injection maps D_{11} and D_{11}^{τ} are obtained from $\mathcal{S}_1^* = \mathcal{L}_2$ as

$$D_{11} = \begin{bmatrix} -0.1556 & -0.3067 \\ 0.0778 & 0.1533 \\ -0.9741 & 1.2111 \end{bmatrix}, D_{11}^{\tau} = \begin{bmatrix} 0.0444 & -0.3667 \\ -0.0222 & 0.1833 \\ -1.1111 & 0.6667 \end{bmatrix}$$

2. The measurement maps $H_{1i}, i = 1, 2$ are found from equation Ker $H_{1i}C_i = \mathcal{S}_1^* +$ Ker C_i as

$$H_{11} = \begin{bmatrix} -0.3123 & 0.4685 \end{bmatrix}, H_{12} = \begin{bmatrix} -0.4472 & 0.4472 \end{bmatrix}$$

3. The canonical projection map P for $\mathcal{S}_1^*$ is given by

$$P = \begin{bmatrix} 0.8944 & -0.4472 & 0 \\ 0 & 0 & 1.0000 \end{bmatrix}$$

4. The maps $M_{1i}, i = 1, 2$ are the unique solutions to $M_i P = H_i C_i,\ i = 1, 2$ and are given by

$$M_{11} = \begin{bmatrix} -0.3492 & 0.9370 \end{bmatrix}, M_{12} = \begin{bmatrix} 1 & 0 \end{bmatrix}$$

5. The induced maps A_{1i} and $A_{1i}^{\tau},\ i = 1, 2$ are found from (6.46) as follows

$$A_{11} = \begin{bmatrix} -3.3444 & -1.1329 \\ -1.2009 & -1.3778 \end{bmatrix}, \ A_{12} = \begin{bmatrix} -0.7214 & -1.9901 \\ -0.3354 & -2.9500 \end{bmatrix},$$

$$A_{11}^{\tau} = \begin{bmatrix} -0.3944 & 0.0745 \\ -1.2423 & -1.1667 \end{bmatrix}, \ A_{12}^{\tau} = \begin{bmatrix} 0.1500 & 1.0510 \\ -0.4153 & -1.5000 \end{bmatrix}$$

6. The maps G_{1i} and G_{1i}^{τ} are obtained by solving LMI (6.45) for $\gamma = 0.5$, $\epsilon_{12} = 0.1$ and $\epsilon_{21} = 0.2$ by using the YALMIP LMI Toolbox [201] which yields

$$G_{11} = \begin{bmatrix} -2.1951 \\ -5.8824 \end{bmatrix}, G_{12} = \begin{bmatrix} -9.4233 \\ 0.5031 \end{bmatrix},$$

$$G_{11}^{\tau} = \begin{bmatrix} -0.2806 \\ 0.3104 \end{bmatrix}, G_{12}^{\tau} = \begin{bmatrix} 1.0041 \\ -0.9763 \end{bmatrix}$$

7. The maps F_{1i}, F_{1i}^{τ}, E_{1i}, and $E_{1i}^{\tau},\ i = 1, 2$ are found according to Theorem 5.12 as follows:

$$F_{11} = \begin{bmatrix} -2.5779 & -3.1898 \\ 0.8534 & -6.8898 \end{bmatrix}, F_{12} = \begin{bmatrix} -10.1448 & -1.9901 \\ 0.1677 & -2.9500 \end{bmatrix}$$

$$F_{11}^{\tau} = \begin{bmatrix} -0.2964 & -0.1884 \\ -1.3507 & -0.8758 \end{bmatrix}, F_{12}^{\tau} = \begin{bmatrix} 1.1541 & 1.0510 \\ -1.3915 & -1.5000 \end{bmatrix}$$

$$E_{11} = \begin{bmatrix} 0.5117 & -1.3713 \\ 0.8633 & -1.5449 \end{bmatrix}, E_{12} = \begin{bmatrix} 2.5244 & -4.2909 \\ -1.0750 & 0.1250 \end{bmatrix}$$

$$E_{11}^{\tau} = \begin{bmatrix} 0.1373 & -0.5414 \\ -1.2081 & 0.8121 \end{bmatrix}, E_{12}^{\tau} = \begin{bmatrix} -0.0242 & 0.5385 \\ -0.3777 & -0.3223 \end{bmatrix}$$

8. Finally, the maps $K_{1i},\ i = 1, 2$ are found from $K_{1i} = P_1 B_i$ as follows

$$K_{11} = K_{12} = \begin{bmatrix} 0.0000 & -0.4472 \\ 0 & -2.0000 \end{bmatrix}$$

The similar procedure can be used for finding the corresponding matrices for generating the residual signal $r_2(t)$.

An input disturbance $d(t)$ is assumed to be a band-limited white-noise with a power of 0.1. The evaluation window length is selected as $T_0 = 5$ seconds. The calculated thresholds are $J_{th_1} = 0.45$ and $J_{th_2} = 0.2$. Figure 6.8 shows the residuals and their evaluation functions corresponding to the healthy operation of the system. As shown in this figure, no false alarm is generated during normal operation of the system. Figure 6.9 shows the residuals and the evaluation functions corresponding to concurrent faults in both actuators where a 40% and a 30% loss of effectiveness (gain) permanent faults are injected in the first and the second actuators at $t = 10$ and $t = 20$ seconds, respectively. These faults can be modeled as $m_1(t) = -0.4u_1(t)$ and $m_2(t) = -0.3u_2(t)$, where $m_1(t)$ and $m_2(t)$ are the fault mode of the first and the second actuators, respectively. According to this figure, the fault in the first actuator is detected at $t = 11.6$ seconds and the fault in the second actuator is detected at $t = 20.5$ seconds. Figure 6.10 shows the residuals and the evaluation functions corresponding to an intermittent float fault in the first actuator of the system between $t = 10$ and $t = 20$ seconds. This fault can be modeled as $m_1(t) = -u_1(t)$. As shown in this figure, the fault is detected and isolated between $t = 10.5$ and $t = 25$ seconds and the evaluation function of r_2 (i.e. J_{r_2}) remains below its corresponding threshold for all time. It should be noted that in all the above scenarios the Markovian jump system remains stable and well-behaved, which makes the task of the FDI problem more challenging.

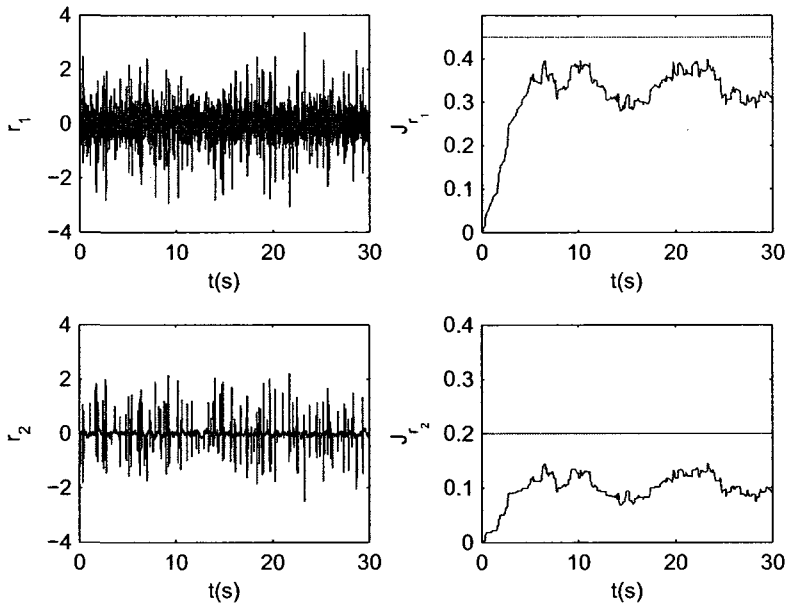

Figure 6.8: Residual signals and their evaluation functions corresponding to the normal mode (healthy operation).

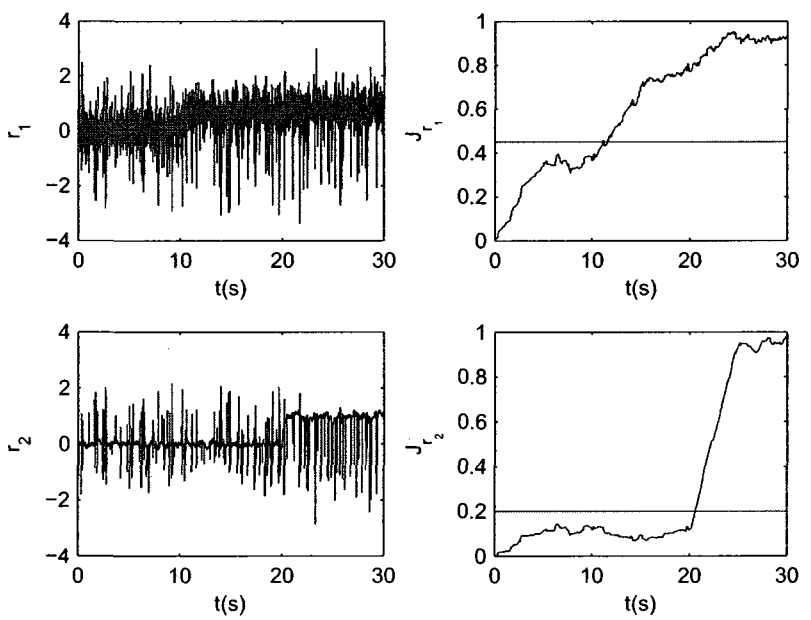

Figure 6.9: Residual signals and their evaluation functions corresponding to concurrent faults in both actuators.

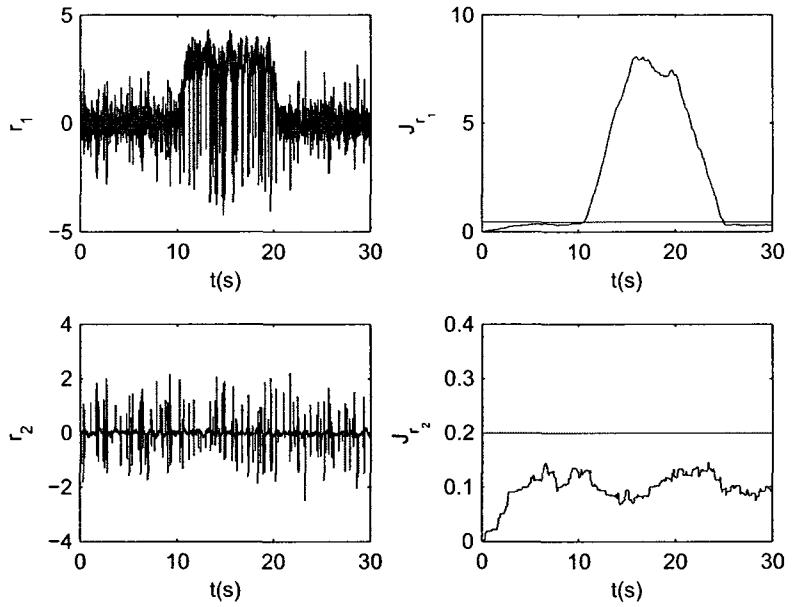

Figure 6.10: Residual signals and their evaluation functions corresponding to an intermittent fault in the first actuator.

6.7 Conclusions

A geometric approach to H_∞-based fault detection and isolation for time-delay system is developed. A set of residual signals is generated so that each residual is only affected by one fault and is decoupled from the others while the H_∞ norm of the transfer function between the unknown disturbance inputs and the residual signals is less than a given positive value. Simulation results demonstrate and illustrate the effectiveness of our proposed method.

Chapter 7

Fault Detection and Isolation of Linear Impulsive Systems

In this chapter, we address the problem of fault detection and isolation for linear impulsive systems. The concept of an unobservability subspace is introduced for linear impulsive systems and it is shown that the algorithm developed for finding unobservability subspaces for Markovian jump system can be used for obtaining unobservability subspaces for linear impulsive systems. The necessary and sufficient conditions for solvability of the fundamental problem of residual generation for linear impulsive systems are obtained by utilizing our introduced unobservability subspace.

This chapter is organized as follows. After a brief literature review, the concept of unobservability subspace is introduced for linear impulsive systems in Section 7.2. In Section 7.3, the necessary and sufficient conditions for solvability of the fundamental problem of residual generation for linear impulsive systems are obtained by utilizing our introduced unobservability subspace. Two case studies, namely, mass-spring system with constraint buffers and systems with impulsive control are considered in Section 7.4 as potential applications of our proposed FDI scheme.

Contributions

The main contributions of this chapter are now summarized as follows:

- The geometric concept of unobservability subspaces is introduced for linear impulsive systems
- The necessary and sufficient conditions for solvability of the fundamental problem of residual generation (FPRG) for linear impulsive systems are derived.

7.1 Introduction

A great deal of attention has recently been devoted to linear impulsive systems [224–226]. Impulsive systems can be viewed as a subclass of hybrid systems in which the states behave according to a continuous-time dynamics and which are also subjected to time-driven or event-driven impulsive effects where the states of the system are changed instantaneously. These systems can be used for modeling biological systems [227], sampled-data systems [228, 229], discrete-event systems [230], constraint mechanical systems [231], intelligent vehilce/highway systems [232] and satellite rendezvous [233]. In the past few years research has been conducted on stability, controllability and observability of these systems [234–236], to just name a few. However, no FDI results have been reported for linear impulsive systems.

In this chapter, we have adopted a geometric approach to the FDI problem of linear impulsive systems. Towards this end, the notion of an unobservability subspace for linear impulsive systems is introduced. It is shown that Algorithm 5.3 developed for the Markovian jump systems in Chapter 5 can be used for obtaining unobservability subspaces for linear impulsive systems. By utilizing the developed geometric framework, necessary and sufficient conditions for generating a set of dedicated residual signals are derived by developing a geometric FDI framework for linear impulsive systems. Using the properties of unobservability subspaces, a

set of residuals is generated such that each residual is affected by one fault and is decoupled from others.

7.2 Unobservability Subspaces for Linear Impulsive Systems

Consider the following linear impulsive system

$$\begin{aligned} \dot{x}(t) &= A_{\mathcal{C}}x(t) + B_{\mathcal{C}}u(t), \quad y(t) = C_{\mathcal{C}}x(t), \quad t \in \mathbb{R} \setminus \mathcal{T} \\ x(\tau_k) &= A_{\mathcal{I}}x(\tau_k^-) + B_{\mathcal{I}}u[k], \quad y[k] = C_{\mathcal{I}}x(\tau_k^-), \quad k \in \mathbb{Z}^+ \end{aligned} \tag{7.1}$$

where $x \in \mathcal{X}$ is the state of the system with dimension n; $u \in \mathcal{U}, y \in \mathcal{Y}$ are input and output signals with dimensions m and q, respectively, $\mathcal{T} = \{\tau_1, \tau_2, ...\}$ is a countable set of impulse times assumed to contain a finite number of elements on any finite time interval, $u[k]$ is a discrete-time control input and $y[k]$ is a discrete-time measurement. The impulse times τ_k can be defined either as a sequence of times which is independent of the state x and results in what is known as *time-dependent impulsive system*, or as a time instant when the state x touches the boundary of a specified region $\mathscr{Z}$ in the state space that is independent of time and results in what is known as *state-dependent impulsive system*. We first start with the definition of an unobservable subspace for impulsive system (7.1) with $B_{\mathcal{C}} = 0$ and $B_{\mathcal{I}} = 0$.

Definition 7.1. *For system* (7.1), *a state* $x_0 \in \mathcal{X}$ *is unobservable with free impulse times if given* t_0, $x(t_0) = x_0$ *yields output responses* $y(t)$ *and* $y[k]$ *which are identically equal to zero for all* $t \geq t_0$ *and all impulse time sets* $\mathcal{T}$.

The above definition of unobservable states is more general than the set introduced in [235], where only continuous-time output $y(t)$ is considered. It is clear that for the case where $C_{\mathcal{C}} = C_{\mathcal{I}}$, these two definitions are identical.

Definition 7.2 ([235]). *For the impulsive system* (7.1), *a subspace* $\mathcal{V}$ *is called invariant if and only if* $A_C\mathcal{V} \subset \mathcal{V}$ *and* $A_I\mathcal{V} \subset \mathcal{V}$.

Let $\mathcal{Q}$ denote the unobservable subspace of the impulsive system (7.1) and $< \mathcal{K}|A_C, A_I >$ denote the largest invariant subspace of (7.1) that is contained in a subspace $\mathcal{K} \subset \mathcal{X}$. The following is our first result.

Lemma 7.1. *For the impulsive system* (7.1), $\mathcal{Q} =< Ker\ C_C \cap Ker\ C_I|A_C, A_I >$.

Proof: The proof follows along the lines that are used in Theorem 4.8 in [235] and is omitted here. ■

We are now in a position to introduce the notions of conditioned invariant and unobservability subspaces for the linear impulsive system (7.1).

Definition 7.3. *A subspace* $\mathcal{W}$ *is said to be conditioned invariant for system* (7.1) *if* $A_C(\mathcal{W} \cap Ker\ C_C) \subseteq \mathcal{W}$ *and* $A_I(\mathcal{W} \cap Ker\ C_I) \subseteq \mathcal{W}$.

It should be noted the above definition is more general than the notion of condition-invariant subspace in [237], where $\mathcal{W}$ is forced to be A_C-invariant. It is clear that the above definition contains the condition-invariant subspaces [237]. It can be shown that $\mathcal{W}$ is conditioned invariant if and only if there exist output injection maps D_C, D_I such that $(A_C + D_C C_C)\mathcal{W} \subseteq \mathcal{W}$, $(A_I + D_I C_I)\mathcal{W} \subseteq \mathcal{W}$. We denote the class of conditioned invariant subspaces of $\mathcal{X}$ for the impulsive system (7.1) by $\mathfrak{W}$. If $\mathcal{W} \in \mathfrak{W}$, we write $\mathfrak{D}(\mathcal{W})$ for the class of maps D_C, D_I. It can be shown that $\mathfrak{W}$ is closed under subspace intersection, and hence for any given subspace $\mathcal{L} \subset \mathcal{X}$, the family of conditioned invariant subspaces that contains $\mathcal{L}$ (denoted by $\mathfrak{W}(\mathcal{L})$) has an infimal element (denoted by $\mathcal{W}^* = \inf \mathfrak{W}(\mathcal{L})$) (constructed below) $\mathcal{W}^*$.

Algorithm 7.1. *The subspace* $\mathcal{W}^*$ *coincides with the last term of the sequence* $\mathcal{W}_k = \mathcal{W}_{k-1} + A_C(\mathcal{W}_{k-1} \cap Ker\ C_C) + A_I(\mathcal{W}_{k-1} \cap Ker\ C_I)$ *with* $\mathcal{W}_0 = \mathcal{L}$.

Remark 7.1. *The above Algorithm is similar to Algorithm 5.2 for the Markovian jump systems. This is due to the fact that the definition of conditioned invariant for impulsive system* (7.1) *coincides with the definition of Markovian jump system* (5.56) *with two modes and* $A_1 = A_{\mathcal{C}}$, $A_2 = A_{\mathcal{I}}$, $C_1 = C_{\mathcal{C}}$ *and* $C_2 = C_{\mathcal{I}}$.

Definition 7.4. *A subspace* $\mathcal{S}$ *is an* unobservability subspace *for system* (7.1) *if there exist output injection maps* $D_{\mathcal{C}}, D_{\mathcal{I}} : \mathcal{Y} \to \mathcal{X}$ *and measurement mixing maps* $H_{\mathcal{C}}, H_{\mathcal{I}} : \mathcal{Y} \to \mathcal{Y}$ *such that* $\mathcal{S}$ *is an unobservable subspace for the following impulsive system:*

$$\begin{aligned} \dot{x}(t) &= (A_{\mathcal{C}} + D_{\mathcal{C}}C_{\mathcal{C}})x(t), \quad y(t) = H_{\mathcal{C}}C_{\mathcal{C}}x(t), \quad t \in \mathbb{R} \setminus \mathcal{T} \\ x(\tau_k) &= (A_{\mathcal{I}} + D_{\mathcal{I}}C_{\mathcal{I}})x(\tau_k^-), \quad y[k] = H_{\mathcal{I}}C_{\mathcal{I}}x(\tau_k^-) \quad k \in \mathbb{Z}^+ \end{aligned} \tag{7.2}$$

In other words, we have

$$\mathcal{S} =< KerH_{\mathcal{C}}C_{\mathcal{C}} \cap KerH_{\mathcal{I}}C_{\mathcal{I}} | A_{\mathcal{C}} + D_{\mathcal{C}}C_{\mathcal{C}}, A_{\mathcal{I}} + D_{\mathcal{I}}C_{\mathcal{I}} > \tag{7.3}$$

We denote for the linear impulsive system (7.1) the class of all unobservability subspaces in $\mathcal{X}$ by $\mathfrak{S}$. Furthermore, $\mathfrak{D}(S)$ denotes the class of maps $(D_{\mathcal{C}}, D_{\mathcal{I}})$ in Definition 7.4.

It should be noted that the above definition also coincides with the unobservability subspace for Markovian jump system (5.56) with two modes and parameters equivalence as in Remark 7.1. Therefore, based on the result of Chapter 5, the class of unobservability subspaces which contains a given subspace has an infimal element. This property is crucial for the application of unobservability subspace to the problem of fault detection and isolation of linear impulsive systems. Let $\mathcal{L} \subset \mathcal{X}$ be an arbitrary subspace and denote $\mathfrak{S}(\mathcal{L})$ as the family of unobservability subspaces that contains $\mathcal{L}$. The following algorithm provides a procedure for constructing $\mathcal{S}^* = \inf \mathfrak{S}(\mathcal{L})$ which is similar to Algorithm 5.3.

Algorithm 7.2. *Let $\mathcal{W}^* = \inf \mathfrak{W}$ and define the sequence $\mathcal{Z}^\mu$ according to*

$$\mathcal{Z}^0 = \mathcal{X}; \quad \mathcal{Z}^\mu = (\mathcal{W} + (A_{\mathcal{C}}^{-1}\mathcal{Z}^{\mu-1} \cap \ Ker\, C_{\mathcal{C}})) \bigcap (\mathcal{W} + (A_{\mathcal{I}}^{-1}\mathcal{Z}^{\mu-1} \cap \ Ker\, C_{\mathcal{I}}))$$

Then $\mathcal{S}^* = \mathcal{Z}^k$, whenever $\mathcal{Z}^{k+1} = \mathcal{Z}^k$.

7.3 Fault Detection and Isolation of Linear Impulsive Systems

In this section the Fundamental Problem in Residual Generation (FPRG) for a linear impulsive system is investigated. This problem was originally considered for linear systems in [3]. The objective in this section is to generalize these results to linear impulsive systems. Consider the following impulsive system

$$\begin{aligned} \dot{x}(t) &= A_{\mathcal{C}}x(t) + B_{\mathcal{C}}u(t) + L_{\mathcal{C}}^1 m_1(t) + L_{\mathcal{C}}^2 m_2(t), \quad t \in \mathbb{R} \setminus \mathcal{T} \\ x(\tau_k) &= A_{\mathcal{I}}x(\tau_k^-) + B_{\mathcal{I}}u[k] + L_{\mathcal{I}}^1 m_1[k] + L_{\mathcal{I}}^2 m_2[k], \quad k \in \mathbb{Z}^+ \end{aligned} \tag{7.4}$$

with the output measurements $y(t)$ and $y[k]$ as in (7.1). The matrices $L_{\mathcal{C}}^1$, $L_{\mathcal{C}}^2$, $L_{\mathcal{I}}^1$ and $L_{\mathcal{I}}^2$ represent the fault signatures and are monic, and $m_i(t) \in \mathcal{M}_i \subset \mathcal{X}$, $i = 1, 2$ denote the fault modes. The fault modes together with the fault signatures can be used to model the effects of actuator faults, sensor faults and system faults on the dynamics of the system. For example, the effects of a fault in the i-th actuator may be represented by $L_{\mathcal{C}}^1$ and $L_{\mathcal{I}}^1$ as the i-th column of $B_{\mathcal{C}}$ and $B_{\mathcal{I}}$, respectively. The failure of the actuator is then represented by $m_1(t) = -u_i(t)$.

Asymptotic stability of the impulsive system (7.4) is now presented where it is assumed that there exists a minimum dwell time $\epsilon > 0$ between each impulse.

Lemma 7.2 ([226]). *The linear impulsive system* (7.4) *with zero input and no fault (healthy mode) is asymptotically stable if there exist a positive definite matrix R such that $RA_{\mathcal{C}} + A_{\mathcal{C}}^\top R < 0$ and $A_{\mathcal{I}}^\top R A_{\mathcal{I}} - R \leq 0$.*

The FPRG problem for the linear impulsive system (7.4) is concerned with the design of a residual generator that is governed by the following filter dynamics

$$\dot{w}(t) = F_{\mathcal{C}}w(t) - E_{\mathcal{C}}y(t) + K_{\mathcal{C}}u(t), \quad r(t) = M_{\mathcal{C}}w(t) - H_{\mathcal{C}}y(t), \quad t \in \mathbb{R} \setminus \mathcal{T}$$

$$w(\tau_k) = F_{\mathcal{I}}w(\tau_k^-) - E_{\mathcal{I}}y[k] + K_{\mathcal{I}}u[k], \; r[k] = M_{\mathcal{I}}w(\tau_k^-) - H_{\mathcal{I}}y[k] \; k \in \mathbb{Z}^+ \tag{7.5}$$

where $w(t) \in \mathcal{F} \subset \mathcal{X}$ such that the response of $r(t)$ is affected by the fault mode $m_1(t)$ and is decoupled from $m_2(t)$, and if $m_1(t)$ is identically zero then $\lim_{t\to\infty} r(t) = 0$ for any input signal $u(t)$.

Toward this end, let us define the extended space $\mathcal{X}^e = \mathcal{X} \oplus \mathcal{F}$ and $\mathcal{U}^e = \mathcal{U} \oplus \mathcal{M}_2$ so that we can rewrite equations (7.4) and (7.5) as follows,

$$\dot{x}^e(t) = A^e_{\mathcal{C}}x^e(t) + B^e_{\mathcal{C}}u^e(t) + L^{e1}_{\mathcal{C}}m_1(t), \quad r(t) = H^e_{\mathcal{C}}x^e(t), \quad t \in \mathbb{R} \setminus \mathcal{T}$$

$$x^e(\tau_k) = A^e_{\mathcal{I}}x^e(\tau_k^-) + B^e_{\mathcal{I}}u^e[k] + L^{e1}_{\mathcal{I}}m_1[k], \quad r[k] = H^e_{\mathcal{I}}x^e(\tau_k^-), \quad k \in \mathbb{Z}^+ \tag{7.6}$$

with $x^e(t) \in \mathcal{X}^e$ and $u^e \in \mathcal{U}^e$, $A^e_{\mathcal{C}} = \begin{bmatrix} A_{\mathcal{C}} & 0 \\ -E_{\mathcal{C}}C_{\mathcal{C}} & F_{\mathcal{C}} \end{bmatrix}$, $B^e_{\mathcal{C}} = \begin{bmatrix} B_{\mathcal{C}} & L^2_{\mathcal{C}} \\ K_{\mathcal{C}} & 0 \end{bmatrix}$, $A^e_{\mathcal{I}} = \begin{bmatrix} A_{\mathcal{I}} & 0 \\ -E_{\mathcal{I}}C_{\mathcal{I}} & F_{\mathcal{I}} \end{bmatrix}$, $B^e_{\mathcal{I}} = \begin{bmatrix} B_{\mathcal{I}} & L^2_{\mathcal{I}} \\ K_{\mathcal{I}} & 0 \end{bmatrix}$, $L^{e1}_{\mathcal{C}} = \begin{bmatrix} L^1_{\mathcal{C}} \\ 0 \end{bmatrix}$, $L^{e1}_{\mathcal{I}} = \begin{bmatrix} L^1_{\mathcal{I}} \\ 0 \end{bmatrix}$, $H^e_{\mathcal{C}} = \begin{bmatrix} -H_{\mathcal{C}}C_{\mathcal{C}} & M_{\mathcal{C}} \end{bmatrix}$ and $H^e_{\mathcal{I}} = \begin{bmatrix} -H_{\mathcal{I}}C_{\mathcal{I}} & M_{\mathcal{I}} \end{bmatrix}$. In order to investigate the criteria for determining whether a nonzero $m_1(t)$ affects the residual signal $r(t)$, the notion of an input observability for the linear impulsive system (7.4) is defined and formalized below.

Definition 7.5. *The linear impulsive system* (7.4) *is said to be (impulsive) input observable if $B_{\mathcal{C}}$ ($B_{\mathcal{I}}$) is monic and the image of $B_{\mathcal{C}}$ ($B_{\mathcal{I}}$) does not intersect with the unobservable subspace of system* (7.4).

Based on the above definitions, the FPRG problem can now be formally stated as the problem of designing a dynamical filter (7.5) such that

(a) r is decoupled from $u^e(t)$ and $u^e(k)$, (7.7)

(b) $m_1(t)$ is input observable or $m_1[k]$ is impulsive input observable in the augmented system (7.6), and (7.8)

(c) $\lim_{t\to 0} r(t) = 0, \quad \text{for } m_1(t) = 0, \forall x^e_0 \in \mathcal{X}^e.$ (7.9)

We need to first derive a preliminary result below in order to obtain the solvability condition for the FPRG problem. The embedding map $Q : \mathcal{X} \to \mathcal{X}^e$ is defined according to [3], namely $Qx = [x^\top, 0]^\top$ where if $\mathcal{V} \subset \mathcal{X}^e$, we have $Q^{-1}\mathcal{V} = \{x | x \in \mathcal{X}, [x^\top, 0]^\top \in \mathcal{V}\}$. Our first result is the generalization of Proposition 1 that was obtained in [3] to a linear impulsive system.

Lemma 7.3. *Let $\mathcal{S}^e$ be the unobservable subspace of system* (7.6). *The unobservability subspace for system* (7.4) *is given by $Q^{-1}\mathcal{S}^e$.*

Proof: First we show that $\mathcal{S} = Q^{-1}\mathcal{S}^e$ is conditioned invariant. Let $x \in \mathcal{S} \cap \mathrm{Ker}C_{\mathcal{C}}$, we need to show that $A_{\mathcal{C}}x \in \mathcal{S}$. This follows by noting that $\left[\begin{smallmatrix} A_{\mathcal{C}}x \\ 0 \end{smallmatrix}\right] = \left[\begin{smallmatrix} A_{\mathcal{C}} & 0 \\ -E_{\mathcal{C}}C_{\mathcal{C}} & F_{\mathcal{C}} \end{smallmatrix}\right]\left[\begin{smallmatrix} x \\ 0 \end{smallmatrix}\right] \in \mathcal{S}^e$ since $\mathcal{S}^e$ is $A^e_{\mathcal{C}}$-invariant. Therefore, $A_{\mathcal{C}}x \in \mathcal{S}$. Similarly, it can be shown that $A_{\mathcal{I}}(\mathcal{S} \cap \mathrm{Ker}C_{\mathcal{I}}) \subset \mathcal{S}$, and hence $\mathcal{S}$ is conditioned invariant. Next, if $x \in \mathcal{S}$, then $Qx \in \mathcal{S}^e$, and therefore $[x^\top, 0]^\top \in \mathrm{Ker}H^e_{\mathcal{C}} \cap \mathrm{Ker}H^e_{\mathcal{I}}$. This shows that $H_{\mathcal{C}}C_{\mathcal{C}}x = 0$ and $H_{\mathcal{I}}C_{\mathcal{I}}x = 0$; and hence $x \in \mathrm{Ker}H_{\mathcal{C}}C_{\mathcal{C}} \cap \mathrm{Ker}H_{\mathcal{I}}C_{\mathcal{I}}$. Finally, according to the definition of the unobservable subspace $\mathcal{S}^e$ (the largest $A^e_{\mathcal{C}}$ and $A^e_{\mathcal{I}}$ invariant subspace in $\mathrm{Ker}H^e_{\mathcal{C}} \cap \mathrm{Ker}H^e_{\mathcal{I}}$), $\mathcal{S}$ is the largest conditioned invariant contained in $\mathrm{Ker}H_{\mathcal{C}}C_{\mathcal{C}} \cap \mathrm{Ker}H_{\mathcal{I}}C_{\mathcal{I}}$, and therefore $\mathcal{S} \in \mathfrak{S}$. ■

We are now in the position to derive our main result on solvability condition for the FPRG problem corresponding to the linear impulsive system (7.4).

Theorem 7.1. *The FPRG problem has a solution for the linear impulsive system* (7.4) *only if*

$$\mathcal{S}^* \bigcap \mathcal{L}^1_{\mathcal{C}} = 0 \quad or \quad \mathcal{S}^* \bigcap \mathcal{L}^1_{\mathcal{I}} = 0 \tag{7.10}$$

where $\mathcal{S}^* = \inf \mathfrak{S}(\mathcal{L}^2_{\mathcal{C}} + \mathcal{L}^2_{\mathcal{I}})$. On the other hand, if the above $\mathcal{S}^*$ and the matrices $T_{\mathcal{C}}$ and $T_{\mathcal{I}}$ and a positive definite matrix R exist such that $RA^0_{\mathcal{C}} + A^{0^\top}_{\mathcal{C}}R + T_{\mathcal{C}}M_{\mathcal{C}} + M^\top_{\mathcal{C}}T^\top_{\mathcal{C}} < 0$ and

$$\begin{bmatrix} A^\top_{\mathcal{I}}RA_{\mathcal{I}} + A^\top_{\mathcal{I}}T_{\mathcal{I}}M_I + M^\top_{\mathcal{I}}T^\top_{\mathcal{I}}A_{\mathcal{I}} - R & M^\top_{\mathcal{I}}T^\top_{\mathcal{I}} \\ T_{\mathcal{I}}M_{\mathcal{I}} & -R \end{bmatrix} \leq 0 \tag{7.11}$$

where the pairs $(A_{\mathcal{C}}^0, M_{\mathcal{C}})$ *and* $(A_{\mathcal{I}}^0, M_{\mathcal{I}})$ *are the factor systems of* $(A_{\mathcal{C}}, C_{\mathcal{C}})$ *and* $(A_{\mathcal{I}}, C_{\mathcal{I}})$ *on* $\mathcal{X}/\mathcal{S}^*$ *respectively, then the FPRG problem is guaranteed to have a solution.*

Proof: **(Only if part)** Let $\mathcal{S}^e$ be an unobservable subspace of system (7.6). To satisfy the condition (7.7), we should have $\mathcal{B}_{\mathcal{C}}^e \subset \mathcal{S}^e$ and $\mathcal{B}_{\mathcal{I}}^e \subset \mathcal{S}^e$. Hence, $\mathcal{L}_{\mathcal{C}}^2 \subset Q^{-1}\mathcal{B}_{\mathcal{C}}^e \subset Q^{-1}\mathcal{S}^e = \mathcal{S}$ and $\mathcal{L}_{\mathcal{I}}^2 \subset Q^{-1}\mathcal{B}_{\mathcal{I}}^e \subset Q^{-1}\mathcal{S}^e = \mathcal{S}$. By invoking Lemma 7.3, we obtain $\mathcal{S} \in \mathfrak{S}(\mathcal{L}_{\mathcal{C}}^2 + \mathcal{L}_{\mathcal{I}}^2)$. For condition (7.8) to hold, according to the Definition 7.5, $\mathcal{L}_{\mathcal{C}}^{e1}$ and $\mathcal{L}_{\mathcal{I}}^{e1}$ should be monic (which is already assumed to hold) and $\mathcal{L}_{\mathcal{C}}^{e1} \cap \mathcal{S}^e = 0$ or $\mathcal{L}_{\mathcal{I}}^{e1} \cap \mathcal{S}^2 = 0$. Thus $Q^{-1}(\mathcal{L}_{\mathcal{C}}^{e1} \cap \mathcal{S}^e) = \mathcal{L}_{\mathcal{C}}^1 \cap \mathcal{S} = 0$ and $Q^{-1}(\mathcal{L}_{\mathcal{I}}^{e1} \cap \mathcal{S}^e) = \mathcal{L}_{\mathcal{I}}^1 \cap \mathcal{S} = 0$. Therefore, the above conditions hold only if equation (7.10) is true.

(if part): Given the unobservability subspace $\mathcal{S}^*$, there exist output injection maps $D_{\mathcal{C}}$, $D_{\mathcal{I}}$ and measurement mixing maps $H_{\mathcal{C}}$, $H_{\mathcal{I}}$ such that $\mathcal{S}^* =< \mathrm{Ker} H_{\mathcal{C}} C_{\mathcal{C}} \cap \mathrm{Ker} H_{\mathcal{I}} C_{\mathcal{I}} | A_{\mathcal{C}} + D_{\mathcal{C}} C_{\mathcal{C}}, A_{\mathcal{I}} + D_{\mathcal{I}} C_{\mathcal{I}} >$ where $H_{\mathcal{C}}$ and $H_{\mathcal{I}}$ are found from Lemma 5.1. Let P be the canonical projection of $\mathcal{X}$ on $\mathcal{X}/\mathcal{S}^*$ and $M_{\mathcal{C}}$ and $M_{\mathcal{I}}$ be unique solutions to $M_{\mathcal{C}} P = H_{\mathcal{C}} C_{\mathcal{C}}$ and $M_{\mathcal{I}} P = H_{\mathcal{I}} C_{\mathcal{I}}$, respectively, and $A_{\mathcal{C}}^0 = (A_{\mathcal{C}} + D_{\mathcal{C}} C_{\mathcal{C}} : \mathcal{X}/\mathcal{S}^*)$ and $A_{\mathcal{I}}^0 = (A_{\mathcal{I}} + D_{\mathcal{I}} C_{\mathcal{I}} : \mathcal{X}/\mathcal{S}^*)$ where $P(A_{\mathcal{C}} + D_{\mathcal{C}} C_{\mathcal{C}}) = A_{\mathcal{C}}^0 P$ and $P(A_{\mathcal{I}} + D_{\mathcal{I}} C_{\mathcal{I}}) = A_{\mathcal{I}}^0 P$. Define $G_{\mathcal{C}} = R^{-1} T_{\mathcal{C}}$ and $G_{\mathcal{I}} = R^{-1} T_{\mathcal{I}}$ where R, $T_{\mathcal{C}}$, and $T_{\mathcal{I}}$ are the solution to inequality (7.11). Let us define $F_{\mathcal{C}} = A_{\mathcal{C}}^0 + G_{\mathcal{C}} M_{\mathcal{C}}$, $F_{\mathcal{I}} = A_{\mathcal{I}}^0 + G_{\mathcal{I}} M_{\mathcal{I}}$, $E_{\mathcal{C}} = P(D_{\mathcal{C}} + P^{-r} G_{\mathcal{C}} H_{\mathcal{C}})$, $E_{\mathcal{I}} = P(D_{\mathcal{I}} + P^{-r} G_{\mathcal{I}} H_{\mathcal{I}})$, $K_{\mathcal{C}} = P B_{\mathcal{C}}$ and $K_{\mathcal{I}} = P B_{\mathcal{I}}$. Define $e(t) = w(t) - P x(t)$. By using equation (7.5) we obtain

$$\begin{aligned}
\dot{e}(t) =& F_{\mathcal{C}} w(t) - E_{\mathcal{C}} y(t) + K_{\mathcal{C}} u(t) - P(A_{\mathcal{C}} x(t) + B_{\mathcal{C}} u(t) + L_{\mathcal{C}}^1 m_1(t)) + L_{\mathcal{C}}^2 m_2(t)) \\
=& F_{\mathcal{C}} w(t) - P L_{\mathcal{C}}^1 m_1(t) - P(A_{\mathcal{C}} + D_{\mathcal{C}} C_{\mathcal{C}}) x(t) - G_{\mathcal{C}} H_{\mathcal{C}} C_{\mathcal{C}} x(t) \\
=& F_{\mathcal{C}} w(t) - P L_{\mathcal{C}}^1 m_1(t) - A_{\mathcal{C}}^0 P x(t) - G_{\mathcal{C}} M_{\mathcal{C}} P x(t) = F_{\mathcal{C}} e(t) - P L_{\mathcal{C}}^1 m_1(t)
\end{aligned}$$

Note that $P L_{\mathcal{C}}^2 = 0$, since $\mathcal{L}_{\mathcal{C}}^2 \in \mathcal{S}^*$. Similarly, it can be shown that $e(\tau_k) = F_{\mathcal{I}} e(\tau_k^-) - P L_{\mathcal{I}}^1 m_1[k]$. Furthermore, according to equation (7.10) at least one of

the terms $PL_{\mathcal{I}}^1 m_1[k]$ or $PL_{\mathcal{C}}^1 m_1(t)$ is nonzero. Also $r(t) = M_{\mathcal{C}} w(t) - H_{\mathcal{C}} y(t) = M_{\mathcal{C}} w(t) - H_{\mathcal{C}} C_{\mathcal{C}} x(t) = M_{\mathcal{C}} e(t)$. Similarly, it can be shown that $r[k] = M_{\mathcal{I}} e(\tau_k^-)$. Consequently, the error dynamics can be written according to

$$\dot{e}(t) = F_{\mathcal{C}} e(t) - PL_{\mathcal{C}}^1 m_1(t), \quad r(t) = M_{\mathcal{C}} e(t), \quad t \in \mathbb{R} \setminus \mathcal{T}$$

$$e(\tau_k) = F_{\mathcal{I}} e(\tau_k^-) - PL_{\mathcal{I}}^1 m_1[k], \quad r[k] = M_{\mathcal{I}} e(\tau_k^-), \quad k \in \mathbb{Z}^+ \tag{7.12}$$

It is clear that the fault mode $m_2(t)$ does not affect the residual $r(t)$ and since the dynamics (7.12) is observable, condition (7.8) also holds. Moreover, for $m_1(t) = 0$ using the result in Lemma 7.2 and the Schur complement, it follows that the above error dynamics is stable and condition (7.9) also holds. ■

Remark 7.2. *It should be noted that for* state-dependent impulsive systems, *a corresponding impulsive region for the detection filters can be obtained as $P\mathscr{Z}$, where P is the canonical projection map defined in Theorem 7.1 and $\mathscr{Z}$ is the region in the state space where the impulses occur. For* time-dependent impulsive systems, *the same sequence of times $\mathcal{T}$ is used for the filters.*

To conclude this section, let us consider a linear impulsive system that has multiple faults and is governed by the following dynamical system

$$\begin{aligned} \dot{x}(t) &= A_{\mathcal{C}} x(t) + B_{\mathcal{C}} u(t) + \sum_{i=1}^{k} L_{\mathcal{C}}^i m_i(t), \quad t \in \mathbb{R} \setminus \mathcal{T} \\ x(\tau_k) &= A_{\mathcal{I}} x(\tau_k^-) + B_{\mathcal{I}} u[k] + \sum_{i=1}^{k} L_{\mathcal{I}}^i m_i[k], \quad k \in \mathbb{Z}^+ \end{aligned} \tag{7.13}$$

with the same output measurement representation as in (7.4) and where $L_{\mathcal{C}}^i, L_{\mathcal{I}}^i,\ i \in \mathbf{k} = \{1, ..., k\}$ are the fault signatures, and $m_i(t) \in \mathcal{M}_i,\ i \in \mathbf{k}$ are the fault modes. We now introduce the generalization to the FPRG problem.

The Extended Fundamental Problem in Residual Generation (EFPRG) [3] for the linear impulsive system (7.13) is defined as the problem of generating k residual

signals $r_l(t),\ l \in \mathbf{k}$ from the impulsive detection filters governed by (7.5) such that a fault in the j-th component m_j can only affect the residual signal $r_j(t)$ and no other residual signals $r_l(t), l \neq j$. The solvability condition for the EFPRG problem is obtained by invoking the solvability condition that was just developed for the FPRG problem.

Theorem 7.2. *The EFPRG problem has a solution for system* (7.13) *only if*

$$\mathcal{S}_i^* \bigcap \mathcal{L}_{\mathcal{C}}^i = 0 \quad or \quad \mathcal{S}_i^* \bigcap \mathcal{L}_{\mathcal{I}}^i = 0,\ i \in \boldsymbol{k}$$

where $\mathcal{S}_i^* = \inf \mathfrak{S}(\sum_{j=1}^N (\mathcal{L}_{\mathcal{C}}^j + \mathcal{L}_{\mathcal{I}}^j))$. *On the other hand, if the above* $\mathcal{S}_j^*, j \in \boldsymbol{k}$ *and the matrices* $T_{\mathcal{C}}^i$ *and* $T_{\mathcal{I}}^i$ *and the positive definite matrices* R^i *exist such that* $R^i A_{\mathcal{C}}^i + A_{\mathcal{C}}^{i^\top} R^i + T_{\mathcal{C}}^i M_{\mathcal{C}}^i + M_{\mathcal{C}}^{i^\top} T_{\mathcal{C}}^{i^\top} < 0$ *and* $\begin{bmatrix} \Phi^i & M_{\mathcal{I}}^{i^\top} T_{\mathcal{I}}^{i^\top} \\ T_{\mathcal{I}}^i M_{\mathcal{I}}^i & -R^i \end{bmatrix} \leq 0$ *where* $\Phi_i = A_{\mathcal{I}}^{i^\top} R^i A_{\mathcal{I}}^i + A_{\mathcal{I}}^{i^\top} T_{\mathcal{I}}^i M_{\mathcal{I}}^i + M_{\mathcal{I}}^{i^\top} T_{\mathcal{I}}^{i^\top} A_{\mathcal{I}}^i - R^i$, *the pair* $(A_{\mathcal{C}}^i, M_{\mathcal{C}})$ *and* $(A_{\mathcal{I}}^i, M_{\mathcal{I}})$ *are the factor systems of* $(A_{\mathcal{C}}, C_{\mathcal{C}})$ *and* $(A_{\mathcal{I}}, C_{\mathcal{I}})$ *on* $\mathcal{X}/\mathcal{S}_i^*$ *respectively, then the EFPRG problem is guaranteed to have a solution.*

Proof: The proof is immediate and follows along the same lines that are developed for the proof of Theorem 7.1. Namely, for generating each residual signal $r_i(t)$, the fault signatures $L_{\mathcal{C}}^1$, $L_{\mathcal{I}}^1$, $L_{\mathcal{C}}^2$ and $L_{\mathcal{I}}^2$ in (7.6) are replaced by $L_{\mathcal{C}}^i$, $L_{\mathcal{I}}^i$, $\sum_{j=1, j\neq i}^k L_{\mathcal{C}}^j$ and $\sum_{j=1, j\neq i}^k L_{\mathcal{I}}^j$, respectively. The remaining derivations follow similarly and are omitted. ■

After constructing the residual signals $r_i(t), i \in \mathbf{k}$, the last step is to determine a threshold J_{th_i} and an evaluation function $J_{r_i}(t)$ (a fault is detected at $t = t_f$ if $J_{r_i}(t) > J_{th_i}$ for all $t \geq t_f$). In this section, the following evaluation function is selected $J_{r_j}(t) = \frac{1}{T_0} \int_{t-T_0}^t r_j^\top(\tau) r_j(\tau) d\tau,\ j \in \mathbf{k}$ where T_0 is the length of the evaluation window. The threshold values J_{th_i} are selected by conducting a worst case analysis of residuals that correspond to the healthy operation of the system that is subject to measurement noise.

7.4 Two Case Studies

7.4.1 Mass-spring system with constraint buffers

In this section, our proposed FDI algorithm is applied to a mass-spring system with constraint buffers as depicted in Figure 7.1. Between collisions the system dynamics are governed by

$$M_1\ddot{q}_1(t) + k_2(q_1(t) - q_2(t)) + k_1 q_1(t) = F_1$$

$$M_2\ddot{q}_2(t) + k_2(q_2(t) - q_1(t)) + k_3(q_2(t) - q_3(t)) + c_2(\dot{q}_2(t) - \dot{q}_3(t)) = 0$$

$$M_3\ddot{q}_3(t) + k_3(q_3(t) - q_2(t)) + c(\dot{q}_3(t) - \dot{q}_2(t)) = F_2$$

where $M_1 = M_3 = 1.5\ kg$, $M_2 = 0.5\ kg$, $k_1 = 1\ N/m$, $k_2 = 0.3\ N/m$ and $k_3 = 0.5\ N/m$. At the instant of collision, the velocities of the masses M_1 and M_2 change according to the conservation law of linear momentum and the loss of kinetic energy so that the system impulse dynamics can be expressed [226] as $M_1\dot{q}_1(\tau_k)+M_2\dot{q}_2(\tau_k) = M_1\dot{q}_1(\tau_k^-) + M_2\dot{q}_2(\tau_k^-)$ and $\dot{q}_1(\tau_k) - \dot{q}_2(\tau_k) = e(\dot{q}_1(\tau_k^-) - \dot{q}_2(\tau_k^-))$ where $e \in [0, 1)$ is the coefficient of restitution. Let us denote $x^\top = [q_1, \dot{q}_1, q_2, \dot{q}_2, q_3, \dot{q}_3]$. The collision instant occurs when $x \in \mathscr{Z} = \{x \in \mathbb{R}^4 : x_1 - x_3 = L,\ \dot{x}_2 > \dot{x}_4\}$. The above system can be written according to model (7.4) with $B_{\mathcal{I}} \equiv 0$ and the fault signatures $L_{\mathcal{I}}^1 = L_{\mathcal{I}}^2 = 0$. The fault signatures $L_{\mathcal{C}}^1$ and $L_{\mathcal{C}}^2$ are selected as the first and the second columns of matrix $B_{\mathcal{C}}$, and they represent faults in actuators F_1 and F_2, respectively. The output measurement is defined as $y(t) = [x_1(t), x_3(t), x_5(t)]^\top$ and $C_{\mathcal{C}} = C_{\mathcal{I}}$. An energy-based controller [226] is designed for the above open loop system. Figure 7.2 shows the position response of the system under the healthy operation where at $t = 100$ seconds a new reference setpoint is considered for the system. Two collisions occurs at $t = 0.15$ seconds and $t = 103$ seconds.

According to Theorem 7.2 results, first we need to construct unobservability subspaces $\mathcal{S}_1^* = \inf \mathfrak{S}(\mathcal{L}_{\mathcal{C}}^2)$ and $\mathcal{S}_2^* = \inf \mathfrak{S}(\mathcal{L}_{\mathcal{C}}^1)$. These unobservability subspaces are

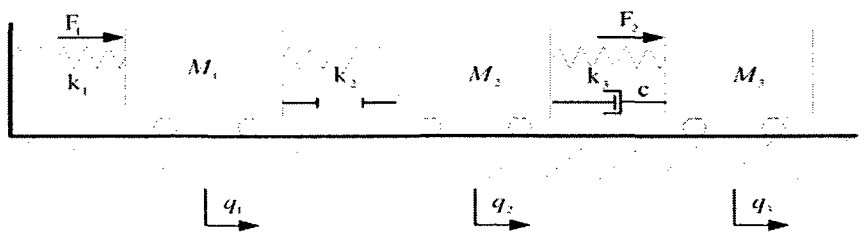

Figure 7.1: The mass-spring system.

obtained by applying Algorithm 5.3. It can be verified that these unobservability subspaces satisfy the necessary conditions of Theorem 7.2. Once the subspaces $\mathcal{S}_1^*$ and $\mathcal{S}_2^*$ are determined, the maps D_C, $D_\mathcal{I}$, M_C, $M_\mathcal{I}$, H_C, $H_\mathcal{I}$ and matrices A_C^i and $A_\mathcal{I}^i$, $i = 1, 2$ are found according to Theorem 7.1. The gain matrices G_C^i and $G_\mathcal{I}^i$ are computed by solving the LMI in Theorem 7.2.

A measurement noise is added to the outputs $y(t)$ and $y[k]$ which is assumed to be a 5% uniform random noise. For the purpose of simulations the evaluation window is selected as $T_0 = 2$ seconds. By considering the worst case analysis of the residuals that correspond to the healthy operation of the system subject to measurement noise, a threshold value of 0.002 is selected for both residual signals r_1 and r_2. Multiple faults scenario is considered where 40% and 60% loss of effectiveness permanent faults are injected in the actuators F_1 and F_2 at $t = 120$ and $t = 140$ seconds, respectively. Figure 7.3 depicts the evaluation functions J_{r_1} and J_{r_2} corresponding to this scenario. One can clearly observe that both faults are detected and isolated with no false alarms is generated due to collisions and impulsive behavior of the system. Figure 7.4 shows the residual evaluation functions corresponding to the above fault scenario that are designed based by using the continuous-time geometric approach proposed in [3] *without* considering the impulsive effects due to collisions. As shown in Figure 7.4, due to collisions two and one false alarms are flagged in the first and the second evaluation functions, respectively. Consequently, our proposed method shown in Figure 7.3 is superior since it guaranteed that no false alarms are generated due to impulsive effects. Moreover, it should be noted that the orders of

the filters that are utilized for the residual r_2 based on our proposed method and the one introduced in [3] are 2 and 4, respectively. This implies that our superior performance was achieved even by using lower dimensional and computationally less complex filters.

7.4.2 System with impulsive control

In this section, the FDI problem of a linear system with impulsive control is considered as the second application of our proposed FDI algorithm. Consider the linear impulsive system (7.4) with parameters $A_C = \left[\begin{smallmatrix} 1.1 & -3 \\ 1 & 2 \end{smallmatrix}\right]$, $B_C = 0$, $A_{\mathcal{I}} = \left[\begin{smallmatrix} 1 & 0 \\ 0 & 1 \end{smallmatrix}\right]$, $B_{\mathcal{I}} = \left[\begin{smallmatrix} -0.9 & -0.18 \\ -0.09 & -0.9 \end{smallmatrix}\right]$ and $C_C = C_{\mathcal{I}} = \left[\begin{smallmatrix} 1 & 0 \\ 0 & 1 \end{smallmatrix}\right]$. The fault signatures $L_{\mathcal{I}}^1$ and $L_{\mathcal{I}}^2$ are selected as the first and the second columns of $B_{\mathcal{I}}$ representing impulsive actuator faults. A periodic impulsive state feedback control is designed with a period of 1 second to stabilize the system [224].

It can be shown that the necessary condition of Theorem 7.2 is satisfied and the EFRPG problem has a solution for the above impulsive control system. A 5% random measurement noise is added to the outputs $y(t)$ and $y[k]$, and where $T_0 = 2$ seconds and $J_{th_1} = J_{th_2} = 0.0001$. A 70% loss of effectiveness single fault is injected in the second impulsive actuator at $t = 10$ seconds. Figure 7.5 shows the residual evaluation functions corresponding to the above fault scenario. As shown in this figure, the fault in the second actuator can be both detected and isolated at $t = 10.4$ seconds.

To the best of our knowledge, no algorithm is available in the literature for FDI of an impulsive actuators. We have shown above that by utilizing our proposed FDI approach, one can detect and isolate faults both in impulsive control systems as well as systems with inherent impulsive phenomenon.

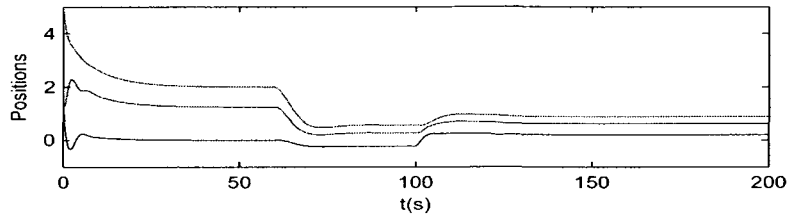

Figure 7.2: The positions response of the healthy system subject to an energy-based controller.

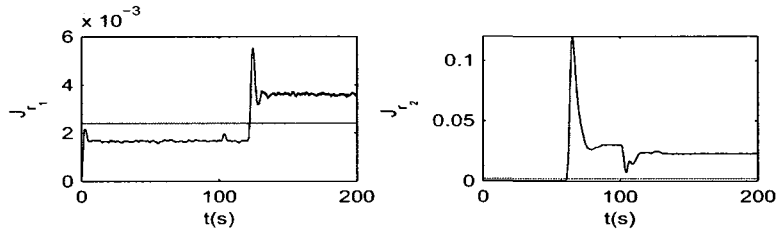

Figure 7.3: Residual evaluation functions corresponding to multiple fault scenario in the actuators F_1 and F_2 (based on our proposed approach).

7.5 Conclusions

A geometric approach to the problem of fault detection and isolation of linear impulsive systems is developed in this chapter. The concept of unobservability subspaces is formalized and an algorithm for constructing these subspaces is presented. By invoking the notion of unobservability subspace, the necessary and sufficient conditions for solving the fundamental problem of residual generation (FPRG) for linear impulsive systems is formally developed. Simulation results demonstrate the effectiveness and capabilities of our proposed scheme.

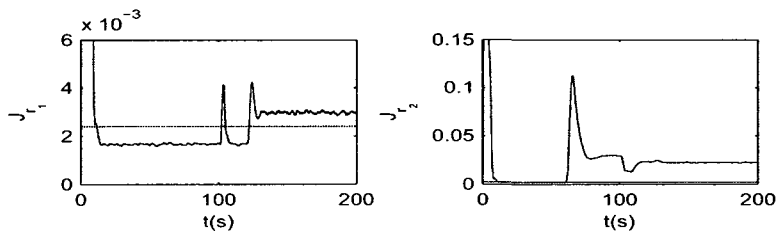

Figure 7.4: Residual evaluation functions corresponding to multiple fault scenario in the actuators F_1 and F_2 (based on the standard continuous-time approach [3]).

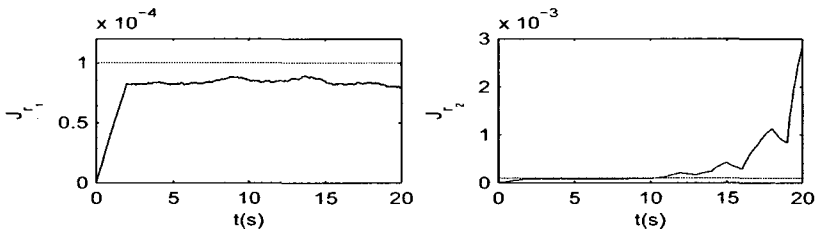

Figure 7.5: Residual evaluation functions corresponding to single fault scenario in the second impulsive actuator (based on our proposed approach).

Chapter 8

Perspectives and Future Directions of Research

In this dissertation, we have been interested in design of fault detection and isolation algorithms in a networked multi-vehicle unmanned systems. This problem is important since one of the main challenges in these systems is developing autonomous cooperative control which can maintain the group behavior and mission performance in the presence of undesirable events such as failures in vehicles. In order to have an autonomous network of unmanned vehicles, fault detection and isolation algorithms should be designed which are capable of detecting and isolating faults in the vehicles. The approach that we proposed was based of geometric FDI framework. We formulated several problems within the domain of multi-vehicle systems and obtained some very interesting results.

In Chapters 3, 4 and 5, we tackled different issues in the design of FDI algorithms for a network of unmanned vehicles such as different FDI architectures, robustness with respect to external disturbances and compensation of the effects of communication links. In Chapter 6, the FDI problem for time-delay systems was investigated. Potential application of our proposed FDI algorithm for time-delay

systems in a network of unmanned vehicles and in networked control systems is in design of an integrated fault diagnosis and controller. We briefly discuss this issue in Appendix B. Finally, in Chapter 7, the FDI problem for linear impulsive systems was investigated and it is shown that our developed geometric framework for the Markovian jump systems can be applied to other classes of systems such as linear impulsive systems. Obviously, there is more work that needs to be done to have a complete theory of fault detection and isolation in a networked multi-vehicle systems. In this chapter, a brief summary of each chapter is provided and a couple of major open problems in each area are identified.

8.1 Research Directions Considered in this Dissertation

In this section, we summarize the major research areas addressed in this dissertation and identify some of the open problems in each area.

8.1.1 Fault Detection and Isolation in a Network of Unmanned Vehicles: Ideal Communication Channels

In Chapter 3, we dealt with the problem of fault detection and isolation for a network of unmanned vehicles without considering the effect of communication channels on the performance of FDI algorithms. It was shown that actuator faults signatures in multi-vehicle systems with relative state measurements are dependent and hence the entire network is overactuated. New coding schemes are developed for both linear and nonlinear systems with dependent fault signatures. Three case studies are considered as potential applications of our novel coding schemes. In the first case study, the FDI problem in a network of unmanned vehicles with relative state

measurement is solved within three different architectures, namely, centralized, decentralized and semi-decentralized. It was shown that the solvability conditions for the centralized and semi-decentralized architectures are identical for vehicles with more than one neighbor. Moreover, it was shown that vehicles cannot perform fault detection and isolation in the fully decentralized fashion without an exchange of information among them. In the second case study, the actuator fault detection and isolation in an F18-HARV aircraft was presented as an example of linear overactuated system. Finally, in the third case study, fault detection and isolation in a satellite with redundant reaction wheels is considered as an example of a nonlinear overactuated system.

The major directions for future research in this area are as follows:

- Development of FDI algorithms for a network of unmanned vehicles with both internal and relative state measurement.
- Investigation of the effects of time-varying network topology on the FDI algorithms.
- Development of robust FDI algorithms with respect to modeling errors and un-modeled dynamics.

8.1.2 Fault Detection and Isolation in a Network of Unmanned Vehicles Subject to Large Environmental Disturbances

In Chapter 4, we proceeded with considering the effects of environmental disturbances on the vehicles and a hybrid fault detection and isolation algorithm was developed for achieving robustness with respect to these disturbances. A hybrid architecture for a robust FDI is introduced that is composed of a bank of continuous-time residual generators and a DES fault diagnoser. It was shown that the proposed

hybrid FDI algorithm is applicable to both linear and nonlinear systems.

The directions for future research in this area are as follows:

- Investigation of the effects of time-varying network topology on the FDI algorithms.
- Development of robust fault identification for a network of unmanned vehicles subject to external disturbances.

8.1.3 Fault Detection and Isolation in a Network of Unmanned Vehicles with Imperfect Communication Links

In Chapter 5, we considered a network of unmanned vehicles in the presence of imperfect communication channels. The packet erasure channel model was considered for communication links and the combination of this model with vehicle dynamics yielded a discrete-time Markovian jump model for the entire network. A geometric approach was developed for fault detection and isolation of both discrete-time and continuous-time Markovian jump systems and a notion of unobservability subspaces was introduced for Markovian jump systems. Our proposed FDI scheme was applied to the FDI problem in formation flight of satellites with imperfect communication links. Moreover, to show the applicability of our proposed algorithms beyond the main focus of this dissertation (network of unmanned vehicles), the actuator fault detection and isolation for an VTOL helicopter is considered as a case study for continuous-time Markovian jump systems.

The major directions for future research in this area are as follows:

- Development of the geometric property of weak controllability for Markovian jump systems and defining the notion of controllability subspaces for MJS.
- Development of FDI algorithms for discrete-time Markovian jump systems which are robust with respect to uncertainties in the transition matrix.

- Development of FDI algorithms for nonlinear Markovian jump systems. This problem has a potential application to a network of vehicles with nonlinear dynamics.

- Development of geometric framework for nonlinear Markovian jump systems and introducing notions such as observability codistribution and controllability distribution.

8.1.4 Fault Detection and Isolation for Time-delay Systems

In Chapter 6, we investigated the problem of fault detection and isolation for time-delay systems, which has its own importance in the development of FDI algorithms for complex industrial systems. Moreover, it was shown how the geometric framework developed in Chapter 5 can be used for time-delay systems. In Chapter 6, we covered broad classes of time-delay systems, namely, retarded, neutral, distributed delay and stochastic time-delay systems. Robust H_∞-based FDI algorithms are developed for each class of time-delay systems. Finally, as discussed in Appendix B, our proposed FDI algorithms for retarded time delay systems and Markovian jump systems have a potential application for an integrated design of FDI/Controller for networked control systems as well as network of unmanned vehicles.

The major future research directions in this area are as follows:

- Integrated FDI/Controller design for a network of unmanned vehicles.

- Study the minimum input sensitivity (H_- index) for time-delay systems. The lowest level of sensitivity of system outputs to system inputs is defined as an H_- index. This has a potential application in investigating a worse-case fault sensitivity.

- Fault detection and isolation for time-delay systems with polytopic uncertainties.

- Development of geometric framework for fault detection and isolation of nonlinear time-delay systems.

- Development of FDI algorithms for systems over ring. Time-delay systems can be modeled as a system over ring. Hence, the FDI problem for time-delay systems can be solved in a broader family of systems, namely systems over ring.

8.1.5 Fault Detection and Isolation for Linear Impulsive Systems

In Chapter 7, we dealt with the problem of fault detection and isolation in linear impulsive systems. This chapter also showed the applicability of our proposed algorithm in Chapter 5 for finding an unobservability subspace in another area of research, namely linear impulsive systems. We solved the fundamental problem of residual generation for linear impulsive systems.

The major directions for future research in this area are as follows:

- Development of FDI algorithms for hybrid impulsive systems where after each impulse the dynamics of the system also switches.

- Development of FDI algorithms for nonlinear impulsive systems.

- Development of geometric framework for nonlinear impulsive systems and introducing the notions such as observability codistribution and controllability distribution.

Appendix A

Finite Unobservability Subspaces for Time-delay Systems

In this section, the detail derivation of Algorithm 6.2 for finding the smallest finite unobservability subspace is presented for a given pair of matrices $(C, A_i), i \in \mathbf{N}_0$. To develop this algorithm, an alternative definition of unobservability subspace is presented, which only depends on the matrices of the system. Based on this alternative definition, an algorithm for constructing the smallest unobservability subspace containing a given subspace is proposed. First, the definition of finite unobservability subspace is reviewed.

Definition A.1. *A subspace $\mathcal{S}$ is called a finite unobservability subspace for system* (6.1) *with matrices $(C, A_i), i \in \boldsymbol{N}_0$ if for some output injection maps $D_i : \mathcal{Y} \to \mathcal{X}$ and measurement mixing map $H : \mathcal{Y} \to \mathcal{Y}$, we have*

$$\mathcal{S} = << Ker\ HC | A_i + D_i C >>_{i \in (\boldsymbol{N})_0} \tag{A.1}$$

Next, we introduce the notion of a common conditioned invariant subspace for given pairs of matrices $(C, A_i), i \in \mathbf{N}_0$.

Definition A.2. *A subspace $\mathcal{W}$ is said to be a common conditioned invariant for*

matrices $(C, A_i), i \in \boldsymbol{N}_0$ *if*

$$A_i(\mathcal{W} \cap Ker\ C) \subseteq \mathcal{W}, \qquad i \in \boldsymbol{N}_0 \tag{A.2}$$

It is clear that if $\mathcal{W}$ is a common conditioned invariant for matrices $(C, A_i), i \in \mathbf{N}_0$, then $\mathcal{W}$ is (C, A_i)-invariant for all $i \in \mathbf{N}_0$. Therefore, there exist maps $D_i : \mathcal{Y} \to \mathcal{X}$ such that $(A_i + D_iC)\mathcal{W} \subseteq \mathcal{W},\ i \in \mathbf{N}_0$. We denote the class of conditioned invariant subspaces of $\mathcal{X}$ for matrices $(A_i, C), i \in \mathbf{N}_0$ by $\mathfrak{W}(\mathfrak{A}, \mathcal{X})$ where $\mathfrak{A} = (A_0, ..., A_N)$. It should be noted that the above definition coincides with the definition of conditioned invariant subspace for Markovian jump system (Definition 5.5) when the matrices C_i for $i \in \mathbf{N}_0$ are identical, i.e. $C_i = C,\ i \in \mathbf{N}_0$. Therefore, the class of common conditioned invariant subspaces is closed under the operation of subspace intersection and the notation $\mathfrak{W}(\mathfrak{A}, \mathcal{L})$ refers to a common conditioned invariant subspace containing $\mathcal{L} \subseteq \mathcal{X}$. Based on Algorithm 5.2, the following algorithm can now be used for constructing an infimal element of $\mathfrak{W}(\mathfrak{A}, \mathcal{L})$ (denoted by $\mathcal{W}^*$):

Algorithm A.1. *The subspace* $\mathcal{W}^*$ *coincides with and is obtained from the last term of the following sequence*

$$\mathcal{W}_0 = \mathcal{L}; \qquad \mathcal{W}_k = \mathcal{W}_{k-1} + \sum_{i=0}^{N} A_i(\mathcal{W}_{k-1} \cap Ker\ C)$$

Next, along the same way as in Theorem 5.3, the following theorem provides an alternative definition of a finite unobservability subspace.

Theorem A.1. *A subspace* $\mathcal{S}$ *is an unobservability subspace for system* (5.56) *if and only if there exist maps* $D_i : \mathcal{Y} \to \mathcal{X}$, *such that*

$$\mathcal{S} = << \mathcal{S} + Ker\ C)|A_i + D_iC >>_{i \in \boldsymbol{N}_0} \tag{A.3}$$

For a given finite unobservability subspace $\mathcal{S}$, the measurement mixing map H's can be computed from $\mathcal{S}$ by solving Ker $HC = \mathcal{S} +$ Ker C. We denote the class of finite unobservability subspaces of $\mathcal{X}$ for matrices $(A_i, C), i \in \mathbf{N}_0$ by $\mathfrak{S}(\mathfrak{A}, \mathcal{X})$.

Next, we try to the characterize the unobservability subspace by means of an algorithm that computes $\mathcal{S}$ without explicitly constructing $(D_0, ..., D_N) \in \mathfrak{D}(\mathcal{S})$. For an arbitrary subspace $\mathcal{S} \subset \mathcal{X}$ let us define a family

$$\mathcal{G} = \{\mathscr{S} : \mathscr{S} = \mathcal{S} + (\bigcap_{i=0}^{N} A_i^{-1}\mathscr{S}) \cap \text{ Ker } C\} \tag{A.4}$$

Below we first show that $\mathcal{G}$ has a unique maximal member.

Lemma A.1. *There exists a unique element $\mathscr{S}^* \in \mathcal{G}$ such that $\mathscr{S} \subset \mathscr{S}^*$ for every $\mathscr{S} \in \mathcal{G}$.*

Proof: Define a sequence $\mathscr{S}^\mu \subset \mathcal{X}$ according to

$$\mathscr{S}^0 = \mathcal{X}; \quad \mathscr{S}^\mu = \mathcal{S} + \bigcap_{i=0}^{N}(A_i^{-1}\mathscr{S}^{\mu-1}) \cap \text{ Ker } C \tag{A.5}$$

The sequence $\mathscr{S}^\mu$ is non-increasing since $\mathscr{S}^1 \subset \mathscr{S}^0$ and if $\mathscr{S}^\mu \subset \mathscr{S}^{\mu-1}$, then

$$\mathscr{S}^{\mu+1} = \mathcal{S} + \bigcap_{i=0}^{N}(A_i^{-1}\mathscr{S}^{\mu}) \cap \text{ Ker } C \subset \mathcal{S} + \bigcap_{i=0}^{N}(A_i^{-1}\mathscr{S}^{\mu-1}) \cap \text{ Ker } C = \mathscr{S}^\mu$$

Therefore, there exist $k \leq n$ such that $\mathscr{S}^\mu = \mathscr{S}^k$ and we set $\mathscr{S}^* = \mathscr{S}^k$. Clearly $\mathscr{S}^* \in \mathcal{G}$. Next, we show that $\mathscr{S}^*$ is the maximal element. Let $\mathscr{S} \subset \mathcal{G}$, then $\mathscr{S} \subset \mathscr{S}^0$ and if $\mathscr{S} \subset \mathscr{S}^\mu$, we have

$$\mathscr{S} = \mathcal{S} + \bigcap_{i=0}^{N}(A_i^{-1}\mathscr{S}) \cap \text{ Ker } C)) \subset \mathcal{S} + \bigcap_{i=0}^{N}(A_i^{-1}\mathscr{S}^{\mu}) \cap \text{ Ker } C = \mathscr{S}^{\mu+1}$$

Consequently, $\mathscr{S} \subset \mathscr{S}^\mu$ for all μ, and hence $\mathscr{S} \subset \mathscr{S}^*$. ■

The next lemma provides an important property of the maximal element $\mathscr{S}^*$ which is used for introducing an alternative characterization of the common unobservability subspace.

Lemma A.2. *Let $\mathcal{S} \in \mathfrak{W}(\mathfrak{A}, \mathcal{X})$ and $(D_0, ..., D_N) \in \mathfrak{D}$, then $\mathscr{S}^*$ is the largest $(A_i + D_iC)$-invariant ($i \in \boldsymbol{N}_0$) that is contained in $\mathcal{S} + ker\ C$).*

Proof: First we show that any $\mathscr{S} \in \mathcal{G}$ is $(A_i + D_iC_i)$-invariant ($i \in \mathbf{N}_0$). We have $\mathscr{S} = \mathcal{S} + \bigcap_{i=0}^{N}(A_i^{-1}\mathscr{S}) \cap \text{ Ker } C$ and

$$(A_j + D_jC)\mathscr{S} = (A_j + D_jC)(\mathcal{S} + \bigcap_{i=0}^{N}(A_i^{-1}\mathscr{S}) \cap \text{ Ker } C)$$

$$\subset (A_j + D_jC)(\mathcal{S} + A_j^{-1}\mathscr{S} \cap \text{ Ker } C)$$

$$\subset (A_j + D_jC)\mathcal{S} + A_j(A_j^{-1}\mathscr{S} \cap \text{ Ker } C) \subset \mathcal{S} + \mathscr{S} \subset \mathscr{S}$$

where we used the relationship $\mathcal{S} \subset \mathscr{S}$. Therefore, $(A_j + D_jC)\mathscr{S} \subset \mathscr{S}$, $j \in \mathbf{N}_0$; and hence $\mathscr{S} \in \mathfrak{W}(\mathfrak{A}, \mathcal{X})$ and $(D_0, ..., D_N) \in \mathfrak{D}(\mathscr{S})$. Consequently, we have $\mathscr{S}^* \in \mathfrak{W}(\mathfrak{A}, \mathcal{X})$. Next we show that for any subspace $\mathcal{W}$ such that it is $(A_i + D_iC)$-invariant ($i \in \mathbf{N}_0$) and is contained in $(\mathcal{S} + \ker C)$, we have $\mathcal{W} \subset \mathscr{S}^*$. If $\mathcal{W} \subset \mathcal{S}$ then it follows that $\mathcal{W} \subset \mathscr{S}^*$, since $\mathcal{S} \subset \mathscr{S}^*$. Therefore, we consider the case where $\mathcal{S} \subset \mathcal{W}$. We have $A_i^{-1}\mathcal{W} \cap \text{ Ker } C = (A_i + D_iC)^{-1}\mathcal{W} \cap \text{ Ker } C$ and as a result $\mathcal{S} + \bigcap_{i=0}^{N}(A_i^{-1}\mathcal{W}) \cap \text{ Ker } C = \mathcal{S} + \bigcap_{i=0}^{N}((A_i + D_iC)^{-1}\mathcal{W}) \cap \text{ Ker } C$. It is clear that $\mathcal{W} \subset \mathscr{S}^0$. If $\mathcal{W} \subset \mathscr{S}^{\mu-1}$, then

$$\mathscr{S}^{\mu} \supset \mathcal{S} + \bigcap_{i=0}^{N}(A_i^{-1}\mathcal{W}) \cap \text{ Ker } C = \mathcal{S} + \bigcap_{i=0}^{N}((A_i + D_iC)^{-1}\mathcal{W}) \cap \text{ Ker } C$$

$$\supset \mathcal{S} + (\mathcal{W} \cap \text{Ker } C)) = \mathcal{W} \cap (\mathcal{S} + \text{Ker } C) = \mathcal{W}$$

where we used the fact that $\mathcal{W} \subset (A_i + D_iC)^{-1}\mathcal{W}$ and the modular distributive rule (if $\mathcal{S} \subset \mathcal{W}$, then $\mathcal{S} + (\mathcal{W} \cap \text{Ker } C) = \mathcal{W} \cap (\mathcal{S} + \text{Ker } C)$). As a consequence $\mathscr{S}^{\mu} \supset \mathcal{W}$; and hence $\mathscr{S}^* \supset \mathcal{W}$. This shows that $\mathscr{S}^*$ is the largest $(A_i + D_iC)$-invariant ($i \in \mathbf{N}_0$) which is contained in $\mathcal{S} + \text{Ker } C$. ■

We are in the position to introduce our proposed alternative characterization of the finite unobservability subspace.

Theorem A.2. *Let $\mathcal{S} \subset \mathcal{X}$ and define $\mathcal{G}$ as in* (A.4). *Then $\mathcal{S} \in \mathfrak{S}(\mathfrak{A}, \mathcal{X})$ if and only if $\mathcal{S} \in \mathfrak{W}(\mathfrak{A}, \mathcal{X})$ and $\mathcal{S} = \mathscr{S}^*$ where $\mathscr{S}^*$ is the maximal element of $\mathcal{G}$.*

Proof: **(If part)** If a) and b) hold, then according to Lemma A.2, we have $\mathcal{S}$ is the

largest $A_i + D_iC$-invariant that is contained in $\mathcal{S} + \ker C$ and hence using Lemma A.1, we have $\mathcal{S} \in \mathfrak{S}(\mathfrak{A}, \mathcal{X})$.

(Only if part) If $\mathcal{S} \in \mathfrak{S}(\mathfrak{A}, \mathcal{X})$, it follows that $\mathcal{S} \in \mathfrak{W}(\mathfrak{A}, \mathcal{X})$ and according to Lemma A.2, we have $\mathcal{S} = \mathscr{S}^*$. ■

Similar to Lemma 5.4, it can be shown that the class of finite unobservability subspaces is closed under the operation of subspace intersection. The notation $\mathfrak{S}(\mathfrak{A}, \mathcal{L})$ refers to a common u.o.s. containing $\mathcal{L} \subseteq \mathcal{X}$. Therefore, $\mathfrak{S}(\mathfrak{A}, \mathcal{L})$ has an infimal element (denoted by $\mathcal{S}^*$). The next algorithm provides a procedure for constructing $\mathcal{S}^{\mathbf{N}_0^*}$.

Algorithm A.2. *Let $\mathcal{W}^* = \inf \mathfrak{W}(\mathfrak{A}, \mathcal{L})$ and define the sequence $\mathcal{Z}^\mu$ according to*

$$\mathcal{Z}^0 = \mathcal{X}; \quad \mathcal{Z}^\mu = \mathcal{W}^* + \bigcap_{i=0}^{N} (A_i^{-1}\mathcal{Z}^{\mu-1}) \cap Ker\ C)$$

Then $\mathcal{S}^{\mathbf{N}_0^*} = \mathcal{Z}^k$, whenever $\mathcal{Z}^{k+1} = \mathcal{Z}^k$.

To analyze the above algorithm note that the sequence $\mathcal{Z}^\mu$ is non-increasing and $\mathcal{Z}^{k+1} = \mathcal{Z}^k$ for $k \geq n - \dim(\mathcal{W}^*)$. Let $\mathcal{Z}^* = \mathcal{Z}^k$. According to Lemma A.2, $\mathcal{Z}^*$ is the largest $A_i + D_iC$, $i \in \mathbf{N}_0$ that is contained in $\mathcal{W}^* + \ker C$ for some $(D_0, ..., D_N) \in \mathfrak{D}(\mathcal{W}^*)$. Let H be the solution to Ker $HC = \mathcal{W}^* + \ker C$. Then $\mathcal{Z}^*$ is an u.o.s. according to Definition A.1. Moreover, it follows that $\mathcal{L} \subset \mathcal{W}^* \subset \mathcal{Z}^*$ ($\mathcal{Z}^* \in \mathfrak{W}(\mathfrak{A}, \mathcal{L})$ and $\mathcal{W} = \inf \mathfrak{W}(\mathcal{L})$); hence $\mathcal{Z}^* \in \mathfrak{S}(\mathfrak{A}, \mathcal{L})$, and consequently $\mathcal{S}^* \subset \mathcal{Z}^*$.

On the other hand, according to Theorem A.2 we have $\mathcal{S}^* = \mathcal{S}^n$ where

$$\mathcal{S}^0 = \mathcal{X}; \qquad \mathcal{S}^\mu = \mathcal{S}^* + \bigcap_{i=0}^{N} (A_i^{-1}\mathcal{S}^{\mu-1}) \cap \text{Ker } C_i, \quad \mu \in \mathbf{n}$$

Since $\mathcal{W}^* \subset \mathcal{S}^*$, it can be shown by induction that $\mathcal{Z}^\mu \subset \mathcal{S}^\mu$, $\mu \in \mathbf{n}$. Indeed, $\mathcal{Z}^0 = \mathcal{S}^0$, and if $\mathcal{Z}^{\mu-1} \subset \mathcal{S}^{\mu-1}$, then

$$\mathcal{Z}^\mu = \mathcal{W}^* + \bigcap_{i=0}^{N} (A_i^{-1}\mathcal{Z}^{\mu-1}) \cap \text{Ker } C \subset \mathcal{S}^* + \bigcap_{i=0}^{N} (A_i^{-1}\mathcal{S}^{\mu-1}) \cap \text{Ker } C = \mathcal{S}^\mu$$

Consequently $\mathcal{Z}^* \subset \mathcal{S}^*$.

Appendix B

Integrated Fault Detection, Isolation and Control for a Network of Unmanned Vehicles

In this appendix, we briefly discuss an integrated design of fault diagnosis and control for a network of unmanned vehicles. Most of the methods that we discussed in this dissertation use an open-loop model of the plant, however, in many cases, the fault detection systems are closed-loop feedback systems. In such situation, faults may be covered by control actions and early detection of faults is clearly more difficult [238, 239]. An integrated approach to control and fault detection using four parameter controller is proposed in [240]. In [241] and [242] an H_∞ optimization technique is used to minimize the fault estimation errors and attenuate the disturbance influence on the fault detection and control problem. In [243], the simultaneous fault detection and control problem is formulated as a mixed H_2/H_∞ optimization problem. In this appendix, we briefly show how an integrated FDI and control can be formulated for a networked control system and specifically for a network of unmanned vehicles.

B.1 Integrated Fault Detection, Isolation and Control for Networked Control Systems

Consider the network control system shown Figure B.1. Usually, there exist two kinds of network-induced time delays, namely, sensor-controller delay τ_{sc} and controller actuator delay τ_{ca}, which are time-varying. The dynamics of the open-loop plant is governed by the following linear continuous-time system:

$$\dot{x}(t) = Ax(t) + Bu(t) + \sum_{i=1}^{k} L_i m_i(t) \tag{B.1}$$

$$y(t) = Cx(t) \tag{B.2}$$

As shown in Figure B.1, the FDI block has access to $y(t - \tau_{sc})$ and $u(t)$, and hence the above open-loop system cannot be considered for the design of an FDI algorithm. To remedy this problem, a new state $X(t)$ can be defined as

$$X(t) = x(t - \tau_{sc}) \tag{B.3}$$

and the state-space representation for the new state can be written as

$$\dot{X}(t) = AX(t) + Bu(t - \tau_{sc}) + \sum_{i=1}^{k} L_i m_i(t - \tau_{sc}) \tag{B.4}$$

$$y(t) = CX(t) \tag{B.5}$$

For simplicity, we consider a linear output feedback control $u(t) = Ky(t)$, so that the closed-loop system can be modeled as

$$\dot{X}(t) = AX(t) + BKCX(t - \tau) + \sum_{i=1}^{k} L_i \bar{m}_i(t) \tag{B.6}$$

$$y(t) = CX(t) \tag{B.7}$$

where $\tau = \tau_{sc} + \tau_{ca}$ is the total induced-delay of the network and $\bar{m}_i(t) = m_i(t - \tau_{sc})$. Consequently, the entire network control system can be modeled as a retarded

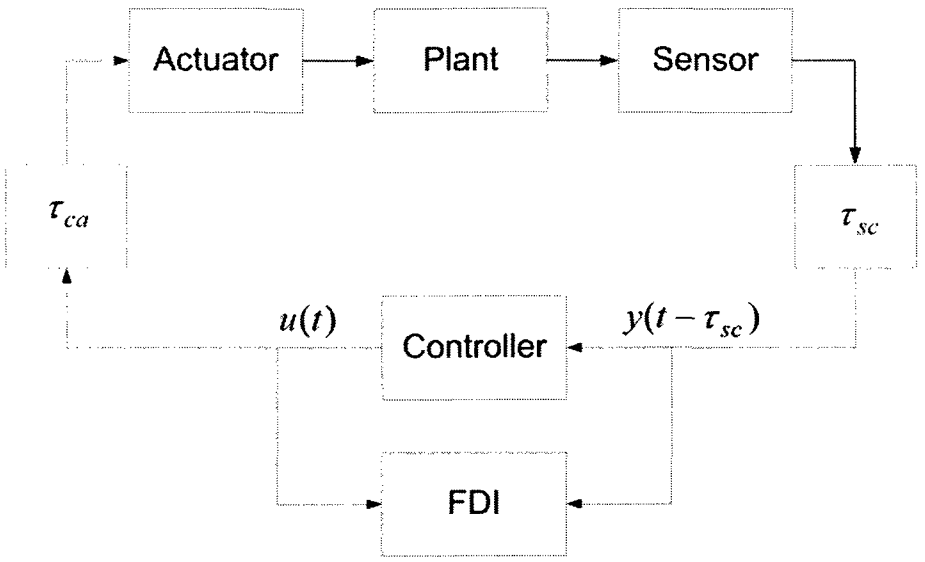

Figure B.1: The structure of a networked control system.

time-delay system and our proposed FDI algorithm for retarded time-delay systems in Chapter 6 can be applied to the FDI problem for networked control systems. Moreover, the design of control can be integrated with the design of fault detection filters as a multiobjective problem. Further work on this problem is considered as one of the directions of future research of this dissertation.

B.2 Integrated Fault Detection, Isolation and Control for a Network of Unmanned Vehicles

In this section, the problem of an integrated fault detection, isolation and control design for a network of unmanned vehicles is investigated. It is shown that our developed FDI scheme in Chapter 6 can be utilized for solving this problem. Consider a network of N homogenous vehicles where each vehicle dynamics is governed by

the following linear model (Equation (5.1)):

$$x_i(k+1) = Ax_i(k) + Bu_i(k) + \sum_{j=1}^{P} L_j m_{ij}(k)$$

$$z_{ij}(k) = C_i(x_i(k) - x_j(k)) \qquad j \in \mathrm{N}_i \tag{B.8}$$

As shown in Figure B.2, a centralized FDI/Control architecture is considered here and it is further assumed that vehicle-controller delay τ_{sc}^i and controller-vehicle delay τ_{sc}^i exist for the communication link of the i-th vehicle. Similar to Chapter 5, the delay between the vehicle and the controller τ_{sc}^i can be considered as a packet dropout and hence the entire network can be modeled as a discrete-time Markovian jump system in (5.5). Here, we assume that the actuators are event-driven. Following the same procedure as in the previous section, the entire network can be considered as a discrete-time Markovian jump system with time delay as follows:

$$x(k+1) = \bar{A}x(k) + \sum A_{\lambda(k)}^i x(k - \tau_{ca}^i) + \sum_{k=1}^{N} \sum_{j=1}^{a} \bar{L}_{kj} m_{kj}(k)$$

$$y(k) = C_{\lambda(k)} x(k)$$

where $\bar{A} = I_N \otimes A$ and the matrices $A_{\lambda(k)}^i$ depend on the controller design. For instance, for a linear output controller $u(k) = Ky(k)$, we have $A_{\lambda(k)}^i = \bar{B}_i K C_{\lambda(k)}$ where $\bar{B}_i$ is the i-th column of $\bar{B} = I_N \otimes B$.

The problem of an integrated FDI/controller design for a network of unmanned vehicles can be solved in the framework of the Markovian jump systems with delay and our proposed FDI algorithm in Section 6.4 can be applied with some modifications to this problem. Further work in this issue is one of the future research directions of this dissertation.

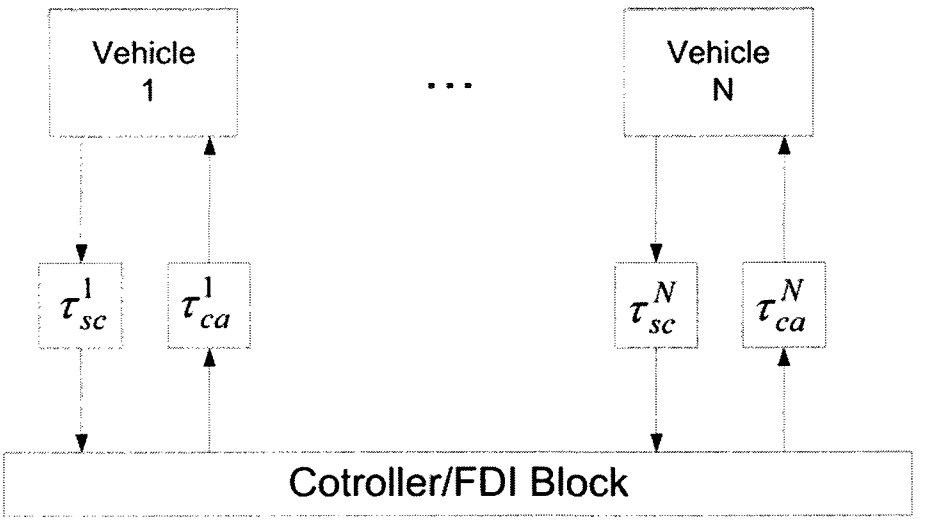

Figure B.2: Integrated FDI/Controller structure of a network of unmanned vehicles.

Bibliography

[1] T. R. Krogstad and J. T. Gravdahl. 6-DOF mutual synchronization of formation flying spacecraft. *Proceeding of IEEE Conference on Decision and Control*, 2006.

[2] E. Earon. ALTAV MK II information. *Pre-release specification, Quanser Inc., Toronto, Canada*, 2007.

[3] M. A. Massoumnia, G. C. Verghese, and A. S. Willsky. Failure detection and identification. *IEEE Transaction on Automatic Control*, 34(3):316–321, 1989.

[4] S. Simani, C. Fantuzzi, and R. J. Patton. *Model-based fault diagnosis in dynamic systems using identification techniques.* Springer, 2003.

[5] R. J. Patton, P. M. Frank, and R. N. Clark. *Fault diagnosis in dynamic systems, theory and applications.* Control Engineering series, Prentice-Hall, New York, 1989.

[6] J. Chen and R. J. Patton. *Robust model-based fault diagnosis for dynamic systems.* Kluwer Academic Publishers, Boston/Dordrecht/London, 1999.

[7] R. J. Patton, P. M. Frank, and R.N. Clark. *Issues of fault diagnosis for dynamic systems.* Springer-Verlog, London, 2000.

[8] M. Basseville and I. V. Nikiforov. *Detection of Abrupt changes: theory and application.* Information and System Science, Prentice-Hall, New York, 1993.

[9] J. Gertler. *Fault detection and diagnosis in engineering systems.* Marcel Dekker, New York, 1998.

[10] R. V. Beard. *Failure accommodation in linear system through self reorganization.* PhD thesis, Massachusettes Inst. Technol, 1971.

[11] H. Jones. *Failure detection in linear systems.* PhD thesis, Massachusettes Inst. Technol, 1973.

[12] M. A. Massoumnia. A geometric approach to the synthesis of failure detection filters. *IEEE Transaction on Automatic Control*, 31(9):839–846, 1986.

[13] J. E. White and J. L. Speyer. Detection filter design: spectral theory and algorithms. *IEEE Transaction on Automatic Control*, 32(7):593–603, 1987.

[14] R. K. Douglas and J. L. Speyer. Robust detection filter design. *Proceedings of the American Control Conference*, pages 91–96, 1995.

[15] J. H. Park and G. Rizzoni. A new interpretation of the fault-detection filter, 1: Closed-form algorithm. *International Journal of Control*, 60(5):767–787, 1994.

[16] J. H. Park and G. Rizzoni. An eigenstructure assignment algorithms for the design of fault detection filters. *IEEE Trans. Autom. Control*, 39(7):1521–1524, 1994.

[17] J. H. Park, G. Rizzoni, and W. B. Ribbens. On the representation of sensor faults in fault-detection filters. *Automatica*, 30(11):1793–1795, 1994.

[18] W. H Chung and J. L. Speyer. A game theoretic fault detection filter. *IEEE Transaction on Automatic Control*, 43(2):143–161, 1998.

[19] R. K. Douglas and J. L. Speyer. h_∞ bounded detection filter. *AIAA Journal of Guidance, Control, and Dynamics*, 22(1):129–138, 1999.

[20] R. H. Chen and J. L. Speyer. A generalized least-squares fault detection filter. *International Journal of Adaptive Control and Signal Processing*, 14:747–757, 2000.

[21] R. H. Chen and J. L. Speyer. Robust multiple-fault detection filter. *International Journal of Robust and Nonlinear Control*, 12(8):675 – 696, 2002.

[22] R. H. Chen, D. L. Mingori, and J. L. Speyer. Optimal stochastic fault detection filter. *Automatica*, 39(3):377–390, 2003.

[23] R. K. Mehra and J. Peschon. An innovations approach to fault detection and diagnosis in dynamic systems. *Automatica*, 7:637–640, 1971.

[24] A. S. Willsky and H. L. Jones. A generalized likelihood approach to the detection and estimation of jumps in linear systems. *IEEE Trans. Autom. Control*, 21:108–121, 1976.

[25] M. Basseville. Detecting changes in signals and systems - a survey. *Automatica*, 24(3):309–326, 1988.

[26] S. G. Tzafestas and K. Watanabe. Modern approaches to system/sensor fault detection and diagnosis. *Journal A. IRCU Lab*, 31(4):42–57, 1990.

[27] J. Y. Keller, L. Summerer, M. Boutayeb, and M. Darouach. Generalized likelihood ratio approach for fault detection in linear dynamic stochastic systems with unknown inputs. *Int. J. Sys. Sci.*, 27(12):1231–1241, 1990.

[28] L. Berec. A multi-model method to fault detection and diagnosis: Bayesian solution. an introductory treatise. *Int. J. of Adaptive Contr. and Signal Processing*, 44(6):1009–1016, 1998.

[29] E. Y. Chow and A. S. Willsky. Analytical redundancy and the design of robust detection systems. *IEEE Trans. Autom. Control*, 29(7):603–614, 1984.

[30] J. Gertler. Survey of model-based failure detection and isolation in complex plants. *IEEE Control Syst. Mag.*, 8(6):3–11, 1988.

[31] J. Chen and H. Y. Zhang. Parity vector approach for detecting failures in dynamic systems. *Int. J. Sys. Sci.*, 21(4):765–770, 1990.

[32] J. Gertler. Fault detection and isolation using parity relations. *Control Engineering Practice*, 5(5):653–661, 1997.

[33] M. A. Massoumnia. *A geoemtric approach to failure detection and identification in linear systems.* PhD thesis, Massachusettes Inst. Technol, 1986.

[34] J. F. Magni and P. Mouyon. On residual generation by observer and parity space approaches. *IEEE Trans. Autom. Control*, 39(2):441–447, 1994.

[35] R. J. Patton and Chen J. A review of parity space approaches to fault diagnosis. *Proceeding of the first IFAC Symp. Fault Detection, Supervision and Safety of Technical Processes, SAFEPROCESS'91*, 1:239–255, 1991.

[36] R. Isermann. Process fault detection based on modeling and estimation methods: A survey. *Automatica*, 20(4):387–404, 1984.

[37] R. Isermann. Experiences with process fault detection via parameter estimation. In S. G. Tzafestas, M. G. Singh, and G. Schmidts, editors, *System Fault Diagnostics, Reliability and Related Knowledge-based Approaches*, volume 1, pages 3–33. D. Reidel Press, Dordrecht, 1987.

[38] P. M. Frank. Fault diagnosis in dynamics system using analytical and knowledge-based redundancy- a survey and some new results. *Automatica*, 26(3):459–474, 1990.

[39] M. Witczak. *Modeling and estimation strategies for fault diagnosis of nonlinear system: from analytical to soft computing approach.* Springer-Verlog, 2007.

[40] J. Gertler. Analytical redundancy methods in failure detection and isolation. *Proceeding of IFAC Fault Detection, Supervision and Safety for Technical Processes*, pages 9–21, 1991.

[41] J. Gertler and D. Singer. A new structural framework for parity equation based failure detection and isolation. *Automatica*, 26:381–388, 1990.

[42] E. A. Garci and P. M. Frank. Deterministic nonlinear observer-based approaches to fault diagnosis: A survey. *IFAC Control Eng. Prac.*, 5:663–670, 1997.

[43] V. Krishnaswami and G. Rizzoni. Robust residual generation for nonlinear system fault detection and isolation. *Proc. IFAC Symp. Fault Detection, Supervision Safety Technical Processes*, pages 163–168, 1997.

[44] C. Guernez, J. P. Cassar, and M. Staroswiecki. Extension of parity space to nonlinear polynomial dynamic systems. *Proceeding of the 3th IFAC Symp. Fault Detection, Supervision and Safety of Technical Processes, SAFEPROCESS'97*, 2:861–866, 1997.

[45] V. Krishnaswami and G. Rizzoni. Nonlinear parity equation residual generation for fault detection and isolation. *Proceeding of the 2th IFAC Symp. Fault Detection, Supervision and Safety of Technical Processes, SAFEPROCESS'94*, 1:317–322, 1994.

[46] A. Shumsky. Robust residual generation for diagnosis of nonlinear systems: parity relation approach. *Proceeding of the 3th IFAC Symp. Fault Detection, Supervision and Safety of Technical Processes, SAFEPROCESS'97*, 2:867–872, 1997.

[47] D. Hengy and P. M. Frank. Component failure detection via nonlinear state observers. *Proceeding of IFAC Workshop on fault detection and Safety in chemical plants*, 1:153–157, 1986.

[48] K. Adjallah, D. Maquin, and J. Ragot. Nonlinear observer-based fault detection. *Proceeding of the third IEEE Conference on Control Application*, pages 1150–1120, 1994.

[49] R. Seliger and P. M. Frank. Fault diagnosis by disturbance decoupled nonlinear observer. *Proceedings of IEEE Conference on Decision and Control*, pages 2248–2253, 1991.

[50] R. Seliger and P. M. Frank. Robust observer-based fault diagnosis in nonlinear uncertain systems. In R. J. Patton, P. M. Frank, and R. N. Clark, editors, *Issues of fault diagnosis for dynamic systems*. Springer Verlag, Englewood Cliffs, NJ, 2000.

[51] W. Chen and M. Saif. Fault detection and isolation based on novel unknown input observer design. *Proceedings of the 2006 American Control Conference*, pages 5129–5134, 2006.

[52] H. Yang and M. Saif. Nonlinear adaptive observer design for fault detection. *Proceedings of the American Control Conference*, pages 1136–1139, 1995.

[53] B. Jiang, M. Staroswiecki, and V. Cocquempot. Fault diagnosis based on adaptive observer for a class of non-linear systems with unknown parameters. *International journal of control*, 77(4):415–426, 2004.

[54] R. Sreedhar, B. Fernandez, and G. Y. Masada. Robust fault detection in nonlinear systems using sliding mode observers. *Proceedings of IEEE Conference on Control Applications*, pages 716–721, 1993.

[55] C. Edwards, S. K. Spurgeon, and R. J. Patton. Sliding mode observers for fault detection and isolation. *Automatica*, 36(4):541–553, 2000.

[56] B. Jiang, M. Staroswiecki, and V. Cocquempot. Fault estimation in nonlinear uncertain systems using robust/sliding-mode observers. *IEE Proceedings on Control Theory Application*, pages 29–37, 2004.

[57] W. Chen and M. Saif. A sliding mode observer-based strategy for fault detection, isolation, and estimation in a class of lipschitz nonlinear systems. *International Journal of Systems Science*, 38(12):943–955, 2007.

[58] X. Yan and C. Edwards. Nonlinear robust fault reconstruction and estimation using a sliding mode observer. *Automatica*, 43(9):1605–1614, 2007.

[59] C. D. Persis and A. Isidori. On the observability codistributions of a nonlinear system. *Systems and Control Letters*, 40:297–304, 2000.

[60] C. D. Persis and A. Isidori. A geometric approach to nonlinear fault detection and isolation. *IEEE Transactions on Automatic Control*, 46(6):853–865, 2001.

[61] C. D. Persis and A. Isidori. On the design of fault detection filters with game-theoretic-optimal sensitivity. *International Journal of Robust and Nonlinear Control*, 12:729–747, 2002.

[62] H. Hammouri, P. Kabore, , and M. Kinnaert. A geometric approach to fault detection and isolation for bilinear systems. *IEEE Trans. Autom. Control*, 46(9):1451–1455, 2001.

[63] N. Meskin, T. Jiang, E. Sobhani, K. Khorasani, and C. A. Rabbath. A nonlinear geometric approach to fault detection and isolation in an aircraft nonlinear longitudinal mode. *Proceeding of American Control Conference*, pages 5771–5776, 2007.

[64] J. Korbicz, J. Koscielny, Z. Kowalczuk, and W. Cholewa. *Fault diagnosis, models, artifical intelligence, application.* Springer-Verlog, Berlin, 2004.

[65] M. Weerasinghe, J. B. Gomm, and D. Williams. Neural networks for fault diagnosis of a nuclear fuel processing plant at different operating points. *Control Engineering Practice*, 6(2):281–289, 1998.

[66] M. J. Fuente and S. Saludes. Fault detection and isolation in a nonlinear plant via neural networks. *Proceeding of the 4th IFAC Symp. Fault Detection, Supervision and Safety of Technical Processes, SAFEPROCESS'2000*, 1:472–477, 2000.

[67] K. Patan and T. Parisini. Identification of neural dynamic models for fault detection and isolation: the case of real sugar evaporation process. *Journal of Process Control*, 15(1):67–79, 2005.

[68] I.A. Al-Zyoud and K. Khorasani. Detection of actuator faults using dynamics neural network for the attitude control subsystem of a satellite. *Proc. IEEE International Joint Conference on Neural Networks (IJCNN-2005)*, pages 1746–1751, 2005.

[69] E. Sobhani, K. Khorasani, and S. Tafazoli. Dynamic neural networkbased estimator for fault diagnosis in reaction wheel actuator of satellite attitude control system. *Proc. IEEE International Joint Conference on Neural Networks (IJCNN-2005)*, pages 2347–2352, 2005.

[70] H.A. Talebi and R.V. Patel. A neural network-based fault detection scheme for satellite attitude control systems. *Proc. IEEE Control Applications Conf.*, pages 1293–1298, 2005.

[71] H.A. Talebi and R.V. Patel. An intelligent fault detection and recovery scheme for reaction wheel actuator of satellite attitude control systems. *Proc. IEEE Control Applications Conf.*, pages 3282–3287, 2006.

[72] Q. Wu and M. Saif. Neural adaptive observer based fault detection and identification for satellite attitude control systems. *American Control Conference*, pages 1054–1059, 2005.

[73] Z. Q. Li, L. Ma, and K. Khorasani. A dynamic neural network-based reaction wheel fault diagnosis for satellites. In *Proc. IEEE International Joint Conference on Neural Networks (IJCNN-2006)*, Vancouver, Canada, July 2006.

[74] Z. Chen, Y. He, F. Chu, and J. Huang. Evolutionary strategy for classification problems and its application in fault diagnosis. *Engineering Applications of Artificial intelligence*, 16(1):31–38, 2003.

[75] R. Sun, F. Tsung, and L. Qu. Combining bootstrap and genetic programming for feature discovery in diesel engine diagnosis. *International Journal of Industrial engineering*, 11(3):273–281, 2004.

[76] D. P. Scharf, F. Y. Hadaegh, and S. R. Ploen. A survey of spacecraft formation flying guidance and control (part i): Guidance. *Proceedings of the American Control Conference*, pages 1733–1739, 2003.

[77] D. P. Scharf, F. Y. Hadaegh, and S. R. Ploen. A survey of spacecraft formation flying guidance and control (part ii): Control. *Proceedings of the American Control Conference*, pages 2976–2985, 2004.

[78] P. K. C. Wang and F. Y. Hadaegh. Coordination and control of multiple microspacecraft moving in formation. *Journal of the Astronautical Sciences*, 44(3):315–355, 1996.

[79] R. W. Beard, J. Lawton, and F.Y. Hadaegh. A coordination architecture for spacecraft formation control. *IEEE Trans. Control Syst. Technol.*, 9(6):777–790, 2001.

[80] M. Mesbahi and F. Y. Hadaegh. Formation flying control of multiple spacecraft via graphs, matrix inequalities and switching. *J. Guid., Contr., & Dyn.*, 24(2):369–377, 2001.

[81] V. Manikonda, P. O. Arambel, M. Gopinathan, R. K. Mehra, and F. Y. Hadaegh. A model predictive control-based approach for spacecraft formation keeping and attitude control. *Proceedings of the American Control Conference*, pages 4258–4262, 1999.

[82] R. S. Smith and F. Y. Hadaegh. Parallel estimation and communication in spacecraft formations. *IFAC World Congress*, 2005.

[83] W. Ren and R. W. Beard. A decentralized scheme for spacecraft formation flying via the virtual structure approach. *AIAA Journal of Guidance, Control and Dynamics*, 27(1):73–82, 2004.

[84] P. Lawson. The terrestrial planet finder. *IEEE Proceedings of Aerospace Conference*, pages 2005–2011, 2001.

[85] C. V. M. Fridlund. Darwin - the infrared space interferometry mission. *ESA Bulletin 103*, 2000.

[86] T. W. Mclain and R. W. Beard. Trajectory planning for coordinated rendezvous of unmanned air vehicles. *Proceeding of the AIAA Conference on Guidance, Navigation, and Control*, AIAA 2000-4369, 2000.

[87] R. W. Beard, T. W. McLain, M. Goodrich, and E. P. Anderson. Coordinated target assignment and intercept for unmanned air vehicles. *IEEE Transactions on Robotics and Automation*, 18(6):911–922, 2002.

[88] A. Tiwari, J. Fung, J. M. Carson, R. Bhattacharya, and R. M. Murray. A framework for Lyapunov certificates for multi-vehicle rendezvous problems. *IEEE Proceedings of the American Control Conference*, pages 5582–5587, 2004.

[89] D. W. Casbeer, D. B. Kingston, R. W. Beard, S. Li T. W. McLain, and R. Mehra. Cooperative forest fire surveillance using a team of small unmanned air vehicles. *International Journal of Systems Sciences*, 37(6):351–360, 2006.

[90] R. W. Beard and T. W. McLain. Multiple UAV cooperative search under collision avoidance and limited range communication constraints. *IEEE Conference on Decision and Control*, pages 25–30, 2003.

[91] Y. Yang, A. A. Minai, and M. M. Polycarpou. Decentralized cooperative search by networked UAVs in an uncertain environment. *IEEE Proceedings of the American Control Conference*, pages 5558–5563, 2004.

[92] Y. Jin, A. A. Minai, and M. M. Polycarpou. Cooperative real-time search and task allocation in UAV teams. *IEEE Conference on Decision and Control*, pages 7–12, 2003.

[93] L. E. Buzogany, M. Pachter, and J. J. d'Azzo. Automated control of aircraft in formation flight. *Proceedings of the AIAA Conference on Guidance, Navigation, and Control*, pages 1349–1370, 1993.

[94] D. F. Chichka, J. L. Speyer, and C. G. Park. Peak-seeking control with application to formation flight. *IEEE Conference on Decision and Control*, pages 2463–2470, 1999.

[95] F. Giuletti, L. Pollini, and M. Innocenti. Autonomous formation flight. *IEEE Control Systems Magazine*, pages 34–44, 2000.

[96] J. D. Wolfe, D. F. Chichka, and J. L. Speyer. Decentralized controllers for unmanned aerial vehicle formation flight. *Proceedings of the AIAA Conference on Guidance, Navigation, and Control*, 1996. AIAA Paper 96-3833.

[97] A. Knoll and J. Beck. Autonomous decision-making applied onto UAV formation flight. *Proceedings of the AIAA Conference on Guidance, Navigation, and Control*, 2006. AIAA Paper 2006-6202.

[98] J. Yuh. Underwater robotics. *Proceedings of the IEEE Conference on Robotics and Automation*, pages 932–937, 2000.

[99] P. Bhatta, E. Fiorelli, F. Lekien, N. E. Leonard, D. A. Paley, F. Zhang, R. Bachmayer, R. E. Davis, D. M. Fratantoni, and R. Sepulchre. Coordination of an underwater glider fleet for adaptive ocean sampling. *Proc. Int. Workshop on Underwater Robotics for Sustainable Management of Marine Ecosystems and Environmental Monitoring*, pages 61–69, 2005.

[100] A. J. Healey. Application of formation control for multi-vehicle robotic minesweeping. *IEEE Conference on Decision and Control*, pages 1497–1502, 2001.

[101] J. G. Bender. An overview of systems studies of automated highway systems. *IEEE Transactions on Vehicular Technology*, 40(1):82–99, 1991.

[102] S. E. Shladover, C. A. Desoer, J. K. Hedrick, M. Tomizuka, J. Walrand, W. Zhang, D. H. McMahon, H. Peng, S. Sheikholeslam, and N. McKeown. Automatic vehicle control developments in the path program. *IEEE Transactions on Vehicular Technology*, 40(1):114–130, 1991.

[103] J. P. Desai, J. Ostrowski, and V. Kumar. Controlling formations of multiple mobile robots. *IEEE International Conference on Robotics and Automation*, 4:2864 – 2869, 1998.

[104] R. Ghabcheloo, A. Pascoal, C. Silvestre, and I. Kaminer. Nonlinear coordinated path following control of multiple wheeled robots with bidirectional communication constraints. *International Journal of Adaptive Control and Signal Processing*, 2006.

[105] P. Ogren, M. Egerstedt, and X. Hu. A control Lyapunov function approach to multi-agent coordination. *IEEE Trans. on Robotics and Automation*, 18:847–851, 2002.

[106] J. R. T. Lawton, R. W. Beard, and B. J. Young. A decentralized approach to formation maneuvers. *IEEE J. Robot. Autom.*, 19(6):933–941, 2003.

[107] W. C. Dickson, R. H. Cannon, and S. M. Rock. Symbolic dynamic modeling and analysis of object/robot-team systems with experiment. *Proceeding of IEEE Conference on Robotics and Automation*, pages 1413–1420, 1996.

[108] C. R. Kube and H. Zhang. The use of perceptual cues in multi-robot box-pushing. *Proceeding of IEEE Conference on Robotics and Automation*, pages 2085–2090, 1996.

[109] T. Vidal, M. Ghallab, and R. Alami. Incremental mission allocation to a large team of robots. *Proceeding of IEEE Conference on Robotics and Automation*, pages 1620–1625, 1996.

[110] D. Kurabayashi, J. Ota, T. Arai, and E. Yoshida. Cooperative sweeping by multiple mobile robots. *Proceeding of IEEE Conference on Robotics and Automation*, pages 1744–1749, 1996.

[111] M. O. Anderson, M. D. Mckay, and B. S. Richardson. Multirobot automated indoor floor characterization team. *Proceeding of IEEE Conference on Robotics and Automation*, pages 1750–1753, 1996.

[112] H. Yamaguchi. Adaptive formation control for distributed autonomous mobile robot groups. *Proceeding of IEEE Conference on Robotics and Automation*, pages 2300–2305, 1997.

[113] A. Fax and R. Murray. Information flow and cooperative control of vehicle formations. *Proceedings of the 2002 IFAC World Congress*, 2002.

[114] A. Fax and R. Murray. Graph laplacians and vehicle formation stabilization. *Proceedings of the 2002 IFAC World Congress*, 2002.

[115] L. E. Parker. Alliance: An architecture for fault tolerant multirobot cooperation. *IEEE Transaction on Robotics and Automation*, 14(2):220–240, 1998.

[116] L. Cheng and Y. Wang. Fault tolerance for communication-based multirobot formation. *Proceedings of the Third International Conference on Machine Leming and Cybernetics*, pages 127–132, 2004.

[117] L. Pollid, F. Giulietti, and M. Innocenti. Robustness to communication failures within formation flight. *IEEE Proceedings of the American Control Conference*, pages 2860–2866, 2002.

[118] W. H Chung and J. L. Speyer. A decectralized fault detection filter. *ASME J. of Dynamic Systems, Measurement, Control*, 123(2):237–247, 2001.

[119] J. L. Speyer. Computation and transmission requirements for a decentralized linear-quadratic-gaussain control problem. *IEEE Transaction on Automatic Control*, 24(2):226–269, 1979.

[120] S. Shankar, S. Darbha, and A. Datta. Design of a decentralized detection filter for a large collection of interacting LTI systems. *Mathematical Problems in Engineering*, 8(3):233–248, 2002.

[121] M. J. Daigle, X. D. Koutsoukos, and G. Biswas. Distributed diagnosis in formations of mobile robots. *IEEE Transaction on Robotics*, 23(2):353–369, 2007.

[122] H. Yang and M. Saif. Robust observation and fault diagnosis in a class of time-delay control systems. *American Control Conference*, pages 478–482, 1997.

[123] H. Yang and M. Saif. Observer design and fault diagnosis for state-retarded dynamical systems. *Automatica*, 34(2):217–227, 1998.

[124] J. H. Liu and P. M. Frank. H_∞ detection filter for state delayed linear systems. *Proc.* 14th *IFAC World Congress Conference*, pages 229–233, 1999.

[125] S. X. Ding, M. Zhong, T. Bingyong, and P. Zhang. An LMI approach to the design of fault detection filter for time-delay LTI systems with unknown inputs. *American Control Conference*, pages 2137–2142, 2001.

[126] B. Jiang, M. Staroswiecki, and V. Cocquempot. H_∞ fault detection filter design for linear discrete-time systems with multiple time delays. *International Journal of System Science*, 34(5):365–373, 2003.

[127] M. Zhong, S. X. Ding, J. Lam, and C. Zhang. Fault detection filter design for LTI systems with time delays. *Proceeding of the* 42th *Conference on Decision and Control*, pages 1467–1472, 2003.

[128] M. Zhong, H. Ye, and G. Wang. Multi-freedom design of fault detection filter for linear time-delay systems. 8th *International conference on control, Automation, Robotics and Vision*, pages 1630–1634, 2004.

[129] B. Leishi, T. Zuohua, and S. Songjiao. RFDF design for linear time-delay systems with unknown inputs and parameter uncertainties. *International Journal of System Science*, 38(2):139–149, 2007.

[130] S. Hashtrudizad and M. A. Massoumnia. Generic solvability of the failure detection and identification. *Automatica*, 35(5):887–893, 1999.

[131] R. N. Clark. A simplified instrument failure detection scheme. *IEEE Trans. Aerosp. Electron. Syst.*, 14(4):558–563, 1978.

[132] S. X. Ding, P. Zhang, P. M. Frank, and E. L. Ding. Threshold calculation using LMI-technique and its integration in the design of fault detection systems. *Proceeding of the* 42th *Conference on Decision and Control*, pages 469–474, 2003.

[133] G. Basile and G. Marro. *Controlled and conditioned invariant subspaces in linear system theory.* Prentice-Hall, 1992.

[134] W. M. Wonham. *Linear multivariable control: A geometric approach.* Springer-Verlag, New York, third edition, 1985.

[135] A. Isidori, A. J. Kerner, C. Gori-Giorgi, and S. Monaco. Nonlinear decoupling via feedback: A differential geometric approach. *IEEE Transactions on Automatic Control*, 26:331–345, 1981.

[136] J. P. Gauthier and I. A. K. Kupca. Observability and observers for nonlinear systems. *SIAM Journal on Control and Optimization*, 32:975–994, 1994.

[137] J. D. Boskovic, S. E. Bergstrom, and R. K. Mehra. Retrofit reconfigurable flight control in the presence of control effector damage. *Proceeding of American Control Conference*, pages 2652–2657, 2005.

[138] N. Meskin and K. Khorasani. Fault detection and isolation of actuator faults in spacecraft formation flight. *Proceeding of IEEE Conference on Decision and Control*, pages 1159–1164, 2006.

[139] N. Meskin and K. Khorasani. Fault detection and isolation in a redundant reaction wheels configuration of a satellite. *Proceeding of IEEE International Conference on Systems, Man, and Cybernetics*, pages 3153–3158, 2007.

[140] N. Meskin and K. Khorasani. Fault detection and isolation of actuator faults in overactuated systems. *Proceeding of American Control Conference*, pages 2527 – 2532, 2007.

[141] N. Meskin and K. Khorasani. Actuator fault detection and isolation for a network of unmanned vehicles. *IEEE Transactions on Automatic Control*, To appear.

[142] H. Schaub and J. L. Junkins. *Analytical Mechanics of Space Systems.* AIAA Educational Series, 2003.

[143] D. McLean, S. Aslam-Mir, and H. Benkhedda. Fault detection and control reconfiguration in flight control. *IEE Colloquium on Fault Diagnosis and Control System Reconfiguration*, pages 1–1, 1993.

[144] A. Barua, P. Sinha, K. Khorasani, and S. Tafazoli. A novel fault-tree approach for identifying potential causes of satellite reaction wheel failure. In *Proc. 2005 IEEE International Conference on Control Applications (CCA-2005)*, pages 1467–1472, Toronto, Canada, August 2005.

[145] N. Tudoroiu and K. Khorasani. Satellite fault diagnosis using a bank of interactive Kalman filters. *To appear in IEEE Transactions on Aerospace and Electronic Systems*, 2007.

[146] K. Watanabe and D. M. Himmelblau. Instrument fault detection in systems with uncertainties. *Int. J. Sys. Sci.*, 13(2):137–158, 1982.

[147] P. M. Frank. Fault diagnosis in dynamic system via state estimation- a survey. In S. G. Tzafestas, M. G. Singh, and G. Schmidts, editors, *System Fault*

Diagnostics, Reliability and Related Knowledge-based Approaches, volume 1, pages 35–98. D. Reidel Press, Dordrecht, 1987.

[148] R. Seliger and P. M. Frank. Fault diagnosis by disturbance decoupled nonlinear observers. *Proc. of the* 30th *IEEE Conf. on Decision and Control*, pages 2248–2253, 1991.

[149] R. J. Patton. Robust fault detection using eigenstructure assignment. *Proc.* 12th *IMACs World Congress on Scientific Computation*, pages 431–434, 1988.

[150] J. Chen. *Robust residual generation for model-based fault diagnosis of dynamic systems.* PhD thesis, University of York, York, UK, 1995.

[151] R. J. Patton and J. Chen. Observer-based fault detection and isolation: robustness and applications. *Contr. Eng. Practice*, 5(5):671–682, 1997.

[152] X. Lou, G. C. Verghese, and A. S. Willsky. Optimally robust redundancy relations for failure detection in uncertain systems. *Automatica*, 22(3):333–344, 1986.

[153] N. E. Wu and Y. Y. Wang. Robust failure detection with parity check in filtered measurements. *IEEE Trans. Aerosp. Electron. Syst.*, 31(1):489–491, 1995.

[154] X. Ding and L. Guo. An approach to time domain optimization of observer-based fault detection systems. *International Journal of Control*, 69(3):419–442, 1998.

[155] N. Viswanadham and K. D. Minto. Robust observer design with application to fault detection. *Amer. contr. Conf.*, pages 1393–1399, 1988.

[156] P. M. Frank and X. Ding. Frequency domain approach to optimally robust residual generation and evaluation for model-based fault diagnosis. *Automatica*, 30(4):786–804, 1994.

[157] M. Kinnaert and Y. B. Peng. Residual generator for sensor and actuator fault detection and isolation- a frequency-domain approach. *International Journal of Control*, 61(6):1423–1435, 1995.

[158] M. Zhong, S. X. Ding, and B. Tang. An LMI approach to robust fault detection filter for discrete-time systems with model uncertainty. *Proceeding of the* 40th *conference on decision control*, pages 3613–3618, 2001.

[159] M. Zhong, S. X. Ding, J. Lam, and H. Wang. An LMI approach to robust fault detection filter for uncertain LTI systems. *Automatica*, 39:543–550, 2003.

[160] A. Casavola, D. Famularo, and G. Franze. A robust deconvolution scheme for fault detection and isolation of uncertain linear systems: an LMI approach. *Automatica*, 41:1463–1472, 2005.

[161] Y. Kim and J. M. Watkins. A new approach for robust and reduced order fault detection filter design. *Proceeding of American Control Conference*, pages 1137–1142, 2007.

[162] M. Sampath, R. Sengupta, S. Lafortune, and K. Sinnamohideen. Failure diagnosis using discrete-event models. *IEEE Transactions on Control System Technology*, 4(2):105–124, 1996.

[163] S. Hashtrudizad, R. H. Kwong, and W. M. Wonham. Fault diagnosis in discrete-event systems: Framework and model reduction. *IEEE Transactions on Automatic Control*, 48(7):1199–1212, 2003.

[164] S. Hashtrudizad, R. H. Kwong, and W. M. Wonham. Fault diagnosis in discrete-event systems: Incorporating timing information. *IEEE Transactions on Automatic Control*, 50(7):1010–1015, 2005.

[165] S. McIlraith, G. Biswas, Dan Clancy, and Vineet Gupta. Hybrid systems diagnosis. *Proceedings of The Third International Workshop on Hybrid Systems: Computation and Control (HSCC 2000)*, pages 282–295, 2000.

[166] S. Narasimhan and G. Biswas. Model-based diagnosis of hybrid systems. *IEEE Transactions on Systems, Man and Cybernetics-Part A: Systems and Humans*, 37(3):348–361, 2007.

[167] D. Berdjag, C. Christophe, and V.t Cocquempot. Nonlinear model decomposition for fault detection and isolation system design. *Proceedings of 45th IEEE Conference on Decision and Control*, pages 3321–3326, 2006.

[168] C. D. Persis and A. Isidori. Fault detection and isolation for state affine systems. *European Journal of Control*, 6:290–294, 2000.

[169] E. Earon. Almost-lighter-than-air-vehicle fleet simulation. *Technical Report, V. 0.9, Quanser Inc., Toronto, Canada*, 2005.

[170] E. O. Elliott. Estimates of error rates for codes on burst-noise channels. *Bell Systems Technical Journal*, 42, 1963.

[171] E. N. Gilbert. Capacity of burst-noise channels. *Bell Systems Technical Journal*, 39, 1960.

[172] N. Meskin and K. Khorasani. Geometric approach to robust fault detection and isolation of Markovian jump systems. *Proceeding of American Control Conference*, pages 2822–2827, June 2008.

[173] Y. Zheng, H. Fang, and Y. Wang. Kalman filter based FDI of networked control system. *Proceeding of the* 5th *World Congress on Intelligent Control and Automation*, pages 1330–1333, 2004.

[174] P. Zhang, S. X Ding, P. M. Frank, and M. Sader. Fault detection of networked control systems with missing measurements. *Proceeding of the* 5th *Asian Control Conference*, pages 1258–1263, 2004.

[175] H. Ye and S. X. Ding. Fault detection of networked control systems with networked-induced delay. *Proceeding of the* 8th *International Conference on Control, Automation, Robotics and Vision*, pages 294–297, 2004.

[176] I. M. Al-Salami, S. X. Ding, and P. Zhang. Statistical based residual evaluation for fault detection in networked control systems. *2006 IAR Annual meeting*, 2006.

[177] S. X. Ding, T. Jeinsch, P. M. Frank, and E. L. Ding. A unified approach to the optimization of fault detection system. *International Journal of Adaptive Control and Signal Processing*, 14(7):725–745, 2000.

[178] S. Li, D. Sauter, and C. Aubrun. Robust fault isolation filter design for networked control systems. *IEEE Conference on Emerging Technologies and Factory Automation*, pages 681–688, 2006.

[179] Z. Mao, B. Jiang, and P. Shi. H_∞ fault detection filter design for networked control systems modeled by discrete markovian jump systems. *IET Control Theory and Application*, 1(5):1336–1343, 2007.

[180] P. Seiler and R. Sengupta. An H_∞ approach to networked control. *IEEE Trans. Autom. Control*, 50(3):356–364, 2005.

[181] J. Xiong and J. Lam. Stabilization of linear systems over networks with bounded packet loss. *Automatica*, 43:80–87, 2007.

[182] V. Gupta, R. M. Murray, and B. Hassibi. On the control of jump linear Markov systems with Markov state estimation. *Proceeding of American Control Conference*, pages 2893–2898, 2003.

[183] R. Krtolica, U. Ozguner, H. Chan, H. Gktas J. Winkelman, and M. Liubakka. Stability of linear feedback systems with random communication delays. *Int. J. Control*, 59(4):925–953, 1994.

[184] L. Xiao, A. Hassibi, and J. How. Control with random communication delays via a discrete-time jump system approach. *Proceeding of American Control Conference*, pages 2199–2204, 2000.

[185] Z. Jin, V. Gupta, and R. M. Murray. State estimation over packet dropping networks using multiple description coding. *Automatica*, 42(9):1441–1452, 2006.

[186] P. Shi, E. K. Boukas, and R. K. Agarwal. Control of Markovian jump discrete-time systems with norm bounded uncertainty and unknown delay. *IEEE Trans. Autom. Control*, 44(11):2139–2144, 1999.

[187] Y. Cao and J. Lam. Robust H_∞ control of uncertain Markovian jump systems with time-delay. *IEEE Trans. Autom. Control*, 45(1):77–83, 2000.

[188] C. E. de Souza and M. D. Fragoso. H_∞ filtering for Markovian jump linear systems. *International Journal of Systen Science*, 33:909–915, 2002.

[189] J. Xing and J. Lam. Fixed-order robust H_∞ filter design for Markovian jump systemswith uncertain switching probabilities. *IEEE Trans. Signal Process.*, 54(4):1421–1430, 2006.

[190] El-Kebir Boukas. *Stochastic switching systems: analysis and design.* Birkhauser, Boston, 2006.

[191] O. L. V. Costa, M. D. Fragoso, and R. P. Marques. *Discrete-Time Markov Jump systems.* Springer-Verlag, London, 2005.

[192] O. L. V. Costa, M. D. Fragoso, and R. P. Marques. *Jump linear systems in automatic control.* Marcel Dekker Inc., New York, 1990.

[193] M. Zhong, H. Ye, P. Shi, and G. Wang. Fault detection for Markovian jump systems. *IEE Proc. Control Theory Application*, 152(4):397–402, 2005.

[194] H. Wang, C. Wang, H. Gao, and L. Wu. An LMI approach to fault detection and isolation filter design for Markovian jump system with mode-dependent time-delays. *Proceedings of the American Control Conference*, pages 5686–5691, 2006.

[195] E. F. Costa and J. B. R. Do Val. Weak detectabilty and the linear-quadratic control problem of discrete-time Markov jump linear systems. *International Journal of Control*, 75(16/17):1282–1292, 2002.

[196] G. Basile and G. Marro. On the robust controlled invariant. *Systems & Control Letters*, 9(3):191–195, 1987.

[197] P. Seiler and R. Sengupta. A bounded real lemma for jump systems. *IEEE Trans. Autom. Control*, 48(9):1651–1654, 2003.

[198] M. C. de Oliveira, J. C. Geromel, and J. Bernussou. Extend H_2 and H_∞ norm characterizations and controller parameterizations for discrete time systems. *International Journal of Control*, 75(9):666–679, 2002.

[199] E. F. Costa and J. B. R. Do Val. On the observability and detectability of continuous-time Markov jump linear systems. *Siam J. Control Optim.*, 41(4):1295–1314, 2002.

[200] G. Marro. The geometric approach toolbox. *http://www3.deis.unibo.it/Staff/FullProf/GiovanniMarro/geometric.htm*, 2007.

[201] J. Lofberg. Yalmip : A toolbox for modeling and optimization in MATLAB. In *Proceedings of the CACSD Conference*, Taipei, Taiwan, 2004.

[202] J. Xiong, J. Lam., H. Gao, and D. W. C. Ho. On robust stabilization of Markovian jump systems with uncertain switching probabilities. *Automatica*, 41(5):897–903, 2005.

[203] K. S. Narendra and S. S. Tripathi. Identification and optimization of aircraft dynamics. *J. Aircraft*, 10(4):193–199, 1973.

[204] J. D. Boskovic, S. E. Bergstrom, and R. K. Mehra. Retrofit reconfigurable flight control in the presence of control effector damage. *Proceedings of the 2005 American Control conference*, pages 2652–2657, 2005.

[205] N. Meskin and K. Khorasani. Fault detection and isolation of retarded time-delay systems using a geometric approach. *Proceeding of IFAC World Congress*, pages 7326–7331, 2008.

[206] N. Meskin and K. Khorasani. A geometric approach to fault detection and isolation of neutral time-delay systems. *Proceeding of American Control Conference*, pages 3293–3298, June 2008.

[207] N. Meskin and K. Khorasani. H_∞-based fault detection and isolation of markovian jump systems with mode-dependent time-delays and uncertain switching probability. *International Journal of Robust and Nonlinear Control*, To appear.

[208] N. Meskin and K. Khorasani. Robust fault detection and isolation of time-delay systems using a geometric approach. *Automatica*, To appear.

[209] F. Kratz, W. Nuninger, and S. Ploix. Fault detection for time-delay systems: a parity space approach. *American Control Conference*, pages 2009–2011, 1998.

[210] B. Jiang, M. Staroswiecki, and V. Cocquempot. Fault identification for a class of time-delay systems. *Proceeding of the American Control Conference*, pages 2239–2244, 2002.

[211] Y. Fuqiang, T. Zuohua, and S. Songjiao. Actuator fault diagnosis for a class of time-delay systems. *Proceeding of* 5th *World Congress on Intelligent Control and Automation*, pages 1798–1802, 2004.

[212] C. Jiang and D. H. Zhou. Fault detection and identification for uncertain linear time-delay systems. *Computer and Chemical Engineering*, 30:228–242, 2005.

[213] S. Zhu and Z. Cheng. Design of robust fault detection and isolation observers for singular time delay systems. *American Control Conference*, pages 5064–5065, 2004.

[214] J. Ren. LMI-based fault detection filter design for a class of neutral system with time delay in states. *Proc.* 16th *World Congress on Intelligent Control and Automation*, pages 5581–5585, 2006.

[215] J. Bokor and G. Balas. Detection filter design for LPV systems: A geometric approach. *Automatica*, 40(3):511–518, 2004.

[216] J. H. Kim and H. B. Park. H_∞ state feedback control for generalized continuous/discrete time delay system. *Automatica*, 35(8):1443–1451, 1999.

[217] M. Darouach. Reduced-order observer for linear neutral delay systems. *IEEE Trans. Autom. Control*, 50(9):1407–1413, 2005.

[218] S. Xu and T. Chen. An LMI approach to the H_∞ filter design for uncertain systems with distributed delays. *IEEE Trans. Circuits Syst. II*, 51(4):195–201, 2004.

[219] S. Xu, T. Chen, and J. Lam. Robust H_∞ filtering for uncertain Markovain jump systems with mode-dependent time delays. *IEEE Trans. Autom. Control*, 48(5):900–907, 2003.

[220] M. S. Mahmoud. Dynamic control of systems with variable state-delay. *International Journal of robust and nonlinear control*, 6:123–146, 1996.

[221] L. Xie, E. Fridman, and U. Shaked. Robust H_∞ control of distributed delay systems with application to combustion control. *IEEE Trans. Autom. Control*, 46(12):1930–1935, 2001.

[222] Y. A. Fiagbedzi and A. E. Pearson. A multistage reduction technique for feedback stabilizing distributed time-lag systems. *Automatica*, 23:311–326, 1987.

[223] F. Zheng and P. M. Frank. Robust control of uncertain distributed delay systems with application to the stabilization of combustion in rocket motor chambers. *Automatica*, 38(3):487–497, 2002.

[224] T. Yang. *Impulsive control theory.* Springer, 2001.

[225] Z. Li, Y. Soh, and C. Wen. *Switched and impulsive systems: analysis, design and application.* Springer, 2005.

[226] W. M. Haddad, V. Chellaboina, and S. G. Nersesov. *Impulsive and hybrid dynamical systems: Stability, Dissipativity, and Control.* Princeton University Press, United Kingdom, 2006.

[227] V. Lakshimikantham, D. D. Bainov, and P. S. Simenov. *Theory of impulsive differential equations.* World Scientific, Singapore, 1989.

[228] T. Hagiwara and M. Araki. Design of a stable feedback controller based on the multirate sampling of the plant output. *IEEE Trans. Autom. Control*, 33:812–819, 1988.

[229] D. A. Lawrence and E. A. Medina. Output regulation for linear systems with sampled measurements. *Proc. of American Control Conf.*, 2001.

[230] A. N. Michel K. M. Passino and P. J. Antsaklis. Lyapunov stability of a class of discrete event systems. *IEEE Trans. Autom. Control*, 39:269–279, 1994.

[231] R. M. Brach. *Mechanical Impact Dynamics.* New York, NY: Wiley, 1991.

[232] J. Lygeros, D. N. Godbole, and S. Sastry. Verified hybrid controllers for automated vehicles. *IEEE Trans. Autom. Control*, 43:522–539, 1998.

[233] X. Liu and A. R. Willms. Impulsive controllability of linear dynamical systems with applications to maneuvers of spacecraft. *Math. Problems in Engineering*, 2:277–299, 1996.

[234] J. Hespanha, D. Liberzon, and A. Teel. Lyapunov characterizations of input-to-state stability for impulsive systems. *Automatica*, in press 2008.

[235] E. A. Medina and D. A. Lawrence. Reachability and observability of linear impulsive systems. *Automatica*, in Press, 2008.

[236] G. Xie and L. Wang. Controllability and observability of a class of linear impulsive systems. *J. Math. Anal. Appl.*, 304:336–355, 2005.

[237] E. A. Medina and D. A. Lawrence. Controlled and conditioned invariants for linear impulsive systems. *Proc. of IEEE Conf. on Deci. & Cont.*, 2006.

[238] D. Henry and A. Zolghadri. Design and analysis of robust residual generators for systems under feedback control. *Automatica*, 41(2):251–264, 2005.

[239] D. Henry and A. Zolghadri. Norm-based design of robust fdi schemes for uncertain systems under feedback control: Comparison of two approaches. *Control Engineering Practice*, 14(9):1081–1097, 2006.

[240] C. A. Jacobson and C. N. Nett. An integrated approach to controls and diagnostics using the four parameter controller. *IEEE Control System Magazine*, 11(6):22–28, 1991.

[241] G. Hearns, M. J. Grimble, and M. A. Johnson. Integrated fault monitoring and reliable control. *UKACC International Conference on Control*, pages 1175–1179, 1998.

[242] S. Kilsgaard, H. H. Niemann M. L. Rank, and J. Stoustrup. Simultaneous design of controller and fault detector. *Proceedings of the 37th IEEE Conference on Decision and Control*, pages 628–629, 1996.

[243] M. J. Khosrowjerdi, R. Nikoukhah, and N. Safari-Shad. A mixed H_2/H_∞ approach to simultaneously fault detection and control. *Automatica*, 40:261–267, 2004.